

NPS ARCHIVE  
1960  
MILANO, V.

NOTES ON THE PRELIMINARY  
DESIGN OF ICEBREAKERS

V. R. MILANO

DUDLEY KNOX LIBRARY  
NAVAL POSTGRADUATE SCHOOL  
MONTEREY, CA 93943-5101

Library  
Naval Postgraduate School  
Monterey, California



DUDLEY KNOX LIBRARY  
NAVAL POSTGRADUATE SCHOOL  
MONTEREY, CA 93943-5101











Notes on the Preliminary Design  
of  
Icebreakers

A Thesis  
Submitted to the Faculty of  
Webb Institute of Naval Architecture  
in Partial Fulfillment  
of the Requirements for the Degree of  
Master of Science  
in  
Naval Architecture

by  
Lieutenant V. R. Milano, USN

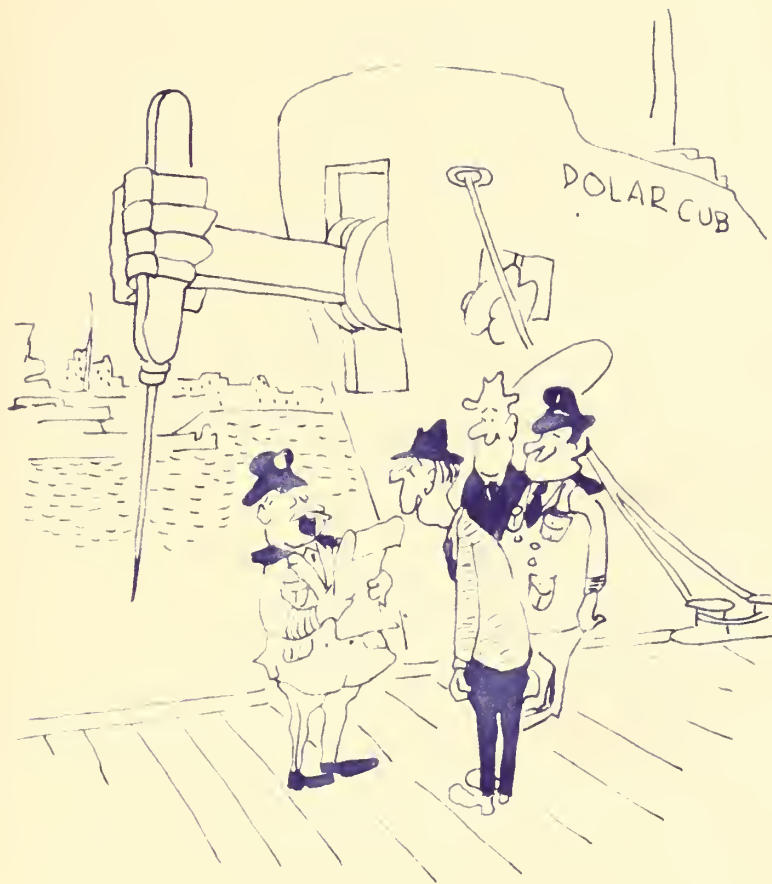
NPS ARCHIVE

1960

MILANO, V

~~MISS~~





"For your outstanding contribution to the  
field of ice-breaking,--"

Maritime Reporter





### Acknowledgements

It would be impossible to credit individually all those persons who have aided and contributed to the preparation of this thesis. <sup>Their</sup> ~~This~~ helpfulness and generosity did, in great part, insure the successful completion of this work.

Special thanks, however, must be given to Doctor Andrew Assur of the U. S. Army Snow, Ice and Permafrost Research Establishment for his continued sincere interest in my work. Without his many helpful suggestions concerning the icebreaker problem and his valuable advice on the problems of ice mechanics, my progress on this thesis problem would certainly have been greatly impaired.

In addition, credit must go to Professor Cedric Ridgely-Nevitt of Webb Institute for his continued interest and assistance in dealing with the difficulties of vessel preliminary design and powering. Also to Professor Lawrence W. Ward and Captain R. A. Hinnners, USN (Ret), of Webb Institute for their guidance and advice and Mr. D. Nevel of the U. S. Army Snow, Ice and Permafrost Research Establishment for his kindness in making available to me his, as yet, unpublished manuscript on the behavior of a wedge on an elastic foundation.



<u>Index:</u>	<u>Page</u>
Section A - List of Symbols	3
Section B - List of Figures and Graphical Aids	13
Section C - The Icebreaker Problem	20
1. Introduction	21
2. Icebreaker Preliminary Design Considerations	28
Section D - Ice Mechanics	35
1. Ice - General	36
2. The Elastic Properties of Ice	46
3. Ice Friction	52
4. The Tensile Strength of Sea Ice	62
Section E - Icebreaker Powering	86
1. Icebreaker Propulsion Machinery	87
2. Propellers and Thrust Predictions	91
Section F - Mechanics of Icebreaking	141
1. Theoretical Predictions of the Stresses in an Ice Field	142
2. Icebreak <sup>ing</sup> <del>up</del> Forces and Vessel Impact Velocity	161
3. Vessel Advance due to Impact	195
4. Vessel Forward Advance and an Evaluation of the Vertical Forefoot	212
5. An icebreakers ability to retract once beset	234





	<u>Page</u>
6. Evaluation of Optimum Flare at Side for Icebreaker Effectiveness	245
7. Icebreakers Ability to break ice without ramming	253
Section G - Preliminary Design Considerations	263
1. Preliminary Estimate of Vessel Proportions	264
2. Evaluation of Transverse and Longitudinal Stability	286
3. Examples of Proposed Preliminary Design Method	304
Section H - Table of Characteristics of Past and Present Icebreaking Vessels	326
Section I - Table of References	345

\* NOTE : NUMBERS IN SUPERSCRIPT REFER TO REFERENCES LISTED  
IN SECTION I



Section A

List of Symbols



- a - Inverse slope of load waterline, i.e. tangent of the angle  
between the centerline plane and the load waterline -  $\tan \psi$
- a<sub>0</sub> - Average distance between ice plates in the ice plate-brine  
pocket model
- a' - Constant depicting ice location in conversion of air temperature  
to ice surface temperature

- A - Non-dimensional coefficient

$$A = \left( \frac{C_b}{C_w} + \frac{k_1^2 C_b}{4k_2^2 C_w^2} \right)$$

- A<sub>a</sub> - Apparent contact area between hull steel and ice surface - sq. ft.
- A<sub>r</sub> - Real contact area between hull steel and ice surface - sq. ft.
- A<sub>t</sub> - Area of contact between hull and ice - sq. ft.
- A<sub>w</sub> - Load waterplane area - sq. ft.
- b - Assumed area of loading when considering stresses in a flat plate  
under a concentrated load - sq. inches
- b<sup>1</sup> - Temperature compensating constant
- b<sub>2</sub> - Width of a wedge at any point x - inches
- b<sub>0</sub> - Average spacing of brine pockets
- b' - Width of a wedge at X = 1; i.e., describes angle
- b<sub>r</sub> - Brine content of sea ice
- B - Maximum beam at load waterline - ft.
- B<sub>1</sub> - Factor related by poissons ratio
- B<sub>2</sub> - Factor related by poissons ratio



- $BM_t$  - Height of transverse metecenter above center of buoyancy - ft.
- BTF - Blade thickness fraction
- c - Radius of circular area over which load P distributed - sq. inches
- CG - Center of Gravity
- CB - Center of Buoyancy
- $C_b$  - Block Coefficient =  $C_p \times C_x$
- $C_o$  - Coefficient of Drag.
- $C_{I_t}$  - Transverse inertia coefficient
- CL - Coefficient of Lift
- $C_{IL}$  - Longitudinal inertia coefficient
- $C_p$  - Prismatic coefficient
- $C_v$  - Vertical prismatic coefficient =  $C_b/C_w$
- $C_w$  - Waterplane coefficient
- $C_x$  - Midship Section coefficient
- D - Propeller diameter - ft.
- $D^1$  - Flexural rigidity of a flat plate =  $Eh^3/12(1 - \nu^2)$
- $D_o$  - Depth Amidships - ft.
- $\epsilon$  - Drag - lift ratio =  $C_o/C_L$
- e - Coefficient of restitution
- E - YOUNG'S MODULUS - psi
- EHP - Effective Horsepower - Hp
- f - Frequency of VIBRATION
- $f_o$  - Dynamic coefficient of friction =  $\mu_o$





- $f_s$  - Static coefficient of Friction =  $\mu_s$
- $F$  - Vertical bow reaction force - tons
- $F_1$   $F'$  - Vertical bow reaction force - lbs.
- $F_b$  - Average area of a brine pocket in surface plane
- $F_f$  - Friction force - lbs.
- $F_o$  - Force tending to move vessel through ice - lbs. equals  $T^1$   
in steady state when inertia energy dissipated
- $g$  - Acceleration of gravity -  $\text{ft}/\text{sec}^2$
- $g^1$  - Length of brine cylinders
- $g_o$  - Average spacing of brine pockets
- $GM_t$  - Transverse metecentric height - ft.
- $GM_L$  - Longitudinal metecentric height - ft.
- $h$  - Thickness of ice sheet or plate - cm or inches equals  $t''$
- $h^1$  - Height of vertical forefoot - ft.
- $h_s$  - Snow thickness - cm or inches
- $H$  - Vessel full load draft - ft.
- $j$  - Slant distance vessel penetrates ice due to compression,  
i.e., length of load waterline to penetrate ice - ft.
- $J$  - Speed Coefficient =  $v_{\infty}/v_D$
- $k$  - Foundation Modulus -  $\text{lb}/\text{in}$
- $k^1$  - Inertia coefficient
- $k_1$  - Nondimensional coefficient defined by  $S = k_1 L/2$



$k_2$  - Nondimensional coefficient defined by

$$GM_2 = \frac{k_2^2 C_w^2 L^2}{H C_8}$$

$K^1$  - Shape factor of loaded area

KB - Distance from base line to vertical center of buoyancy - ft.

KG - Distance from base line to vertical center of gravity - ft.

$KM_t$  - Distance from base line to transverse metecenter - ft.

$KM_L$  - Distance from base line to longitudinal metecenter - ft.

$l$  -  $\sqrt[4]{D/a} = \sqrt[4]{Eh^3/12(1-\nu^2)k}$

$l^1$  - Characteristic length =  $\sqrt[4]{Eh^3/12k}$

L - Length between perpendiculars - ft. = LBP

LOA - Length overall - ft.

LCF - Longitudinal center of floatation

LWL - Load waterline length - ft.

m - metecenter

$m^1$  - added mass - lb/sec<sup>2</sup>/ft.

$m^{11}$  - vessel mass - lb/sec<sup>2</sup>/ft.

M - Bending moment at upper fibers of wedge - inch lb.

n - Distance from amidships to longitudinal center of floatation - ft.

N - Propeller shaft RPM

$N^1$  - Normal load - lbs.

$\phi l$  - Distance from forward perpendiculars to vertical portion of forefoot - ft.

$P_m$  - Plastic mean flow pressure - psi



- $p_o$  - propeller pitch at the 0.7 radius - ft.
- $P$  - Propeller Horsepower = 0.98 SHP = PHP - Hp
- $P$  - Applied concentrated load - lbs.
- $q$  - Uniformly distributed load on wedge - lb/inches
- $Q$  - Propeller torque - ft. lbs.
- $Q^1$  - Compressive force against the ships side at the bow exerted by  
ice - lbs.
- $Q^1_n$  - Component of  $Q^1$  normal to the shell - lbs.
- $Q^1_t$  - Component of  $Q^1$  tangent to the shell - lbs.
- $r$  - Ship resistance at any speed  $v$  - lbs.
- $r^1$  - Total distance vessel travels in horizontal direction - ft.
- $r_o$  - radius of assumed concentrated loadings of wedge
- $r_b$  - one half width of included brine pockets
- $R_t$  - Resultant force acting normal to the stern - lbs.
- $s$  - Distance from intersection of stern and load waterline to the  
longitudinal center of floatation - ft.
- $s^1$  - Vessel accelerating distance - ft.
- $s_b$  - Salinity of brine
- $s_1$  - Relative insulation value of snow as versus ice
- $s_o$  - Salinity of ice
- $s_s$  - Relative amounts of solid salts
- $S$  - Shape factor of loaded area





- SHP - Shaft Horsepower - Hp
- t - Thrust deduction factor
- $t^1$  -  $M/PX$
- $t^{11}$  - Thickness of ice sheet - cm or inches = h
- T - Propeller thrust - tons
- $T^1$  - Propeller thrust - lbs.
- $T_1$  - Ideal propeller thrust
- $T_0$  - Propeller thrust at bollard condition - tons
- $T_0^1$  - Propeller thrust at bollard conditions - lbs.
- u - tangent of hydrodynamic pitch angle =  $\tan \beta$
- U - Non dimensional coefficient

$$U = \frac{f_s - \tan \alpha \cos \beta}{f_s \tan \alpha + \cos \beta}$$

- v - Vessel speed - ft/sec.
- $v^1$  - Relative brine volume
- $v_a$  - Propeller Speed of Advance - ft/sec. =  $v (1 - w)$
- $v_e$  - Extensional velocity of sound wave through infinite solid medium - ft/sec.
- $v_o$  - Longitudinal velocity of sound wave in infinitely long bar - ft/sec.
- $v_r$  - Transverse velocity of sound wave over surface of extended solid medium - ft/sec.
- V - Vessel speed - knots
- w - Wake fraction
- W - Vessel displacement - tons



x - distance along wedge from apex

X - Non-dimensional coefficient

$$X = \frac{\cot \alpha \cos \beta - f_0}{\cos \beta + f_0 \cot \alpha}$$

X<sub>h</sub> - nondimensional hub diameter =  $\frac{\text{hub diameter}}{\text{propeller diameter}}$

X<sup>1</sup> - Vessel impact speed variable

y - Horizontal vessel travel due to ice compression - ft.

$\bar{y}$  - Distance from edge of flat plate to the centroid of loaded area

Y - Non-dimensional coefficient

$$Y = \frac{\cos \beta}{\cos \beta + f_0 \cot \alpha}$$

Z - Non dimensional coefficient

$$Z = \frac{\cos \beta \cos^2 \alpha}{\cos \beta + f_0 \cot \alpha} = Y \cos^2 \alpha$$

$\alpha$  - angular ~~use~~ <sup>RISE</sup> of forefoot - degrees

$\beta$  - Angle between center line plane and the normal to the shell plate  
at the bow - degrees

$\beta$  -  $\tan^{-1} \frac{v_a}{\pi N D}$

$\beta_0$  - Non-dimensional parameter =  $b_0/a_0$

$\beta_1$  - Hydrodynamic pitch angle

$\beta$  - Angle measured in the plane normal to the ships side at the bow,  
between the centerline plane and the ships side - degrees

$\gamma'$  - Specific weight of sea water lb/ft<sup>3</sup>.

$\gamma_0$  - Non dimensional parameter =  $g^1/g_0$

$\epsilon$  - Average ratio of length of brine pocket to the width of brine pocket



$\eta_h$  - Hull efficiency =  $(1 - t / 1 - w)$

$\eta_m$  - Mechanical efficiency  $\approx 0.98$

$\eta_b$  - Blade efficiency

$\eta_i$  - Ideal propeller efficiency

$\eta_o$  - Open water propeller efficiency

$\eta_r$  - Relative rotative efficiency

$\eta$  - Propeller coefficient

$$\eta = \frac{N}{60} \sqrt{\frac{D^5}{V}} \varphi$$

$\eta_D$  - Dynamic coefficient of friction =  $f_D$

$\eta_s$  - Static coefficient of friction =  $f_s$

$\nu$  - Poisson's ratio

$\rho$  - Density - lb. sec<sup>2</sup>/ft.

$\rho_o$  - Non dimensional parameter

$$\rho_o = \frac{c r_o}{1 + F_b}$$

$\sigma$  - Propeller coefficient

$$\sigma = \frac{T D}{\pi r^2}$$

$\sigma_i$  - Tensile strength of sea ice - psi

$\sigma_1$  - Empirically determined ice strength in the region of ice deterioration - psi

$\sigma_c$  - Compressive strength of ice - psi

$\sigma_F$  - Tensile strength of fresh water ice - psi

$\sigma_o$  - Tensile strength of ice without internal cavities - psi

$\sigma_r$  - Bending stress in upper fibers of wedge - psi



$\sigma_{max}$  - Tensile strength of material - psi for ice

$$\sigma_{max} = \sigma'$$

$r$  - Non dimensional distance of loading

$$r = \frac{r}{r'}$$

$\tau_s$  - shear strength - psi

$x$  - Non dimensional distance measured along wedge =  $x'$

$\varphi$  - Angle between the centerline plane and the load waterline, i.e.

$$a = \tan \varphi$$

$\varphi'$  - Function representing the reduction in strength of ice due to brine inclusions

$\psi$  - Angle between the centerline plane and the ships side at a transverse bow section

$\Delta d$  - Change in vessel draft - ft.

$\Delta \psi$  - Change in vessel trim - radians

$\theta_a$  - Air temperature - °C

$\theta_i$  - Temperature at the interface between ice and snow - °C

$\theta_w$  - Water temperature - °C

$\phi$  - Propeller Coefficient

$$\phi = \frac{V_a}{V_w} \cdot \frac{D^5}{V_w^2} \cdot \frac{1}{r^2} \cdot \frac{1}{r^2}$$

$\nabla$  - Volume of water displaced - cu. ft.

$\lambda$  - Advance coefficient =  $\tan \delta = \frac{V_a}{\pi N D}$





Section B

List of Figures and Graphical Aids



Figure

1. Partial phase diagram for ice
2. Strength Conditions of Sea Ice
3. Young's Modulus of ice as a function of ice temperature
4. Laminar Structure of a sea ice crystal
5. Model of brine inclusions in sea ice
6. Model of reinforced brine pockets
7. Relative tensile strength of sea ice
8. Series B3-50 propeller data
9. Ballard Pull available for B3-50 series propeller as  
a function of shaft horsepower and propeller diameter
10. Shaft RPM necessary to develop maximum ballard pull -  
series B3-50 propeller
11. Series B4-55 propeller data
12. Ballard pull available for series B4-55 propeller as a  
function of shaft horsepower and propeller diameter
13. Shaft RPM necessary to develop maximum ballard pull,  
series B4-55 propeller
14. Comparison of propeller data for various series propellers
15. to 20. Propeller thrust developed versus ship speed for series  
B3-50 propeller
  15. Propeller diameter 5 ft
  16. Propeller diameter 10 ft
  17. Propeller diameter 15 ft



Figure

18. Propeller diameter 20 ft
19. Propeller diameter 25 ft
20. Propeller diameter 30 ft
21. to 26. Propeller thrust developed versus ship speed for  
series B4-55 propeller
21. Propeller diameter 5 ft
22. Propeller diameter 10 ft
23. Propeller diameter 15 ft
24. Propeller diameter 20 ft
25. Propeller diameter 25 ft
26. Propeller diameter 30 ft
27. Variation of  $\delta / \mu^{2/3}$  as a function of  $\phi / \mu^{1/3}$   
for series B3-50 propeller
28. Variation of  $\delta / \mu^{2/3}$  as a function of  $\phi / \mu^{1/3}$   
for series B4-55 propeller
29. Variation of thrust coefficient as a function of speed  
coefficient for series B3-50 propeller
30. Variation of thrust coefficient as a function of speed  
coefficient for series B4-55 propeller
31. Variation of lift coefficient as a function of thickness -  
cord ratio and blade section angle of attack
32. Variation of drag coefficient as a function of thickness -  
cord ratio and blade section angle of attack



- Figure 33. Comparison of force required to overcome sea ice based on various flat plate formulae
34. Force required to overcome perennial sea ice as a function of ice temperature based on flat plate theory
35. Loci of points of maximum  $\epsilon'$  for solution of wedge problems
36. Strength characteristics of perennial sea ice
37. Strength characteristics of normal one season sea ice
38. Strength characteristics of young sea ice
39. Vessel added mass parameter  $k'$  as a function of length to beam ratio and half beam to draft ratio
40. Icebreaker total hull resistance as a function of ship speed in open water
41. Vessel speed parameter for acceleration in open water
42. Icebreaker total hull resistance as a function of ship speed in *brash* filled channel
43. Vessel speed parameter for acceleration in *brash* filled channel
44. Representation of load waterplane inclination
45. Variation of propeller diameter to draft ratio as a function of full load draft
46. Variation of propeller diameter to beam ratio as a function of vessel beam





Figure

47. Variation of vessel draft as a function of length between perpendiculars
48. Variation of vessel beam as a function of length between perpendiculars
49. Variation of beam to draft ratio as a function of length between perpendiculars
50. Variation of propeller loading factor  $T_0/D^2$  as a function of length between perpendiculars
51. Variation of non dimensional ratio  $T_0/\omega$  as a function of length between perpendiculars
52. Variation of non dimensional forefoot function  $C$  as a function of length between perpendiculars
53. Variation of vessel advance factors  $\tau$  and  $\ell$  as a function of length between perpendiculars
54. Evaluation of vessel energy lost due to vertical forefoot striking ice sheet
55. Vessel energy effectively used due to vertical forefoot striking ice sheet
56. Variation of non dimensional quantity  $U$  as a function of  $\alpha$  and  $\beta$  for  $f_s = 0.4$
57. Variation of non dimensional quantity  $U$  as a function of  $\alpha$  and  $\beta$  for  $f_s = 0.5$



58. to 60. Thickness of ice a vessel can break continuously as  
a function of ballard pull available and sea ice  
surface temperature

58. Perennial Sea Ice

59. Normal one season sea ice

60. Young sea ice

61. Variation of  $\cot \alpha \cos \beta$  as a function of  $\alpha$  and  $\beta$

62. Range of variation of waterplane coefficient as a  
function of speed length ratio

63. Non dimensional quantity A as a function of block  
coefficient and waterplane coefficient

64. Non dimensional quantity  $Z$  as a function of  $\alpha$  and  $\beta$

65. Non dimensional quantity  $X$  as a function of  $\alpha$  and  $\beta$

66. Non dimensional quantities  $X$  and  $Z$  as a function  
of  $\alpha$  and  $\beta$

67. Variation of prismatic coefficient as a function of  
speed-length ratio and displacement-length ratio

68. Variation of block coefficient as a function of speed  
length ratio and prismatic coefficient

69. Variation of midship section coefficient as a function  
of speed length ratio

70. Variation of waterplane coefficient as a function of  
prismatic coefficient

71. Variation of transverse inertia coefficient as a function  
of waterplane coefficient



- Figure
- 72. Variation of longitudinal inertia coefficient as  
a function of waterplane coefficient
  - 73. Variation of vertical prismatic coefficient as  
a function of prismatic coefficient and speed  
length ratio
  - 74. Variation of depth amidships as a function of length  
between perpendiculars and length to draft ratio
  - 75. Variation of longitudinal center of floatation as a  
function of waterplane coefficient
  - 76. Solution for vessel displacement in sample problem



Section C

The Icebreaker Problem





## Part 1

### Introduction

The true icebreaker, as distinguished from the vessel strengthened for ice, is a unique type of sea going vessel. It must be capable of continuous operation in areas of the world seldom seen by the conventional vessel and under environmental conditions which are often extremely severe. The vessel must be strong and powerful so as to be able to withstand and overcome its element - ice, and it must be self sufficient so as to be capable of long sustained operation far from any possible source of supply or material assistance.

Primarily, icebreakers are vessels designed to force passage through ice filled waters so as to accomplish several allied functions. One of the most important of these functions is that of escorting or leading conventional thin skinned vessels through the ice field by breaking a channel in the ice wide enough for the escorted vessels to pass through. Another of these functions is that of keeping a given waterway or channel free of solid ice to such an extent that conventional vessels may traverse the waterway without danger. The icebreaker is often called upon to free vessels beset by ice in the various waterways, rivers or lakes and at times even in polar regions. Lastly, the icebreaker must be capable of long periods of independent operation in polar regions for the purpose of



carrying out valuable hydrographic or oceanographic survey and also to provide logistic support to remote ice-locked stations.

The history of ice breakers is comparatively short when compared with the history of navigation. The first true icebreaker was probably "EISBRECHER I" which was built in Hamburg in 1871 and worked between Hamburg and Cuxhagen. It had a displacement of 500 metric tons and an engine power of 600 IHP. Since that time many changes and innovations have occurred in icebreaker design practice until today there exist such goliaths as the 8000 ton, 21000 SHP "Glacier" in the United States and the 16000 ton, 40000 SHP atomic powered "Lenin" in Russia.

Many new theories as regards icebreaking were developed during this evolutionary period. The spoon shaped bow of the "MURTAJA" in 1890 was a revolutionary change. Its effectiveness in solid ice was gratifying, however, in snow covered ice or ice slush it proved a failure since the spoon shape tended to push the snow and slush forward with the bow quickly absorbing the vessels forward energy. At about the same time, on the great lakes, the effectiveness of forcing a passage through ice by backing the vessel through it was observed. The adaption of bow propellers was a natural consequence, beginning in 1888 with the ferry boat "ST. IGNACE" with a stern shaft power of 2000 IHP and a forward shaft power of 1000 IHP. The primary function of this bow propeller was to wash water and ice from the forward end of the vessel thereby reducing the friction between



the ice and the vessel. Unfortunately, the wash of the forward propeller was unsymmetrical due to direction of propeller rotation and the single forward propeller always produced a side force which made steering and maneuvering to one of the sides more difficult. On many subsequent installations this condition was alleviated by the use of twin forward screws. The use of these bow propellers proved very effective in bays, rivers and lakes. In later years, however, when they were employed on polar icebreakers serious shortcomings became evident. In these polar regions where the ice is very thick and hard and breaking by ramming was a necessity, considerable propeller damage resulted. Consequently, bow propellers are seldom used on present arctic breakers.

In 1926 oil fired boilers began to replace the previously used coal fired installations, thus greatly increasing the icebreakers cruising range. At about the same time heeling tanks were introduced which could heel the vessel several degrees by means of pumping water between opposing wing tanks, thus helping to free a vessel beset by ice friction. 1932 saw the introduction of direct current diesel electric propulsion with its inherent high SHP/weight ratio and greatly increased vessel maneuverability through feasible pilot house engine control.

Despite these various evolutionary changes in icebreaker design, it is also true that basic icebreaker hull form has changed little through the years. Vessel displacements and powering have been increased and





propeller shaft configuration and number have been varied but through it all the basic hull shape and configuration has remained about the same. In fact, to the present day, little, if any, factual test or experimental data exists as to the effect of variation of hull form on ice breaking effectiveness. Limited personal experiences as to an existing vessel's effectiveness have been about the only guide available to the designer. Consequently, each new icebreaker is no more than a scaled up model of some existing vessel which it is felt has proven effective. No doubt the present hull form is effective, but is it as effective as it could be for its given displacement and power? It is amazing that even today, little, if any, theoretical evaluations or actual test data concerning icebreaking and ice breaking vessels is to be found in the literature. Has no one ever considered changing the present hull form in search of a more effective one, perhaps a hull form which broke ice upward which is considerably easier to do than downward, or a hull form that attempted to conserve the major portion of potential energy developed by ramming so that a quasi-constant vertical bow reaction force is maintained against the ice surface and only a small additional propeller thrust is necessary to break even heavy ice in a continuous forward motion? This latter method would at least keep the vessel's bow from falling back down when the ice broke after each ram and would be efficient which cannot be said of the present hull shape and method. Perhaps these things and others have been





thought of but since comparatively few icebreakers are built there is little incentive for publication. Since World War II, however, interest in the polar regions has materially increased. More nations of the world are finding that they have increasing interests and commitments of a military, commercial and scientific nature in these areas. Yet the majority of existing icebreaker type vessels are obsolete and unable to successfully cope with the present demands of operations in the Arctic and Antarctic. New, more powerful and more effective icebreaking vessels will, no doubt, be built. To do this most effectively it would seem that a more positive program of theoretical analysis, research and test is necessary both in the field of ice mechanics and ICEBREAKER Naval Architecture.

This paper attempts to present a discussion of the mechanics of ice breaking plus a means of approaching the preliminary design or design study of the conventional type of icebreaking vessel. It is only one of the many possible approaches and by no means purported to be the best, most logical or most correct possible. However, it is an approach and one which attempts to make effective use of what little is known about ice and ice breaking. Throughout the paper many assumptions are made and conclusions drawn. To the author they seemed reasonable and justifiable. Others might tend to disagree or object violently. However, to lend authority or credence to an objection or opposing view, justification must



be presented to substantiate the objection. If this paper accomplishes even this end it shall have, to a degree, achieved its purpose, for only through published critical discussion and differences of opinion will the elements of icebreaker design be critically re-evaluated so as to stimulate a real desire towards determining the most effective means of breaking ice.

There are many types of icebreakers and each is designed so that it may best cope with the ice and environmental conditions of its particular service. It would be impossible for this paper to treat the particular problems of each of the various icebreaker types. Consequently, to bring the problem within reasonable limits, we shall consider the case of the large polar icebreaker (arctic or antarctic) with no bow propellers and with two stern propellers. Invariably, many of the items discussed herein will apply with equal validity to any type breaker and one with any powering configuration, however, in those instances where definition must be made, reference will always be to the twin stern screw polar icebreaker. It should also be noted that throughout the paper, full load displacement condition is used synonymously with design conditions and that when reference is made to vessel displacement, draft, beam, etc., it is always to the full load or design condition unless specifically noted to the contrary. Since only the twin stern screw vessel is considered, all references to vessel length are to length between perpendiculars. One final comment is in order. Snow cover on an ice surface will greatly effect the physical



and elastic properties of that ice. Since so little is actually known quantitatively about the effects of the snow cover all references to ice, its strength and properties, is in every case to ice with no snow cover.



## Part 2

### Icebreaker Preliminary Design Considerations

In order to commence a logical preliminary design of an arctic ice-breaker, there are certain items of information concerning the proposed vessel, its service and general area of normal operation which must be known to the designer. These items of information need not be known with great accuracy for the ship will invariably be a compromise as regards its service, area of operation and characteristics. However, in order to allow for as realistic and accurate preliminary vessel parameter estimates as is possible, it behooves the designer to acquaint himself as thoroughly as is possible with these requirements which will either restrict or control his selection of vessel parameters.

Generally speaking, those items which will have the most immediate effect upon the design are:

(a) Physical size limitations imposed on the vessel

1. Draft restrictions
2. Minimum beam considerations

(b) Normal operating area

1. Arctic
2. Antarctic

(c) Operational requirements

1. Convoying ability (high power and high length to beam ratio)





2. Independent operation (low length to beam ratio)
3. Maximum thickness of ice which it is desired the vessel be able to overcome.
4. Month of year during which it is desired vessel be <sup>FIRST</sup> ~~just~~ able to successfully penetrate ice.
5. Mean air temperature typical of area of operation during period described in 4 above.

The desired draft of the proposed vessel must be considered early in the design stage. Often there are draft limitations due to the restricted depths of water found in the vessel's proposed area of operation. If no such draft restrictions exist then the draft should be selected large enough to accomodate large diameter propellers. This is desirable so as to develop maximum possible thrust yet still allow for sufficient propeller tip immersion so as to prevent the propeller tips from striking the bottom surface of a floating ice sheet and in addition, prevent air from being drawn down by the propeller. Unfortunately, however, most areas of operation in the arctic and antarctic impose some draft limitations. Consequently, a serious study of the vessels most probable area of operation should be made and the maximum safe operating draft determined. In most instances, for the arctic breaker, this limit seldom exceeds 29 to 30 feet.

The minimum desirable extreme beam at the full load waterline is another item which must be considered early in the design. If the proposed



vessel is to be capable of efficient convoy service in the ice, it is often desired that the extreme vessel beam be equal to or greater than the beam of the largest vessel which the icebreaker may have to escort through pack ice. The channel that an icebreaker leaves is often about a foot or two feet wider than the vessel itself, dependent upon the thickness and hardness of the ice encountered. Hence, some decision as to the minimum acceptable extreme beam must be made. Such a vessel will normally have a relatively low length to beam ratio, in the range of about 4 to 4.8. These values are rather low and tend to produce a vessel with either poor or mediocre directional stability. In order to escort vessels through the ice effectively and safely it is necessary for the escorting icebreaker to have good directional stability so as to be able to maintain as steady and straight a course through the ice as is possible. Such a requirement would dictate a rather high length to beam ratio, probably around 5.5 or 6. Unfortunately, however, this would restrict the permissible extreme beam. Consequently a compromise choice of beam must be made. Some authorities on icebreaking feel, and the author tends to agree, that the minimum extreme beam should not be such an overriding consideration. It is felt that in convoying it is much more vital to have adequate directional stability so that the vessel will not tend to veer off sharply when the bow strikes a piece of ice a glancing blow, hence producing a channel in the ice which is straighter and easier for the escorted ships to follow. Due to this high length to beam ratio, however, the extreme beam may be limited to a value



less than the beam of the escorted vessels. However, since most vessel convoying in ice is done during the summer months, the ice will normally be open, with a considerable number of leads and not under pressure. Under these circumstances, as the icebreaker forces a lead or traverses a floe, the ice will be able to move aside giving way to the icebreaker and leaving a resultant channel astern the breaker which is considerably wider than the vessels extreme beam. If, perchance, the ice is not open, but rather concentrated with almost ten tenths coverage and possibly still under pressure, then practical experience has shown that it is best to use two icebreakers to escort, the first icebreaker with good directional stability forcing the channel and the second trimming off the edges of the channel so as to insure adequate width of channel and straightening any irregularities caused by passage of the first breaker. There are considerable pro and cons on this topic of length to beam ratio and minimum extreme beam which is acceptable in a good convoying icebreaker. It is felt, however, that the tide of opinion is changing and that more and more people involved in icebreaking are becoming convinced that directional stability is of paramount importance in an arctic icebreaker, hence the proponents of higher length to beam ratios are increasing.

If the escorting of vessels through the ice is not to be a primary task of the proposed icebreaker, then lower length to beam ratios are acceptable and in fact, desirable. This will produce a short stubby vessel capable of quick sharp turns which can wind itself through the ice, taking advantage of





every lead in its forward progress. Such a vessel will have poor directional stability. Maneuverability, however, is much more important when forcing independent passage through heavy ice so that complete advantage may be taken of leads, polynays and the evasion of areas of rafted or heavily snow covered ice.

There is no doubt that the selection of length to beam ratio and minimum extreme beam for an icebreaker vessel is a compromise. Consequently, it behooves the designer to understand, as completely as is possible, the needs of the proposed vessel before making the selection of values.

In addition to the consideration of vessel convoying in ice, the beam must be sufficient to insure adequate intact and damaged stability. As a result of their normally large beams, this type vessel has a large transverse metecentric height. Consequently, intact stability is normally very good -so good in fact as to often prove a discomfort to the crew. This stability, however, must not be assumed to be adequate merely because of a high initial metecentric height. Icebreaker operations are often such as to make such a high metecentric height desirable and necessary and not ~~solely~~ <sup>SOLELY</sup> the by product of a beamy vessel. Most characteristic is the serious reduction in stability which occurs when the vessel rides up onto the ice, especially with iced top ~~hampers~~ <sup>HAMPER</sup>

One other item which should be seriously considered prior to the commencement of an icebreaker design study is the probable area of normal vessel operation and the periods during which the vessel will actually be operating in ice. Environmental conditions differ in the arctic as compared to the antarctic and vessels which can operate with success during normal periods in the arctic often experience serious difficulty in the antarctic. The month of year





during which the icebreaker is first expected to be able to penetrate the ice will materially effect its requirements; the thickness of ice normally found in the area, past records of ice growth rates, history of ice pressure during various months of the year, rafting, snow cover experienced, etc., all should be considered so as to more realistically determine the probable needs of the vessel. Considerable study of ice conditions both in the arctic and antarctic have been made for a number of years by such organizations as the Hydrographic Office, U. S. Navy Civil Engineering Corps., U. S. Army Snow, Ice and Permafrost Research Establishment, Navy Electronics Laboratory, etc.. Each of these organizations has a wealth of ice data and information concerning past ice experience at various times of the year and under various operating conditions which is readily available to the designer. Consequently, it behooves the designer of an icebreaking vessel to avail himself of as much of this data and past history as is possible so that he can more realistically realize the actual needs of the proposed vessel.

In this paper we attempt to make direct use of several of these environmental factors which can be reasonably predicted from past records. Among the items we consider are mean air temperature during the month of first expected ice penetration and probable snow cover during this time. Based on this data we can estimate the probable ice surface temperature which might be expected. Other items we consider are normal ice thickness encountered in the past in the general area of operation and at the desired times of the year and



the type of pack ice experienced prior to natural weather breakup, i.e., perennial sea ice (old ice), normal one season sea ice or new formations of young sea ice. Based on these estimates of ice thickness and type of ice expected and on our previous estimate of ice surface temperature we may, with some degree of accuracy, determine the vertical bow reaction force which it shall be necessary for our vessel to develop in order to overcome the expected ice and force passage so as to accomplish its mission.

These are but a few of the items of information which past ice history can provide to aid the designer. Much more exists, equally pertinent, and all of which can be used to aid the designer to more realistically visualize his problem and provide a vessel which will be more effective in coping with its expected environment.



Section D

Ice Mechanics



## Part 1

### Ice - General

Ice may exist in any one of several allotropic forms, depending on the ambient temperature and the pressure exerted on the ice. These forms are illustrated by the phase diagram, figure / . It can be seen that as temperature decreases and the pressure increases from atmospheric up to approximately 30,000 psi, water solidifies into the common ice form, Form I. As the temperature is furthered lowered and the pressure increased to the 30,000 to 31,000 psi range, Form I ice may be changed to Form II or Form III ice. At 50,000 psi, Form III ice passes instantaneously through an unstable Form IV (shaded area) into Form V at temperature ranges from approximately  $-13^{\circ}$  F to  $2^{\circ}$  F. At temperature ranges from about  $-13^{\circ}$  to  $-30^{\circ}$  F., increases beyond 50,000 psi cause direct conversion of Form II into Form V ice.

Only the common form, Form I, is found under natural environmental conditions and has, consequently, practical engineering significance. Figure / shows the decrease in the melting point of Form I ice in relation to pressure. It is this decrease in melting point temperature that is responsible for regulation of ice, i.e., the fusion of two pieces of ice at temperatures near the melting point brought together with slight pressure.

### Supercooling

Even though the normal freezing point of water is  $0^{\circ}$  C. ( $32^{\circ}$  F.), it may be appreciably supercooled before freezing begins, particularly if the





PARTIAL PHASE DIAGRAM  
FOR  
ICE

TEMPERATURE - DEGREES F

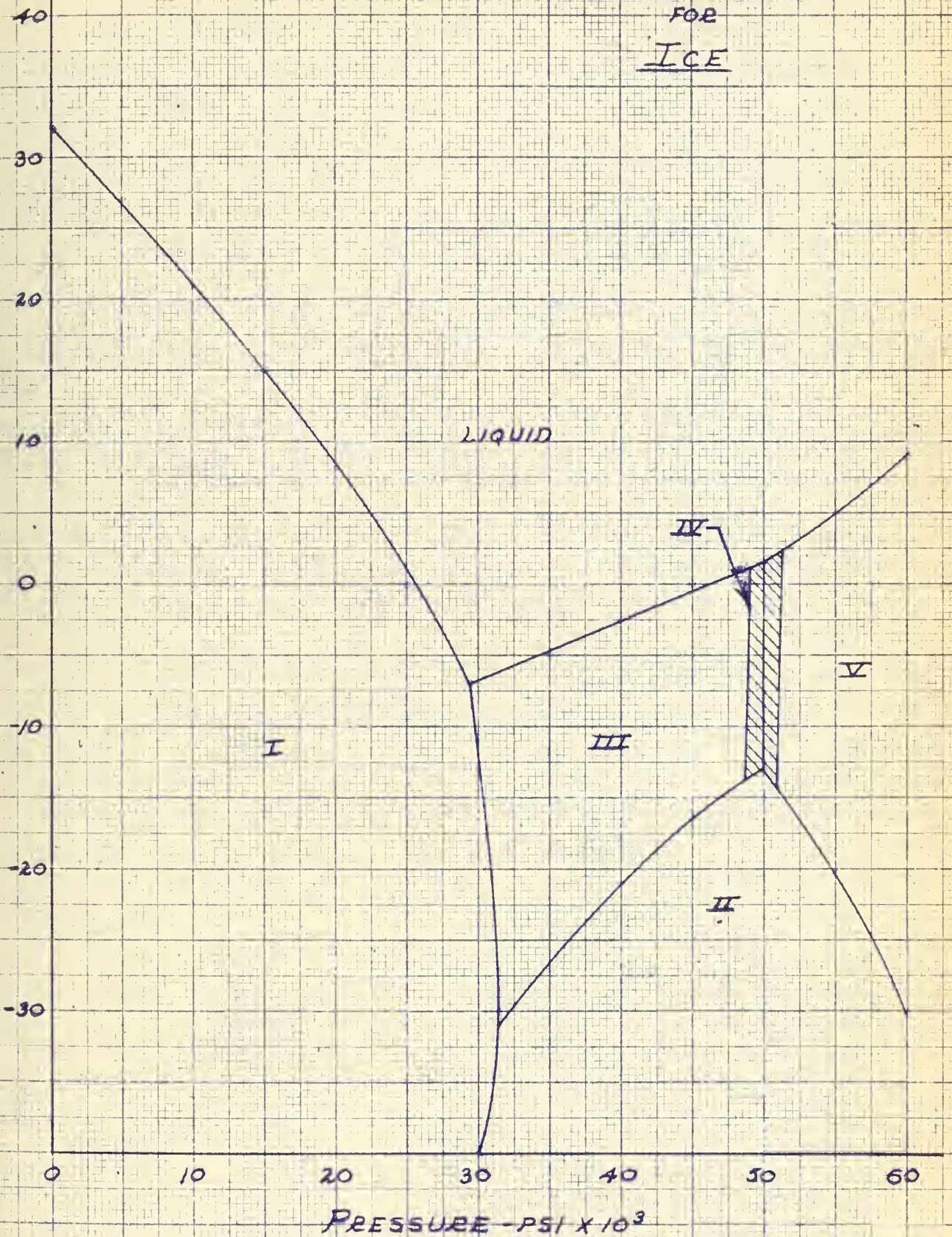


FIG. 1



water is of high purity. In open water occurring in nature, the degree of supercooling varies from a few hundredths of a degree to about  $-1.2^{\circ}\text{C}$ . ( $29.8^{\circ}\text{F}$ ). After supercooling has occurred, freezing may be initiated by seeding or by such measures as impact or splashing. The rate at which crystallization occurs depends on the degree of supercooling; in slightly supercooled water, such as is normally encountered in nature, the rate of crystallization may be sufficiently slow so that supercooled water will coexist with ice in quiet ponds or lakes for a measurable period of time.

### Freezing

The formation of ice, as a rule, depends on the removal of heat from the upper surface by convection or radiation to the air. Generally, the air temperature must be appreciably below  $0^{\circ}\text{C}$ . for freezing to occur; otherwise the rate at which heat is supplied from the earth and from the lower layers of water will be greater than the rate of its removal. As heat is removed at the upper surfaces during and prior to the formation of ice, the colder water sinks, and warmer, less dense water rises; this convection assists in cooling the entire body of water. However, because water has its maximum density at about  $4^{\circ}\text{C}$ . ( $39.2^{\circ}\text{F}$ .) the convection essentially ceases after this temperature is reached by the entire body of water. Thereafter, the densest, warmest water remains at the bottom. As a consequence, the rate at which heat will be supplied from the bottom will be markedly reduced and the freezing at the surface accelerated. Note here that





if the initial ice surface formed is covered with snow, the rate of increase in ice thickness will be markedly reduced due to the excellent insulating properties of the snow.

### Melting

Both warm air and solar radiation are important factors in the melting of ice occurring naturally. In the Polar regions where air temperatures are low, the solar radiation is by far the more important. The radiation is absorbed within the ice, particularly by impurities which accumulate at grain boundaries, hence in fresh water, ice thaws along the crystal boundaries and becomes extremely weak while still of appreciable thickness. In sea ice the radiation is absorbed, particularly in regions where there is an accumulation of salt, causing thawing to start at these sites. Because of the internal absorption of radiation by ice, appreciable melting will take place when the surface temperature of the ice is still lower than the freezing point. This thawing along the grain boundaries and at impurity sites is due to the effect of the impurities in lowering the melting point of the ice since all substances that dissolve in water depress the freezing point and for dilute solutions the depression is proportional to the amount of impurity.

### Effect of Impurities on Ice

In any body of natural water there will be some dissolved minerals and other impurities. Sea water at one extreme is an obvious example but even fresh water has impurities. When ice crystals form, they tend to reject these impurities which then form a layer of concentrated impurities about the



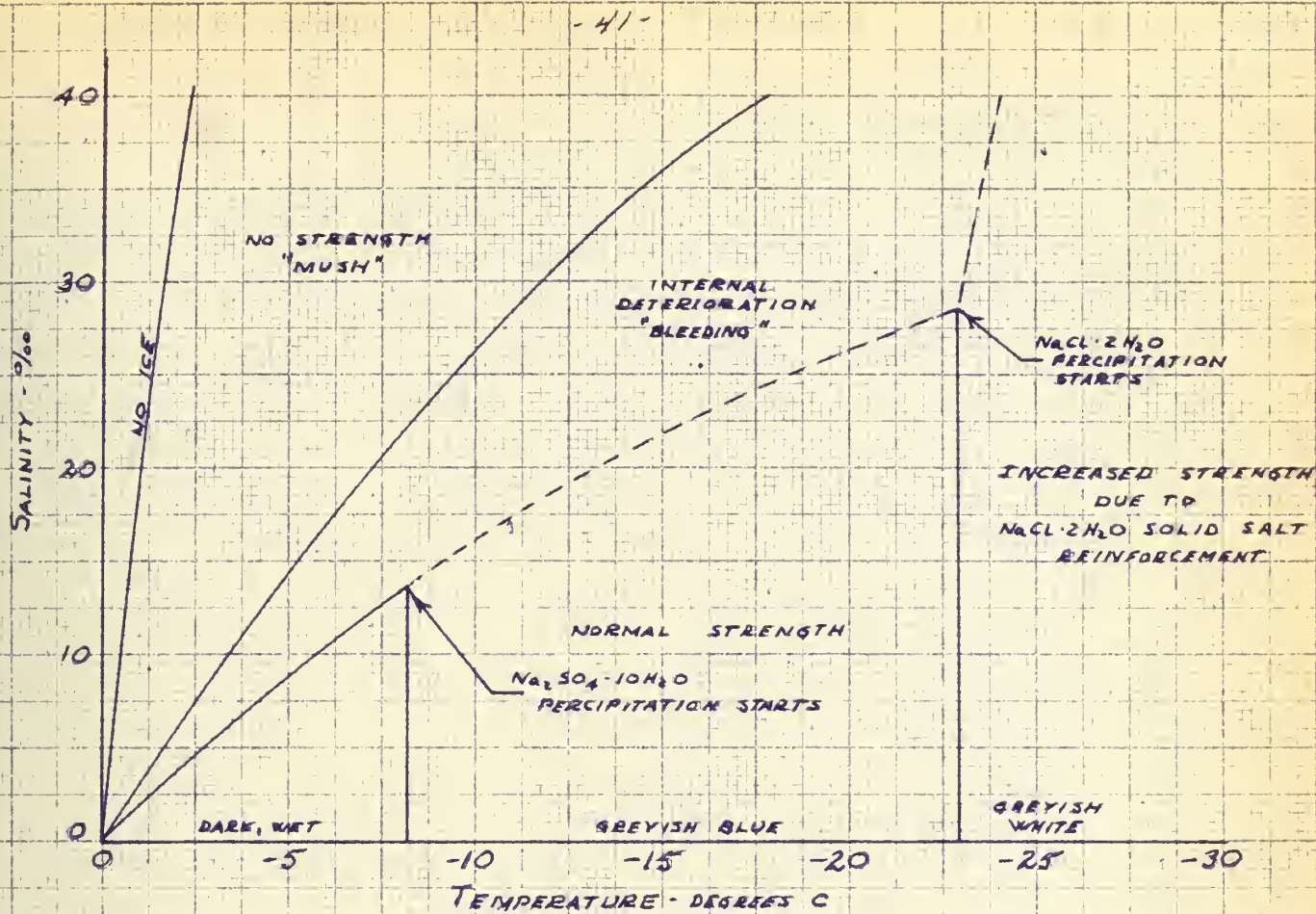
crystal at the grain boundaries, and this layer has a lower melting point than the crystals themselves. This may greatly <sup>A</sup>ffect the physical properties of the ice even though the amount of impurity is small. Melting will always begin at these boundaries between ice crystals and at a temperature below  $0^{\circ}$  F. ( $32^{\circ}$  F.). Fresh water ice becomes rotten as thawing, starting at the inner crystal boundaries, separates the ice into needles or columns. This ice is said to be candled. As a result of this crystal structure in bulk, the physical properties of ice may vary widely, especially when the temperature is near the melting point.

In formation of sea ice, the effect of salt content is very pronounced. Freezing of the water does not begin until a temperature of  $28.6^{\circ}$  F. is reached in undiluted sea water, and the structure produced is porous, containing pockets of brine from which solid salt crystals begin to <sup>PRE</sup>~~RE~~PRECIPITATE when the ice cools to about  $17^{\circ}$  F. The structure, and consequently, the strength properties of sea ice improve with time as the concentrated brine drains and as the salinity of the ice becomes gradually smaller. Newly formed salt water ice of relatively high salinity is flexible and elastic as compared to fresh water ice which is harder and brittle.

The general relation of sea ice strength as a function of temperature and salinity is shown in Figure 2. Here we see that as salinity increases the temperature must be considerably lowered before the ice has any appreciable strength.







## STRENGTH CONDITIONS OF SEA ICE

NORMAL STRENGTH REFERS TO A WIDE RANGE OF STRENGTH CONDITIONS REPRESENTED BY A RELATIVE STRENGTH OF  $\approx 0.5$  AS SHOWN IN FIGURE 7 PRIOR TO PRECIPITATION OF  $\text{NaCl} \cdot 2\text{H}_2\text{O}$  SALT

BLEEDING REFERS TO THAT CONDITION OF INTERNAL DETERIORATION OF THE TOTAL ICE SHEET DUE TO THE FORMATION OF INCREASED BRINE. THE ICE IS FAIRLY WEAK THOUGH STILL COHERENT. AT ITS MORE ADVANCED STAGE THE CAVITIES IN SEA ICE ARE IN HYDRAULIC CONTACT WITH THE SEA WATER UNDERNEATH

MUSH CONSISTS OF INCOHERENT PLATES WITHOUT INTERNAL BRIDGING. MUSH CAN BE CONSIDERED A SORT OF ICE UNTIL NO ICE IS PRESENT AND EVERYTHING IS TRANSFORMED INTO BRINE. THE STRENGTH OF SUCH ICE IS PRACTICALLY NON-EXISTANT.



## Crystallography

It is generally agreed that when ice forms at the surface of a body of water it crystallizes in the hexagonal system and that the ice sheets which form are usually composed of prismatic ice crystals oriented with their long axis (optic or "c" axis) vertical and at right angles to the surface. Hence a normal ice sheet consists of long, vertical ice crystals, each usually several centimeters square in cross section.

The main difference between fresh water and salt water ice is the presence of brine inclusions in the later, forming systematically arranged <sup>holes</sup> ~~beles~~. As diagrammed below, in figures 4 and 5, a sea ice crystal consists of parallel pure ice plates in the direction of growth. The brine inclusions are between the plates, the amount strongly dependent upon temperature and, at a given temperature, is proportional to salinity. An enlarged sketch of the brine inclusions shows them drawn as circular cylinders between the laminar plates of pure ice. In nature they do not necessarily have this exact shape, in fact an elliptical shape might be more near correct, but this will suffice for the purpose of illustration. Note that the brine inclusions are shown as continuous cylinders although vertical interruptions are usually observed.

## Sea Ice

Ice met at sea is for the most part of two kinds, icebergs originating from glaciers, and sea-ice formed on the sea itself by the freezing of sea water. Sea ice proper accounts for probably 99% of the ice met with at sea; bergs are important inasmuch as they constitute a danger to navigation, but





they are common only in a limited number of localities. Suffice it to say that from the ship point of view they are to be avoided and no attempt is ever made to overcome them. A certain amount of ice may also originate in rivers or estuaries as fresh water ice, but it is already in a state of decay by the time it reaches the open sea and its importance is no more than local.

Fresh water freezes at  $32^{\circ}$  F. but sea water freezes at various lower temperatures, depending on the salinity; the greater the salinity, the lower the freezing point. Average sea water, with a salinity of about 35 parts per thousand does not freeze in the open sea until the temperature has fallen to  $28.6^{\circ}$  F.

Ice forms first in shallow water, near a coast or over shoals and banks and in areas of low salinity. It spreads from these areas as centers. Such ice broken up and carried seaward by winds or currents starts further ice formation in deeper water. Ice in deeper water which has not melted during the previous season also acts in the same way. Wave action ordinarily hinders the formation of ice to some extent, however, the presence of old ice *damps* down any sea or swell and, at the same time by cooling the water tends to assist the beginning of the freezing process.

The first sign of freezing is an oily or opaque appearance of the water, due to the formation of ice spicules and then plates known as frazil crystals. These consist of fresh water free of any salt, and increase in number until the sea is covered by sludge or slush of a thick soupy consistency. If low



temperatures continue, the ice crystals coagulate into small discs on the surface. By fusion at their edges these in turn assume the characteristic pancake form. As the process continues, these pancakes adhere to each other to form continuous sheets of young ice.

While the original ice spicules and plates are free from salt, a network of ice crystals forms as further plates are added, in the pockets of which, sea ice is trapped. The crystals grow at the expense of the enclosed sea water; the remaining water thus becomes saltier and therefore, heavier. Rapidly formed sea ice therefore, holds more brine between its crystals than ice of comparatively slow growth. Ice is a poor conductor of heat and the rate of its formation drops appreciably after the first 4 to 6 inches have formed; a snow cover if present, still further reduces the conductivity. The enclosed brine is itself seldom frozen except at very low temperatures; it tends to sink through the surrounding crystal network due to its density.

Sea ice may grow to a thickness of 3 to 4 inches in the first 24 hours and from 2 to 3 more in the second 24 hours. The original surface of the ice is often below water level, and the original surface of the ice is rarely if ever, visible after the first few days. The ice frequently reaches a thickness of 5 feet and sometimes 7 to 10 feet in one season.

Sea ice, other than fast ice in sheltered bays or along the coast, is continually in motion as a result of the effects of wind, tidal streams and current. In its motion the ice must open and shut like a concertina; there





are always a certain number of leads and lanes present, otherwise the ice could not move. In summer these leads normally remain open, but in winter they are soon frozen over with young ice. Apart from the movement of the ice, the occurrence of swells also tends to break up the ice. Due to these various motions, the ice is continuously breaking up, even throughout the winter.

In other instances the ice may not be broken up but rather, subjected to pressure as moving floes are driven together or moving floes pressed against fast ice. Rafting or hummucking occurs according to the degree of pressure. Definite ridges may thus be found, the longer the pressure lasts the greater the ridges. Pressure ridges may be as high as 50 feet when grounded against a coast, but in deep water away from land the greatest height is from 20 to 30 feet and more usually from 10 to 15 feet.

The release of pressure gives rise to lines of weakness in ice fields, in the form of cracks, lanes or leads. These are often parallel with pressure ridges but an ice field does not necessarily crack in its thinnest part and cracks are frequently found passing through ridges and hummucks of considerable height.



## Part 2

### The Elastic Properties of Ice

Ice is generally accepted to be a plastic material and consequently should be described by Maxwell's equation:

$$\tau - f_s = \gamma \frac{dr}{dt}$$

in which

$\tau$  = shearing stress in psi

$f_s$  = elastic limit in psi

$\gamma$  = viscosity in lb/sec/in

$\frac{dr}{dt}$  = rate of deformation

In much of the work that has been reported, it has been assumed that  $f_s = 0$  that is, that ice is truly a viscous material. Although the elastic limit is very small, an analysis of the flow of glaciers indicates that it is not zero. There is evidence that the viscosity of ice depends considerably on the orientation of the optic axis relative to the applied stress. Thus, results of tests show ice to be elastic if the stress is applied perpendicular to the optic axis but otherwise to behave as a plastic. In the case where plastic behavior should occur, tests also indicate that if the rate of loading is great enough, i.e. greater than  $0.5 \text{ Kg/cm}^2 - \text{sec}$ , the ice will behave as an elastic substance rather than plastically. Hence, since the normal mode of loadings of ice is parallel to the optic axis, i.e. normal to the ice sheet, all tests are conducted at rates of loading well in excess of  $0.5 \text{ Kg/cm}^2 - \text{sec}$ .



A large number of determinations of the elastic properties of ice have been reported, but there is a marked lack of agreement, especially among the early results and they must be considered unreliable. Most of the early determinations were made using static loading and assuming ice to be truly elastic rather than plastic. More recently, measurements have also been made using sonic (dynamic) means. In these instances, consistent results have been attained and, although possibility of error does still exist, the values obtained do represent the most reliable to date.

Some question does exist as to the assumption that ice is or behaves as an elastic isotropic material when subjected to stresses. As mentioned above, the elastic behavior may be *INSURED* by the rate of loading, and in addition, it has been shown that if crystallization of the ice is sufficiently rapid, the ice will consist of many crystals variously oriented and could, for practical purposes be considered isotropic. The truth of this last statement was borne out by the fact that although specimens for a variety of tests were cut in many random directions from ice block samples, no great variation in elastic properties were noted. Such minor variations as were observed could be explained by internal flaws which were present in some of the specimens.

The principles involved in the sonic determination of Youngs modulus,  $E$ , and poissons ratio,  $V$ , are based on the principles of the velocity of sound waves through a solid medium. It can be shown that the velocity of a sound wave in an infinitely long rod, called the longitudinal velocity, is given by

$$v_o = \sqrt{\frac{E}{\rho}}$$



also, the velocity of a sound wave through an infinite solid medium, called extensional velocity, is given by

$$v_e = \sqrt{\frac{E(1-\nu)}{2(1+\nu)(1-2\nu)}}$$

It can also be shown that ~~the~~ the transverse wave over the surface of an extended solid is related to the shear waves which occur in <sup>THIN</sup> ~~their~~ plates. Vibrations of this type were first discussed by Rayleigh in his Scientific Papers, Vol. 2, Cambridge University Press, 1900 and are commonly called "Rayleigh Waves". A mathematical treatment is given by Love in his A Treatise on the Mathematical Theory of Elasticity, 4th Edition, Cambridge University Press, 1927. This velocity may be written as

$$v_r = k \sqrt{\frac{E}{2(1+\nu)}}$$

Therefore, if we can determine these three velocities for ice experimentally, we can determine Youngs Modulus and poisson ratio for the material since

$$\frac{v_o}{v_e} = \sqrt{\frac{(1+\nu)(1-2\nu)}{(1-\nu)}}$$

once  $\nu$  determined from the above  $E$  may be obtained from

$$E = \frac{v_o^2}{\nu}$$





and checked by determining  $K$  from

$$\frac{\sigma_r}{\sigma_s} = K \sqrt{\frac{E}{2(1+\nu)}}$$

then substituting to obtain  $E$  from

$$\sigma_r = K \sqrt{\frac{E}{2(1+\nu)}}$$

$$E = \frac{2\sigma_r^2(1+\nu)}{K^2}$$

Tests have indicated that the values of Youngs Modulus varies somewhat with temperature, especially in the range - 30° C. to 0° C. The results of these experiments are shown in Figure 3. Values of Poissons ratio remain relatively constant over this temperature range and may be taken as

$$\nu = 0.365 \pm 0.007$$

from 0 to -15° Centigrade.

These values in Figure 3 are representative of the variation of Youngs Modulus for fresh water ice. For the case of salt water ice there is evidence that the values of Youngs Modulus should be considerably lower, more a function of temperature and definitely dependent upon brine content (temperature and salinity). Unfortunately, however, little if any, experimental data exists in the present day literature to corroborate this evidence and show just what the range of values of Youngs Modulus for sea ice should be.



-50-

ICE  
TEMPERATURE VARIATION  
OF  
YOUNG'S MODULUS

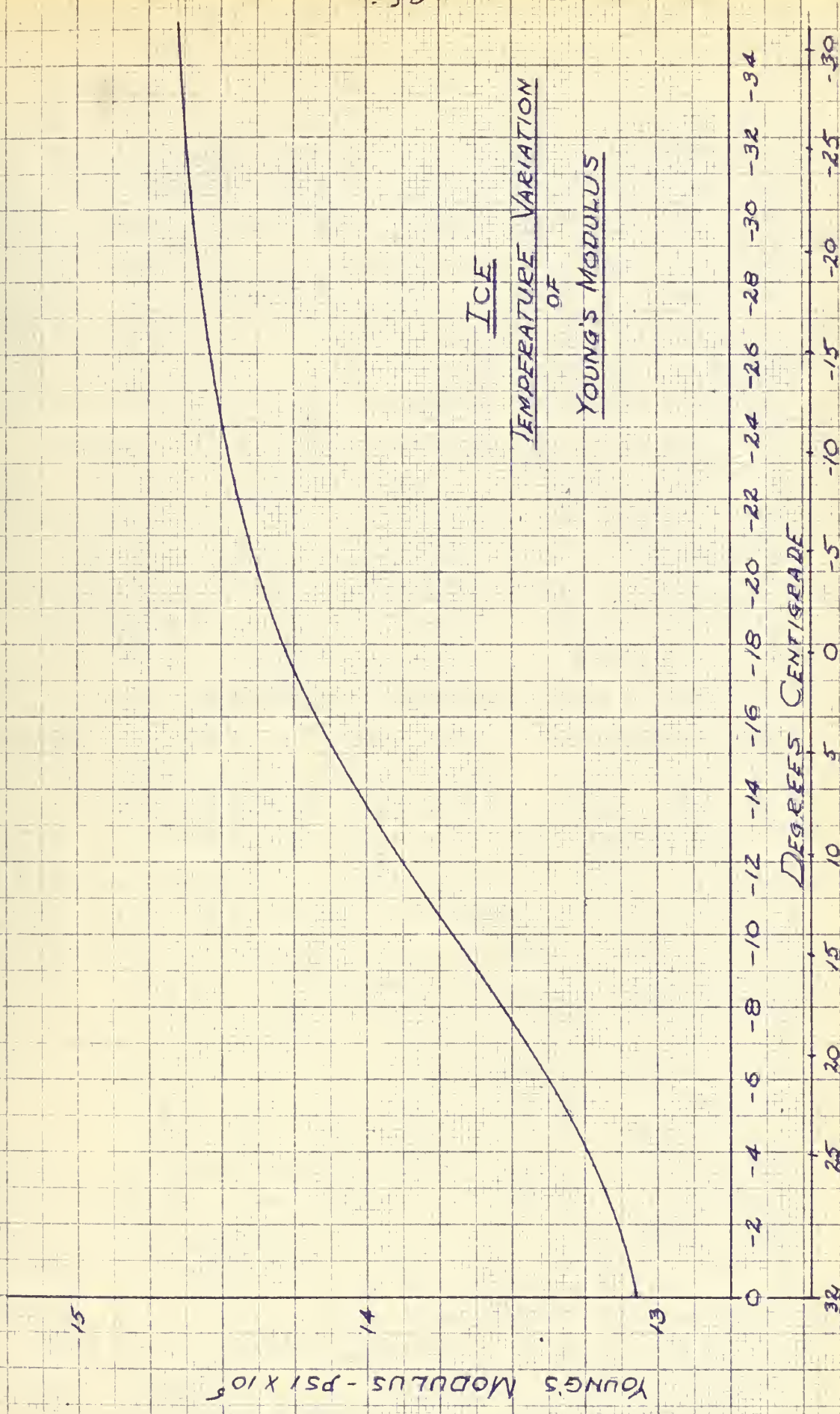


FIG. 3



In addition, since <sup>THIS</sup> ~~the~~ paper deals with the icebreaker problem, some question must be raised as to the accuracy of the sonic methods for the determination of Youngs Modulus. The sonic stresses are very small while the working stresses due to the operation of an icebreaker are very large and it is possible that the sonic method gives somewhat inaccurate information of stress-strain relationships for use in solving the icebreaker problem.

We must, however, accept these probable inherent inaccuracies since the data presented above represents the most accurate and reliable published to date. Possibly, future experimentation will provide a more accurate and realistic representation of the values of Youngs Modulus for sea ice. For the icebreaker problem, however, it is felt that the values quoted above are adequate. Since the ice sheet is considered as a semi infinite flat plate on an elastic foundation, and since only the fourth root of Youngs Modulus enters into the determination of stresses within the plate, it is felt that what errors exist in our above listed values of Youngs Modulus could not be such as to materially effect the determination of stresses within the ice sheet.





### Part 3

#### Ice Friction

The experimental relations known as the classical laws of dry friction have been known for several hundred years. These laws as stated by Coulomb are:

1. Frictional force for a constant load is independent of apparent area of contact.
2. Frictional force is directly proportional to the load, that is, to the total force which acts normal to the sliding surface.
3. Static friction force differs from <sup>KINETIC</sup> ~~static~~ friction force; however, the <sup>KINETIC</sup> ~~static~~ friction is independent of the velocity of the slides.
4. Frictional force depends upon the nature of the materials in contact.

The second of these laws of dry friction may be expressed as

$$F_f = \mu N'$$

where

$F_f$  = frictional force

$N'$  = normal load

$\mu$  = coefficient of friction - either static or <sup>KINETIC</sup> ~~static~~

These static or <sup>KINETIC</sup> ~~static~~ coefficients, according to law four, are dependent upon the nature of the materials in contact, but, according to law one,





independent of the apparent area of contact.

The characteristics of hydrodynamic friction, on the other hand, are quite different. In many cases it is exactly opposite to the characteristics of dry friction. For a Newtonian fluid the force of resistance is related to the apparent area of contact, the velocity gradient, and to the viscosity according to the relation

$$F = \eta A_a \frac{dv}{dx}$$

where

$F$  = Tangential resistance force

$\eta$  = Absolute viscosity

$A_a$  = Apparent contact area

$dv/dx$  = velocity gradient

Measurement of the frictional force, its variation with load, apparent area and velocity enable one to distinguish between the presence of dry and fluid friction. These criteria have been applied to friction on ice. Experimental measurements do indicate that the frictional force is nearly a linear <sup>function</sup> ~~friction~~ of the load, and related to the materials of the two surfaces. The variation of frictional force with apparent area and velocity is very small. These several relations indicate that friction of materials on ice is primarily of the dry friction variety.

The resistance experienced in the process of sliding one surface over another, which is generally termed friction, is not a simple phenomenon but



probably arises through the action of several different mechanisms.

One mechanism of dry friction is undoubtedly related to the presence of asperities on the surface. Several theories have been proposed to explain this relationship. According to this surface roughness theory, the asperities are considered to be rigid with an average slope angle equal to  $\phi$ . The applied tangential force supposedly has a component parallel to the slope which is sufficient to lift the normal load over the rigid asperities by the relation

$$F \cos \phi = N' \sin \phi$$

hence coefficient of friction

$$\mu = \frac{F}{N'} = \tan \phi$$

In 1920, however, Hardy<sup>(125)</sup> pointed out that the lifting mechanism cannot be the principal mechanism of frictional resistance since experiments with flat clean metal surfaces indicated friction practically independent of surface roughness. He proposed adhesion as the dominant force of friction. Holm<sup>(96)</sup> in 1938 suggested that this adhesive force acts only over the real area of contact which is a fraction of the apparent or geometric area of surface contact. As can be shown, this real area of contact between a sliding body and a stationary surface composed of a single material is a function of the normal load applied and may be expressed as

$$A_r = \frac{N'}{p_m}$$

where  $p_m$  = plastic mean flow pressure of softest material.



The resistance force due to friction therefore equals the product of the shear stress in the contact region times the real area of contact, i.e.

$$F = \tau_s A_r$$

where

$\tau_s$  = shear stress of weaker material

Therefore

$$F = \tau_s \frac{N}{p_m}$$

This indicates a linear relationship between friction force and normal load which satisfies the second classic law of friction. Since we said coefficient of friction

$$\mu = \frac{F}{N'}$$

then

$$\mu = \frac{F}{N'} = \frac{\tau_s}{p_m}$$

where both shear strength  $\tau_s$  and mean flow pressure  $p_m$  are bulk properties of the weaker material, and explain classic law four regarding the dependence of friction force upon the nature of the materials in contact.

Two factors which effect the strength of a material and hence  $\tau_s$  and  $p_m$  are temperature and time. It was reasoned, therefore, that the temperature variation of the coefficient of friction should be a critical test between surface roughness and adhesion theories. Since the geometric slope of the asperities is independent of temperature there should be no change in  $\mu$  with temperature according to the surface roughness theory



but since both  $\tau_s$  and  $\rho_m$  are temperature sensitive, a temperature variation of  $\mu$  would be expected by the adhesion theory. Experimental measurements indicate that the temperature variation of  $\mu$  was very similar to the ratio of the variations of  $\tau_s$  and  $\rho_m$ , hence, tending to substantiate the adhesion theory.

If we apply this general theory of friction to the case of friction on ice we have

$$\tau_s \approx 300 \text{ psi}$$

The mean flow pressure  $\rho_m$  is often taken as 1.1 Y where Y = yield stress or proportional limit of the material. In the case of ice, the elastic limit has been reported as lying between 7 and 14 psi. These values are low and in conflict with the assumption of ice as an elastic medium with elastic behavior up to the yield point and with a tensile strength of about 200 psi. Some justification lies in the belief that these reported values of 7-14 psi are but the limits of proportionality and that the elastic limit must be higher. However, as an approximation, if we assume

$$\tau_s = 300 \text{ psi}$$

$$\rho_m = 14 \text{ psi}$$

Then

$$\mu = \frac{\tau_s}{\rho_m} = 21.4$$

This calculated value is much higher than experimentally obtained values.

The lower actual values of friction on ice could indicate error in the measurement of  $\tau_s$  and  $\rho_m$  or, as is more reasonable, indicate the presence of an





intermediate lubricating fluid. The mechanism by which this lubricating fluid - water - was formed or converted from ice was not, however, easily explained.

(96)

In the 19th century Thompson presented papers regarding the possibility of ice melting due to the lowering of the melting temperature by the application of pressure. Reynolds, in 1901, supported this theory by noting that several investigators had experimentally found a decrease in the slipperiness of ice at low temperatures. Reynolds interpreted this fact as indicating insufficient pressure available to lower the melting point to the low ambient temperature. Quantitatively, however, it must be noted that approximately 100 atmospheres of pressure are required to lower the melting temperature by 1° C. The tremendous pressure necessary to supply this melting temperature depression places the pressure melting mechanism in doubt as the source of lubricant supply. As regards Reynolds observation of temperature dependency, in the case of sea ice, it can be attributed to the precipitation of solid salts at the lower temperatures as explained by ASSUR in 1958.

(96)

Bowden and Hughes agreed that water must be the lubricant but felt that its formation was the result of frictional heating of the ice-slider interface. Depending upon the relative thermal conductivity of the slider and ice, part of the frictional heat is lost to the slider and part is used in melting ice. Thus, theoretically, the coefficient of friction between BRASS and ice should be greater than between ebonite and ice. Experiments substantiated this fact. In 1947, however, this theory was cast in doubt. It



was reasoned that if this heat melting theory were true, direct heating of the sliding runners would facilitate melting and further reduce friction. Experimental results did not show the expected frictional reduction.

<sup>(96)</sup>  
Bell in 1948 also questioned this friction melting theory and proposed instead a plastic flow theory in which pressure and frictional heat caused increased plasticity of the solid ice surface, rather than a complete phase change to liquid. However, work of Nakaga and Matsumato in 1953 <sup>(126)</sup> shows experimental evidence of the existence of a liquid water film on ice surfaces below temperature of 0° C. This liquid film is supposedly present at all times and is not supercooled water, but rather, water in equilibrium with its vapor phase on one side and with ice crystals on the other. What effect this film has on frictional resistance or whether it is the one theorized to have been due to pressure or frictional heat is not known, however, despite Bell's contention of plastic flow, and the inability to conclusively demonstrate experimentally the pressure or friction heating theories, it does seem pretty conclusive that what lubrication does occur during sliding on ice is due to an interposed liquid film.

Despite all the theories, and published experimental results, very little actual reliable data exists on the static and dynamic coefficients of friction of steel on ice. The variation of these coefficients with temperature, though recognized, has not been determined with any degree of reliability. The effect of normal loading is also elusive. Previously we



stated that the real area of contact could be represented as

$$A_r = \frac{N'}{p_m}$$

which indicates that it is independent of apparent area of contact as measured by standard geometric means and directly proportional to the first power of the normal applied load. This is in agreement with the first two classic laws of friction but is only applicable for a low ratio of loading to mean flow pressure. At higher ratios of loading to mean flow pressure, the real area of contact is an appreciable portion of the apparent area. Since the real area cannot exceed the apparent area, the ratio  $A_r/A_a$  must approach a limit of unity at extreme loads and may be expressed analytically as

$$\frac{A_r}{A_a} = 1 - e^{-BN'}$$

where B is a constant

hence as

$$\begin{array}{ll} N' \rightarrow 0 & A_r \rightarrow 0 \\ N' \rightarrow \infty & A_r \rightarrow A_a \end{array}$$

In addition, for low values of normal load the expression

$$e^{-BN'} \approx 1 - BN'$$

Therefore

$$\frac{A_r}{A_a} = 1 - (1 - BN') = BN'$$

and real area is a linear function of normal load as required by the second





classic law of friction. In this instance of low normal load

$$B = \frac{A_r}{A_n} \times \frac{1}{N'}$$

but

$$A_r = \frac{N'}{P_m}$$

Therefore

$$B = \frac{1}{A_n P_m}$$

Now this real area - load relation is recognized but has not, unfortunately, been confirmed experimentally over the entire loading range. Reliable determination of  $P_m$  at low normal loads and of the constant  $B$  at higher loadings are lacking. Hence, though we recognize the effect of normal loadings as it effects real contact area and hence friction coefficients, our expressions still require reliable experimental verification.

In addition, it is known that a snow cover will materially effect the coefficients of dynamic and static friction. However, since it has been shown that the effect is dependent upon the type of snow cover, water content, temperature, normal load and velocity, what data does exist on the effect of snow on friction, is unreliable and difficult to use.

Consequently, for the ship problem we must attempt to select those values of coefficients of friction which appear to be most reliable and consistent with published experimental results. It must be kept in mind, however, that the values are only representative and not necessarily applicable to all engineering situations. For the case of the ship problem, the most representative values are those published by Arnold and Alabrieff (1938) which are given





for polar salt water ice as

coefficient of static friction	0.30 to 0.50
--------------------------------	--------------

coefficient of dynamic friction	0.10 to 0.20
---------------------------------	--------------



## Part 4

### The Tensile Strength of Sea Ice

The most comprehensive study of the strength of sea ice to date is that made by Dr. A. ASSUR of the U. S. Army Snow, Ice and Permafrost Research Establishment in his paper Composition of Sea Ice and its Tensile Strength,  
(80)  
(1958). In this paper, which is partially paraphrased here, Dr. ASSUR attempts to analyze the strength of sea ice in terms of brine content rather than in terms of salinity and temperature as has often been attempted in the past.

The laminar structure of sea ice crystals, shown in figures 4 and 5, where plates of fresh water ice are separated by layers with brine inclusions has been known since the turn of the century. The earliest attempt to study the relation of strength to internal cavities in sea ice is that of Tsunkov (1939) whose relation

$$\sigma' = \sigma_0 \left( 1 - \sqrt{\frac{\alpha}{\pi}} \sqrt{r} \right)$$

where  $\sigma_0$  = strength of ice without pores

$r$  = porosity - internal cavities without ice -

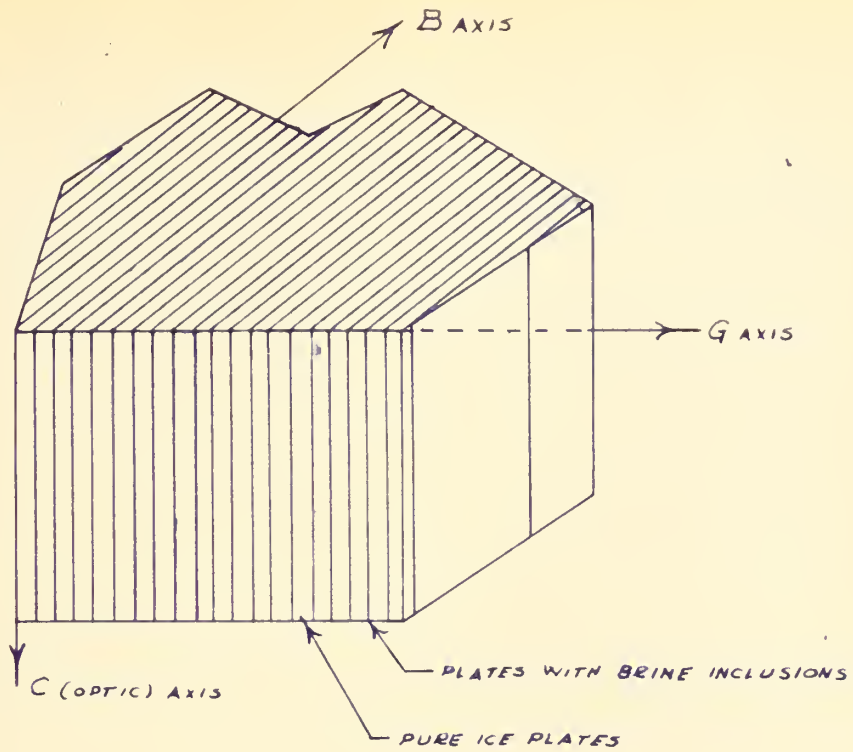
Tsunkov used air content

is based on the assumption of cavities in the form of uninterrupted circular cylinders.

Further progress was made by Weeks and Anderson in their study of the geometry of brine inclusions, leading to the formulation of sea ice strength as

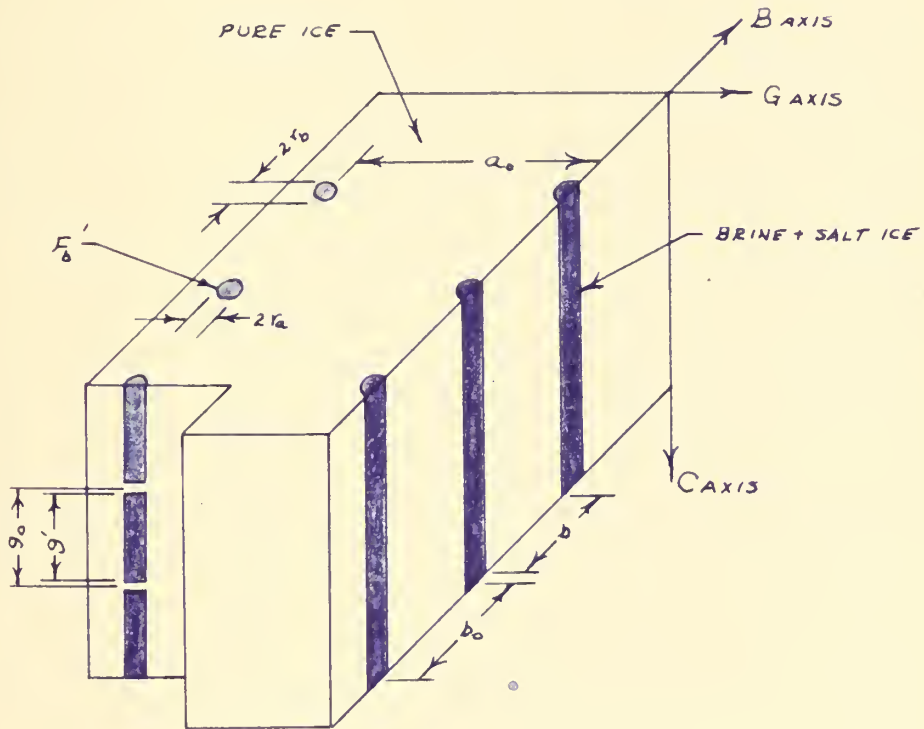
$$\sigma' = \frac{\sigma_0}{K} (1 - \alpha)$$





LAMINAR STRUCTURE OF A SEA ICE CRYSTAL

FIG 4



MODEL OF BRINE INCLUSIONS

• FIG 5



where  $\sigma_f$  = strength of fresh water ice

$K$  = stress concentration factor for brine inclusions

and proposed two models for  $\lambda$  i.e.

$$\lambda = \sqrt{\frac{8\sigma_f}{\pi}}$$

$$\lambda = \frac{0.2116\sigma_f + 0.0011}{0.0322}$$

$$\lambda = \frac{2r_b}{b_0}$$

where  $2r_b$  = width of brine pockets

$b_0$  = spacing of brine pockets

The first of these models is based on the assumption of circular cylinders as was Tsunkov's. The second is elliptical and assumes changes in the brine pocket shape within a plane only.

THIS

The formulation for sea ice strength was a novel approach to sea ice physics in that it is similar to the approach used to compute strength of perforated plates and it does try to explain the known fact that the flexural strength of sea ice measured while in contact with the water is far below that as measured in air in the laboratory. However, this difference in tensile strength between fresh and salt water ice explained in terms of stress concentration factors is not supported by experimental evidence. In addition, neither this nor any previous formulation attempted to explain the more complicated case of reinforcement of the ice due to precipitated salts at low temperatures, i.e. below about  $-8^{\circ}\text{C}$ .

The present development by Dr. Assoe, therefore, is based on the concept of

$$\sigma' = \sigma_0 (1 - \varphi')$$

where





$\sigma'$  = strength of sea ice

$\psi'$  = friction representing the reduction in strength due to brine inclusions

$\sigma_o = C \sigma_f \frac{\sigma(-10)}{\sigma_\phi}$  = basic strength of sea ice computed directly from sea ice data

$\sigma_f$  = strength of fresh water ice

$C$  = coefficient

$\sigma_\phi$  = strength of fresh water ice at given temperature  $\phi$

$\sigma_{(-10)}$  = strength of fresh water ice at a temperature of  $-10^\circ \text{C}$ .

Note the factor  $\frac{\sigma(-10)}{\sigma_\phi}$  is needed in order to reduce the strength of fresh water ice to  $-10^\circ \text{C}$ . so that the effect of temperature upon the strength of fresh water ice bridges (i.e. platlets) in a sea ice crystal need not be considered, and what remains is solely the effect of brine inclusions. The choice of  $-10^\circ \text{C}$ . here is an arbitrary one. It is interesting to note here that for most instances the value of  $C < 1$ . This can be explained by the fact that all tests for the strength of fresh water ice are conducted in air, on core samples, by the ring test, i.e. loading a hollow cylindrical core perpendicular to its axis until failure. Now we know that ice in the presence of its liquid phase is weaker than ice tested in air, therefore  $C$  should be less than one since the sea ice has brine inclusions, hence the interstitial liquid weakens the minute ice bridges.

In order to determine  $\psi' = f(r')$  a general three dimensional



geometrical model is developed to account for the effect of brine volume on the ice strength. In order to do this, of course, the brine volume must be determined as a function of temperature and salinity considering the precipitation of salts and numerically deriving the phase relations in sea ice. It is interesting to note the radical effect on sea ice produced by precipitated salts such as  $\text{Na}_2\text{SO}_4 \cdot 10\text{H}_2\text{O}$  and  $\text{NaCl} \cdot 2\text{H}_2\text{O}$

It is because of these salts that we can no longer maintain, as many publications still do, that sea ice is three times weaker than fresh water ice. It is true that sea ice can be weaker, but at low temperatures, i.e. below about  $-8^\circ\text{C}$ ., where these salts begin to precipitate the sea ice can equal or even exceed the strength of the fresh water ice. The present theory, therefore, attempts to explain the wide variations in sea ice strength in terms of brine volume and precipitated salts.

Based on many actual tests it was found that at a given temperature the reduction in strength of sea ice is proportional to  $\sqrt{\text{salinity}}$ . But since brine volume at a given temperature is proportional to salinity then the reduction in strength is proportional to  $\sqrt{v'}$ . Therefore, in the selection of a geometrical model for ice crystals with brine inclusions it seemed desirable to have one which represented the reduction in ice strength due to brine inclusions as a function of  $\sqrt{v'}$ .

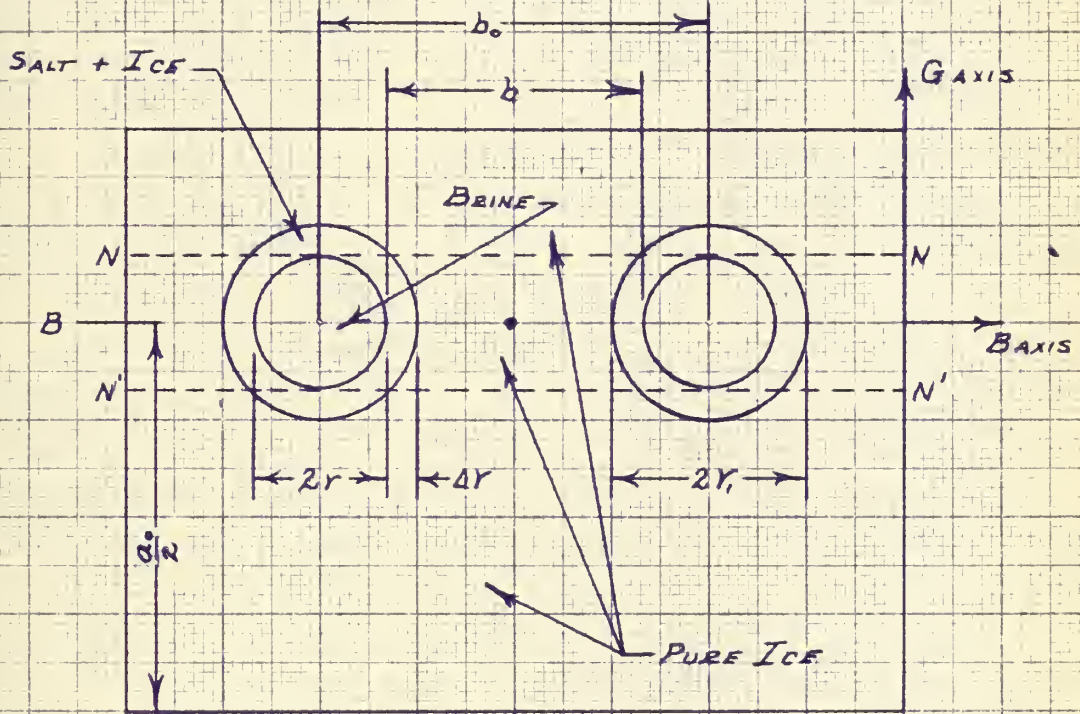
If we introduce the notation as shown on figures 5 & 6

$v'$  = relative volume of brine

$F_b'$  = average area of a brine pocket in the BG plane







MODEL  
OF  
REINFORCED BRINE POCKETS

FIG. 6



$a_o$  = average distance between plates

$b_o$  = average spacing of brine pockets

$g'$  = length of brine cylinders in direction

$g_o$  = average spacing of brine cylinders

Then we may say that

$$v' = \frac{F'_b g'}{a_o b_o g_o} \quad (1)$$

Introducing the dimensionless parameters

$$\gamma_o = \frac{g'}{g_o}$$

$$\beta_o = \frac{b_o}{a_o}$$

equation (1) becomes

$$v' = \frac{\gamma_o}{\beta_o} \frac{F'_b}{a_o} \quad (2)$$

The most convenient way to measure  $F'_b$  is to find the maximum length  $2r_b$  and the maximum width  $2r_a$  of individual brine pockets in the  $B-G$  plane and averaging

$$F'_b = \frac{\pi}{4} (2r_b \cdot 2r_a)$$

under the assumption of an elliptical shape which is a good approximation.

If a tensile stress is applied in the direction of the  $G$  axis, then it acts upon a reduced cross section of

$$v = \frac{2r_b g'}{a_o g_o} = \frac{\gamma_o}{\beta_o} \cdot \frac{2r_b}{a_o} \quad (3)$$





If the basic strength of ice itself is designated as  $\sigma_0$  then the effective strength due to the reduction in cross section becomes

$$\sigma' = \sigma_0 \left( 1 - \frac{\gamma}{\beta_0} \frac{2r_b}{a_0} \right) \quad (4)$$

Now all depends on how  $2r_b$  and  $\gamma$  vary with the brine volume  $v'$

If we assume that the average length and spacing of the brine cylinders and therefore  $\gamma$  stay constant then the changes in brine volume are reflected only in the cross section in the  $\theta-\phi$  plane. If we assume also that this cross sectional shape of the brine pocket stays geometrically similar then all linear dimensions of the brine pocket in the cross section change proportionately to the square root of the brine volume, therefore

$$\sigma' = \sigma_0 (1 - \text{CONSTANT} \sqrt{v'})$$

Based on many tests with actual sea ice this assumption appears most reasonable and does produce a model which satisfies our previous criteria that the ice strength decreases as a function of  $\sqrt{v'}$

If we introduce another non dimensional parameter

$$\beta_0 = \frac{2r_b}{\sqrt{F_b'}}$$

then

$$2r_b = \beta_0 \sqrt{F_b'}$$

and from (3)

$$\sigma' = \frac{\gamma_0 \beta_0}{\beta_0} \frac{\sqrt{F_b'}}{a_0}$$

also from (1) we see that

$$\sqrt{F_b'} = \sqrt{\frac{\beta_0}{\gamma_0}} a_0 \sqrt{v'}$$



so that

$$\gamma' = \gamma_0 \left( 1 - \rho_0 \sqrt{\frac{\gamma_0}{\beta_0}} a_0 \sqrt{r'} \right) \quad (5)$$

Therefore the non-dimensional criteria

$$\rho_2 = \rho_0 \sqrt{\frac{\gamma_0}{\beta_0}}$$

has to be constant if the strength of ice is to reduce proportional to  $\sqrt{r'}$

Now if we consider the brine pockets as elliptical cylinders and let

$\epsilon = \frac{r_b}{r_a}$  be the average ratio of the length of the elliptical brine pockets (in the  $\mathcal{D}$  direction) to the width of the pockets (in the  $\mathcal{G}$  direction), then

$$F_b' = \pi r_b \cdot r_a = \frac{\pi r_b^2}{\epsilon} \quad \text{as before.}$$

Since

$$\rho_0 = \frac{2 r_b}{\sqrt{F_b'}}$$

we have

$$\rho_0 = 2 \sqrt{\epsilon / \pi}$$

Therefore, equation (5) becomes

$$\gamma' = \gamma_0 \left( 1 - 2 \sqrt{\frac{\gamma_0 \epsilon}{\pi \beta_0}} \sqrt{r'} \right) \quad (6)$$

From microstudies of ice crystals, reasonable values of  $\beta_0$ ,  $\gamma_0$

and  $\epsilon$  are determined so that the petrographic constant  $\rho_2$  may be determined

$$\rho_2 = 2 \sqrt{\frac{\gamma_0 \epsilon}{\pi \beta_0}} = 1.5958$$

Therefore

$$\gamma' = \gamma_0 \left( 1 - 1.5958 \sqrt{r'} \right) \quad (7)$$

In order to determine  $\gamma_0$  it was necessary to evaluate the results of a considerable number of ring tests performed on sea ice core samples in



the field so as to obtain the trend in variation of tensile strength as a function of brine volume. This, in essence, proved to be a straight line VARIATION for the region above  $-8.2^{\circ}$  C, (prior to salt precipitation) variation, and since we've shown that

$$\sigma' = \sigma_0 - \sigma_0 \rho_2 \sqrt{v'}$$

we can equate the slope of this straight line variation to  $\sigma_0 \rho_2$  and thus it was determined that

$$\sigma_0 \rho_2 = 22.66 \pm 0.50$$

$$\sigma_0 = 14.20 \pm 0.31 \text{ kg/cm}^2$$

hence

$$\sigma' = 14.20 (1 - 1.57 \sqrt{v'}) \quad (8)$$

for that portion of the sea ice condition above  $-8.2^{\circ}$  C.

The above test results also indicated that as the ice temperature continued to rise a point was reached where the ice strength fell off very rapidly (deterioration - complete loss of strength). For this region, the test results indicated the empirical relationship

$$\sigma_s = \sigma' [1 - 40(v' - 0.09)] \quad (9)$$

As previously mentioned, as the brine volume in sea ice drops - temperature decreases - various salts begin to precipitate out which act to strengthen the ice (i.e. below  $-8.2^{\circ}$  C.). Figure 6 represents a model of reinforced brine pockets. For simplicity, circular pockets are drawn. The initial radius  $r_i$  shows the brine pocket when the salt started to precipitate,  $r$  is the radius after salt is precipitated, but the pockets are not drawn to scale.



If the salt particles together with ice are deposited on the walls of the brine inclusions, there is effective reinforcement at the place of highest stress concentration (in the B-B plane at the walls). The small bubble in the center is a symbol for stress concentration or local defects on the B-B plane.

If Young's modulus of this salt ice mixture does not differ much from its value for ice, all that matters is the reinforcement, which will act as soon as a small amount of salt is precipitated. Since a rapid transition from a high stress concentration to normal stress occurs near the wall, the width of the salt-ice reinforcement does not matter, once a certain minimum value is exceeded. This model holds well for the precipitation of  $\text{Na}_2\text{SO}_4 \cdot 10\text{H}_2\text{O}$  as evidenced by considerable test results. Using a test evaluation procedure similar to that used to determine  $\sigma_0$  we may evaluate  $\sigma'_0$  as

$$\sigma'_0 = 18.74 \pm 0.27 \text{ kg/cm}^2$$

Therefore

$$\sigma' = 18.74 (1 - 1.576 \sqrt{\sigma'}) \quad (10)$$

for the region between  $-8.2^\circ \text{C.}$  to  $-22.9^\circ \text{C.}$  where  $\text{Na}_2\text{SO}_4 \cdot 10\text{H}_2\text{O}$  salt precipitates out. The actual increase in strength, therefore, due to the presence of the salt is

$$\frac{18.74}{14.20} = 1.334 \pm 0.035$$

or an increase of one third.

Now let us consider the strength behavior of ice when  $\text{NaCl}$  precipitates, which it does in much larger quantities than  $\text{Na}_2\text{SO}_4$ . Test results indicate that the presence of  $\text{NaCl}$  (in the form of  $\text{NaCl} \cdot 2\text{H}_2\text{O}$ ) increases the ice strength





appreciably though, it was at first thought, in another manner than does  $\text{Na}_2\text{SO}_4 \cdot 10\text{H}_2\text{O}$ . Later indications seem to indicate however, that the model used for precipitation of  $\text{Na}_2\text{SO}_4 \cdot 10\text{H}_2\text{O}$  also applies to the precipitation of  $\text{NaCl} \cdot 2\text{H}_2\text{O}$  and that the value of  $\delta_s'$  could be evaluated as for the case of  $\text{Na}_2\text{SO}_4 \cdot 10\text{H}_2\text{O}$  (personal correspondence). This produces a value of

$$\delta_s' \approx 23.65 \text{ kg/cm}^3$$

therefore

$$\delta' = 23.65 (1 - 1.576 \sqrt{S'}) \quad (11)$$

for the region below  $-22.90^\circ \text{C}$ . where  $\text{NaCl} \cdot 2\text{H}_2\text{O}$  salt precipitates out. The actual increase in strength, therefore, due to the presence of this salt is

$$\frac{23.65}{19.20} = 1.667$$

or an increase of  $2/3$ .

Having determined the relationship of tensile strength of sea ice as a function of included brine volume, it was necessary to determine the variation of brine volume with temperature so as to be able to show variations in tensile strength of sea ice with temperature.

The only attempt to compute the brine content of sea ice was that reported by Malingren (1933) and Zussov (1945). These attempts had one thing in common, that is, that brine content  $b_r$  is

$$b_r = \frac{S_o}{S_b}$$

where

$S_o$  = salinity of the ice

$S_b$  = salinity of brine

This equation states that all the salts measured in  $S$  are dissolved in the brine inclusions, which is not so, and the correct relationship should be

$$b_r = \frac{S_o - S_s}{S_b}$$



where  $S_s$  = relative amount of solid salts.

The assumption that  $S_s = 0$  is not reasonable nor permissible.

In order to determine the relative brine volume in sea ice, therefore, it was necessary to determine the exact concentration of different ions and salts in sea ice, after the freezing of sea water, as a function of temperature at the salinity of normal sea water so as to determine the phase diagram for sea ice. For given sea ice the values shown in the phase diagram for salts and brine have to be altered in proportion to the salinities, however, from this information it is possible to determine the amounts of precipitated salts as a function of temperature. Where the amount of precipitated salts were computed, the amounts of ions in solution could be determined by subtraction from the initial amounts known to exist in sea water. Once the absolute amount of ions were known, their total was obtained and the relation

$$b_r = \frac{S_o}{S_b}$$

could be applied to obtain the amount of brine. Dividing the amount of brine of 34.325 (the salinity of normal sea water in parts per thousand) gives the amount of brine in standard sea ice of one part per thousand salinity as a function of temperature. Since theoretical densities of sea ice vary little depending on temperature and salinity, an average value of 0.926 was assumed so that the relative brine volume could be computed as strictly proportional to salinity. In this way the variation of relative brine volume could be computed as a function of temperature for a salinity of 1 part per thousand and multiplied by the salinity to get variation with temperature at any other salinity.



Knowing this variation of relative brine volume as a function of temperature for a given salinity, it is possible to apply equations (8), (9), (10) and (11) in order to obtain the variation in tensile strength as a function of temperature. These results are shown in figure 7 for representative salinities met in sea ice. The strength is given in terms of a computed basic strength of  $14.20 \text{ Kg/cm}^2$  (202 psi) equivalent to the tensile strength of an imaginary sample if all the brine pockets are filled with ice. It should be recalled that values shown in figure 7 represent the tensile strength as a function of ice temperature and not ambient air temperature.

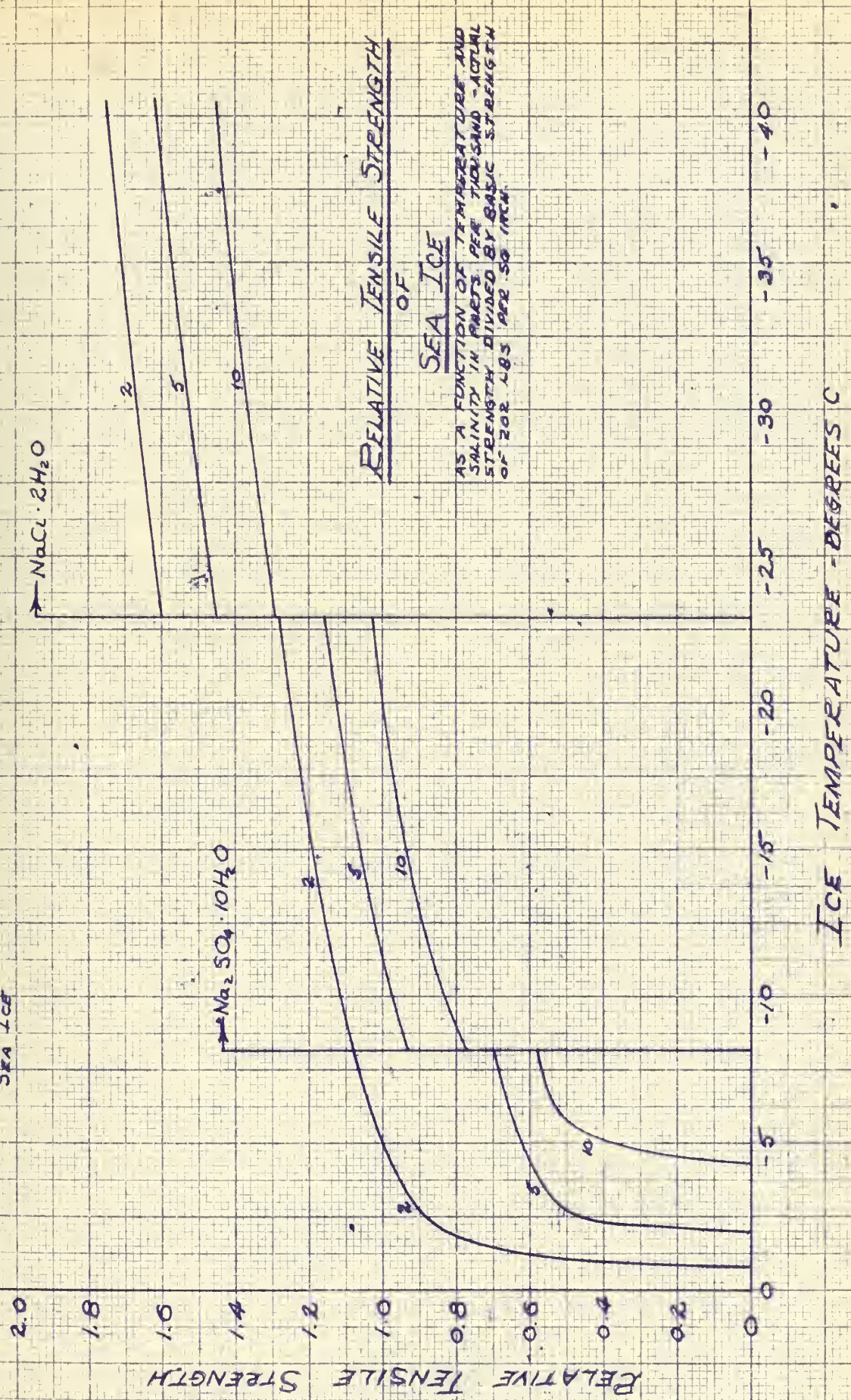
For the portion of figure 7 below  $-8.2^\circ \text{ C.}$  and  $-22.9^\circ \text{ C.}$  the sudden increases in strength is due to the presence of precipitated  $\text{Na}_2\text{SO}_4 \cdot 10\text{H}_2\text{O}$  below  $-8.2^\circ \text{ C.}$  and precipitated  $\text{NaCl} \cdot 2\text{H}_2\text{O}$  below  $-22.9^\circ \text{ C.}$  The presence of these salts, even in small amounts, increases the strength of the ice by one third in the case of the  $\text{Na}_2\text{SO}_4 \cdot 10\text{H}_2\text{O}$  and by two thirds in the case of the  $\text{NaCl} \cdot 2\text{H}_2\text{O}$ . There is very little change in strength with temperatures in this region. Note that although the strength increase is shown to occur instantaneously at  $-8.2^\circ \text{ C.}$  and  $-22.9^\circ \text{ C.}$ , there is in reality a finite transition temperature zone. However, since the mechanics of this transition is complicated and the transition temperature zone small, we may, for practical engineering application, ignore it and consider the transition instantaneous.

In the case of perennial sea ice, it is suspected that a great part of the ENRICHED  $\text{Na}_2\text{SO}_4 \cdot 10\text{H}_2\text{O}$  does not redissolve <sup>ABOVE</sup> ~~about~~  $-8.2^\circ \text{ C.}$  This explains the fact that the strength of perennial ice is about one third above the strength of comparable one season ice even if the effect of salinity





2 - PERENNIAL SEA ICE  
5 - NORMAL ONE SEASON SEA ICE  
10 - FIRST FORMATIONS OF YOUNG SEA ICE



RELATIVE TENSILE STRENGTH  
OF  
SEA ICE

AS A FUNCTION OF TEMPERATURE AND  
SALINITY IN PARTS PER THOUSAND - ACTUAL  
STRENGTH DIVIDED BY BASIC STRENGTH  
OF 200 LBS PER SQ INCH

Fig 7





is considered. Hence the higher values for perennial sea ice in the temperature range of  $-1.3^{\circ}$  C. to  $-8.2^{\circ}$  C. Above  $-1.3^{\circ}$  C. all the  $\text{Na}_2\text{SO}_4 \cdot 10\text{H}_2\text{O}$  goes into solution and the ice strength breaks down completely.

As previously mentioned, the temperature involved in the sea ice strength variation depicted in figure 7 is the ice temperature and not air temperature. Since we wish to use this data to predict icebreaker performance in the preliminary design stage it would be advantageous to be able to convert seasonal air temperature to ice temperatures so as to facilitate use of figure 7. In addition, since for our icebreaker problem we will consider the ice sheet as a semi-infinite flat plate on an elastic foundation which is caused to fail due to bending stresses in the outer fiber, and since we will subsequently show that it is the strength of the top most fiber of the ice sheet which dictates its breaking we can see that we are really interested in the ice surface temperature for application to figure 7. Doctor Assel in a subsequent work (Unpublished - personal correspondence) has developed a relationship between ice surface temperature and air temperature which is ideal for our problem here. This relationship is given for conditions of negative air temperature as

$$\theta_o = \alpha_o (\theta_a - \theta_w) \frac{h}{h + 5.1 h_s} + 0.1 \quad ^{\circ}\text{C} \quad (12)$$

where

- $\theta_o$  = temperature at the interface between ice and snow
- $\theta_a$  = air temperature ( $^{\circ}\text{C}.$ ) averaged over a number of days  
 depending on  $\frac{h + 5.1 h_s}{h + 5.1 h_s}$ . For  $\frac{h + 5.1 h_s}{h + 5.1 h_s} = 60$  it is  
 4 days.



$\theta_w$  = water temperature ( $^{\circ}\text{C}.$ ) which is dependent upon salinity but can usually be taken as  $-0.17^{\circ}\text{C}.$

$\alpha'_0$  = constant dependent upon location of ice. For  $\theta_a$  measured at a shore station  $\alpha'_0 = 0.84$ . For  $\theta_a$  measured above the ice sheet as for an icebreaker  $\alpha'_0 \approx 0.80$

$h$  = ice thickness - cm

$h_s$  = snow depth - cm

$s_i$  = relative insulation of snow versus ice.  $s_i$  is 5 to 6 for normal conditions in the arctic, 4 to 5 under extreme cold for wind-swept snow, 8 to 12 for old snow and 12-19 for a normal snow cover during the winter in moderate latitudes.

$b'$  = a temperature value which is about  $\pm 1.0^{\circ}\text{C}.$  in the middle of the winter, increasing during cooling periods and decreasing during warming periods. During late winter  $b'$  decreases to about  $-0.4^{\circ}\text{C}.$

For the purpose of the paper, however, we shall not consider the effect of a snow cover since so little is known of its effect on ice <sup>FRICITION</sup> function, its compressive strength, etc. Consequently, we shall consider ice as without a snow cover, hence  $h_s = 0$  and our expression above becomes

$$\theta_0 = \alpha'_0 (\theta_a - \theta_w) + b' \quad ^{\circ}\text{C} \quad (13)$$

Now assuming the values suggested by Dr. Assur for  $\alpha'_0$  and  $b'$  and using

$\theta_w = -0.17$  we have

$$\theta_0 = (0.86 \theta_a + 0.11) - 0.4 \quad ^{\circ}\text{C} \quad (14)$$



Now it is true that there is some question as to the choice of  $b'$ . However, since the modern arctic icebreaker attempts to get through the ice as soon as is possible at the close of winter it seems logical to use that value for  $b'$  which is characteristic of late winter. It should be reiterated that the above expression does not hold for positive air temperatures and breaks down, in general, in late spring. It is desired, however, that our icebreaker be capable of penetrating the ice as early in the season as possible, preferably no later than early spring. Consequently, temperature conditions in the Arctic and Antarctic during this time will be such as to make expression (14) applicable.

As a guide to the mean air temperature conditions existing in the Arctic and Antarctic during various months of the year, table 1 and 2 show representative mean temperatures experienced at various stations throughout the year.



## Mean Maximum and Minimum Temperatures °F.

TABLE 1  
ANTARCTICA

		Argentine Islands	Cape Adare	Cape Denison	Debenham Islands	Fromheim
		LAT 65-15S	71-18S	67-00S	68-08S	78-38S
		LONG 64-16W	170-09E	142-40E	67-06W	163-37W
JAN	MAX	39	37	34	39	27
	MIN	31	30	26	30	1
FEB	MAX	-	-	29	36	-
	MIN	-	-	21	27	-
MAR	MAX	36	22	18	34	-
	MIN	28	14	10	25	-
APR	MAX	30	16	6	30	12
	MIN	23	5	-2	20	-54
MAY	MAX	28	3	6	14	- 4
	MIN	21	-11	-2	1	-59
JUNE	MAX	27	- 5	3	10	13
	MIN	21	-19	-3	-10	-73
JULY	MAX	18	- 1	0	18	9
	MIN	7	-18	-8	-6	-66
AUG	MAX	5	- 4	6	17	-12
	MIN	-7	-23	- 3	-5	-74
SEPT	MAX	18	- 4	4	25	15
	MIN	5	-19	-6	13	-64
OCT	MAX	30	5	8	-	16
	MIN	22	-11	-3	19	-40
NOV	MAX	32	24	22	36	23
	MIN	23	9	21	26	-18
DEC	MAX	36	36	31	40	32
	MIN	30	27	23	29	2

Weather Data for the Antarctic





GAUSS	Laurie Island	Little America	Port Charcot	Port Circoncision	Water Boat Point
66-02S	60-45S	78-34S	65-03S	65-10S	64-48S
89-54E	44-43W	163-56W	64-00W	64-12W	62-43W
34	42	31	35	38	50
24	24	18	30	33	27
30	43	11	36	38	49
22	24	-19	27	31	25
23	43	21	37	38	42
10	18	-45	23	30	20
10	40	10	36	27	47
-3	6	-49	10	19	20
11	37	17	29	27	38
1	-8	-58	-3	19	4
8	35	20	32	26	38
-9	-18	-49	-10	15	14
-3	37	-9	31	28	39
-14	-20	-62	- 4	15	-16
6	38	- 4	32	27	35
- 7	-14	-62	16	16	2
16	41	8	32	34	36
0	- 3	-38	2	20	14
24	40	18	34	38	42
12	14	-26	23	23	13
33	41	30	34	-	48
24	22	7	27	-	27

TABLE 1 (Cont.)



Mean Temperature °F.

ARCTIC AREA

	Adak	Attu Attie	Barter Island	Dutch Harbor	Galena	Kodiak
LAT	51-57N	52-54N	70-80N	53-54N	64-48N	57-48N
LONG	176-36W	173-20E	143-50W	166-32W	156-54W	152-24W
JAN	31	31	-15	32	- 5	30
FEB	32	29	-10	32	-12	32
MAR	33	31	-12	34	11	33
APR	37	34	5	36	21	37
MAY	40	39	19	41	41	43
JUNE	44	43	33	46	55	50
JULY	49	51	41	51	60	54
AUG	51	53	38	53	54	55
SEPT	48	47	28	49	44	50
OCT	42	42	13	42	26	42
NOV	37	36	1	37	4	35
DEC	33	31	-15	33	-10	31

WEATHER DATA FOR THE ARCTIC

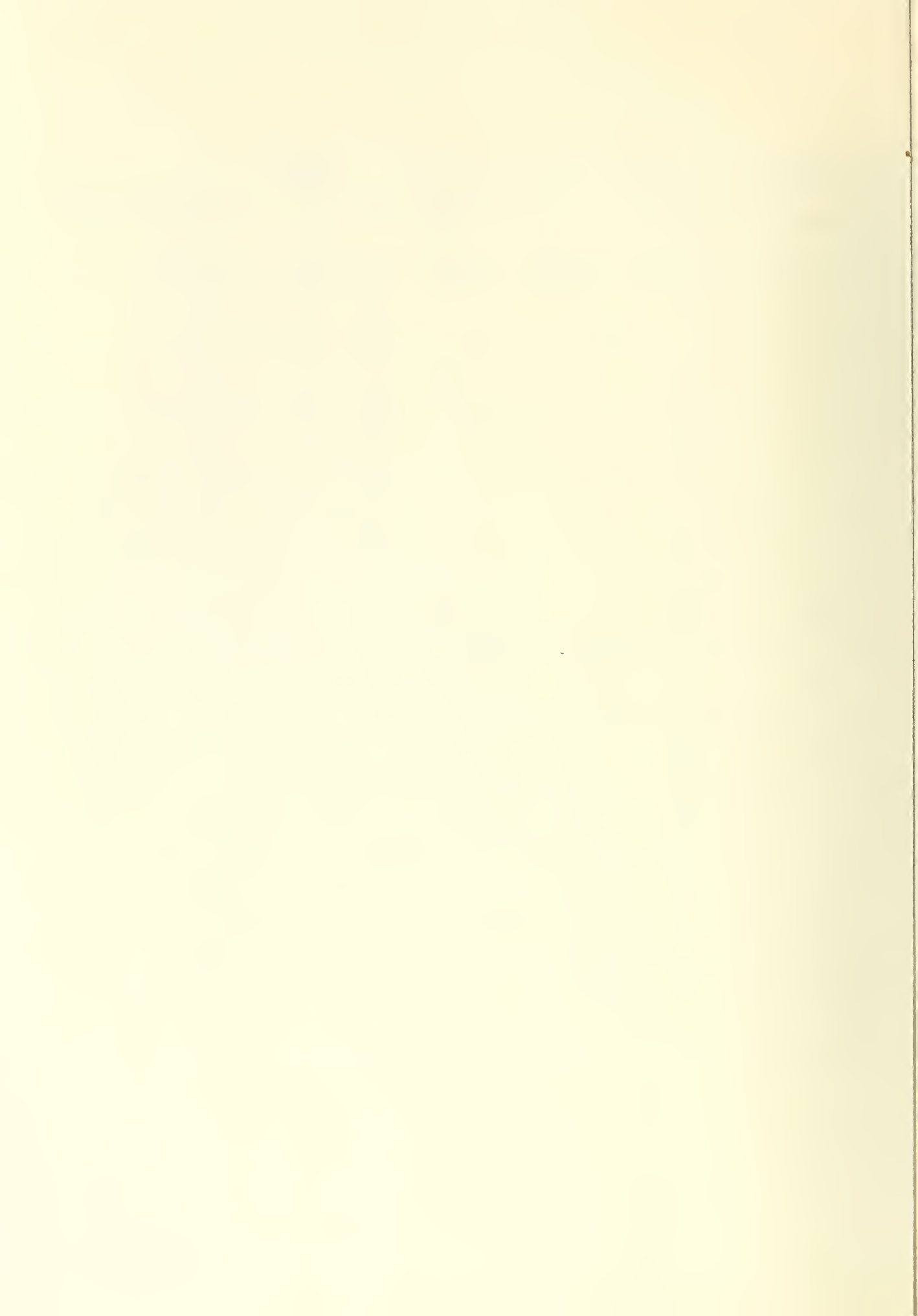


TABLE 2 (CONT)

Wales	Arctic Bay	Churchill	Clyde River	Coral Harbor	Isachsen	Mould Bay	Pangnirtung
65-37N	73-00N	58-47N	70-25N	64-11N	78-47N	76-16N	66-09N
168-03W	85-18W	94-11W	68-17W	83-17W	103-32W	119-50W	65-30W
0	-21	-19	-16	-25	-37	-32	-16
0	-27	-17	-19	-21	-33	-31	-16
-3	-16	- 6	-13	-13	-26	-21	- 7
13	- 4	14	- 2	1	-20	-11	8
26	19	30	19	19	10	12	25
37	36	43	34	35	30	30	37
46	44	54	41	46	38	38	45
45	42	52	40	46	33	34	44
40	30	42	32	33	16	19	37
30	15	27	21	19	- 5	- 2	25
18	- 4	6	4	8	-22	-16	11
4	-16	-11	-11	-12	-31	-26	- 8

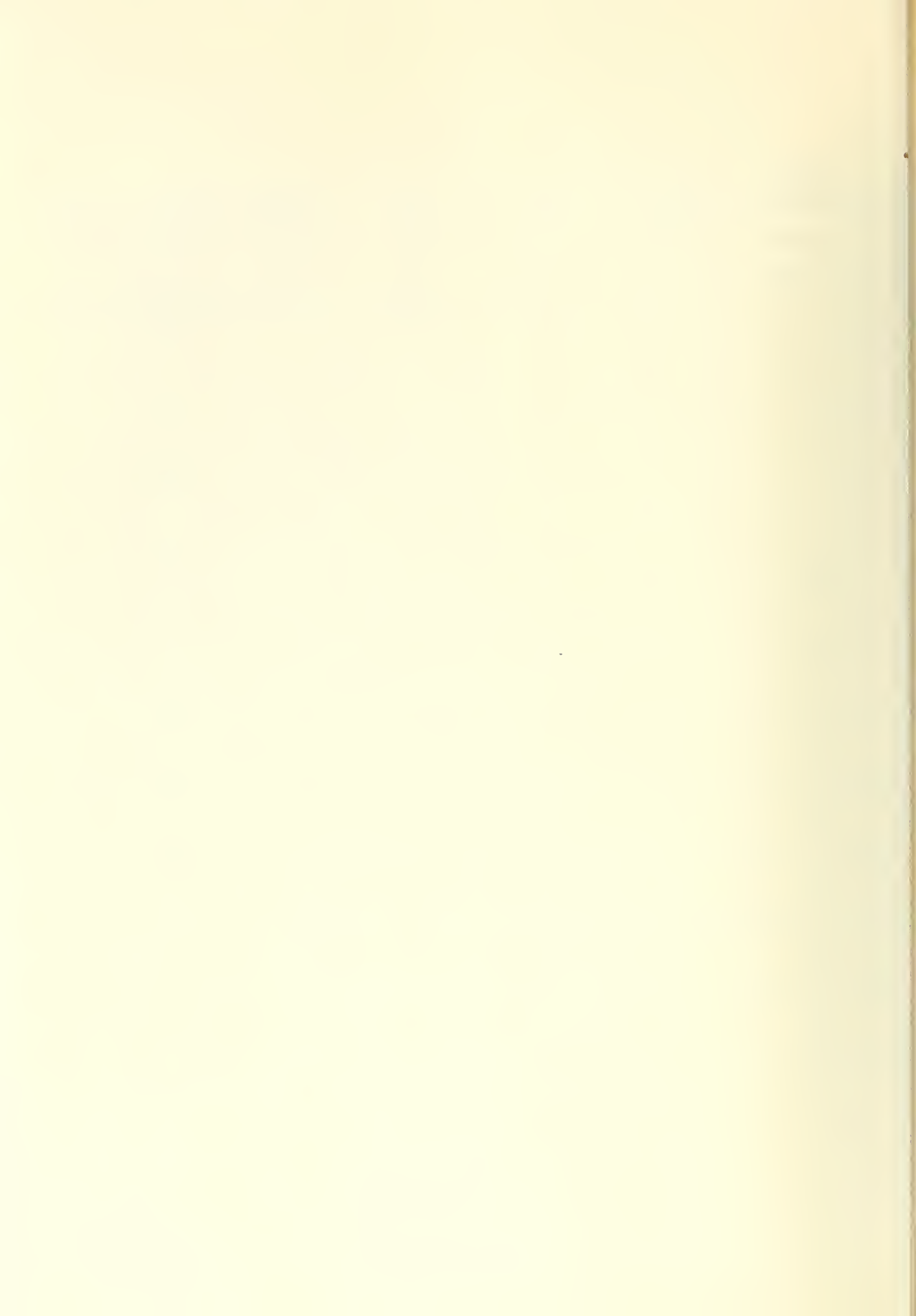


Angmagss- alik	Godthaab	Ivigtest	Scoresby Sound	Upernavik	Stykkis- holmur	Petsame	Utsjoki
55-37N	64-11N	61-12N	70-30N	72-47N	65-05N	69-33N	70-05N
57-33W	51-43W	48-10W	23-00W	56-07	22-46W	31-13E	27-52E
17	14	19	1	- 7	29	18	10
14	14	19	2	-10	28	10	11
18	19	24	2	- 7	28	17	16
24	25	31	10	7	33	29	24
33	33	40	24	25	40	39	34
41	40	46	35	35	47	48	45
44	44	50	40	41	50	56	52
42	43	47	38	41	49	53	50
37	38	41	32	33	45	43	42
30	31	34	19	25	39	34	30
23	24	27	9	15	33	28	19
19	18	21	4	2	29	20	13



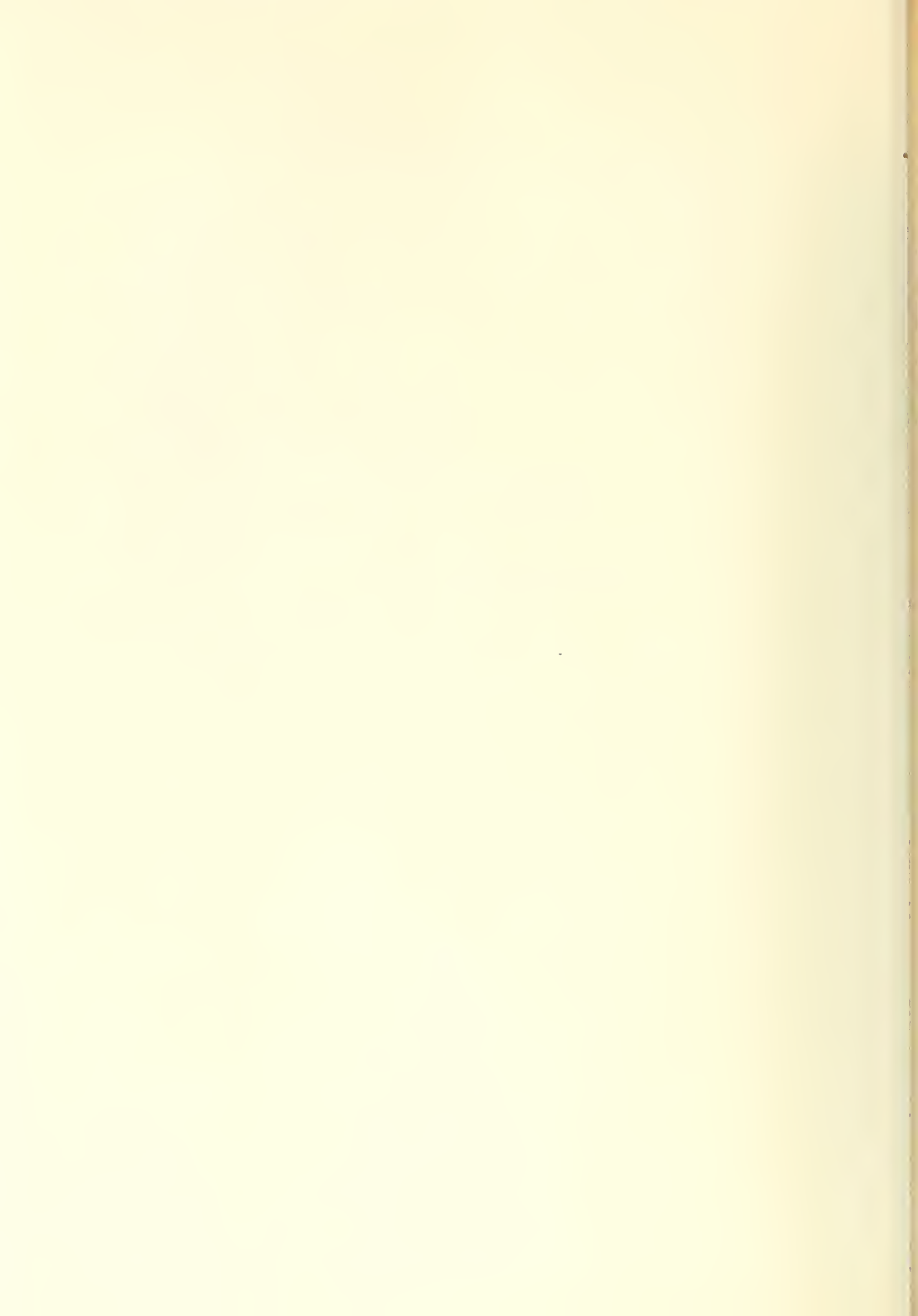


Bear Island	Green Harbor	Jan Wagen	Vardo	Anadyr	Cape Deznev	Cape Shmidt	Wrangel Island
74-28N	78-02N	70-59N	70-22N	64-47N	66-02N	68-55N	70-58N
19-17E	14-15E	8-18E	31-06E	177-34E	169-52W	179-29E	178-23W
18	3	23	22	-10	- 7	-20	-11
17	-3	22	21	- 8	-10	-15	-13
15	-2	21	23	- 5	- 2	-10	- 10
19	8	25	29	7	9	- 4	1
28	23	30	35	24	22	18	17
35	36	26	42	40	35	34	33
40	42	41	48	51	42	39	37
39	40	42	48	50	41	37	35
36	32	38	43	39	36	30	29
30	22	32	35	23	24	17	18
23	11	27	28	6	9	- 1	4
20	6	23	24	-6	1	- 8	-5



Section E

Icebreaker Powering



## Part 1

### Icebreaker Propulsion Machinery

The selection of main propulsion machinery for icebreaking vessels is completely governed by the severe requirements of ice breaking service and the long range operation it requires. The need is for a propulsion plant which is extremely reliable, rugged and capable of withstanding the frequent and often extended periods during which the propeller and shafting are subjected to serious and sudden shock from both solid and broken ice.

When breaking a channel through an ice field or forcing a lead, the propellers often operate at bellard condition while at the same time often sustaining hard serious contact with pieces of solid ice forced into the propeller stream by the ice breaking action of the bow. While operating against heavy pack ice, the engines are continuously reversed rapidly in order to allow the continuous maneuvering necessary to keep the vessel from becoming beset and to augment the rudder in forcing a straight channel through the ice. The plant must be capable of developing maximum thrust (hence maximum power) at zero speed of advance, requiring the development of practically full power at reduced shaft RPM. In addition, due to the nature of icebreaking, the propulsive system must be amenable to direct, positive and simple control from the bridge.

Few kinds of propulsion machinery offer the degree of flexibility, ruggedness and reliability required for this icebreaking service. Reciprocating steam engines have been successfully used in the past while Diesel

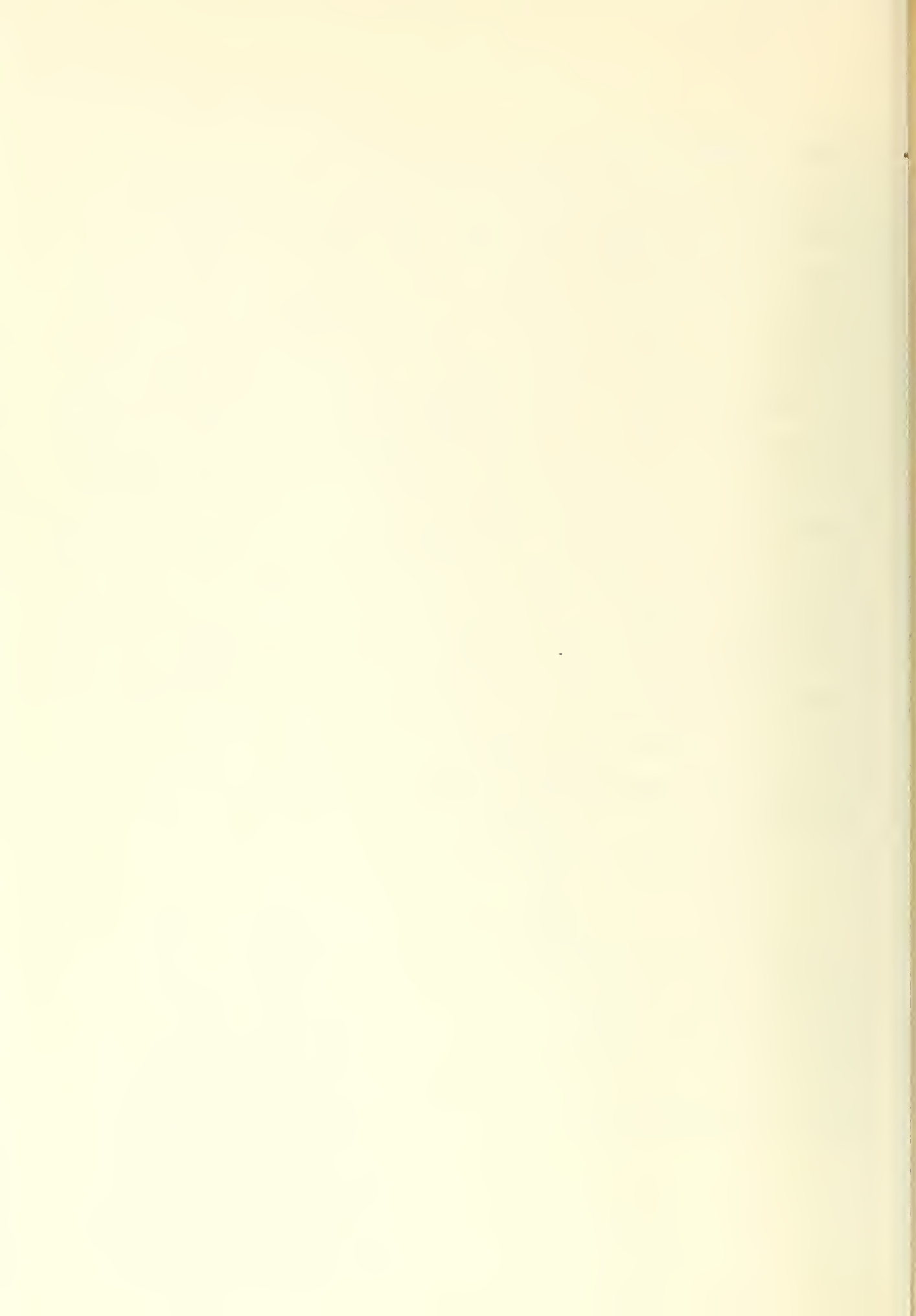


Electric systems are most often the choice for present day applications. Both types of plants offer the necessary characteristics of high continuous torque over a wide range of shaft RPM. Each system has its inherent advantages, and although steam is seldom used on modern day arctic icebreakers, it must be stated that this type of machinery has an excellent record of ice breaking performance in the many vessels in which it has been used. Among the advantages enjoyed by a reciprocating steam plant when in comparison with a Diesel Electric unit are: lower first cost, lower maintenance cost, a requirement for less qualified personnel and the fact that the plant is reliable and simple to operate. Among the disadvantages may be listed higher total plant weight, higher weight of fuel and water, greater plant space required, less flexibility in a multiscrew multiple engine installation and a larger margin of excess fuel capacity required for any given cruising range during which icebreaking work is anticipated due to the greatly increased specific fuel consumption when breaking ice. It should be noted that for a comparable normal 15000/16500 SHP installation, the estimated all purpose fuel consumption for the two type plants is:

Diesel Electric - 0.50 lb. at full power

Steam - 0.86 lb. at full power for a 440 psi plant

Admittedly, there are many points in favor of the steam plant installation. The present trend, however, is towards a greater general adaption of Diesel Electric propulsion. The most important reason for this trend in icebreaking vessels is the lower fuel consumption and correspondingly larger cruising radius. For arctic breakers, the multiplicity of power generation units is an





advantage since it is possible to cruise at lower speeds with the engines operating at <sup>their</sup> ~~the~~ maximum efficiency. Future developments may, of course, reverse this present trend. The adaption of nuclear power to icebreaker power plants may well be the greatest stimulus yet foreseen. Fuel consumption would no longer be a controlling factor since the use of nuclear power would allow continuous icebreaking operation for prolonged periods of time. Furthermore, the fears of being beset by pack ice for the winter period will no longer plague operating personnel, since there would be no problem of fuel shortage to force drastic reductions in heating and other auxiliary functions, and the vessel could become fully operational as soon as ice conditions permitted. It must be noted, however, that even if nuclear power made a return to steam desirable, the propulsion system would in all probability be of a turboelectric d-c direct drive type. Hence, in reality, the present trend would not really be reversed, but rather, result in a combination of the two systems. However, since only one nuclear icebreaker actually exists (the Russian "Lenin") and since no others are presently contemplated, let us, for the purpose of this paper consider only the Diesel Electric installation.

The Diesel Electric system is essentially a constant power system, though the torque and shaft RPM are still in direct proportion to the horsepower. The design speed for this type unit is that speed at which the propeller has been designed to absorb full horsepower at the highest efficiency. If the brake horsepower of a diesel unit is known, the shaft horsepower may be estimated with an assumed efficiency of 94% for the generator and 92% for the



propulsion motor - hence, an overall efficiency of 86.4%.

For those vessels with bow propellers it is possible by the sacrifice of a relatively small regulating effect to distribute the available total power in an arbitrary proportion between the forward and after screws. Normally, the power is equally distributed amongst all screws, however, when breaking ice, all power may be applied to the after screws. Several existing installations are so flexible that as much as 75% of installed power may be applied to the forward shafts, which is often advantageous when operating in rafted lake or river ice.

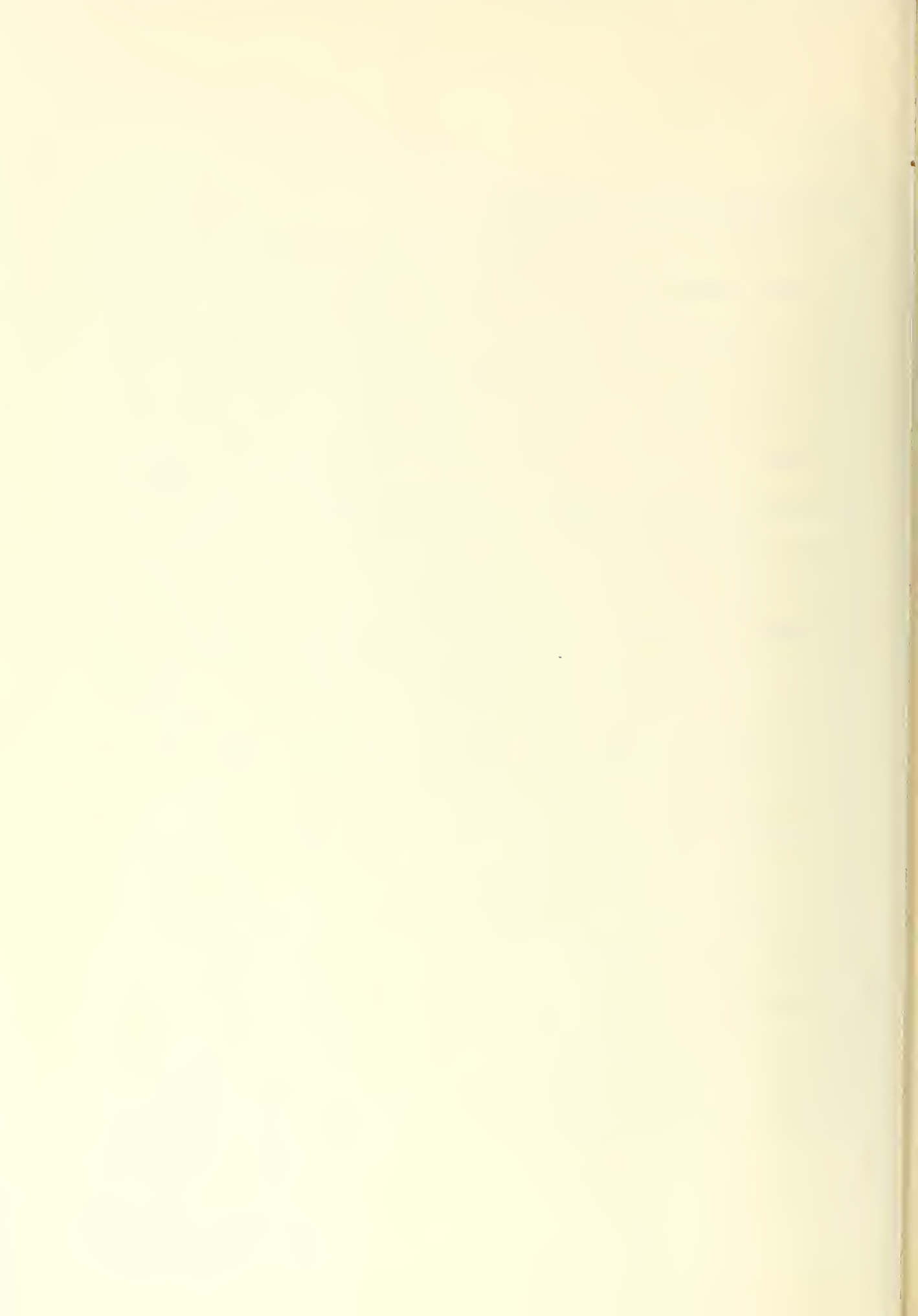
In the arctic icebreaker, bow propellers are seldom installed since service experience has shown that <sup>their</sup> ~~there~~ presence is often a serious disadvantage. Consequently, all power is normally distributed between two after propellers. If a triple screw arrangement is used, half total power is normally applied to the centerline screw and one quarter total power to each of the two outboard screws.



## Part 2

### Propellers and Thrust Predictions

Propellers for use on icebreaking vessels are normally designed so as to develop maximum thrust at a zero speed of advance. Some authorities advocate a somewhat higher design speed, in the vicinity of three to six knots, since it would be desirable to develop maximum thrust at the speed at which an icebreaker normally is able to proceed through one year pack ice. However, as shown by Bridewiser in a thesis entitled The Estimation of Tugboat Tow-  
(98)  
line Pull and Effects of Types of Propelling Systems, the effect of design speed on developed propeller thrust is very small for the diesel electric installation. For example, at a ship speed of three knots the percentage difference between thrust developed for a propeller design speed of 0 knots and 6 knots is only 2.2% and at a ship speed of six knots this percentage difference is only 1%. This very small percentage difference is mainly due to the constant efficiency of the power plant and what little variation that does exist is due to the slight variance in propeller efficiency. Consequently, the propeller design speed is not too vital a criteria<sup>on</sup> when considering the thrust developed at speeds of advance through ice pack. When breaking heavier ice by ramming, however, it is quite easy for the vessel to become stuck due to riding up too far onto the ice sheet. In such an instance it is highly desirable that the propeller develop the maximum possible thrust so that the vessel may extract itself. Heeling tanks are often a great help at such a time in order to break the vessel free from the ice. However, the thrust is still necessary in order to insure the commencement of astern motion. Since a difference in





propeller design speed of from zero to six knots can modify the ballard pull by as much as 11% it would seem logical that a propeller design speed of zero knots is the most desirable for the arctic icebreaking vessel.

The propeller diameter should naturally be chosen as large as possible, however, the propeller should never work below the baseline and at the same time should be so situated that the blade tip will clear the bottom of the ice at all conditions of trim.

Professor Laurens Troost conducted a series of open water tests on modern propeller forms in Holland, the results of which are published in the paper (112) Open Water Test Series with Modern Propeller Forms. From these tests, a series of propellers was arranged and plotted on a new  $\mu - \gamma$  coordinate system which greatly facilitates propeller thrust calculations in the preliminary design stage. The constants involved are:

$$\mu = \frac{N}{60} \sqrt{\frac{\rho D^5}{\phi}}$$

$$\gamma = \frac{T \cdot D}{2\pi \phi}$$

$$\phi = \sigma_a \sqrt{\frac{\rho D^3}{\phi}}$$

In the icebreaking problem, we can determine the force necessary to overcome ice of a given thickness (see section F-2). Since the force which can be developed by an icebreaker at its bow is a function of the propeller thrust available and the kinetic energy developed in ramming, we must know the thrust which may be developed by a well designed propeller so that we may determine





the percentage of thrust developed which is applied to the development of ice breaking force. Consequently, if we consider the Troost data and a propeller design speed of zero knots we may reason as follows:

$$PHP = \frac{2\pi\phi N}{33000} = P$$

where  $P$  = propeller horsepower

$$= \eta_m \times \text{shaft horsepower}$$

$$= \frac{EHP}{\eta_p \eta_r \eta_h}$$

$$\eta_m = \text{mechanical efficiency} \approx 98\%$$

$$\eta_h = \text{hull efficiency} = \left( \frac{1-t}{1-u} \right)$$

$$\eta_p = \text{open water screw efficiency}$$

$$\eta_r = \text{relative rotative efficiency}$$

Therefore

$$N = \frac{33000P}{2\pi\phi}$$

also

$$\mu = \frac{N}{60} \sqrt{\frac{P D^5}{\phi}}$$

Therefore

$$\mu = \frac{33000P}{120\pi\phi} \sqrt{\frac{P D^5}{\phi}}$$

and

$$\phi^{3/2} = \frac{33000P}{120\pi\mu} \sqrt{P D^5} \quad (31)$$

In addition

$$\delta = \frac{T'D}{2\pi\phi}$$

Therefore

$$\phi^{3/2} = \left( \frac{T'D}{2\pi\delta} \right)^{3/2} \quad (32)$$

If we equate (31) and (32) we obtain

$$T' = \left( 275 \sqrt{P \pi \phi} \right)^{2/3} P^{2/3} D^{2/3} = \frac{\delta}{4^{2/3}}$$



If for the density of sea water at approximately  $29^{\circ}$  F. (when in equilibrium with sea ice) we assume

$$\rho = 1.925 \frac{\text{lb}}{\text{ft}^3}$$

Then

$$T' = 156 (\rho D)^{2/3} \frac{\gamma}{4^{1/3}}$$

Now in the ballard condition it is found that the thrust deduction value drops to almost zero. If  $F_0$  is the towrope pull and  $T_0$  the propeller thrust in this zero ship-speed condition, it is mostly found in model experiments as well as in full scale tests that for single screw vessels

$$t = 1 - \frac{F_0}{T} \approx 0.035$$

Theoretically this should be zero, but the propeller sets up a flow around the stern such that the zero value is not quite attained. Hence the towrope pull obtained at zero speed is not equal to the thrust developed, but rather, must be modified to account for the above phenomenon<sup>on</sup>. Since this thrust deduction is a function of water column flow along the hull we may assume without too much error that for a twin screw vessel the value is one half that of a single screw vessel, hence

$$t = 1 - \frac{F_0}{T} \approx 0.0175$$

Therefore, because of this small remaining thrust deduction factor, the ballard pull becomes

$$T' = (0.9825) (156 \rho^{2/3} D^{2/3} \frac{\gamma}{4^{1/3}})$$

$$T' = 153.3 \rho^{2/3} D^{2/3} \frac{\gamma}{4^{1/3}} \quad (33)$$

Therefore, for a given  $P$  and  $D$ ,  $T^1$  is proportional to  $\frac{\gamma}{4^{1/3}}$  and the highest



values for thrust  $T^1$  will be found on the  $\mu - \delta$  diagram for that part of the line

$$\phi = \sqrt{a} \left( P \frac{D^3}{Q} \right)^{1/2} = 0$$

where  $\delta / \mu^{2/3}$  is a maximum.

Then since

$$\mu = \frac{N}{80} \sqrt{\frac{D^3}{Q}} \quad \text{and} \quad Q = \frac{33000 P}{2\pi N}$$

we may determine the corresponding propeller RPM by substitution as

$$N = 213.5 \left( \frac{\mu^2 P}{D^3} \right)^{1/3} \quad (34)$$

In our icebreaker problem, however, we are interested not only in the thrust developed at zero speed, but also at various other speeds. As previously stated, for the diesel electric unit the power is constant (PHP = const). In addition, a large amount of testing has indicated pretty definitely that changes in local pitch from root to tip do not seem to have a marked effect on total propeller efficiency, and that it is the pitch at about 0.7 radius that governs the blade efficiency, provided that the pitch changes at root and tip are not extreme, thus giving negative or extremely high angles of <sup>INCIDENCE</sup> ~~incidence~~. Consequently, for our analysis, it is sufficient to assume a constant pitch propeller, feeling assured that the results will apply equally well to a variable pitch blade. Therefore, the value of  $P_0/D$  obtained from the  $\mu - \delta$  diagram for the point of maximum  $\delta / \mu^{2/3}$  is constant also. Hence, since

$$PHP = \frac{2\pi Q N}{33000} = P$$

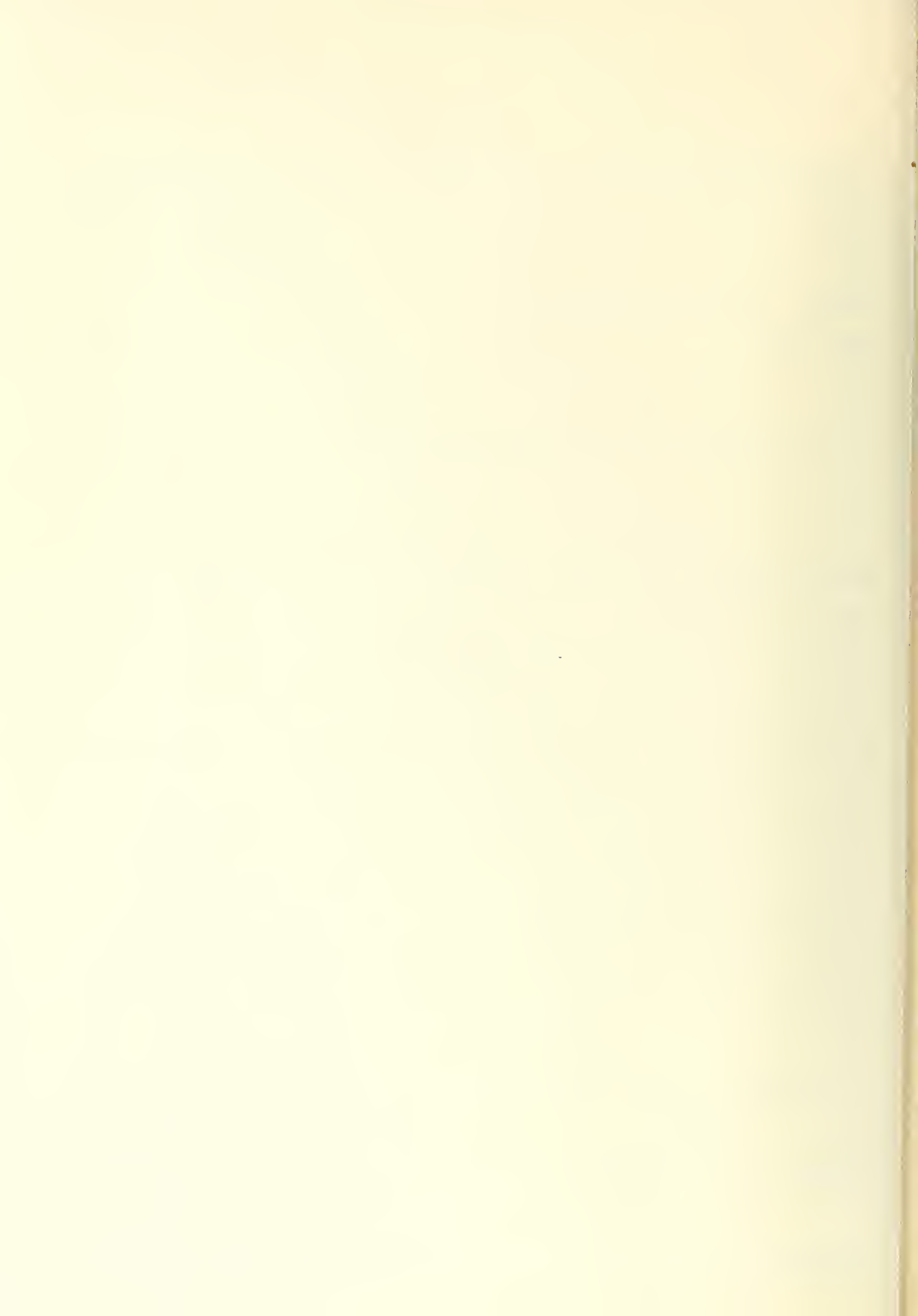
if we assume values of  $N$  we can calculate corresponding values of  $Q$  since

$$Q = \frac{33000 P}{2\pi N}$$

Knowing  $Q$ , we can determine  $\mu$  since

$$\mu = \frac{N}{80} \sqrt{\frac{D^3}{Q}}$$

Therefore, with values of  $\mu$  and  $P_0/D$  we can enter the  $\mu - \delta$  DIAGRAM



and pick off values of  $\delta$  and  $\phi$ . With these values we may determine propeller thrust as

$$\delta = \frac{T' D}{2 \pi \phi}$$

$$\therefore T' = \frac{2 \pi \phi \delta}{D}$$

(35)

at a corresponding vessel speed determined by

$$\phi = v_a \sqrt{100^3 / \phi}$$

$$\therefore v = \frac{\phi}{100} \sqrt{\frac{\phi}{100^3}} \quad \text{ft/sec.}$$

$$V = 1.542 \frac{\phi}{100} \sqrt{\frac{\phi}{100^3}}$$

knots

(36)

Very little information exists as to the wake fraction of ice breaking vessels. Dr. Jansson, in his paper on ice breaker design lists average values of 0.14 and 0.18 for two models which he tested and which had stern propellers only. Nordstrom, Edstrand and Lindgren in their paper Model Tests with Ice-breakers reporting work done at the Swedish State Tank, list values of from 0.123 to 0.105 covering a speed range from 9 to 14 knots for models which were designed with a bow propeller but which had the bow propeller removed and a dummy boss and cove substituted. Model tests at the David Taylor Model Basin for several classes of coast guard icebreakers list a value of 0.235 for the wind class breakers, 0.207 for the <sup>MACKINAW</sup> ~~Ulickman~~, 0.205 for the Cactus class and 0.200 for the Glacier. In the case of the wind class and the Mackinaw, each was built with three screws, one forward and two aft (wind class later modified to remove the bow propeller and replace it with a blank covering) and since the values given for wake fraction for these vessels did not specify the status





of the forward screw, and since the presence of a bow screw materially alters the wake fraction of the stern screws, these listed values are not too reliable. In addition, it is known that the wake fraction varies slightly with speed over the normal operating speed range, but at the lower speeds, as the bellard condition is approached, this wake fraction varies more radically. Unfortunately, little if any information exists concerning the variation of wake fraction at these lower speeds. Consequently, for the purposes of preliminary design, we must be satisfied with the selection of a single representative value of wake fraction, which we must assume to apply throughout the entire speed range of operation. This, of course, admits to a certain inherent error, however, until such time as accurate test data does exist we must content ourselves with the fact that the error is constant and allows reasonable prediction of vessel performance. In this paper, since we are considering solely the case of the twin screw icebreaker without bow propeller, and since it is best to overestimate the value of this wake fraction, when it cannot be determined accurately, we shall therefore assume

$$\omega = 0.18$$

Therefore

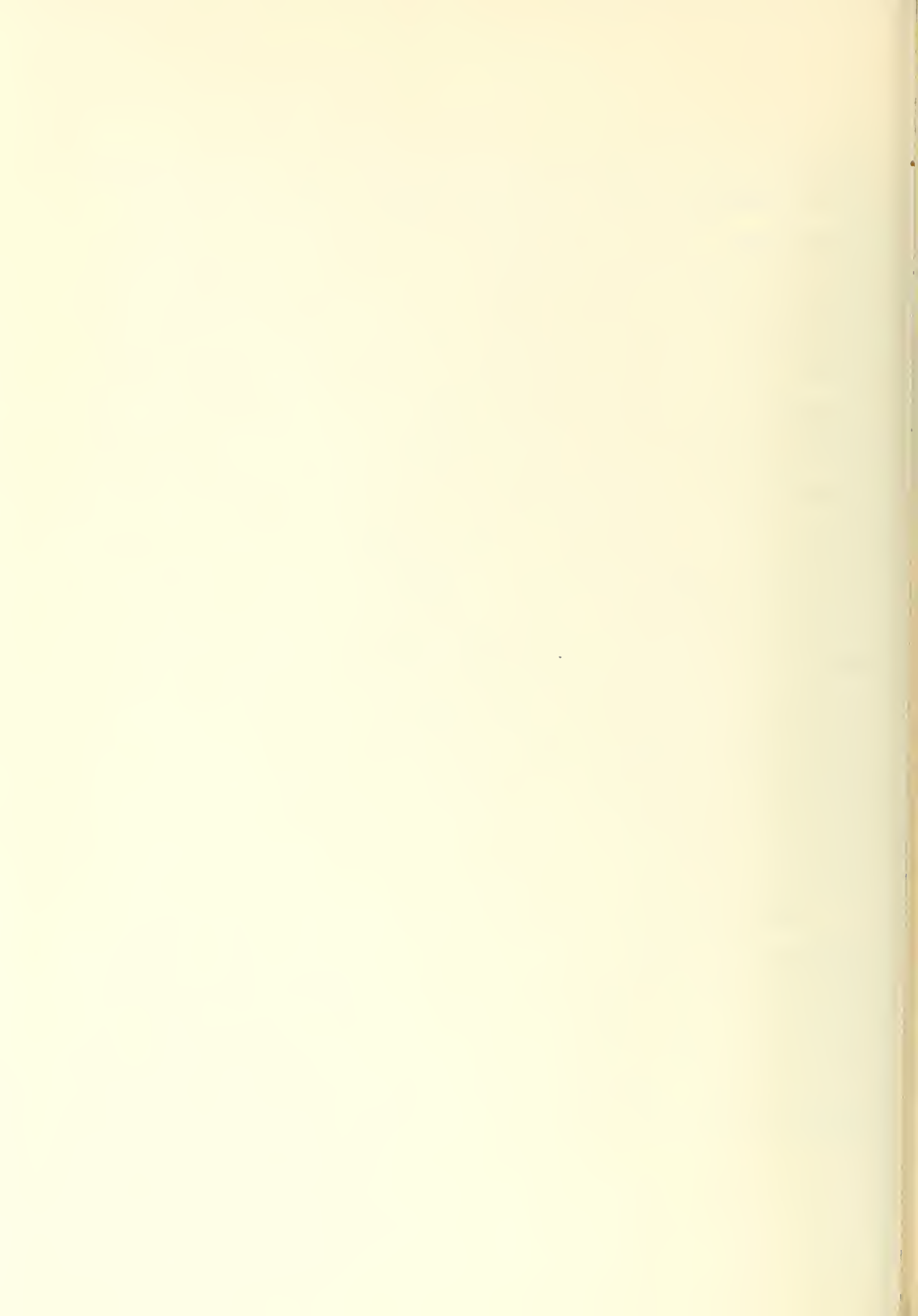
$$V = 0.722 \phi \sqrt{\frac{P}{\rho D^5}} \quad \text{knots} \quad (37)$$

In regards to the developed area ratio which we shall use to determine the specific Troest propeller series to use we need not be too concerned since the value is not too critical as far as the preliminary propeller design is concerned. It must be remembered, however, that blade area does effect overall propeller efficiency somewhat. In an ideal fluid, with no friction, it would



not matter what the blade area was since we would get the same lift forces from a thin blade as from a wide blade, hence the same thrust force and torque force. In a real fluid, however, we have a drag force as well as lift. The components of this drag force are such as to decrease the thrust obtained and to increase the torque required on the shaft to produce this thrust. Hence the larger the blade area, the more frictional resistance and hence drag. Therefore, a narrow blade is best for maximum efficiency. Careful consideration must, however, be given to the problem of cavitation since too narrow a blade will give rise to serious cavitation problems. The area of the blade, therefore, is normally chosen from a cavitation standpoint such that the blade width or area is as small as possible, yet sufficient to prevent the peak negative pressure from approaching the vapor pressure of water. It is interesting to note that in icebreaker propellers, the full sections, necessitated from strength considerations, makes it impossible to avoid cavitation completely, especially at high loading and low speed. Consequently, for the purposes of the selection of preliminary characteristics the best course of action is to select a developed blade area ratio which is characteristic of present day practice.

When considering the number of blades for use with a twin screw ice breaking vessel it may be said that there is very little effect on efficiency despite the number of blades. The most common arrangement is either a three or four bladed wheel. Some authorities hold that the general rule of thumb is that the three bladed wheel is more efficient than the four bladed one, However, for moderate or high blade area ratios it is possible to design a



four bladed wheel which will have efficiencies equal to or greater than the corresponding three bladed propeller. Consequently, the choice of whether to use a three or four bladed propeller is almost entirely a question of vibration and that the number of blade impulses per minute is the deciding factor. Of course, since the requirements of icebreaking differ greatly from those normally encountered on sea going vessels, there are many theories concerning the selection of number of blades. The Glacier and wind class were both designed with <sup>three</sup> ~~these~~ bladed propellers. Both have shown blade failures. This may perhaps be taken as an indication that icebreakers should be fitted with four bladed propellers. In this case, perhaps, large ice pieces could not get in between the blades and cause failure. Others, however, feel that the three bladed wheel is best. Each blade of a three bladed propeller is stronger than that of a propeller with more blades and the greater gap obtained with the three bladed propeller as compared with propellers with more blades, is more favorable from the point of view of ice passing through the blades. Consequently, the choice of number of blades is purely an arbitrary one and subject to the opinions of the designer. Despite the choice, however, the problem of vibrations must be considered and it must be insured that the blade frequency is different from criticals or harmonics thereof of the hull or shaft vibration frequencies.

For the purposes of this paper, therefore, we shall consider both the three and four bladed propeller. Experience dictates that the developed area - disc area ratio normally used in ice breaking type vessels falls into the





range of from 0.35 to 0.54 for the three bladed propeller and from 0.50 to 0.60 for the four bladed propeller. For the purpose of this paper, therefore, we will select the Troost propeller series B3.50 and B4.55 as representative of present practice.

By applying expressions (33) and (34) to these series propellers we may determine the variation of maximum ballard pull attainable as well as the shaft RPM necessary to obtain this ballard pull both as a function of shaft horsepower available per shaft and propeller diameter. This has been done for a range of shaft horsepower and propeller diameters and the results are shown in figures <sup>9, 10, 12, 13</sup> 15, 16, 18 and 19. By the use of this plotted data we may, for a known shaft horsepower per shaft and given propeller diameter, determine with reasonable accuracy the ballard pull which will be developed per shaft and the shaft RPM necessary for its attainment.

By comparing the results obtained from these two series we may further substantiate our previous statement that the number of blades used is not very critical in the preliminary analysis. Since for the B3-50 propeller

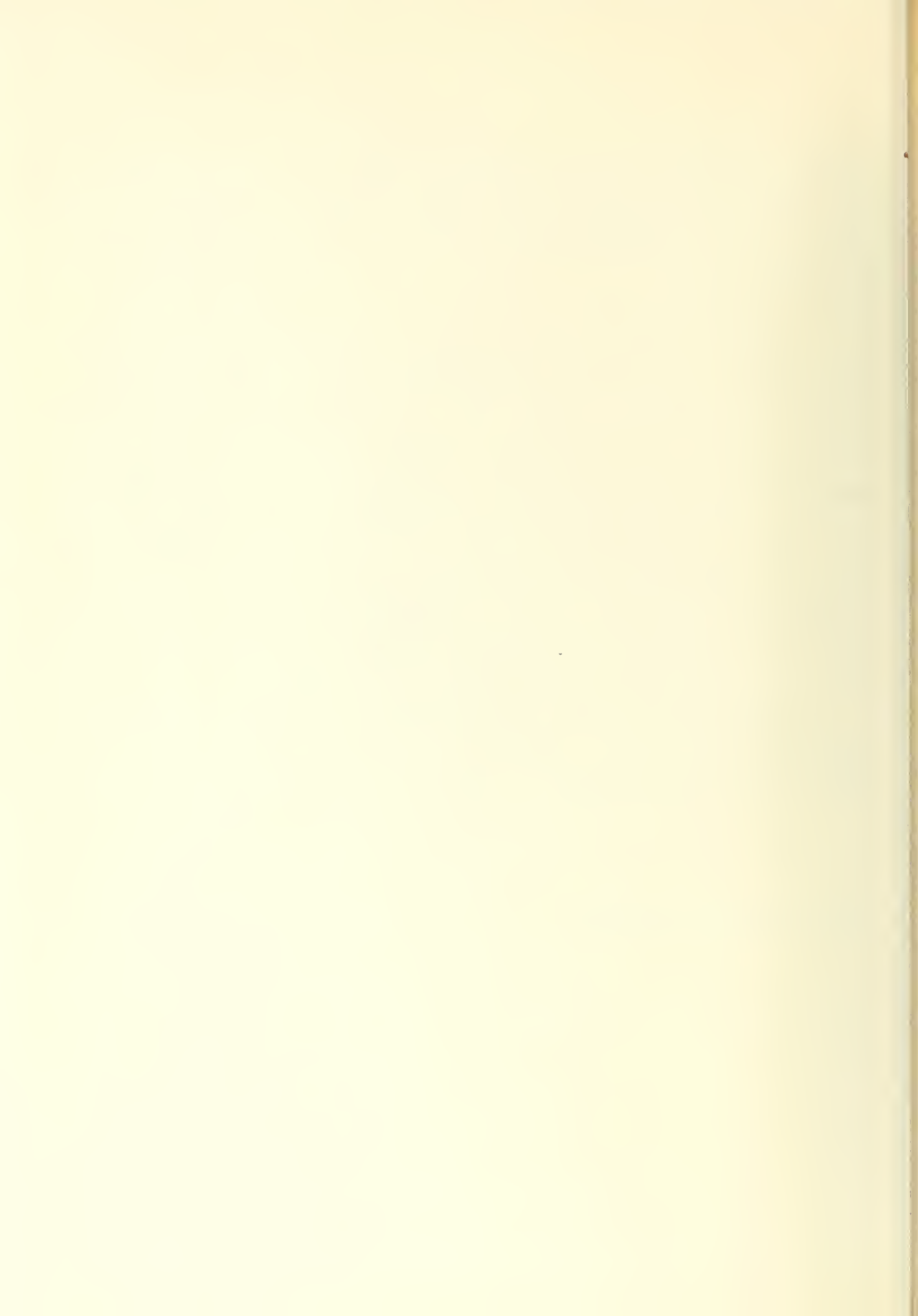
$$T' = 74.2 \rho^{2/3} D^{2/3}$$

$$N = 818 \left( \frac{\rho}{D^5} \right)^{1/3}$$

and for the B4-55 propeller

$$T' = 72.2 \rho^{2/3} D^{2/3}$$

$$N = 803 \left( \frac{\rho}{D^5} \right)^{1/3}$$





Series Propeller B3-50

$u$	$x$	$y^{2/3}$	$\frac{\delta}{y^{2/3}}$	$\frac{p_0}{D}$
3.5	0.95	2.31	0.412	1.19
4.0	1.10	2.52	0.437	1.02
5.0	1.355	2.92	0.464	0.81
6.0	1.575	3.31	0.477	0.675
7.0	1.77	3.66	0.483	0.58
8.0	1.93	4.00	0.483	0.50

$P_0$  = pitch at 0.7 radius

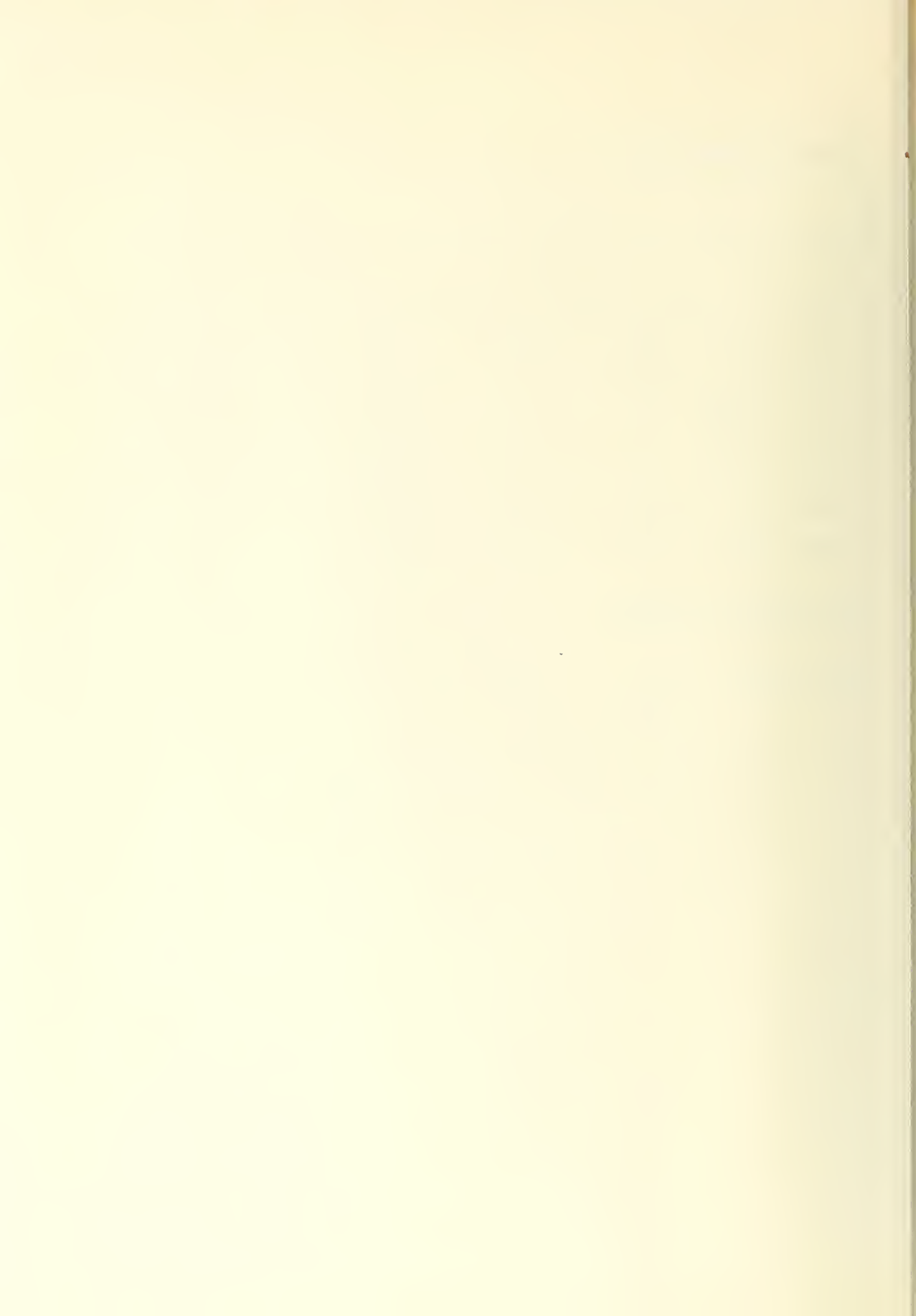
From plot max  $\frac{\delta}{y^{2/3}} = 0.4838$  AT  $y = 1.5$   
 $\frac{P_0}{D} = 0.54$

$$T' = 153.3 P^{2/3} D^{2/3} \frac{\delta}{y^{2/3}} \quad (33)$$

$$T' = 74.2 N^{1/3} D^{2/3} \quad (33A)$$

$$N = 213.5 y^{2/3} \left( \frac{P}{D^2} \right)^{1/3} \quad (34)$$

$$N = 313 \left( \frac{P}{D^2} \right)^{1/3} \quad (34A)$$



SERIES B3.50  
PROPELLER DATA

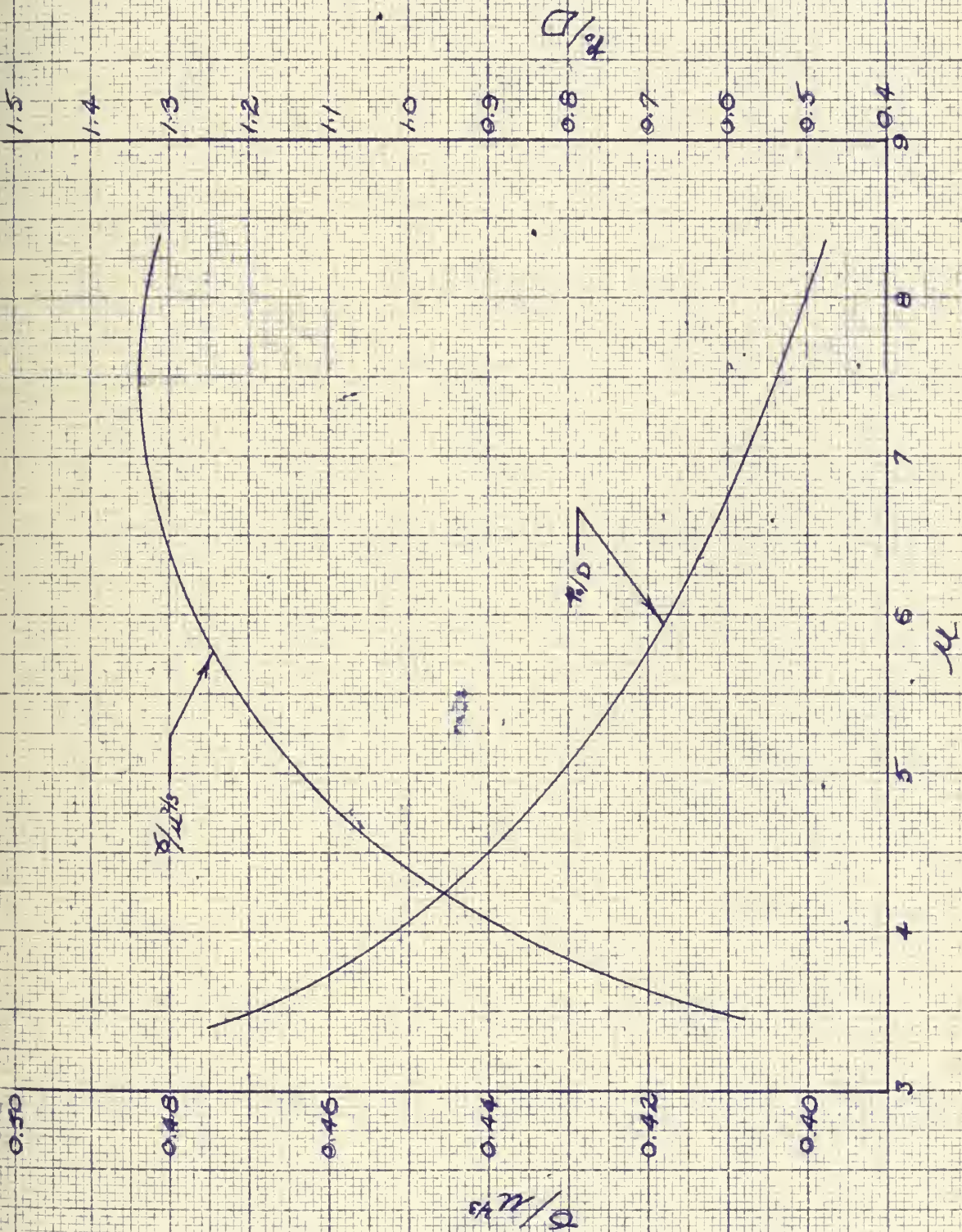
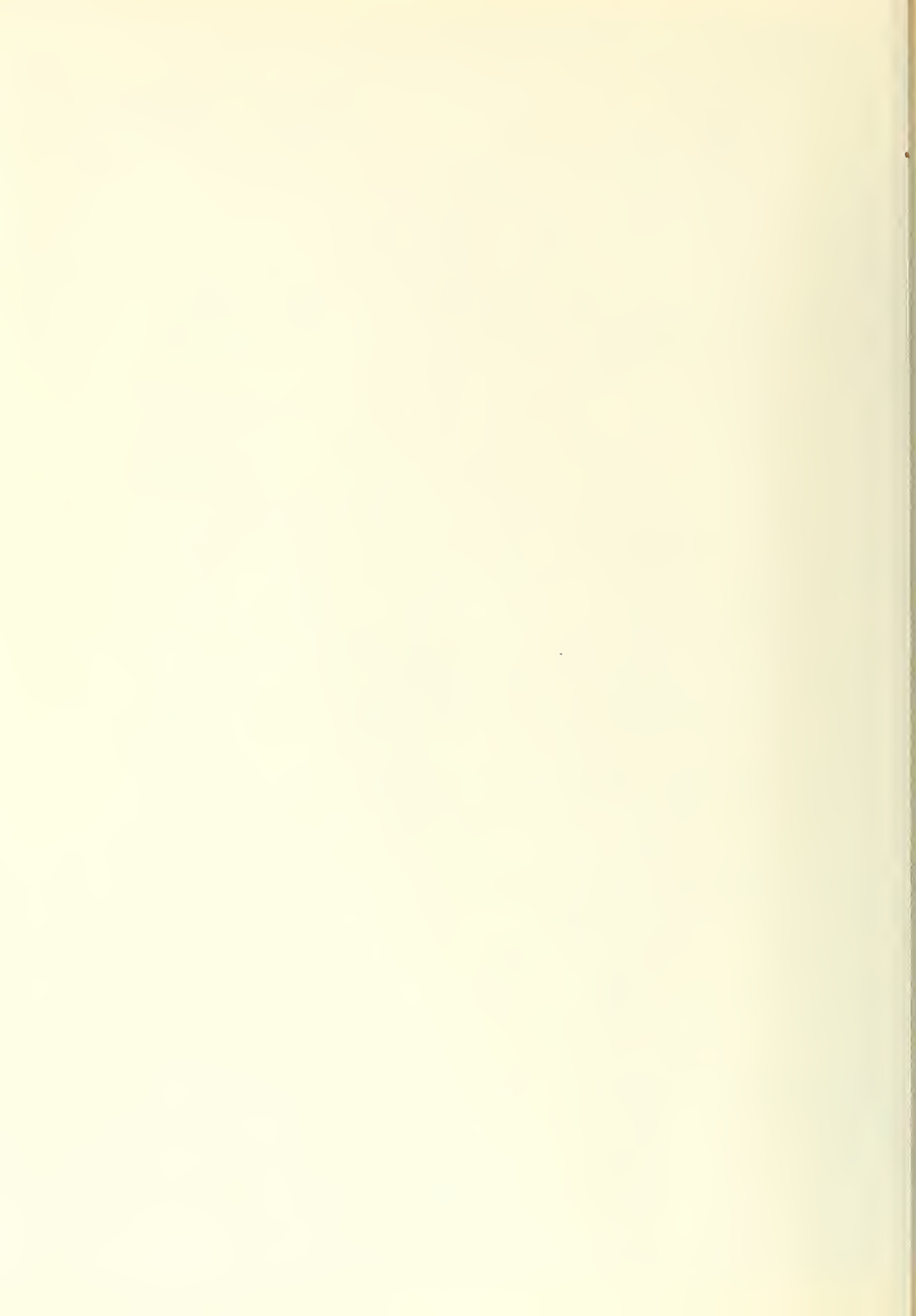


Fig 8





-102-

# BOLLARD PULL VS SHAFT HORSEPOWER FOR TROOST B-3.50 PROPELLER PER SHAFT

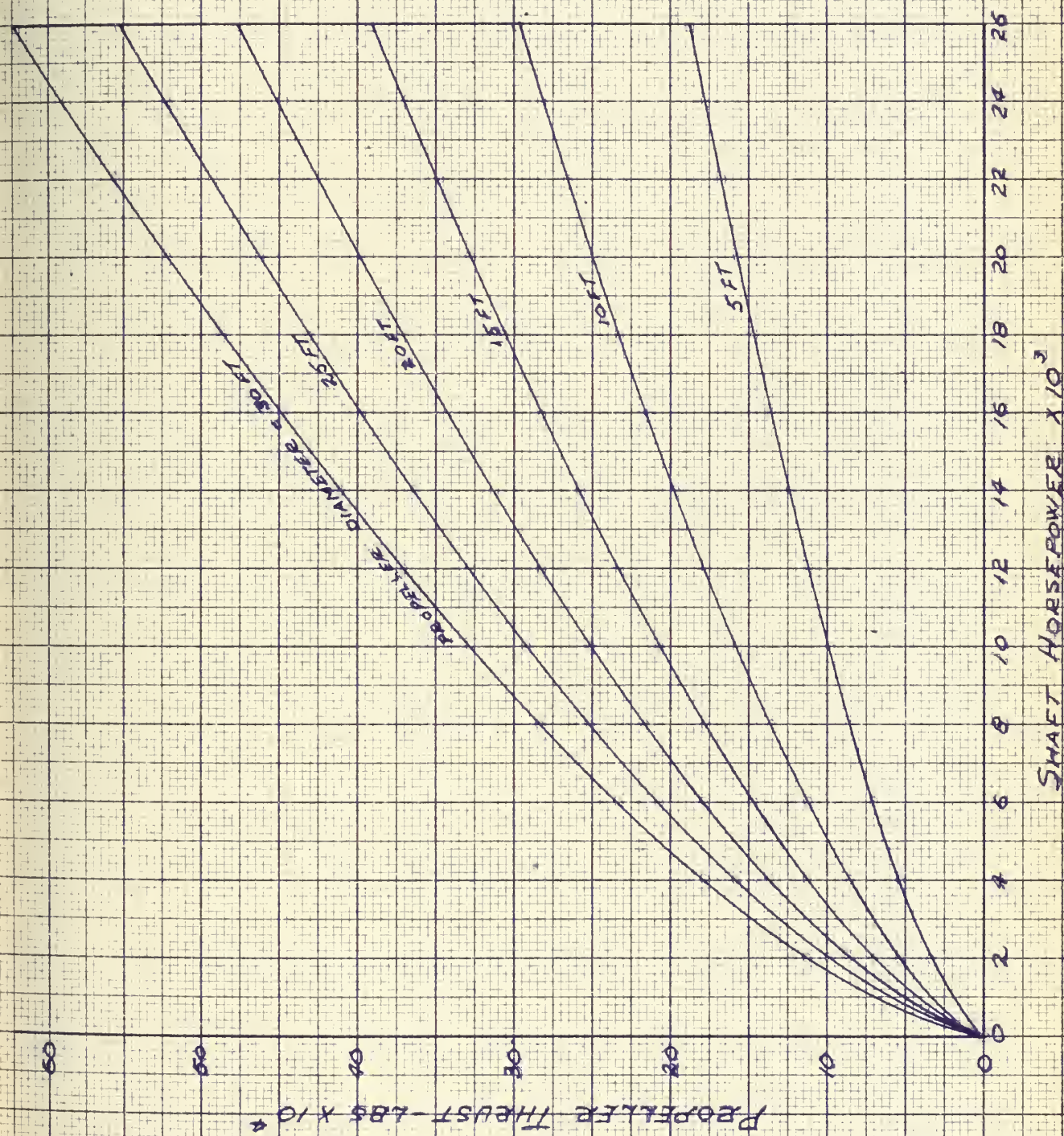
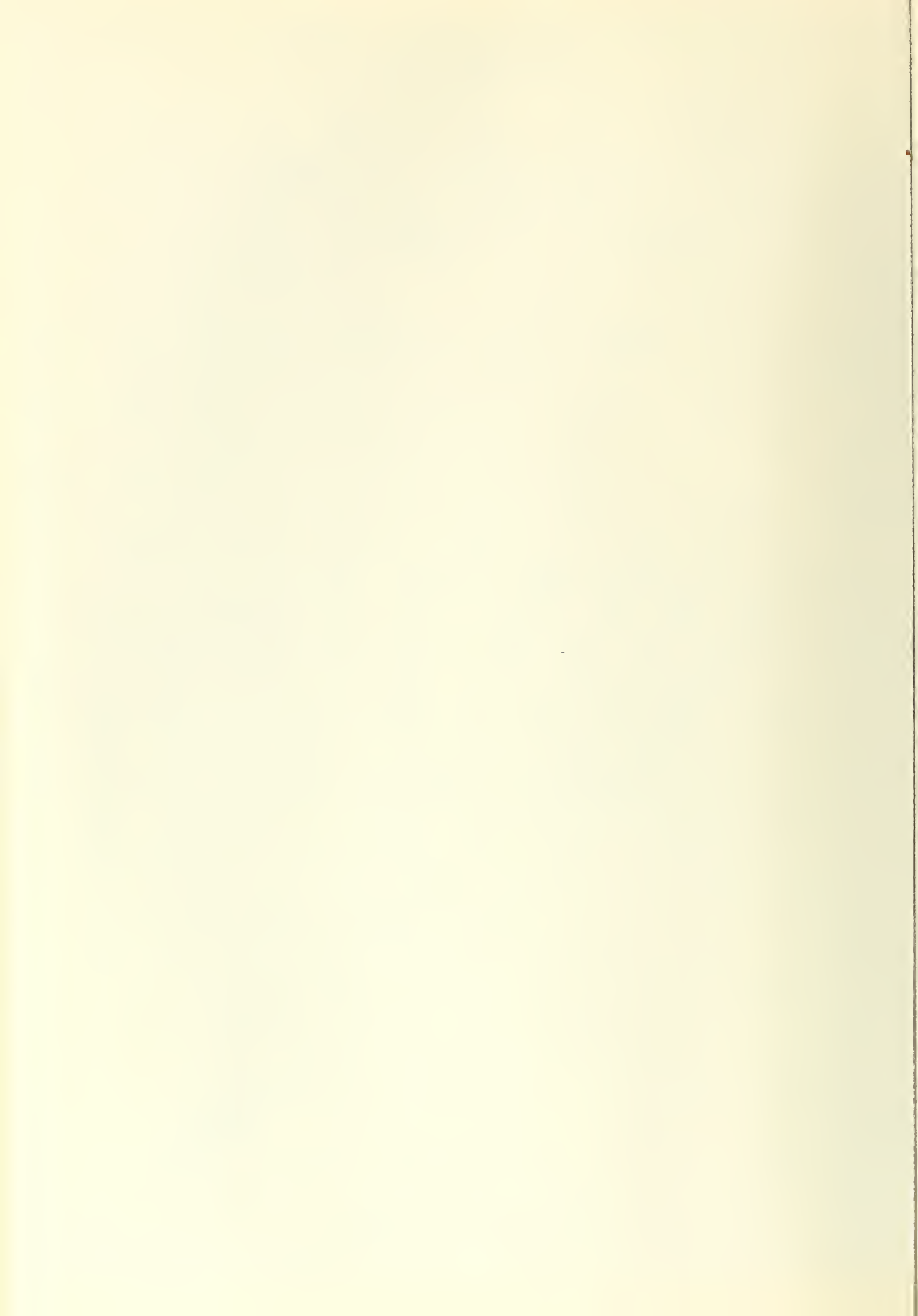


Fig 9





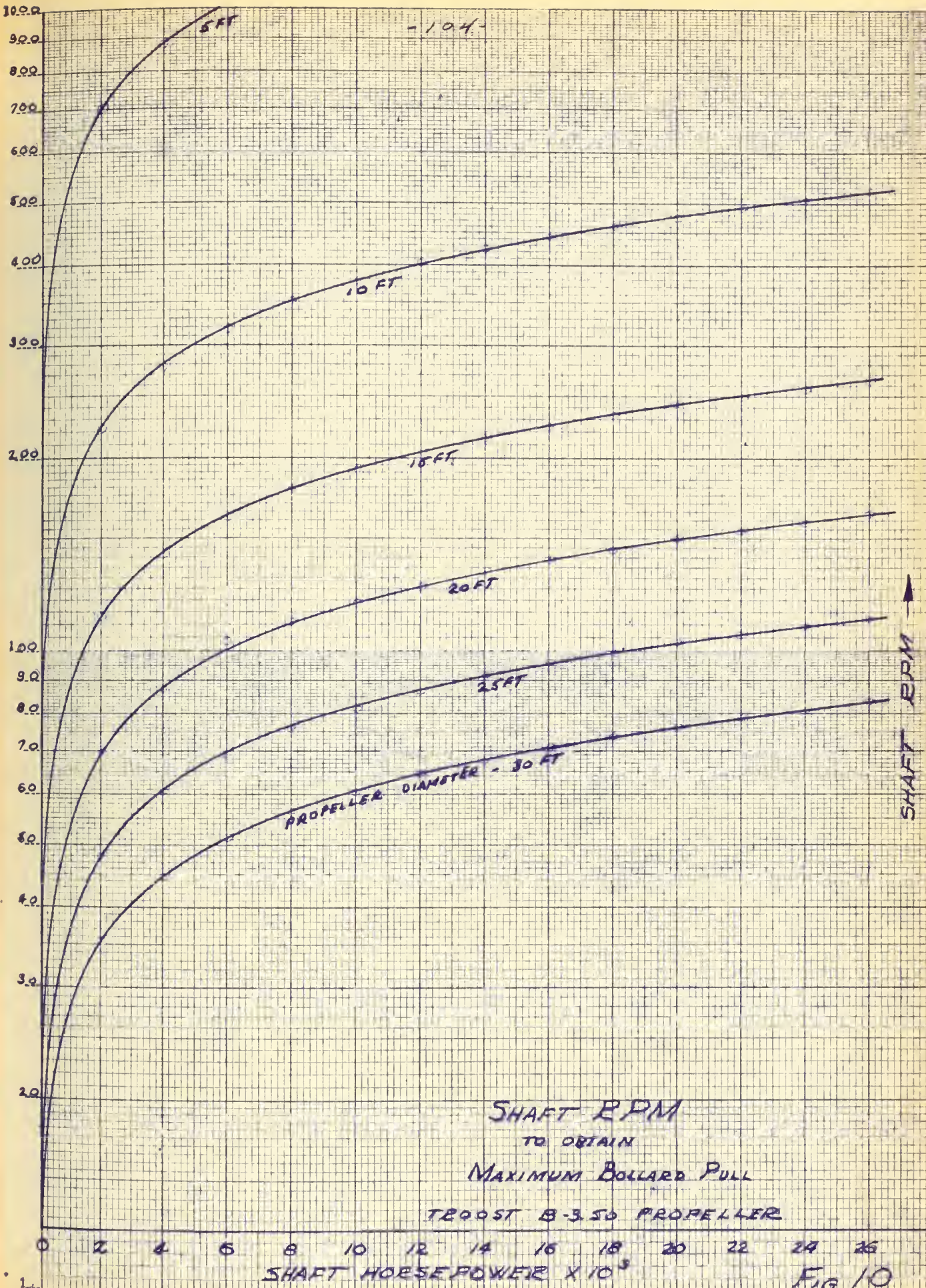


FIG 10





Series Propeller B4-55

$u$	$\delta$	$u^{2/3}$	$\frac{\delta}{u^{2/3}}$	$P_0/D$
3	0.83	2.08	0.399	1.4
4	1.115	2.52	0.442	1.0
5	1.35	2.92	0.462	0.775
6	1.55	3.31	0.469	0.63
7	1.72	3.66	0.471	0.54
7.5	1.80	3.83	0.471	0.50

$P_0$  = pitch at 0.7 radius

From plot max  $\frac{\delta}{u^{2/3}} = 0.471$  AT  $u = 7.3$

$$P_0/D = 0.515$$

$$T' = 155.3 P^{2/3} L^{1/3} \frac{\delta}{u^{2/3}} \quad (33)$$

$$T' = 12.2 P^{2/3} L^{1/3} \quad (33B)$$

$$N = 213.5 \frac{u^{4/3}}{D^{5/3}} \quad (34)$$

$$N = 503 \left( \frac{P}{D^5} \right)^{1/3} \quad (34B)$$



SERIES B4.55  
PROPELLER DATA

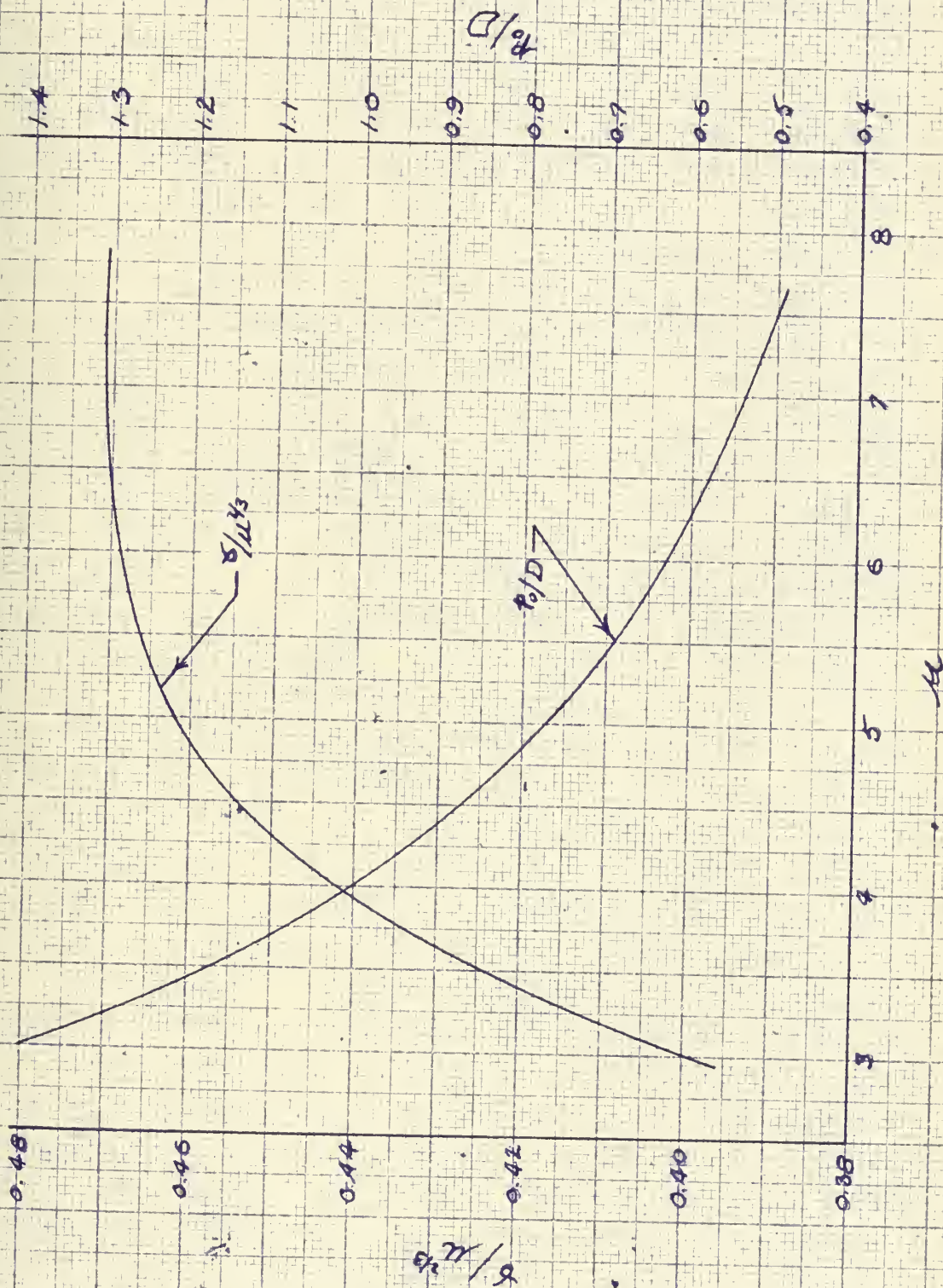
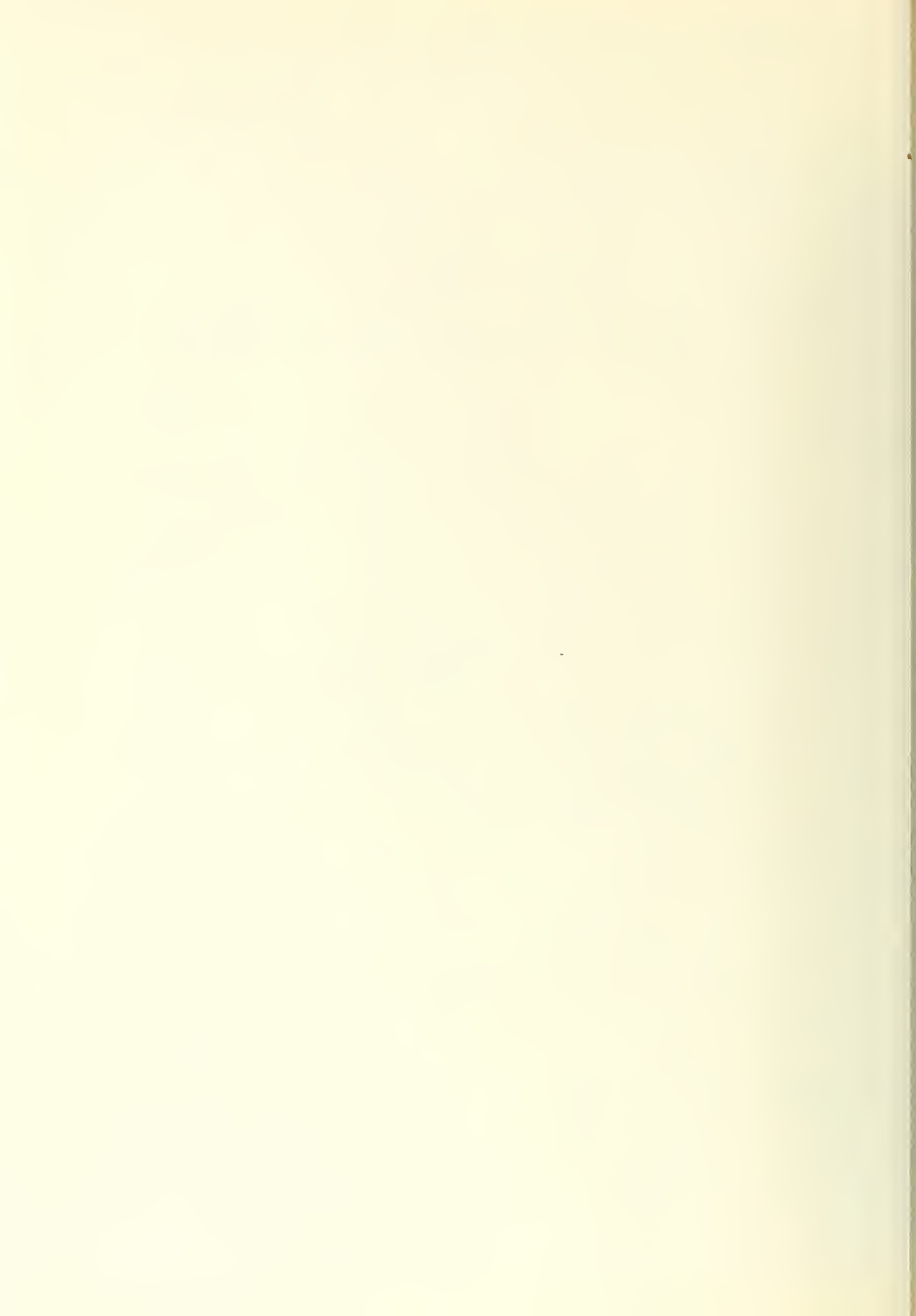
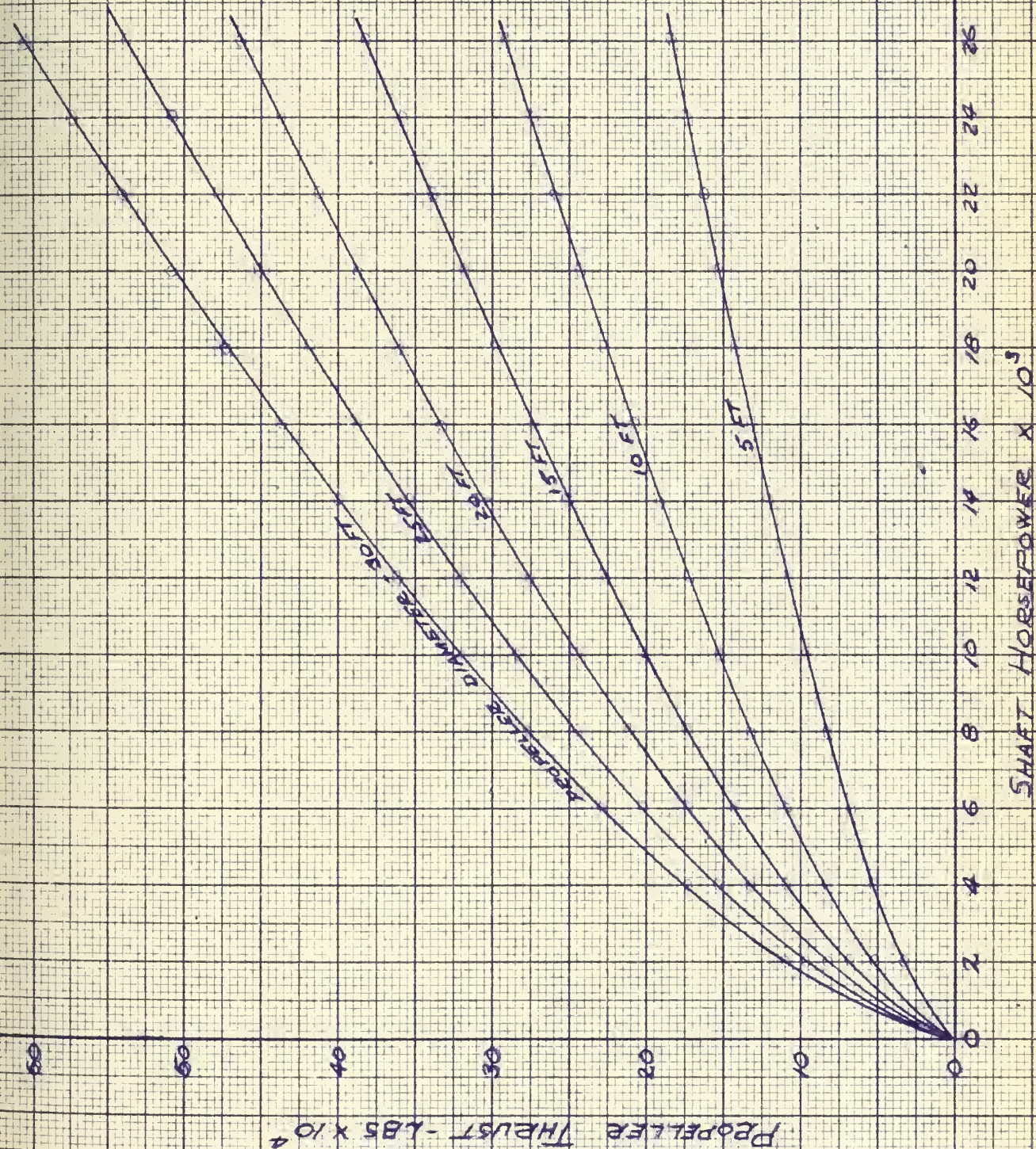


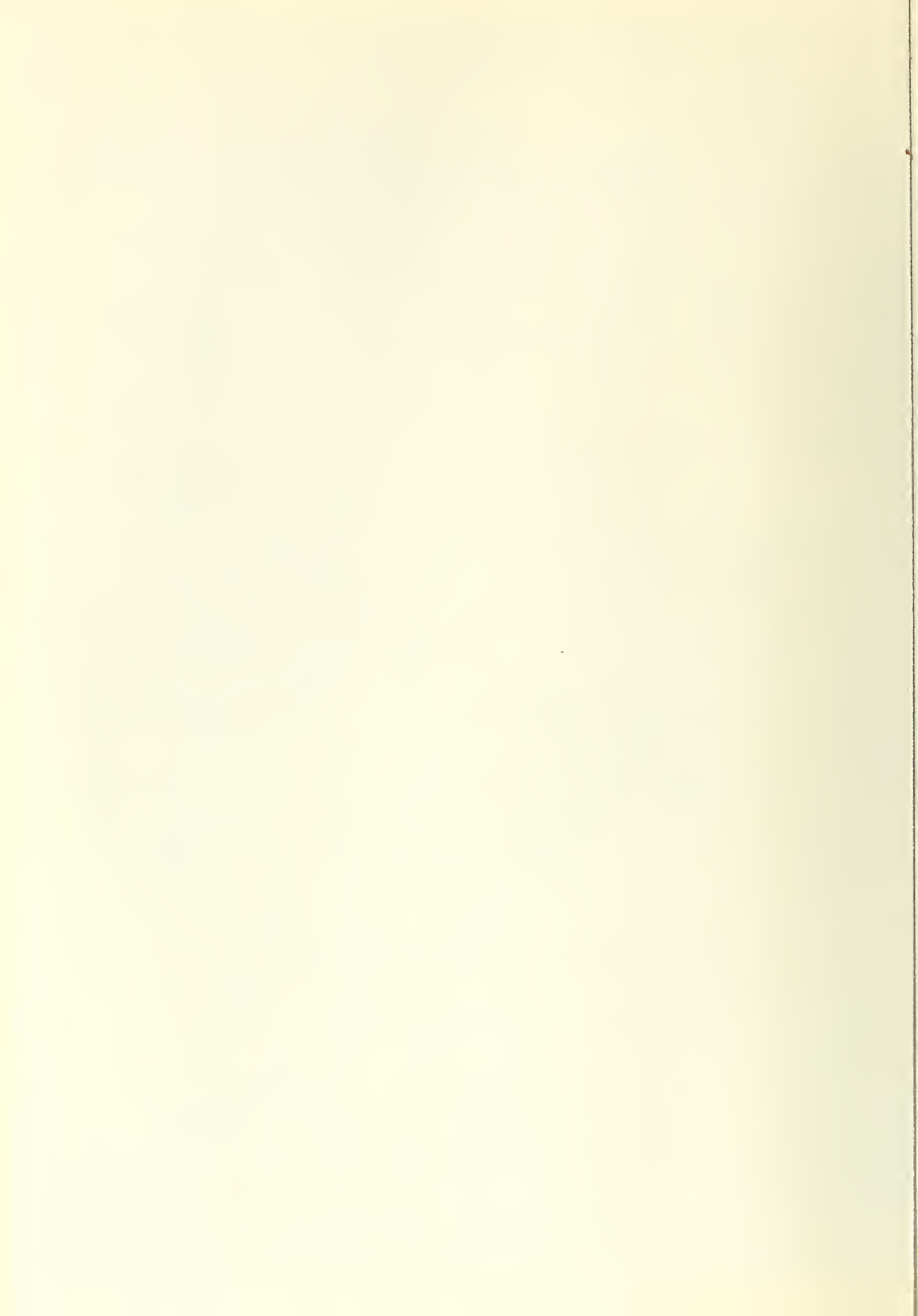
FIG 11



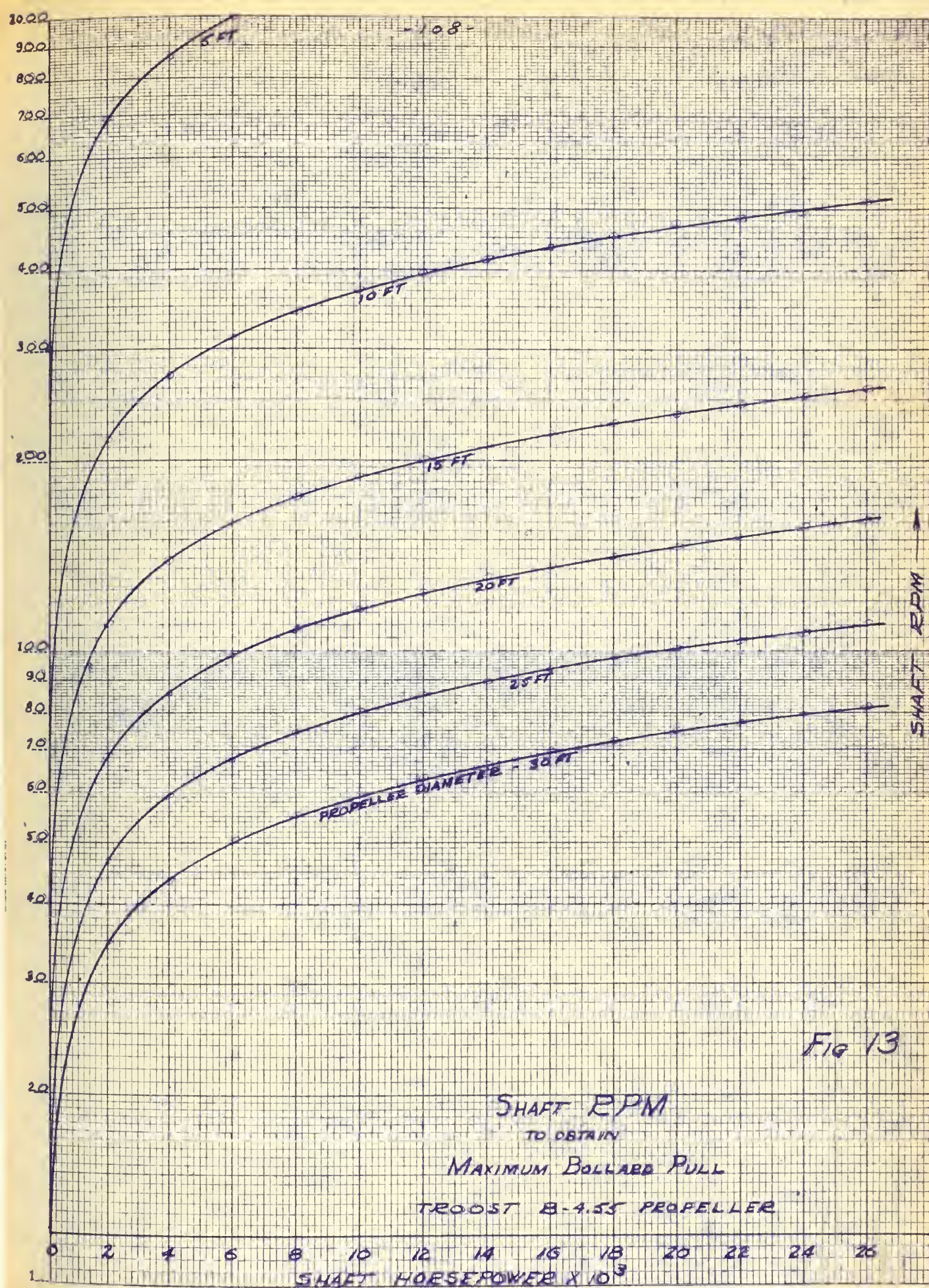


-107-  
 BOLLARD PULL  
 VS  
 SHAFT HORSEPOWER  
 FOR  
 TROOST B-4.55 PROPELLER  
 PER SHAFT













we see that the percentage difference in predicted ballard pull between the three and four bladed propellers - all other factors remaining constant - is only about 2.7% and the percentage difference in shaft RPM required is only about 1.8%.

We may, in a like manner reaffirm another previous statement of ours. We mentioned that the propeller series used is not critical in the preliminary analysis so long as that used is typical of those normally found in a particular type service. For this purpose we may examine several propeller series, holding the number of blades constant, and observe the percentage variation in ballard pull obtainable and shaft RPM necessary for its attainment. For the three bladed propeller let us consider the Troost series B3-35, B3-50 and B3-65 propellers and for the four bladed propeller consider the Troost series B4-40, B4-55 and B4-70 propellers. Considering these series we find that

$$T'_{B3.35} = 14.7 P^{2/3} D^{4/3}$$

$$T'_{B3.65} = 67.5 P^{2/3} D^{4/3}$$

$$T'_{B4.40} = 25.7 P^{2/3} D^{4/3}$$

$$T'_{B4.70} = 21.4 P^{2/3} D^{4/3}$$

also that

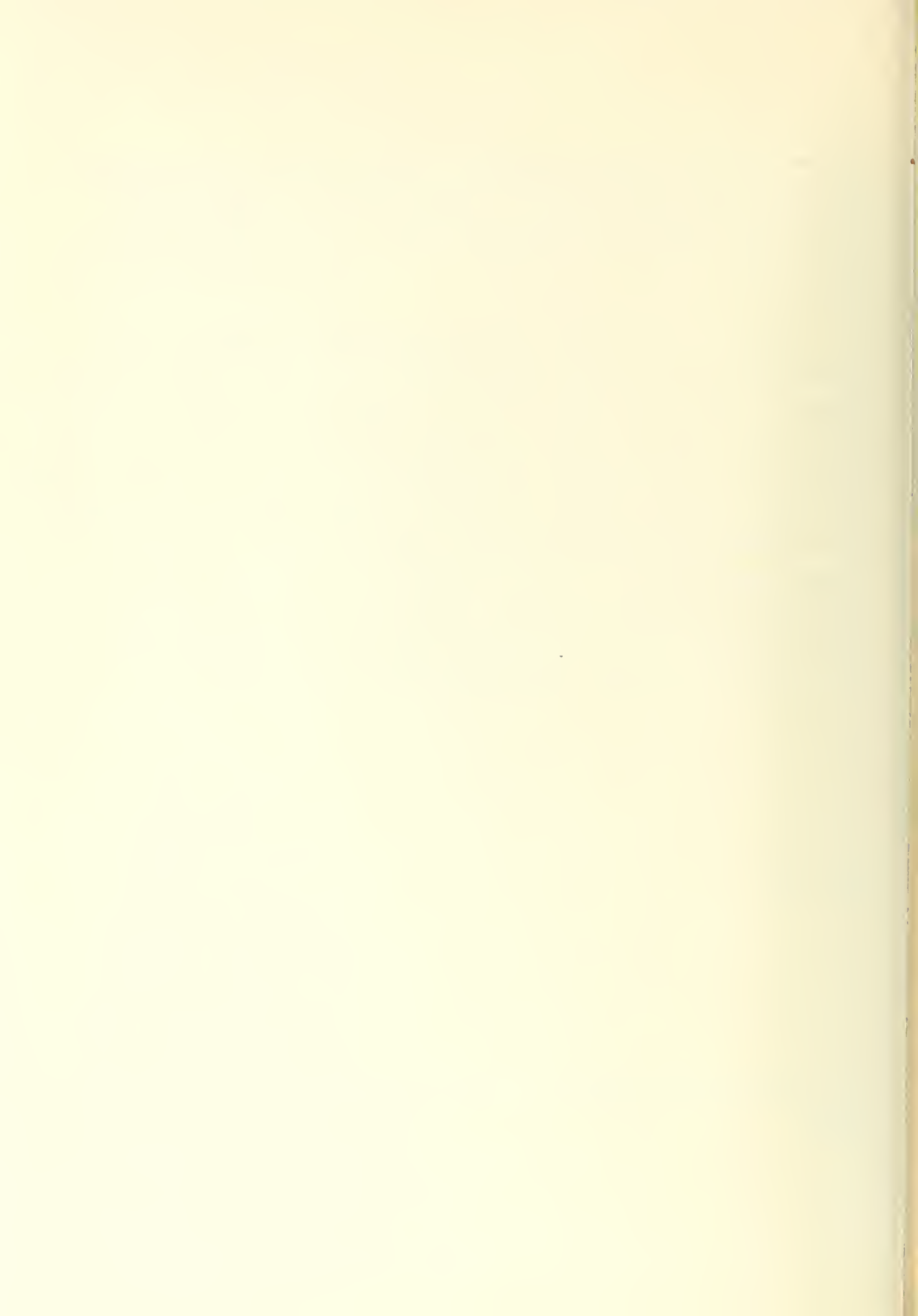
$$N_{B3.35} = 803 (P/D^5)^{1/3}$$

$$N_{B3.65} = 143 (P/D^5)^{1/3}$$

$$N_{B4.40} = 124 (P/D^5)^{1/3}$$

$$N_{B4.70} = 826 (P/D^5)^{1/3}$$

Hence the percentage difference between the ballard pull attainable with the series



Blade Area Comparison

		B3-35			B3-65			B4-40			B4-70		
$\mu$	$\delta$	$4^{2/3}$	$\delta/4^{2/3}$	$\delta$	$4^{2/3}$	$\delta/4^{2/3}$	$\delta$	$4^{2/3}$	$\delta/4^{2/3}$	$\delta$	$4^{2/3}$	$\delta/4^{2/3}$	$\delta$
3.0				0.82	2.08	0.394				0.84	2.08	0.404	
3.5	0.88	2.31	0.381				0.92	2.31	0.398				
4.0	1.03	2.52	0.408	1.08	2.52	0.428	1.06	2.52	0.421	1.11	2.52	0.441	
5.0	1.30	2.92	0.446	1.30	2.92	0.446	1.35	2.92	0.463	1.33	2.92	0.456	
6.0	1.54	3.31	0.466	1.495	3.31	0.452	1.60	3.31	0.484	1.52	3.31	0.459	
7.0	1.75	3.66	0.478	1.653	3.66	0.452	1.81	3.66	0.494	1.695	3.66	0.463	
7.5				1.73	3.84	0.451	1.89	3.84	0.493	1.78	3.84	0.464	
7.6										1.80	3.865	0.465	
7.65				1.745	3.88	0.450							
7.8							1.925	3.94	0.488				
8.0	1.925	4.00	0.482										
8.3	1.975	4.10	0.482										

$\max \delta/4^{2/3} = 0.4822$    
  $\max \delta/4^{2/3} = 0.4516$    
  $\max \delta/4^{2/3} = 0.4774$    
  $\max \delta/4^{2/3} = 0.465$

$T' = 14.9 \rho^{2/3} D^{1/3}$    
  $T' = 16.5 \rho^{2/3} D^{1/3}$    
  $T' = 15.7 \rho^{2/3} D^{1/3}$    
  $T' = 11.4 \rho^{2/3} D^{1/3}$

$N = 803 (P/D^5)^{1/3}$    
  $N = 143 (P/D^5)^{1/3}$    
  $N = 177 (P/D^5)^{1/3}$    
  $N = 326 (P/D^5)^{1/3}$



# COMPARISON SERIES

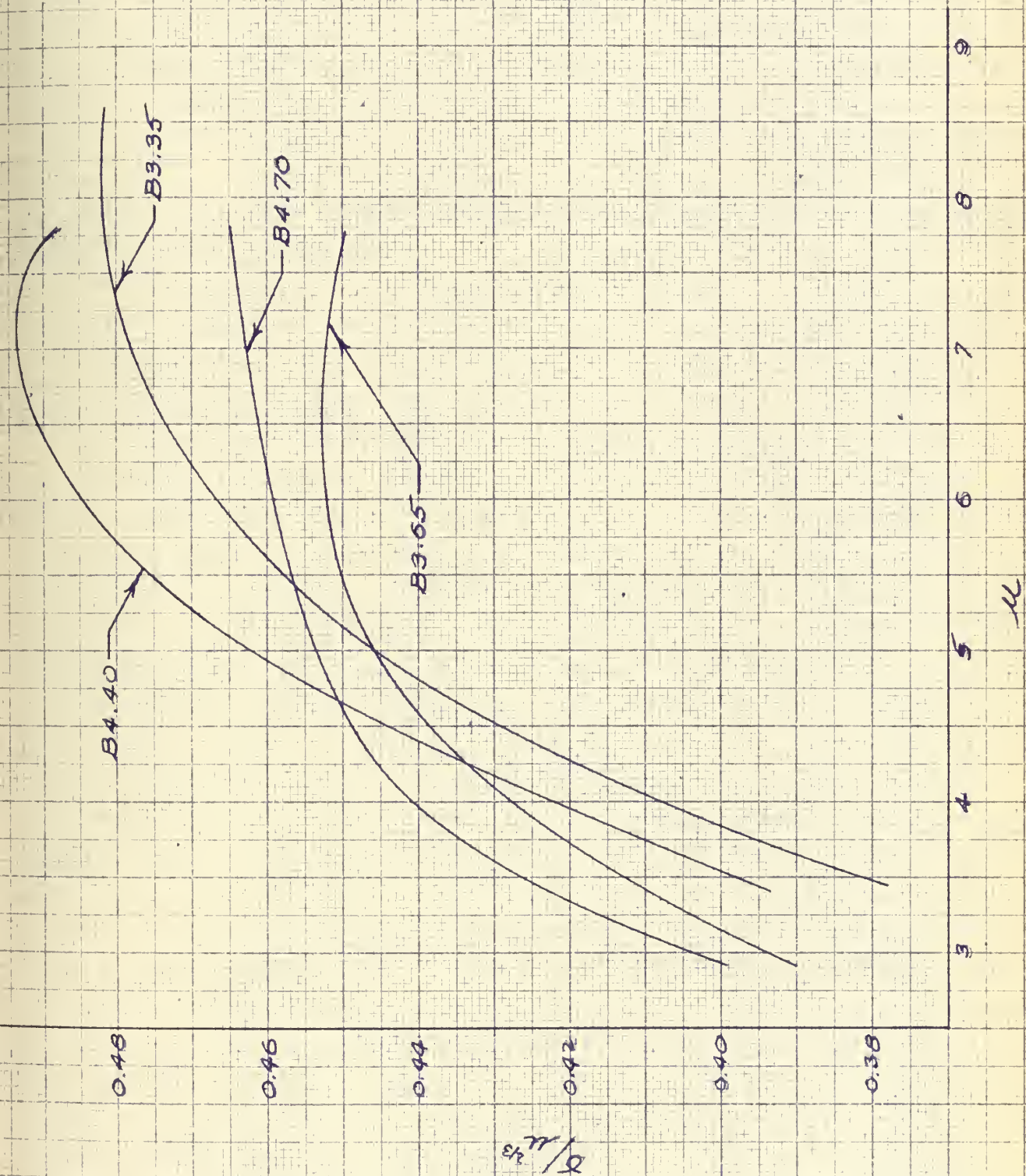


FIG 14







B3-35 and B3-50 = 0.94%

B3-50 and B3-65 = 6.33%

B3-35 and B3-65 = 7.23%

B4-40 and B4-56 = 4.63%

B4-56 and B4-70 = 1.11%

B4-40 and B4-70 = 5.68%

and the percentage difference between the shaft RPM required to obtain maximum ballard pull with the series

B3-35 and B3-50 = 5.22%

B3-50 and B3-65 = 10.1%

B3-35 and B3-65 = 16.2%

B4-40 and B4-55 = 1.13%

B4-55 and B4-70 = 2.78%

B4-40 and B4-70 = 4.04%

Hence we can see that for the three bladed propeller a variation in developed blade area ratio as large as 85% produces only about 7% variation in obtainable ballard pull and about a 16% variation in shaft RPM required. Likewise for the four bladed propeller a variation in developed blade area ratio of as large as 75% produces only about 6% variation in developed ballard pull and about 4% variation in shaft RPM required.



Consequently, we see that the actual choice of propeller series is not too critical and that the results given in figures 9, 10, 12, and <sup>13</sup>19 for the B3-50 and B4-55 propellers are quite satisfactory for preliminary powering analysis.

As previously mentioned, we are interested not only in the ballard pull which may be developed, but also in the thrust which we may expect at various speeds of advance. Consequently, we wish to investigate the variation of propeller thrust as a function of ship speed for a range of shaft horsepowers and propeller diameters. To do this, we proceed as previously outlined. The pitch diameter ratio is constant over the speed range since we have designed for ballard condition, hence our values of  $\delta$  and  $\mu$  lie on a line of constant  $P/D$ . In addition, since we are considering the diesel electric installation, the propeller horsepower is also constant. Therefore, in order to obtain an orderly variation of propeller thrust with ship speed we may proceed down the constant  $P/D$  line of the Troost series charts and select corresponding values of  $\mu$ ,  $\delta$  and  $\phi$ . From these we may determine our propeller thrust and vessel speed by our previously developed relationships

$$T = \frac{2\pi \phi \delta}{D} \quad \text{lbs} \quad (35)$$

$$V = 0.722 \phi \sqrt{\frac{P}{\rho D^5}} \quad \text{knots} \quad (37)$$

For the value of  $Q$  we may combine

$$Q = \frac{33000 P}{2\pi N}$$

and

$$\mu = \frac{N}{60} \sqrt{\rho D^5 / Q}$$



eliminating N to obtain

$$Q = 24.8 \frac{\rho^{1/3} D^{5/3}}{4^{1/3}}$$

If we substitute the value of Q into (35) and (37) we obtain our desired expression for propeller thrust

$$T = 156 \frac{\rho^{2/3} L^{4/3}}{4^{2/3}} \quad \text{lbs} \quad (38)$$

and for ship speed

$$V = 2.54 \phi \left( \frac{\rho}{D^{2/3} 4^{1/3}} \right)^{1/3} \quad \text{knots} \quad (39)$$

This investigation was carried out for the Troost Series propellers B3-50 and B4-55 for shaft horsepowers ranging from 4000 to 28000 per shaft and for propeller diameters ranging from 5 feet to 30 feet. The results of this investigation are shown in figures <sup>15</sup> 21 to <sup>26</sup> 32. Interpolation may be used for intermediate values of shaft horsepower per shaft but for intermediate values of propeller diameter it is necessary to use the figure for that diameter closest to the propeller diameter desired. So doing will naturally introduce some error in thrust predictions, however, the error will be slight and usually insignificant as regards preliminary powering analysis.

If it is required to have more accuracy for intermediate propeller diameters than can be obtained from figures <sup>15</sup> 21 to <sup>26</sup> 32 in predicting variations of propeller thrust as a function of ship speed we may proceed as follows. " Returning to our original expressions

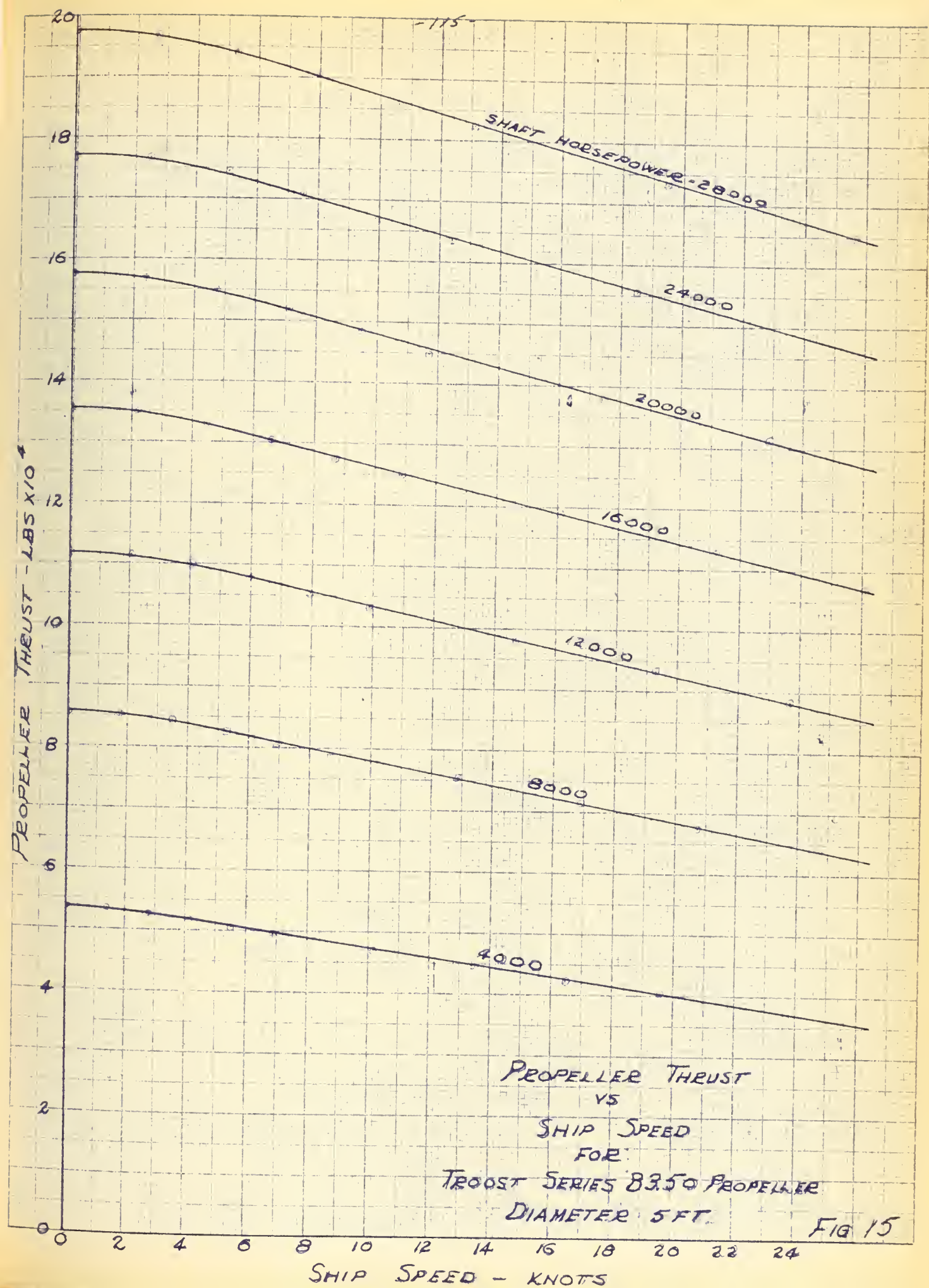
$$T = 156 \frac{\rho^{2/3} D^{4/3}}{4^{2/3}} \quad \text{lbs} \quad (38)$$

$$V = 2.54 \phi \frac{\rho^{1/3}}{D^{2/3} 4^{1/3}} \quad \text{knots} \quad (39)$$

we can determine from the Troost data the variation of  $\frac{\phi}{4^{1/3}}$  as a function











PROPELLER THRUST  
VS  
SHIP SPEED  
FOR

TROOST SERIES B3.50 PROPELLER  
DIAMETER - 10 FT

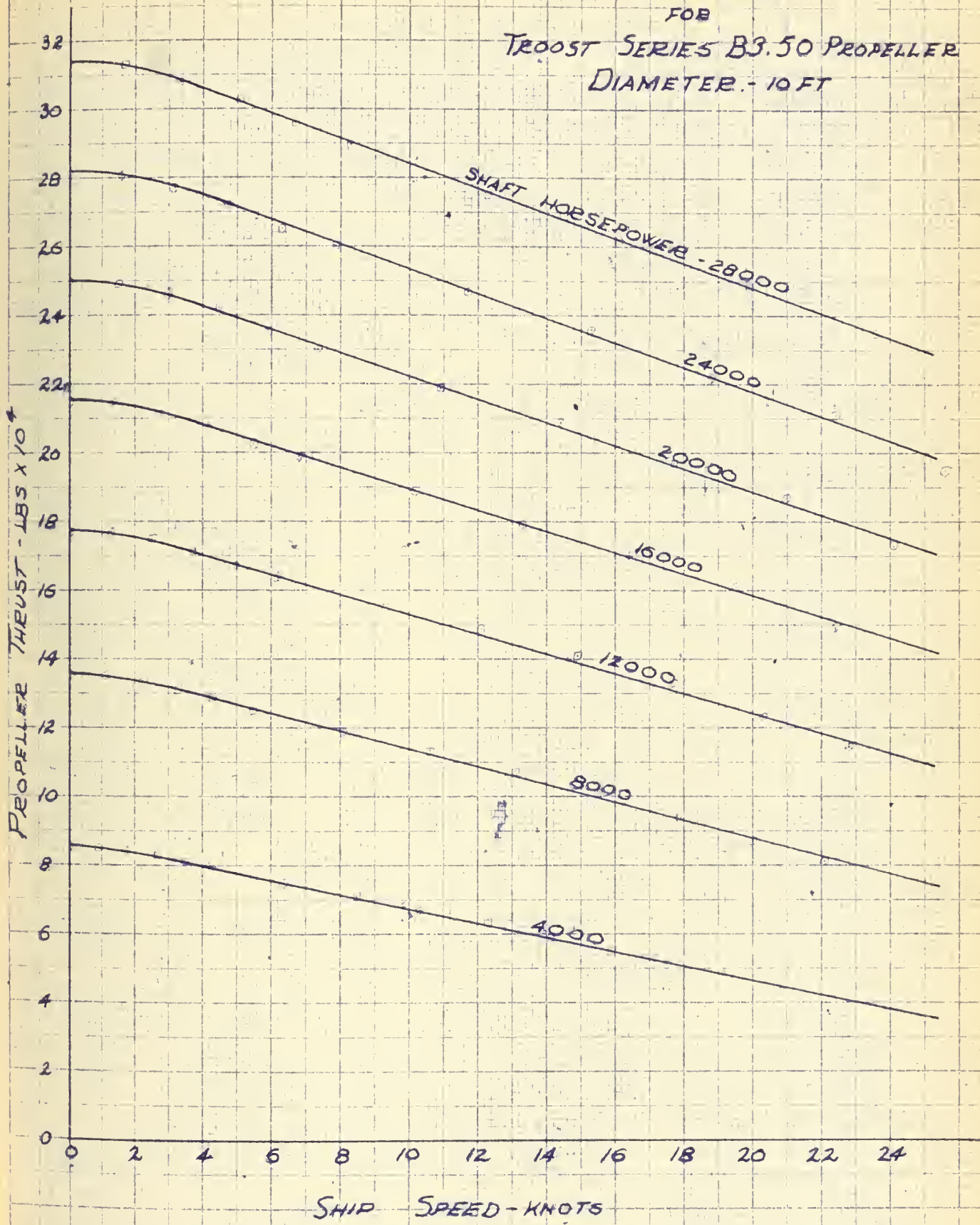


FIG 16



PROPELLER THRUST  
VS  
SHIP SPEED  
FOR  
TROOST SERIES B3.50 PROPELLER  
DIAMETER 15 FT.

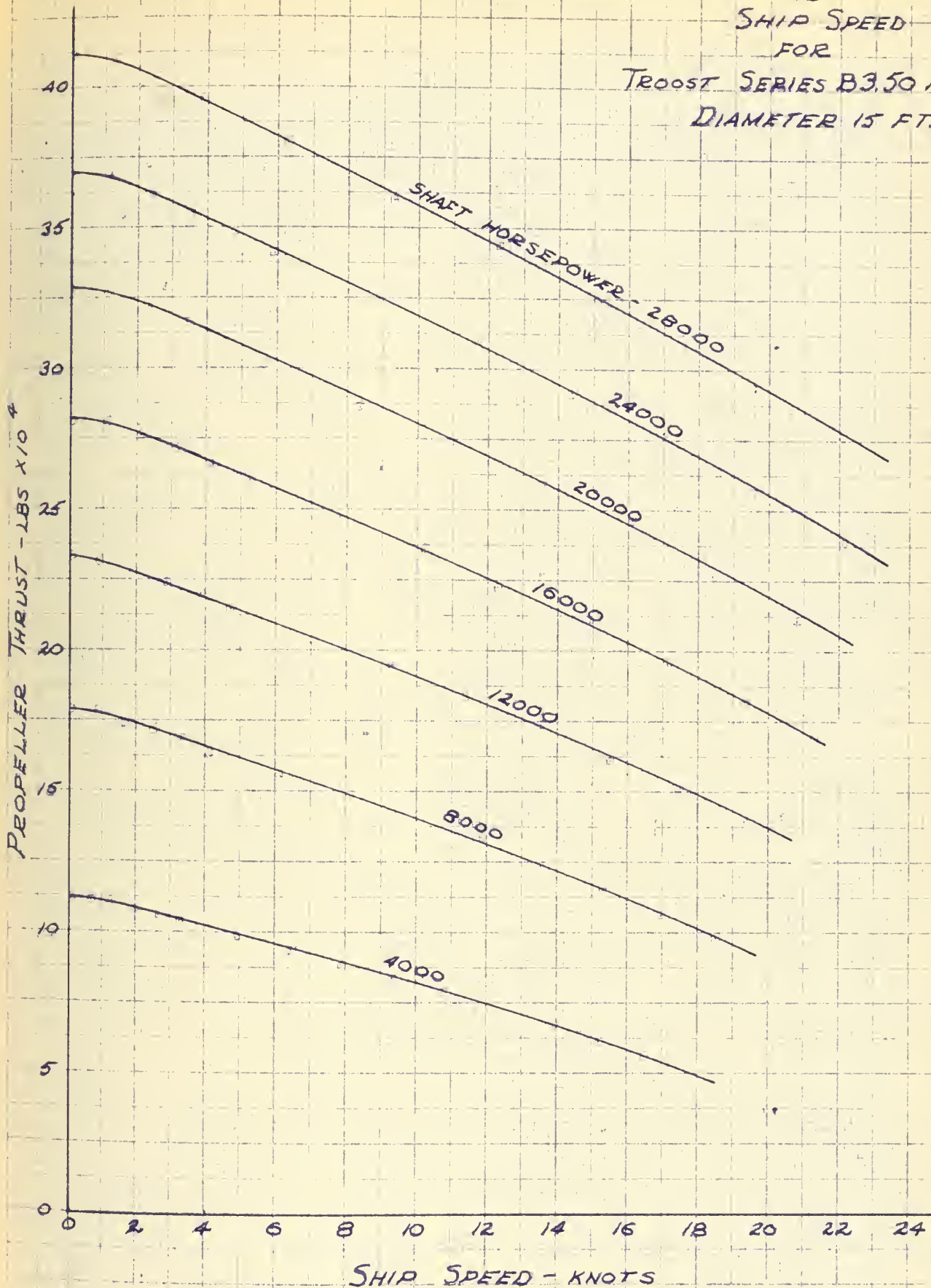
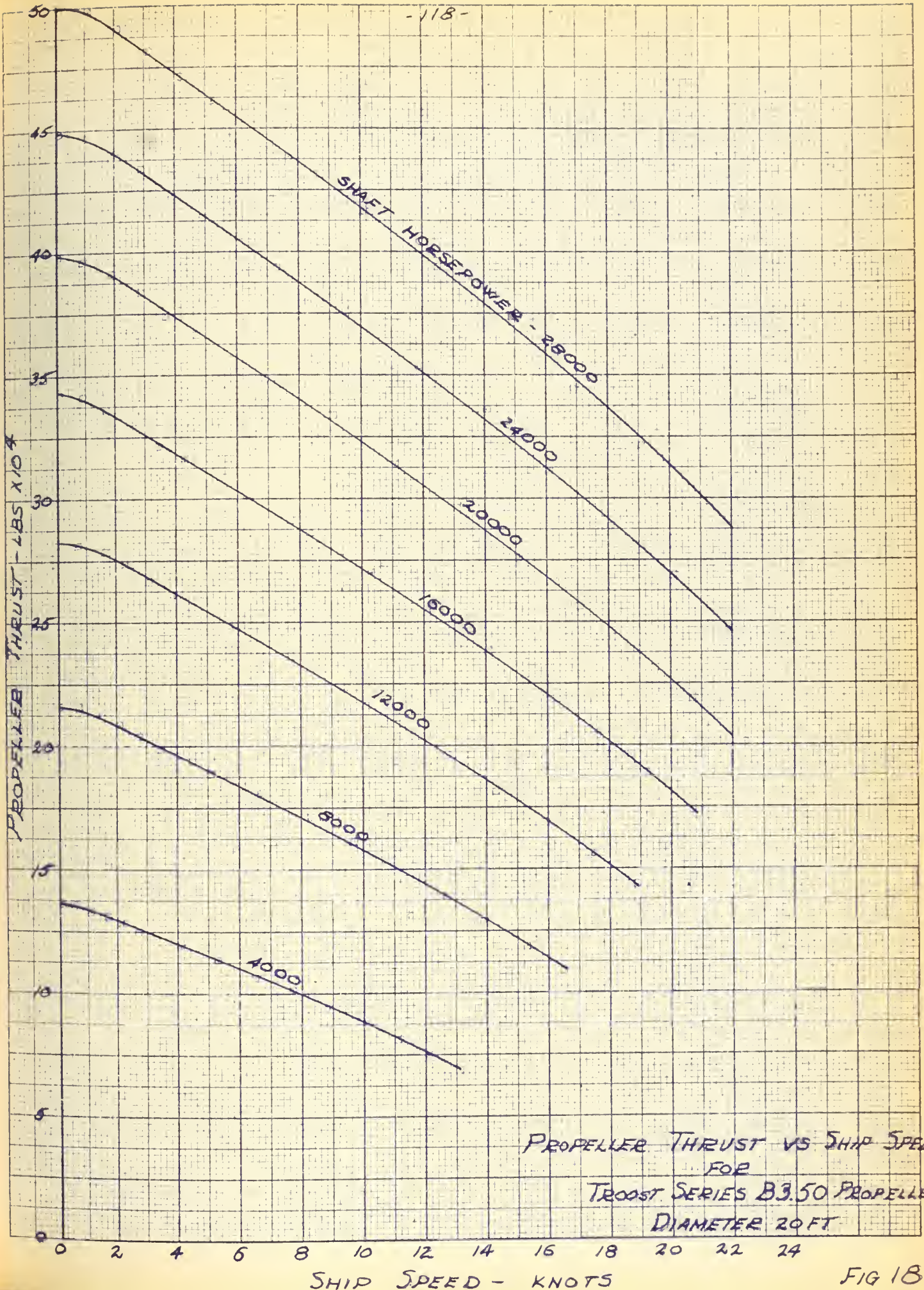


FIG 17







PROPELLER THRUST VS SHIP SPEED  
FOR  
TROOST SERIES B3.50 PROPELLER  
DIAMETER 20 FT

FIG 18





# PROPELLER THRUST

VS

## SHIP SPEED

FOR

### TROOST SERIES 83.50 PROPELLER

### DIAMETER 25 FT

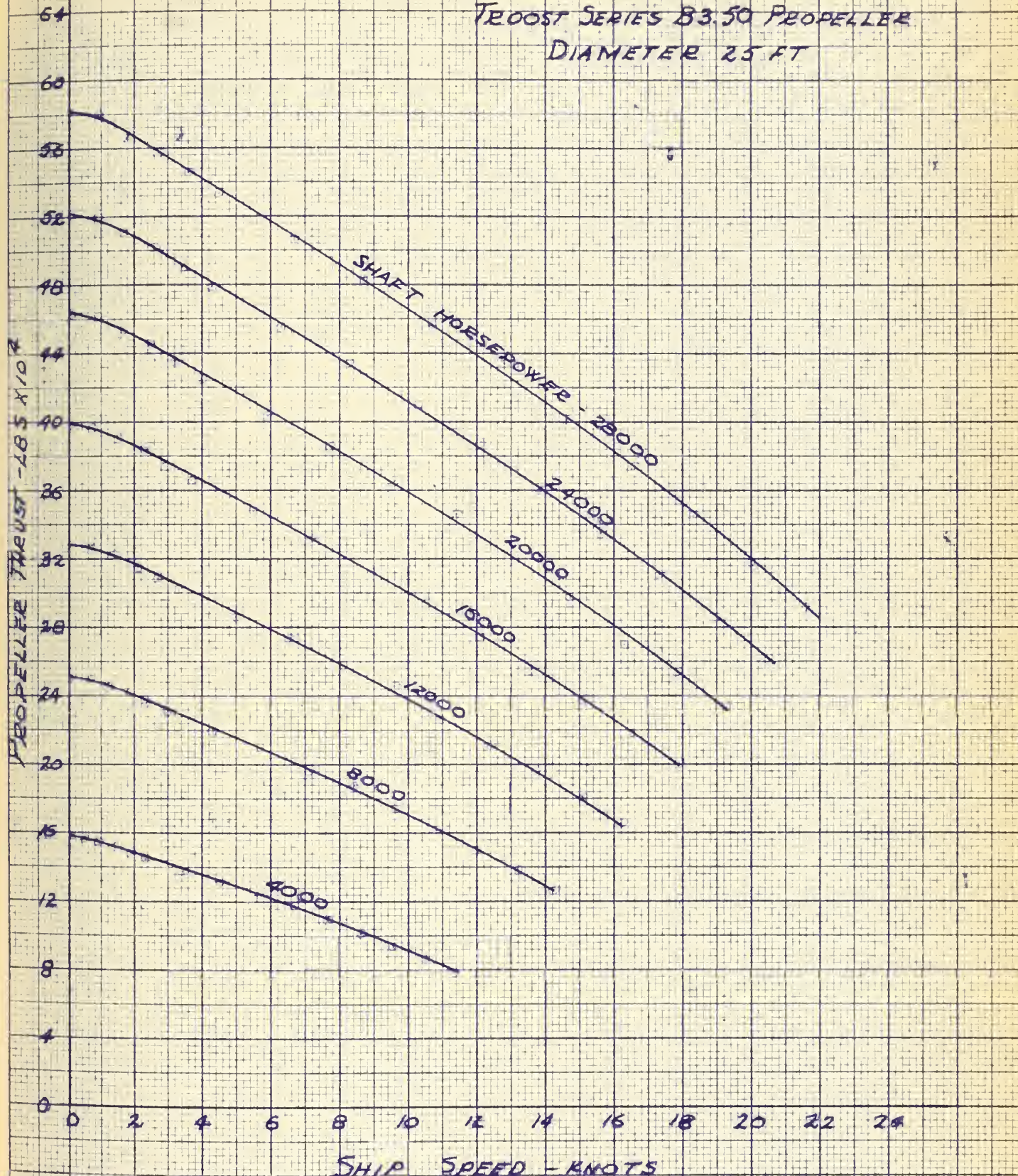


Fig 19





# PROPELLER THRUST VS

SHIP SPEED  
FOR

TROOST SERIES B3.50 PROPELLER  
DIAMETER 30 FT

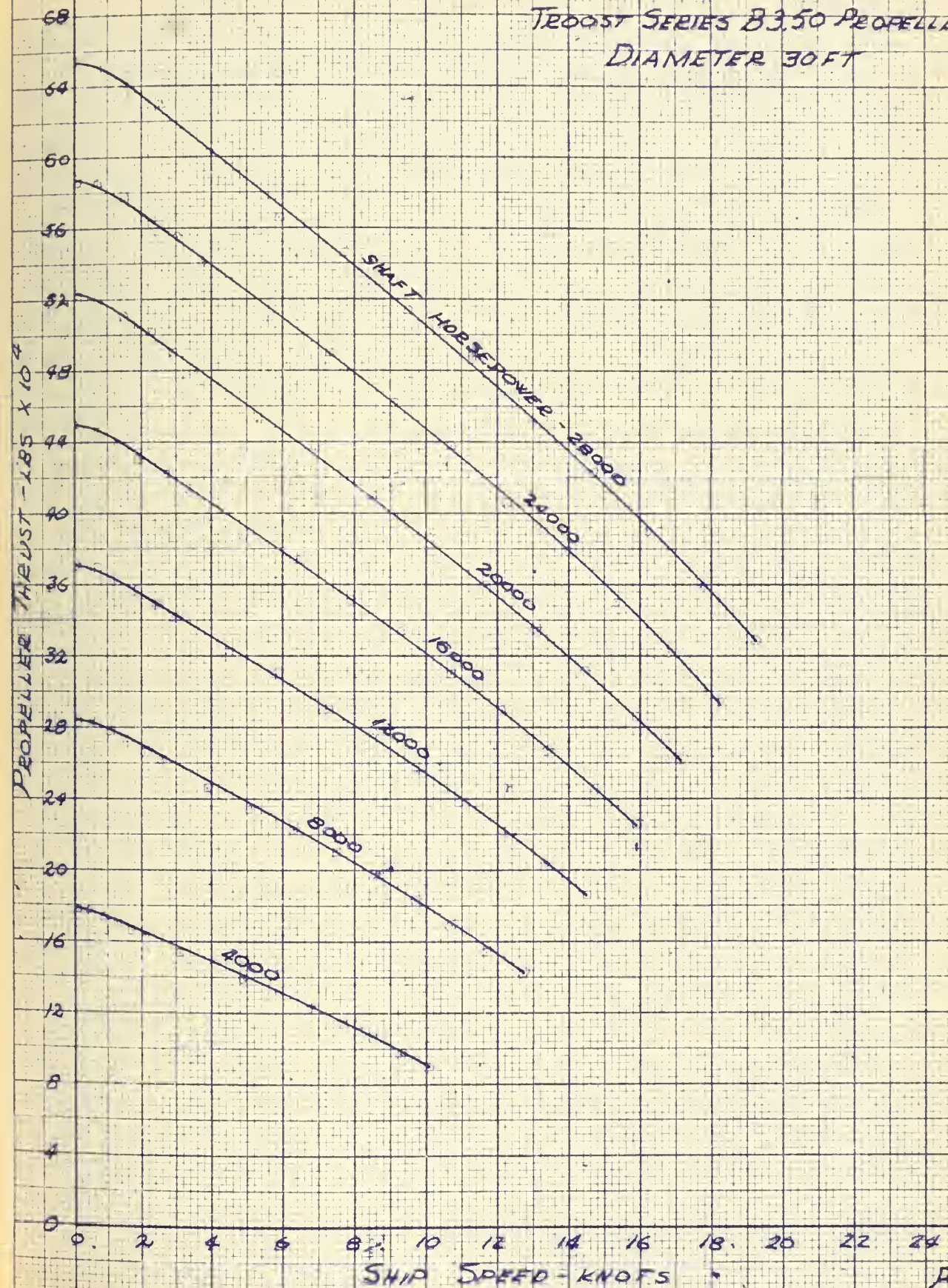
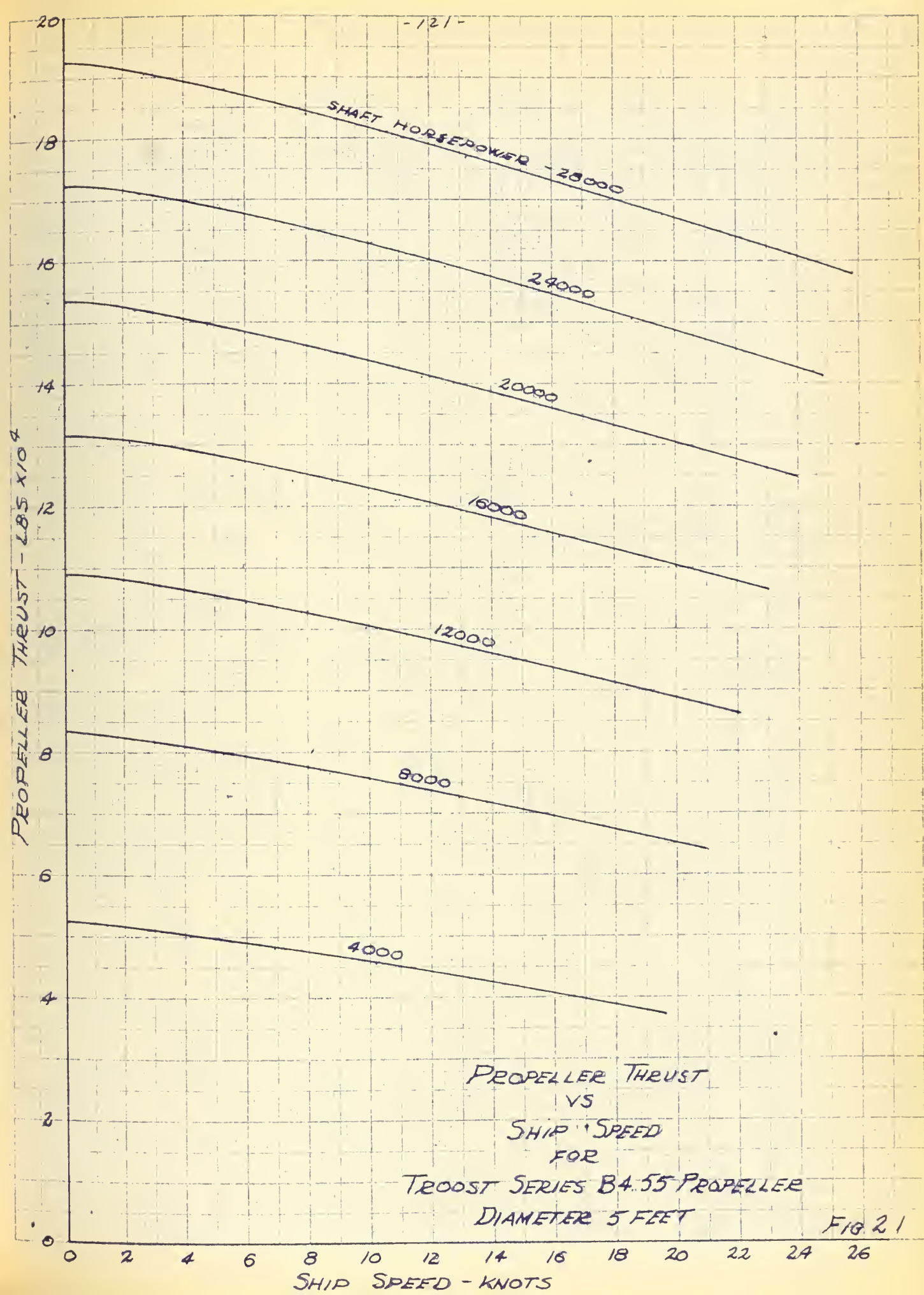
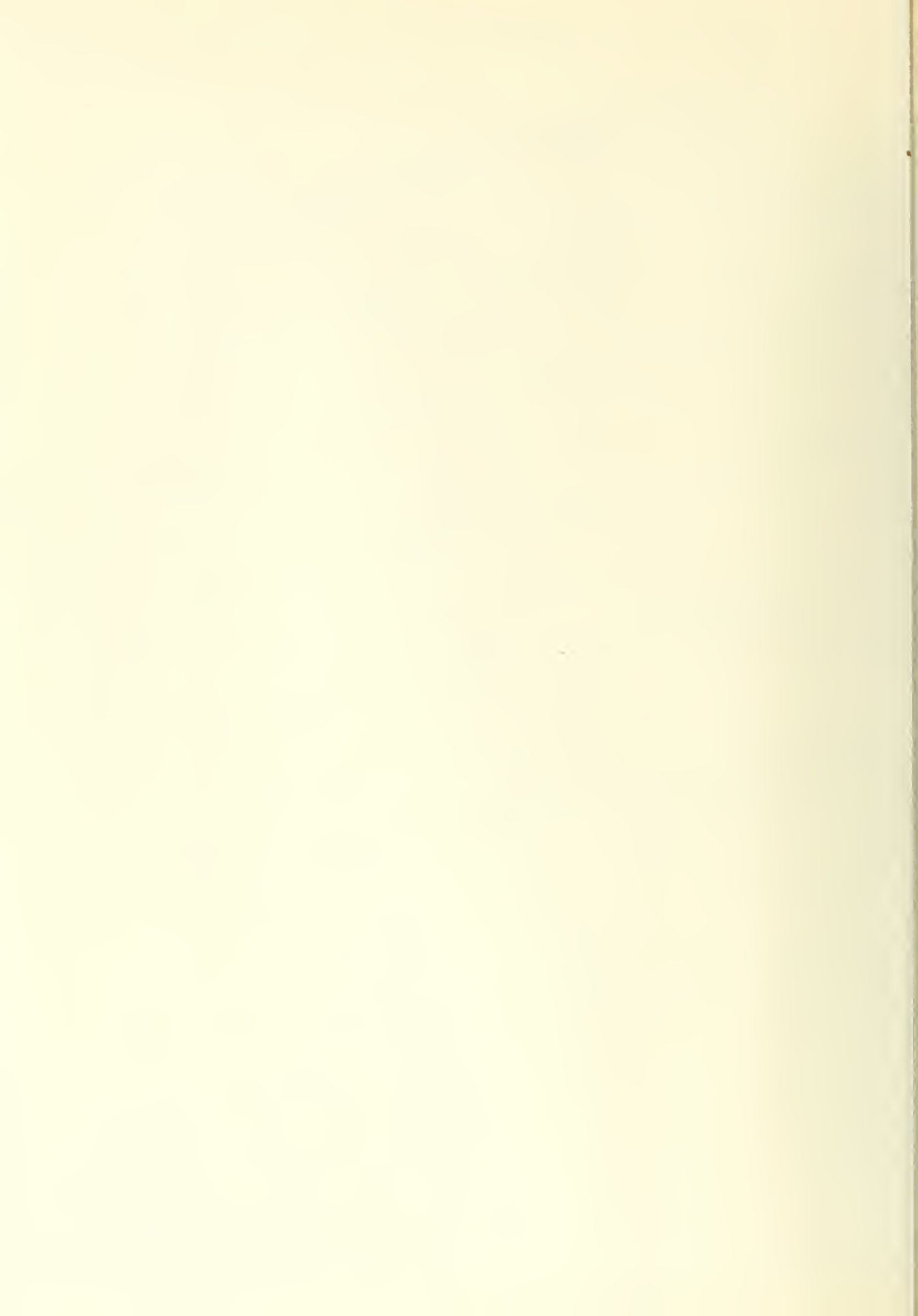


FIG 20









PROPELLER THRUST  
VS  
SHIP SPEED  
FOR

TROOST SERIES B4.55 PROPELLER  
DIAMETER 10 FEET

PROPELLER THRUST - LBS X 10<sup>4</sup>

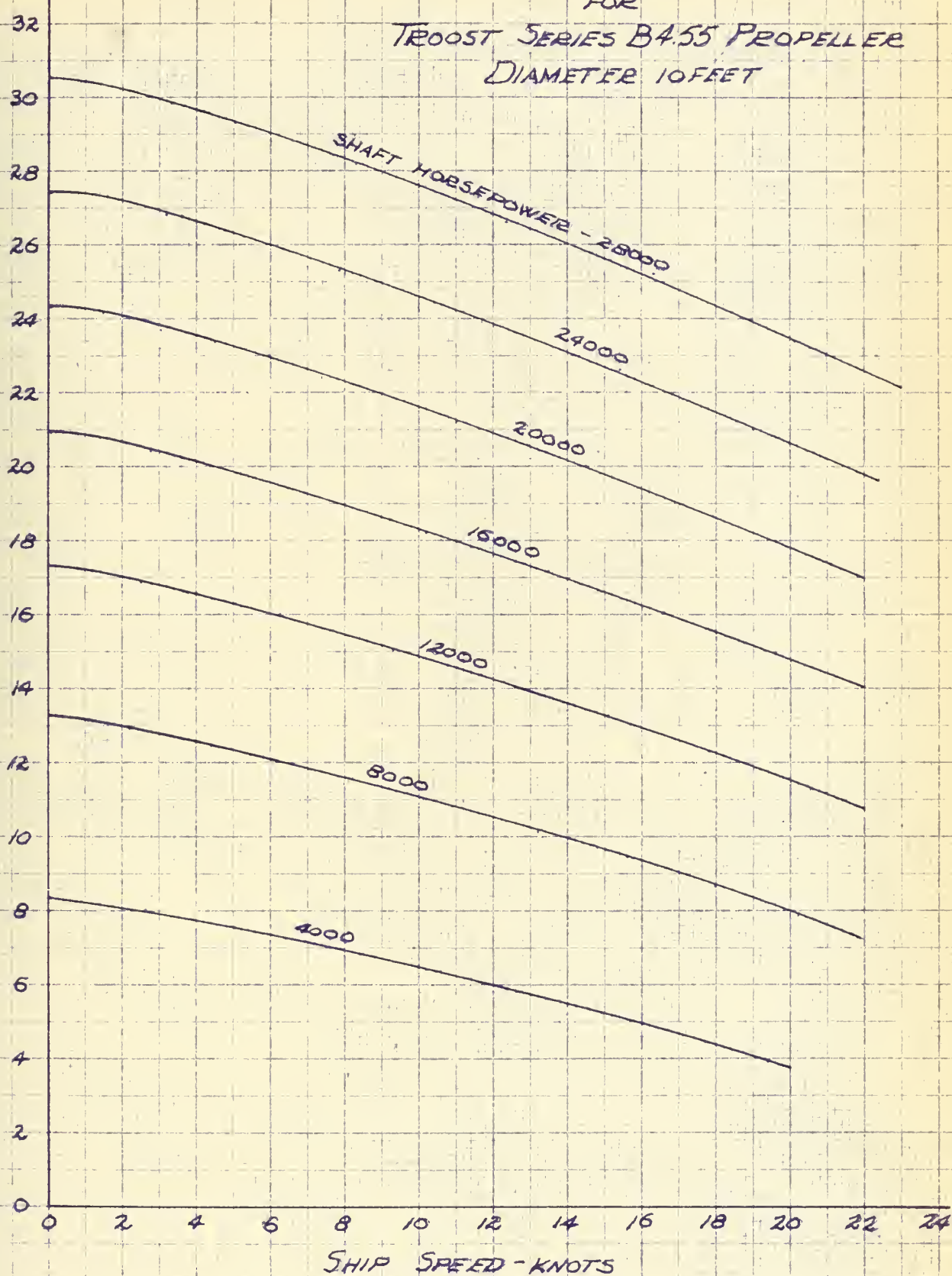


FIG 22





# PROPELLER THRUST VS

SHIP SPEED

FOR

TROOST SERIES B4.55 PROPELLER

DIAMETER 15 FEET

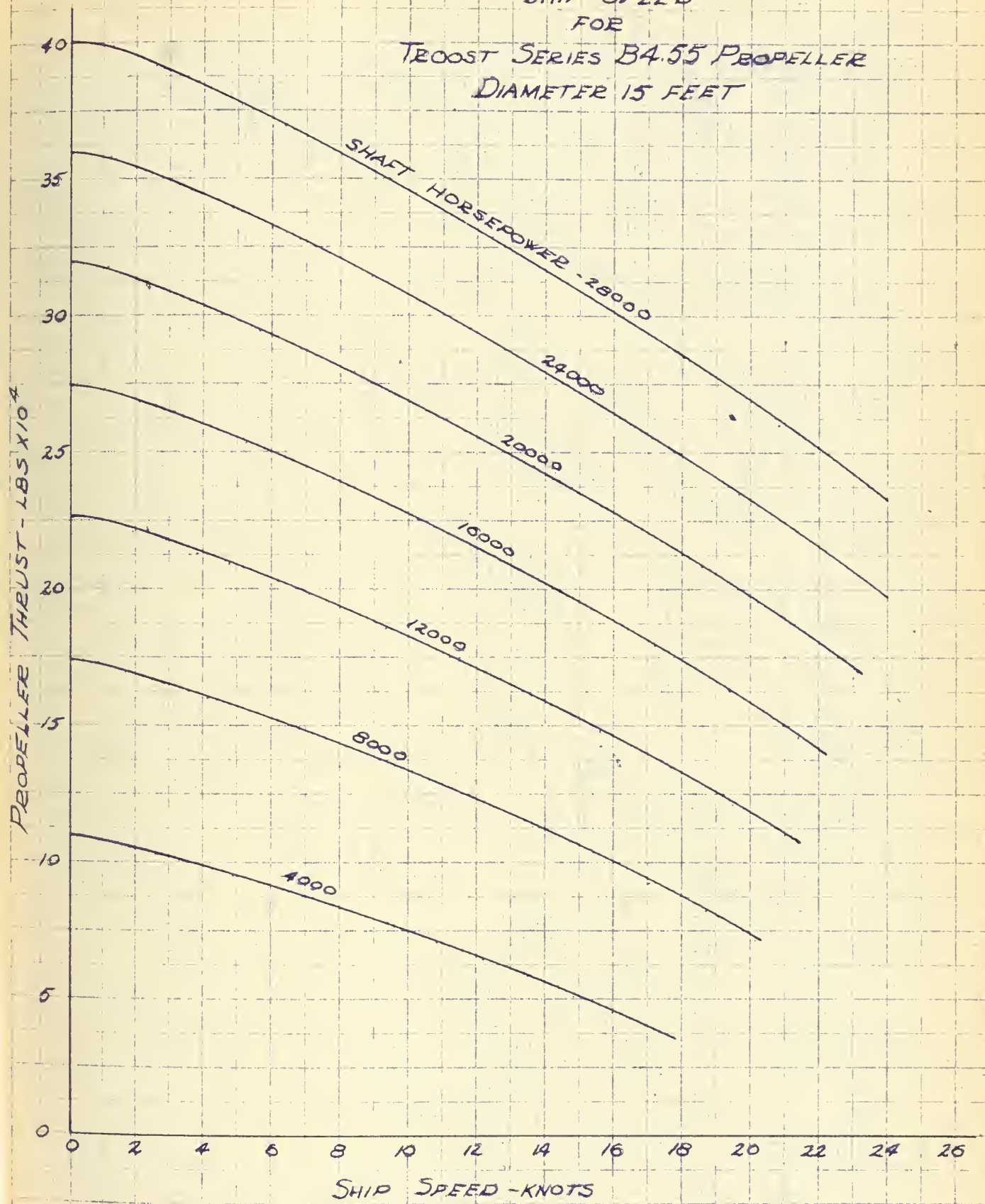


FIG 23



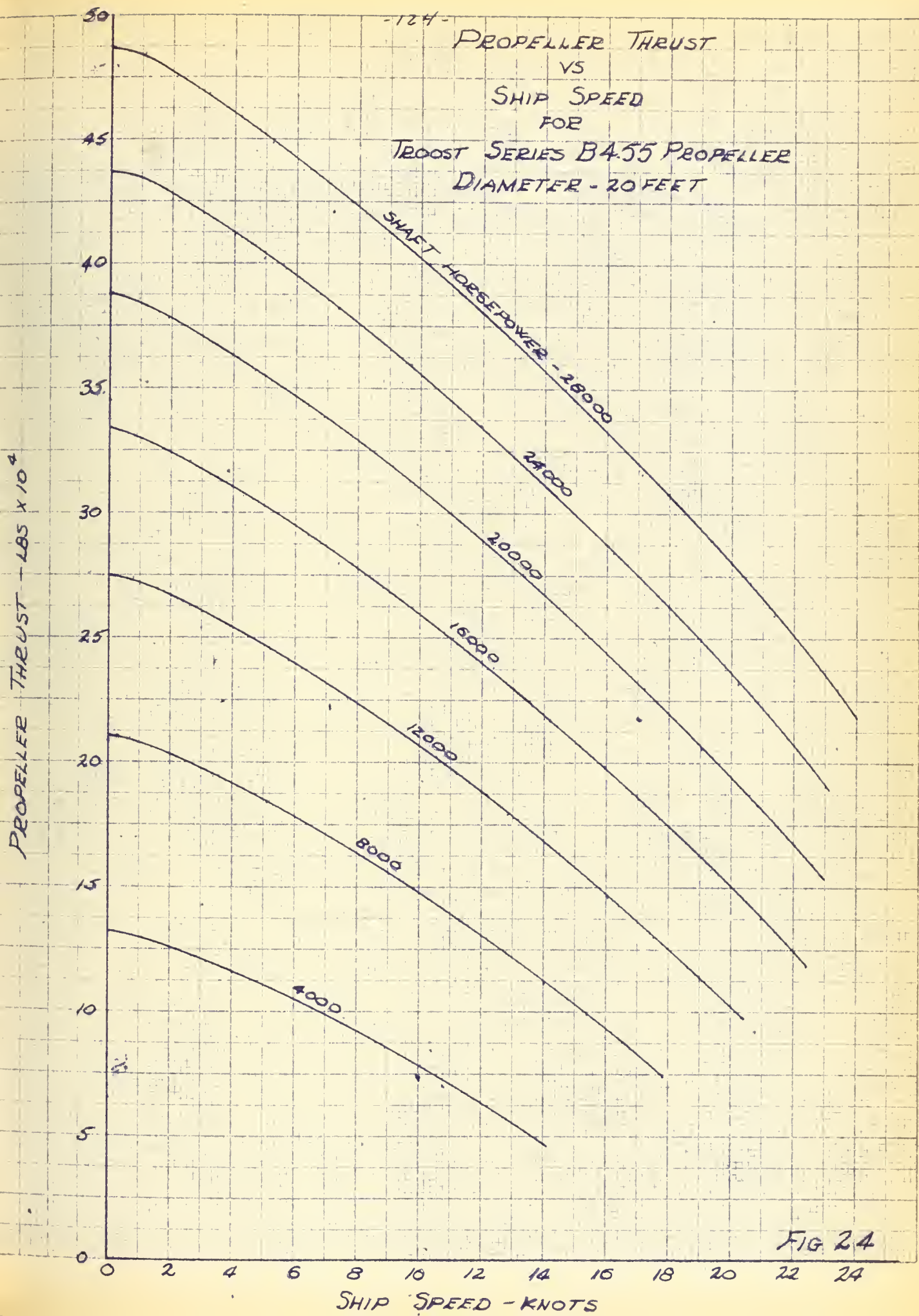


FIG 24





PROPELLER THRUST  
VS  
SHIP SPEED  
FOR  
TROOST SERIES B4.55 PROPELLER  
DIAMETER - 25 FEET

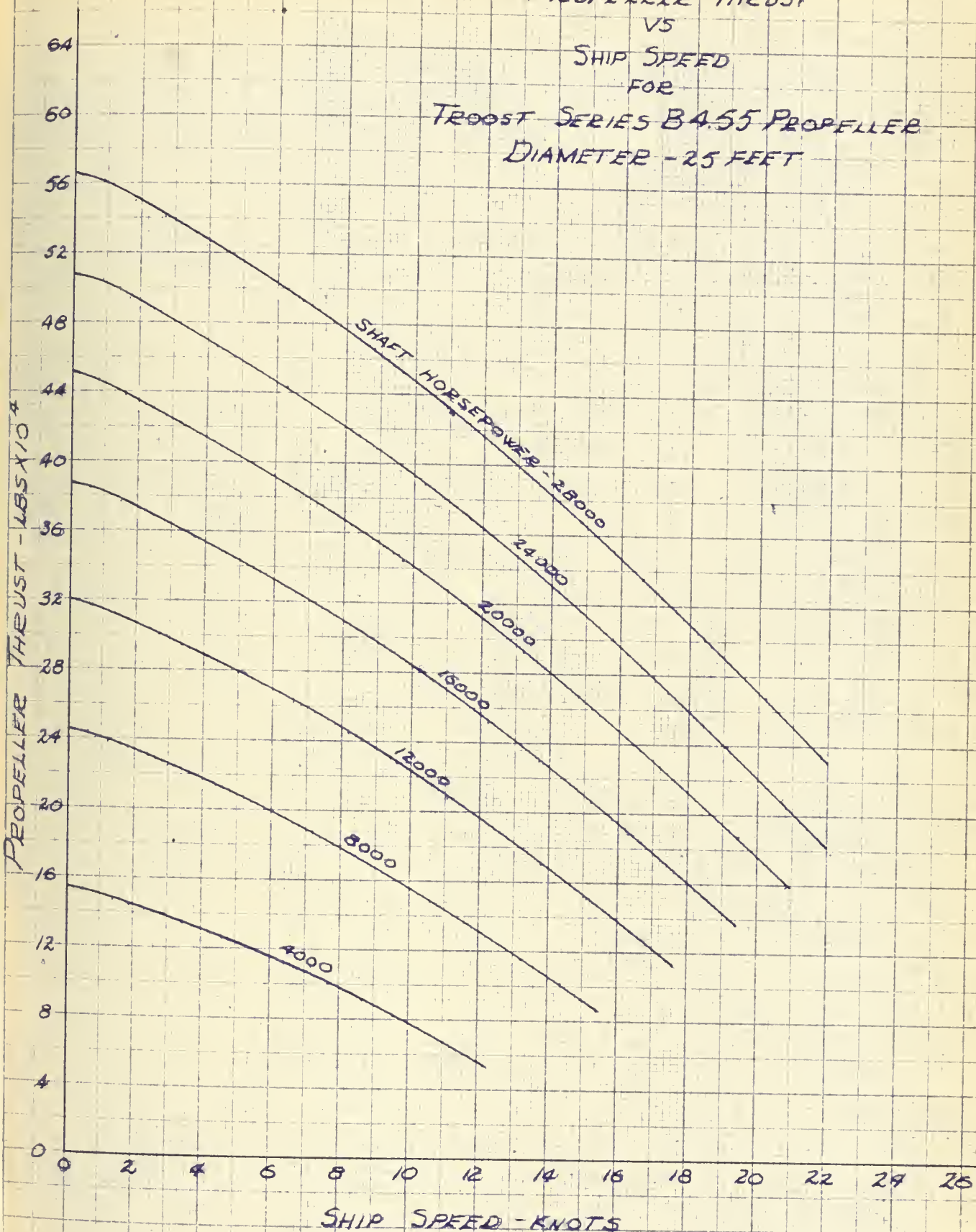
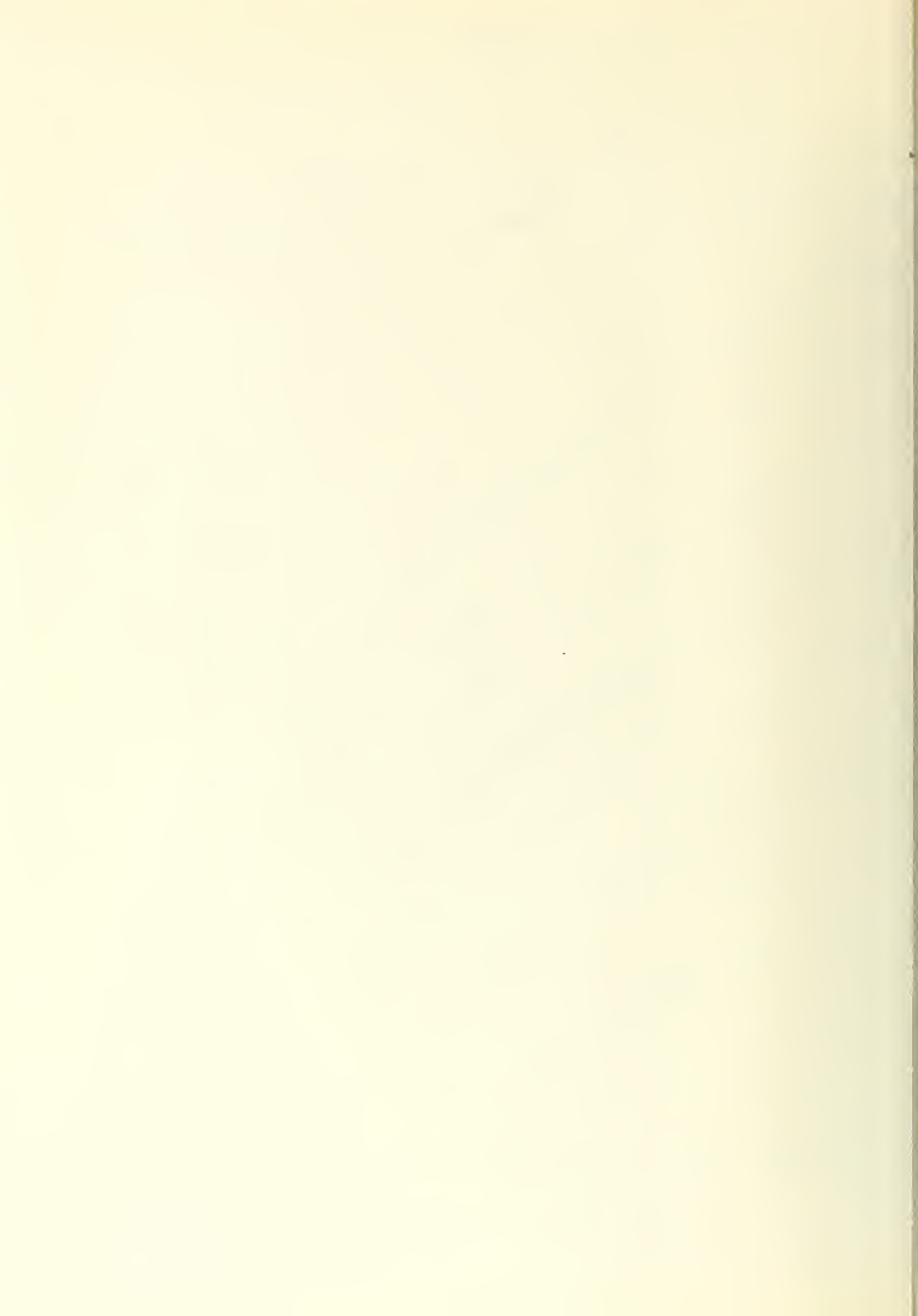
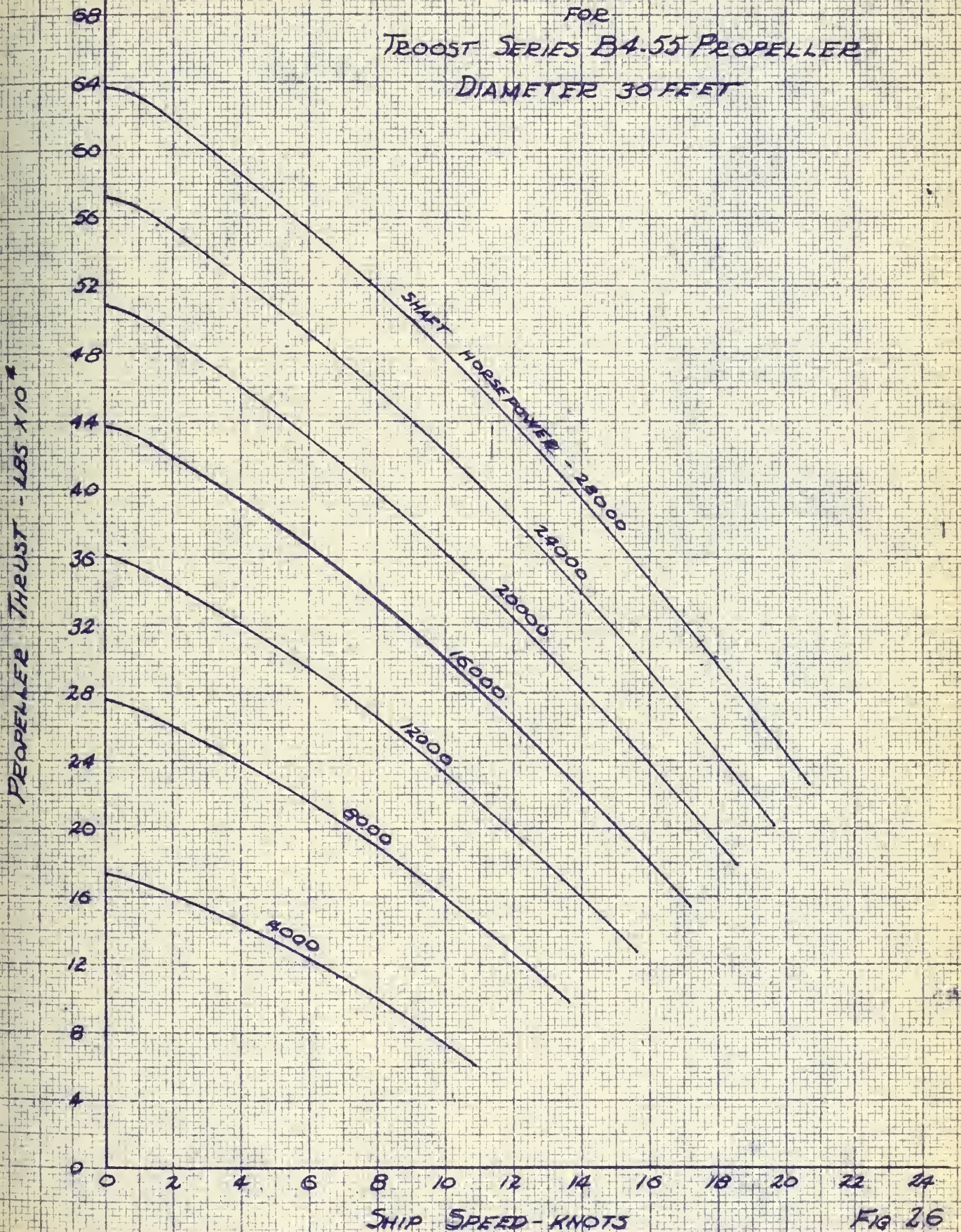


FIG 25





PROPELLER THRUST  
VS  
SHIP SPEED  
FOR  
TROOST SERIES B4.55 PROPELLER  
DIAMETER 30 FEET







of  $\phi^{1/3}$ . Hence for a given propeller diameter and shaft horsepower per shaft we may determine the value of  $\phi^{1/3}$  for any desired ship speed from

$$\phi^{1/3} = \frac{VD^{2/3}}{2.54 P^{1/3}}$$

We can then select the corresponding value of  $\delta^{1/3}$  and determine the thrust at the given speed as

$$T' = 156 P^{2/3} D^{2/3} \delta^{2/3} \text{ lbs/shaft}$$

For this purpose an investigation of the variation of  $\delta^{1/3}$  as a function of  $\phi^{1/3}$  was made for the Troost series propellers B3-50 and B4-55. The results are shown in figures <sup>27</sup>33 and <sup>28</sup>34.

We can, if we wish, eliminate the use of figures <sup>27</sup>33 and <sup>28</sup>34 by means of an empirical relationship determined by curve fitting. If we carry this through we find that for the Troost series B3-50 propeller the straight line variation

$$\delta^{1/3} = 0.484 - 0.1 \phi^{1/3}$$

gives a maximum possible error in  $\delta^{1/3}$  of only about 2%. In like manner, for the Troost series B4-55 propeller the straight line variation

$$\delta^{1/3} = 0.487 - 0.119 \phi^{1/3}$$

gives a maximum possible error in  $\delta^{1/3}$  of only about 4%. Hence if we can accept these percentage errors in our preliminary powering analysis we have for the series B3-50

$$\delta^{1/3} = 0.489 - 0.0394 \frac{VD^{2/3}}{P^{1/3}}$$

Hence

$$T' = 156 P^{2/3} D^{2/3} \left[ 0.489 - 0.0394 \frac{VD^{2/3}}{P^{1/3}} \right] \quad (40)$$

And for the series B4-55

$$\delta^{1/3} = 0.487 - 0.0468 \frac{VD^{2/3}}{P^{1/3}}$$





VARIATION OF  $\delta/\mu^{2/3}$  AS A FUNCTION  
OF  $\phi/\mu^{1/3}$  FOR TBOOST SERIES  
B9.50 PROPELLER

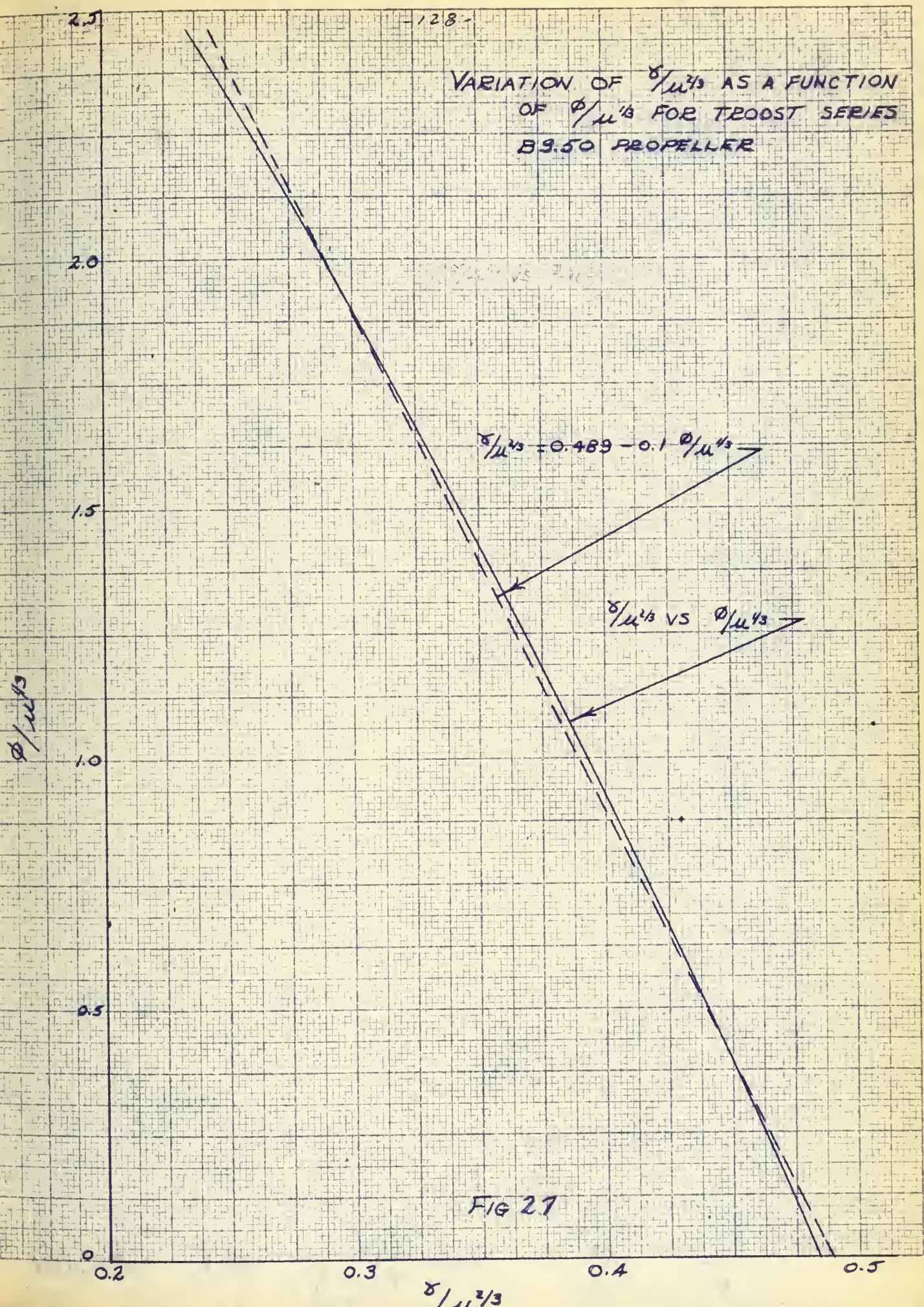


FIG 27





VARIATION OF  $\delta/\mu^{1/3}$  AS A FUNCTION  
OF  $\phi/\mu^{1/3}$  FOR TROOST SERIES  
B 4.55 PROPELLER

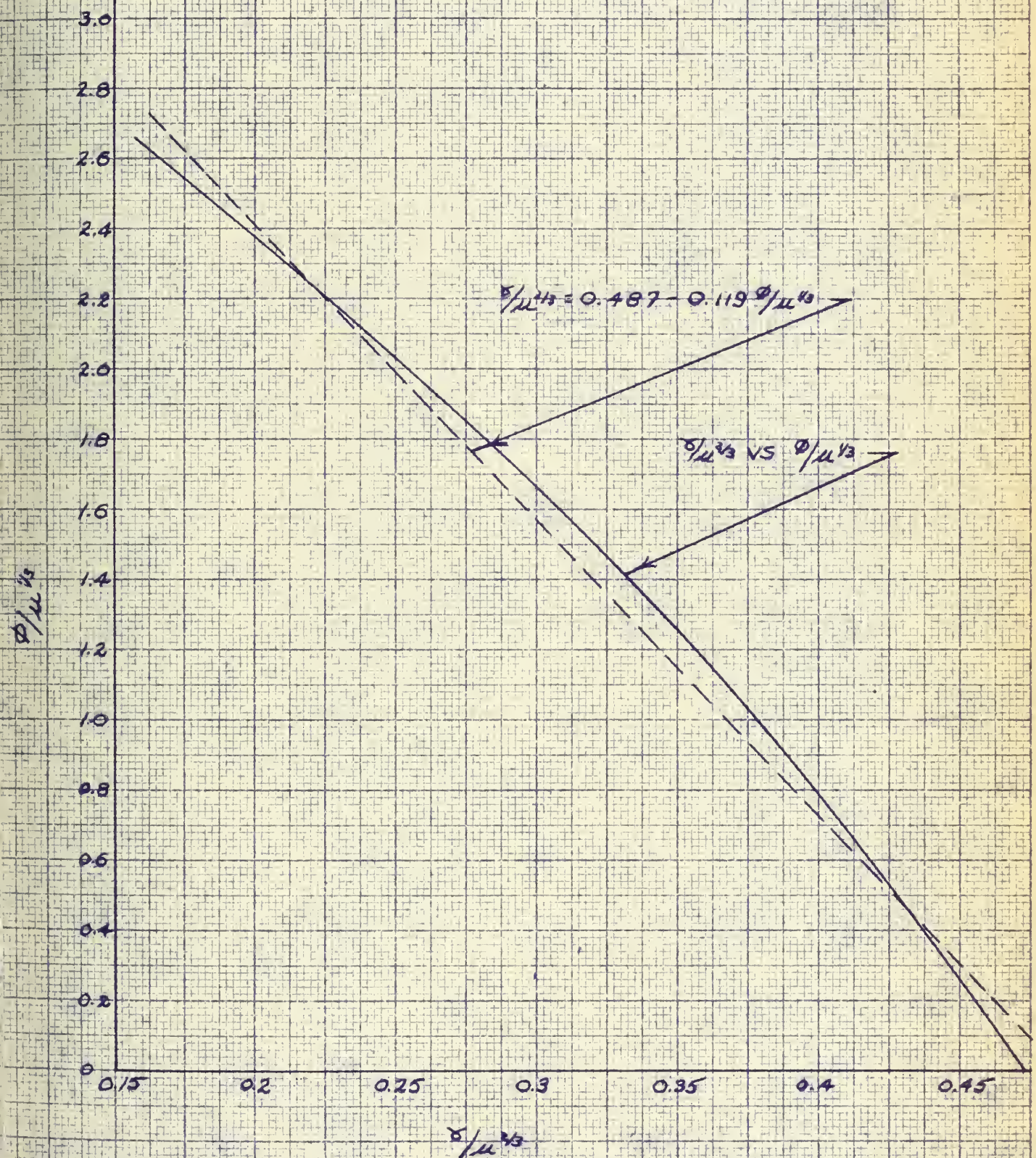


FIG 28





hence

$$T' = 156 P^{1/3} D^{1/3} (0.48) = 0.0468 \frac{V D^{4/3}}{P^{1/3}} \quad (41)$$

The thrust produced by a given propeller can be materially affected by the size of hub installed and the thickness of the propeller blades. This is especially true in the case of icebreakers which often employ detachable blade propellers with their inherently large hubs and blades of very thick section so as to achieve reasonable root stresses when operating in ice. Because of this fact, the values of propeller thrust predicted for a given blade from data presented in this section should be modified to reflect the influence of hub diameter and blade thickness.

Let us first consider the effect of propeller hub diameter. Shultz, in his paper The Ideal Efficiency of Optimum Propellers having Finite Hubs and Finite Number of Blades <sup>(110)</sup> reports on work done at the Taylor Model Basin on the effect of hub diameter on developed propeller thrust. His results are presented as plots of the variation of ideal thrust Coefficient ( $C_{t_i}$ ) as a function of advance coefficient ( $\lambda$ ) for various ratios of hub diameter to propeller diameter. In order to make use of this data, let us consider

$$\eta_i = \text{ideal propeller efficiency} = \frac{\tan \beta}{\tan \beta_i}$$

where

$$\tan \beta = \frac{v_a}{\pi n D} = \frac{101.3 V (1-w)}{\pi N D}$$

$$\tan \beta_i = \frac{p_0}{\pi D}$$

at zero angle of attack

Therefore

$$\eta_i = \frac{101.3 V (1-w)}{N p_0}$$

In addition

$$\lambda = \text{advance coefficient} = \tan \beta$$

$$= \frac{v_a}{\pi n D} = \frac{101.3 V (1-w)}{\pi N D}$$



Previously we stated that for the B3-50 series propeller  $\tau_0/D = 0.57$  and for the B4-55 series propeller  $\tau_0/D = 0.515$ . Substituting for propeller pitch

and using our selected value of  $\tau = 0.18$  we have

$$\lambda = \frac{26.45V}{ND}$$

$$\eta_i = \frac{154.3V}{ND}$$

B3-50 series

$$\lambda = \frac{26.45V}{ND}$$

$$\eta_i = \frac{151.8V}{ND}$$

B4-55 series

Noting that speed coefficient  $J$  is defined as

$$J = \frac{v_a}{ND} = \frac{23.3V}{ND}$$

we have

$$\lambda = 0.318 J$$

B3-50 and B4-55 series

$$\eta_i = 1.855 J$$

B3-50 series

$$\eta_i = 1.94 J$$

B4-55 series

Over the normal range of  $J$  for icebreaker operation we may now investigate the variation of  $C_{Tc}$  as a function of propeller hub diameter. This was done for the three and four bladed propeller and the results are presented as figures ~~35A and 35B~~ <sup>29 & 30</sup>.

The data presented in this section on developed propeller thrust was obtained from the Troost propeller series wherein the test propellers used had values of hub diameter to propeller diameter of

$$X_h = 0.180 \quad 3 \text{ blade series}$$

$$X_h = 0.167 \quad 4 \text{ blade series}$$

The actual thrust developed by a given propeller, therefore, is

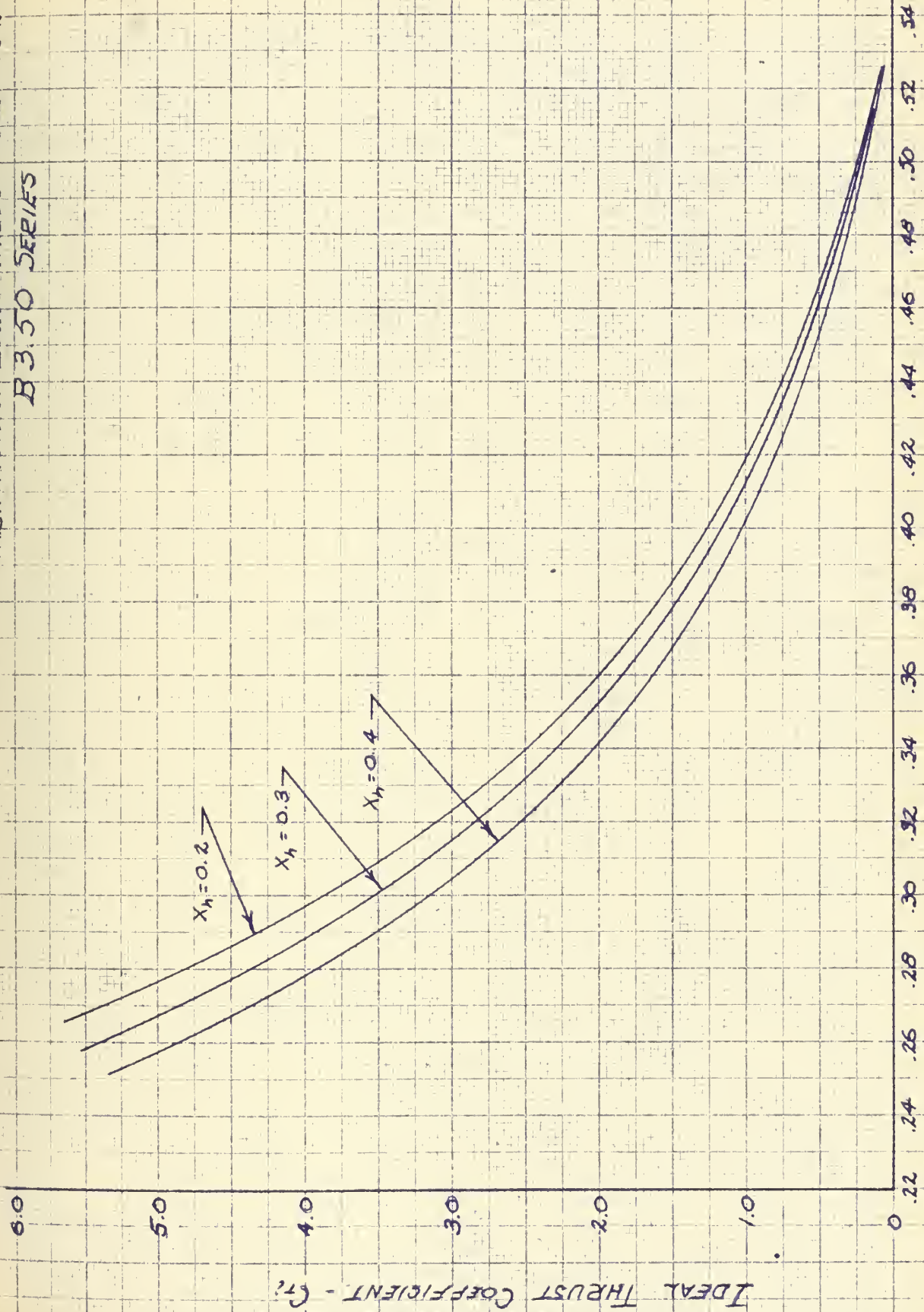
$$T = K T_{\text{Troost}}$$

where  $K$  is a constant representing the reduction in propeller thrust due to





# VARIATION OF IDEAL THRUST COEFFICIENT B3.50 SERIES

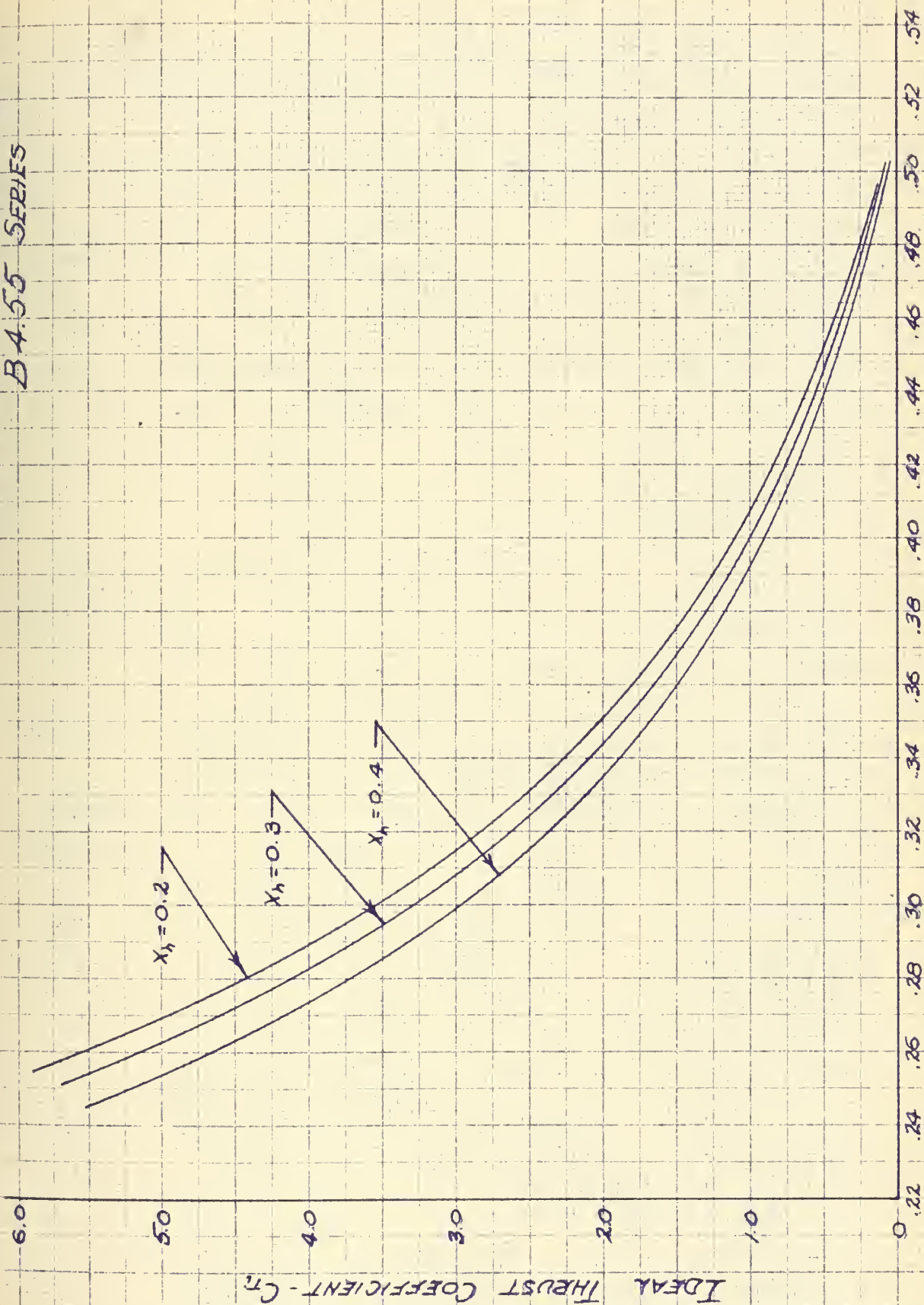


SPEED COEFFICIENT -  $J = V_a/hd$

FIG 29



VARIAION OF IDEAL THRUST COEFFICIENT  
B4.55 SERIES



SPEED COEFFICIENT -  $J = \frac{v_0}{a_0}$

FIG 30





hubs whose  $X_h$  is larger than those actually used by Troost. For the conventional solid propeller blades used on icebreakers

$$X_h \approx 0.21 - 0.22$$

For the built up or detachable blade propeller

$$X_h \approx 0.32 - 0.35$$

Due to these increased hub diameters, the ideal thrust coefficient is reduced about 3% with the solid propeller and about 14% with the detachable blade propeller. Consequently, the thrust data presented in figures 9, 12 AND 15 through 26 must be modified so that

$$T_{ACTUAL} = 0.97 T \quad \text{solid propeller}$$

$$T_{ACTUAL} = 0.86 T \quad \text{detachable blade propeller}$$

to take account of propeller hub diameter.

Let us now consider the effect upon developed propeller thrust of varying blade thickness. Burrill in his paper Calculation of Marine Propeller Performance Characteristics (99) considers the effect of varying propeller thickness to cord ratio upon the lift and drag coefficients of a normal OGIVAL propeller blade. By means of this data we can estimate the effect of blade thickness upon developed thrust.

It can be shown that the propeller efficiency  $\eta_p$  may be expressed as

$$\eta_p = \eta_b \eta_o$$

where

$$\eta_b = \text{blade efficiency} = \left( \frac{1 - 2 \epsilon}{1 + \frac{2 \epsilon}{3 \mu}} \right)$$

$$\epsilon = \text{Drag lift ratio} = c_d / c_l$$

$$\mu = \text{Tangent of hydrodynamic pitch angle}$$

$$= \tan \beta_c = \frac{p_o}{\pi D} \quad \text{at zero angle of attack}$$





If we consider first the Troost series B3-50 propeller whose sections all have a zero angle of attack, we have

$$y = \frac{p}{\pi D}$$

We have previously shown that for optimum performance with this propeller

$$p_{0,D} = 0.54$$

therefore

$$y = 0.172$$

and

$$\eta_0 = \frac{1 - 0.344\epsilon}{1 + 3.88\epsilon}$$

Based on data published by Burrill in his paper Calculation of Marine Propeller Performance Characteristics, we can determine the value of  $\epsilon$  as a function of blade thickness-cord ratio for blades of the normal ogival shape. A reproduction of this data are shown as figures 31 AND 32

From data on the series B3-50 propeller we can determine that the thickness-cord ratio ( $t/c$ ) at the seven tenths radius is

$$t/c = 0.0467$$

Therefore, from figure 31 we can determine that the lift coefficient for the blade section is

$$C_L = 0.235$$

and from figure 32 the drag coefficient as

$$C_D = 0.007$$

hence

$$\epsilon = 0.0383$$

and

$$\eta_0 = 0.801$$

For a typical three bladed propeller used on present day icebreakers

$$t/c \approx 0.09$$



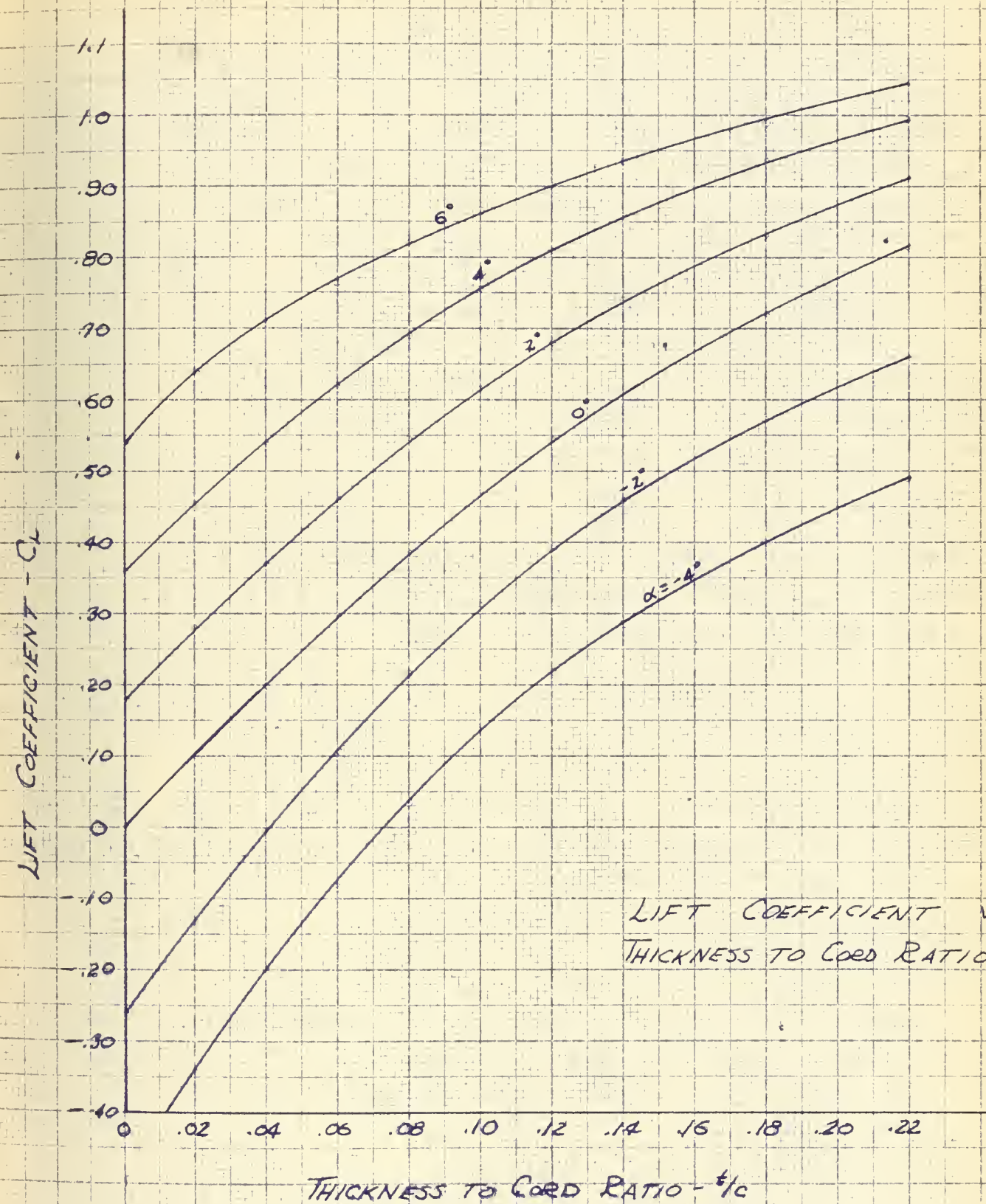


FIG 31





# VARIATION OF DRAG COEFFICIENT AS A FUNCTION OF THICKNESS CORD RATIO

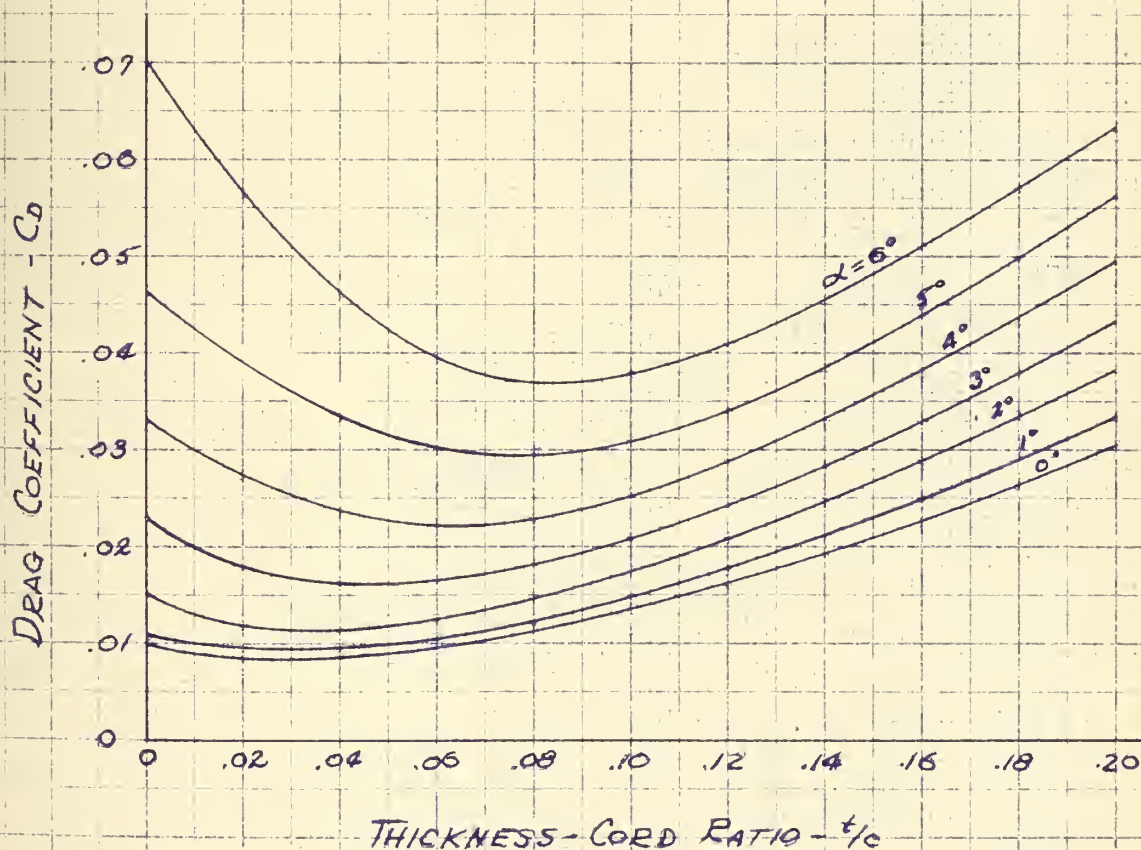
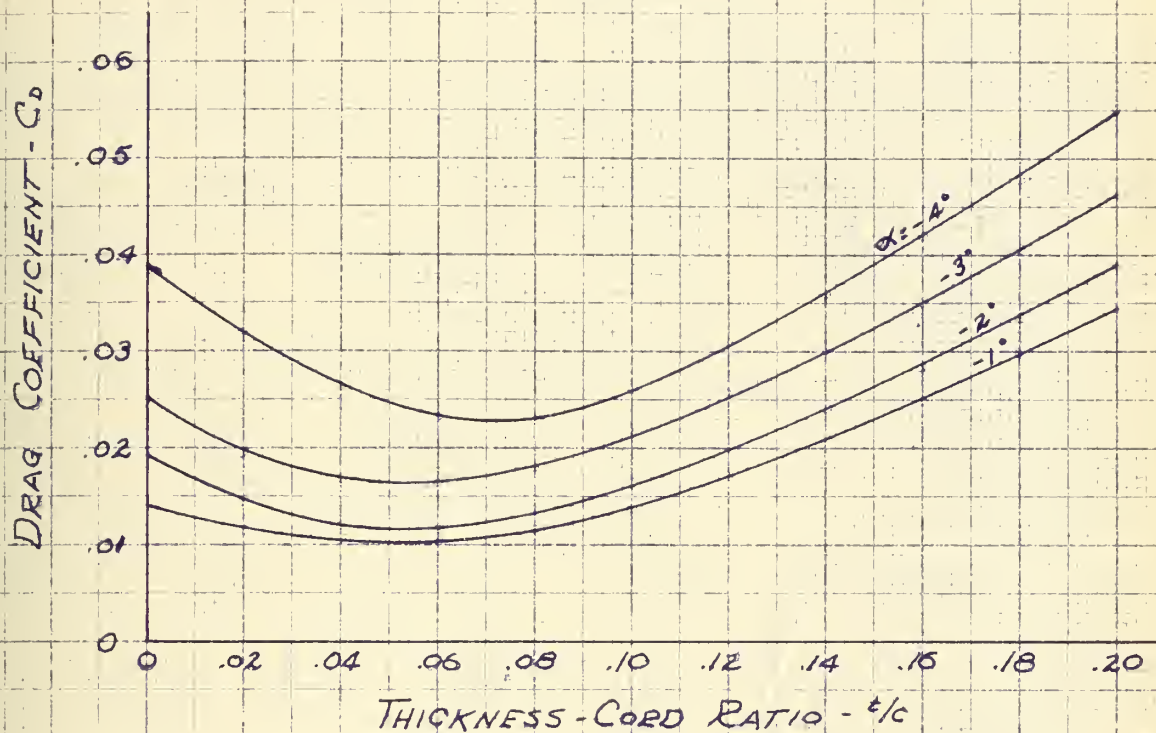


FIG 32





at the 0.7 radius. This large thickness is necessary from a strength viewpoint for operation in ice. In order for the blade section to develop the same lift as our B3-50 series propeller, it must be designed with an angle of attack of

$$\alpha = -2.4^\circ \quad (\text{Figure 31})$$

and a resulting pitch of

$$\begin{aligned} p_o &= \pi D \tan(\beta_c - \alpha) \\ &= 0.406 D \end{aligned}$$

With this angle of attack and thickness-cord ratio, the drag coefficient of the section from figure <sup>32</sup> ~~35E~~ is

$$C_D = 0.017$$

hence

$$\epsilon = 0.0724$$

and

$$\gamma_o = 0.762$$

Consequently, by use of the thicker blade section, we have suffered a 11.5% reduction in blade efficiency and hence propeller efficiency. Since thrust delivered is a direct function of propeller efficiency this percentage reduction will be reflected in the thrust delivered.

In like manner, for the B4-55 series propeller we have

$$\epsilon_c = 0.073$$

Hence from figure 31 for zero angle of attack

$$C_L = 0.355$$

and from figure 32

$$C_D = 0.0108$$

hence

$$\epsilon = 0.0304$$



For this propeller, however, we have shown that for optimum performance

$$p_o/D = 0.515$$

therefore

$$y = 0.164$$

and

$$\gamma_o = \frac{1 - 0.328 \epsilon}{1 + 4.07 \epsilon}$$

Based on our above value of  $\epsilon$  we have for this propeller

$$\gamma_o = 0.833$$

There is little data available on the characteristics of four bladed propellers presently used on ice breakers. However, since from a strength viewpoint a propeller blade is similar to a cantilever beam, and since the blade sections of a four bladed propeller must have about the same unit strength as the three bladed type, it would seem reasonable to assume that

$$\tau_c \approx 0.07$$

for the four bladed propeller sections at the 0.7 radius. In order for this blade section to develop the same lift as our B4-55 series propeller section, it must be designed with an angle of attack of

$$\alpha = -1^\circ \quad (\text{Figure 31})$$

and a resulting pitch of

$$p_o = \pi D \tan(\beta_o - \alpha) \\ = 0.457 D$$

With this angle of attack and thickness-cord ratio, the drag coefficient for the section from figure 32 is

$$C_D = 0.0128$$

hence

$$\epsilon = 0.03605$$

and

$$\gamma_o = 0.862$$



Hence, there results a 2.05% reduction in blade efficiency due to the use of the thicker blade section, which reduction is directly reflected in developed propeller thrust.

Based on the above development, therefore, we may say that as a first approximation

$$T_{ACTUAL} = K_L T_{TROOST}$$

Where  $K_L$  is a reduction factor to reflect the effect of thicker blade sections. The values of  $K_L$  may be stated as

$$K_L = 0.885 \quad \text{3 bladed propeller}$$

$$K_L = 0.98 \quad \text{4 bladed propeller}$$

In review, therefore, we note that we cannot use propeller thrust values directly as obtained from Troost data and as shown in figures 9, 12 and 15 through <sup>25</sup>32. Rather, these values must be modified so as to reflect the thicker blade sections and larger propeller hub used on actual icebreaker installations. Consequently, in all our subsequent work, where reference is made to propeller thrust, actual thrust shall be used, where

$$T_{ACTUAL} = K_1 K_L T_{TROOST}$$

and	$K_1 = 0.97$	solid propeller
	$= 0.86$	built up propeller
	$K_L = 0.885$	3 bladed propeller
	$= 0.98$	4 bladed propeller





141

Section F

Mechanics of Icebreaking



## Part 1

### Theoretical Predictions of the Stresses in an Ice Field

The nature of the action of an icebreaker in breaking ice is two fold. The ship forms a channel of open water in moving through the ice. The end of this channel is basically shaped in the form of the bow plan at the water-line. As the ship moves into this wedge, it exerts a force in the plane of the ice sheet and, in addition, a force normal to the ice sheet as the ship rides up onto the ice. The nature of the stresses arising from these two sets of forces is different.

The forces exerted in the plane of the ice sheet cause a state of plane stress to be established in the ice which ultimately produces failure in the form of long radial cracks emanating from the stern of the vessel. The second set of forces, normal to the ice field, produce bending in the ice sheet which eventually causes the ice to crack radially from the center of loading due to tension in the bottom most fibres of the ice. As this loading increases the radial cracks lengthen and increase in number until finally a circumferential crack, roughly at right angles to the radial cracks, is formed caused by tension on the uppermost fibres of the ice sheet. The details of the icebreaking process, as well as the overall effects, depend upon which type of failure occurs first. For the case of relatively thin ice there is considerable photographic evidence to show that the radial cracks are sufficient to cause the ice to fail before any bending forces can be generated, hence failure of the ice is due to forces arising from the ramming motion of the vessel in the plane of the ice sheet. In the case of greater ice thickness, however, it seems pretty certain from



experimentation that failure is primarily due to the forces normal to the ice field. Here what minor cracks are caused by the stresses in the plane of the ice sheet are lengthened and increased in number by the tension bending stresses in the bottom of the ice sheet, then as loading is increased, circumferential cracks are formed due to tension in the top of the ice sheet and the ice fails by breaking at these circumferential cracks. This later case is characterized by the vessel riding up onto the ice sheet to generate normal forces and is most characteristic for the general arctic and antarctic conditions. It is this later case which shall be our primary interest.

To illustrate the nature of the stresses which arise in an ice field during the passage of an ice breaker, it is convenient to consider the ice field as a continuous, semi-infinite flat plate resting on an elastic foundation, which is subjected to a concentrated load (the vessel) applied at its free edge. In doing this we may neglect the case of failure due to plane stresses and consider only that case which treats with the bending stresses in the ice field as the more critical condition and that upon which the design of an arctic or antarctic icebreaker should be based. Now as the vessel climbs up onto the ice, the ice shelf will deflect due to static and dynamic loading. Due to the deflection there will be set up a potential energy in the ice shelf. When we consider the expression for the deflection we must, by virtue of the dynamic loading, consider this a dynamic problem. Now it can be shown that the natural frequency of a flat rectangular plate may be expressed as

$$f = \frac{\pi}{2} \sqrt{\frac{g D'}{4h} \left( \frac{m^2}{a^2} + \frac{n^2}{b^2} \right)}$$





where

$$m = n = 1$$

$a \text{ \& } b$  = plate dimensions

$$D' = \frac{Eh^3}{12(1-\nu^2)} \quad \text{flexural rigidity of the plate}$$

$d$  = weight per unit volume of plate

$h$  = thickness of plate

hence if  $a = b \rightarrow \infty$  as would be true in an ice field then we may assume for practical application that

$$f = 0$$

Consequently, it would seem reasonable that for our problem, the ice shelf may be considered as a flat rectangular plate under a static concentrated edge load.

The first study of a flat plate on an <sup>elastic</sup> ~~electric~~ foundation was by Hertz, who gave the solution for an infinite plate under the action of a concentrated load. Later Dinuik and Schleicher developed Hertz's solution for a round symmetrically loaded plate. Max Wyman of the University of Alberta also treated this problem of the round, symmetrically loaded flat plate on the elastic foundation and applied his results to the problem of vehicle travel on ice. <sup>(124)</sup>

<sup>(121-123)</sup> Westergaard, in the United States, gave the solution for an infinite plate loaded by a single row of concentrated forces. In addition, during his work on concrete pavement analysis he developed the solution for a semi-infinite flat plate on an elastic foundation loaded by a concentrated force at any point on the plate as well as for the case where the concentrated load is at a free edge. Utilizing Westergaard's method, N. M. Gersevanov at the Institute of Foundations and Substructures studied the unlimited plate, the plate limited by one straight and two parallel straight edges and loaded periodically



by forces in a single row or in a rectangular grid. Shiparo, at the U. S. Army Snow, Ice and Permafrost Research establishment, treated the problem of an infinite strip plate on an elastic foundation under the action of a point load using the Westergaard-Gersevanov method but employing Fourier integrals rather than series solutions.

The above mentioned solutions to the semi-infinite plate problem, have, on occasion, been considered for the investigation of the icebreaker problem. Chenea, Ormondroyd and Naghdi attempted to do so in a joint work in 1950 during an investigation of structural stresses in icebreaking vessels. Unfortunately, however, they did no more than determine the solution of the flat plate problem and neither they nor any others before them applied the results to the evaluation of ice breaker effectiveness.

For the purposes of this paper we will review and compare several solutions to the flat plate problem to see how effectively they predict ice sheet failure. As previously mentioned, we shall not consider stresses in the plane of the plate.

In 1950, Professor Ormondroyd suggested the use of an expression first developed by S. Timoshenko. The expression holds for a semi-infinite slab supported on an elastic foundation and carrying concentrated loads spaced at intervals of "a" along the free edge. When "a" is made very large, the maximum stress on the under surface of the slab just under the load becomes

$$\sigma_{max} = 0.529(1 + 0.54\sqrt{v}) \frac{P}{b} \left[ \log_{10} \left( \frac{Eh^3}{2b^4} \right) - 0.71 \right] \quad (15)$$

where

$$b = \sqrt{1.6C^2 + h^2} - 0.675h \quad \text{for } C < 1.724h$$

$$= C \quad \text{for } C > 1.724h$$

C = radius of circular area over vessel load P distributed which



If  $c = 0$  then  $P$  is a concentrated load and  $b = 0.325 h$ . Therefore, if we use the value of poissons ratio previously developed and a value of

$k = 64 \frac{lb}{in^3} = 0.03705 \frac{lb}{in^3}$  we may substitute and rearrange our expression to give

$$P = \frac{\sigma_{max} h^2}{0.633 \left[ \log_{10} \left( \frac{E}{0.000414 h} \right) - 0.71 \right]} \quad (16)$$

as the concentrated vertical force required to cause failure in the bottom most fibers of the slab.

(122 & 123)

A somewhat similar solution was developed by Westergaard in his work on concrete pavements for air fields. In this work he expressed the stress in the bottom fibers of the slab directly under the load as

$$\sigma_{max} = \frac{12(1+\nu)}{\pi(3+\nu)} \frac{P}{h^2} \left[ K' + 0.8659 - \frac{\nu}{4} - B_1 + \frac{1-\nu}{4} S + B_2 \frac{r}{\rho} \right] \quad (17)$$

$S$  &  $K'$  = shape factors of loaded area defined by

$$K' = \frac{1}{2} + \ln \frac{\rho}{a'} \quad \text{WHERE} \quad a' = \sqrt{1.6 a^2 + h^2} - 0.675 h \quad \text{for } a < 1.724 h$$

$$a' = a \quad \text{for } a > 1.724 h$$

$$S = -\frac{r^2}{2a^2} \cos 2\theta \quad \text{for load distributed over a circular area of radius } r = a$$

$B_1$  &  $B_2$  factors related by

$$4(B_1 - 0.8659) = 0.28 + \frac{\nu}{3} + \nu^2$$

$$4B_2 = 1.18(1 + 2\nu)$$

If we consider the case of the concentrated load, i.e.  $r = \rho = 0$  we have

$$S = 0$$

$$K' = \frac{1}{2} + \ln \frac{\rho}{0.325 h}$$

If we again use our value of poissons ratio and foundation modulus  $k$ ,

substitute in (17) and rearrange we have

$$P = \frac{\sigma_{max} h^2}{1.548 \left[ 0.275 + \ln \sqrt{\frac{E}{0.00431 h}} \right]} \quad (18)$$





(18)

It is interesting to note that if this expression is compared to that quoted by Ormondroyd (16) we find that

$$\frac{P_{16}}{P_{18}} = 1.44$$

This variation could be due to certain approximations in Westergaards development. For instance, the expression stated for the determination of  $B_1$  and  $B_2$  are the result of a curve fitting process and may therefore contain certain inherent inaccuracies. It is doubtful if this would account for as much as a 44% difference.

An expression for the maximum stress on the bottom surface of a slab calculated to that developed by Westergaard is given by Roark as

$$\sigma_{max} = \frac{0.863 (1+\nu) P}{h^2} \left[ \ln \frac{l}{b} + 0.201 \right] \quad (19)$$

Substituting for poissons ratio and foundation modulus  $k$  and rearranging we have

$$P = \frac{\sigma_{max} h^2}{1.178 \left[ \ln \frac{l}{0.325 h} + 0.201 \right]} \quad (20)$$

Each of the above expressions may be used to predict the force  $P$  required to cause failure in the ice sheet due to tension in the bottom most fibers. Little use, however, has been made of them in the past. Kari, in a discussion on icebreaker design gives an empirical expression to use in predicting the resistance of ice to rupture. This expression is given as

$$P = 9340 (h+24) \quad (21)$$

Since this expression fails to consider the effect of temperature on sea ice strength, its reliability is quite doubtful. In a paper on the bow characteristics of icebreakers, Simpson suggests the use of an expression originally developed for a circular flat plate freely resting on a circular rim. This



is given as

$$P = \frac{\pi h^2 \delta}{3} \quad (22)$$

This expression too, is not felt to be too reliable since, although it has a temperature dependence in  $\delta$  it does not account for the elastic foundation. In addition, the circular plate configuration does not closely enough approximate the physical ice breaking picture.

It must be recalled that in all of the above expressions for the solution of the flat plate problem certain simplifying assumptions have been made. Firstly, that the flat plate is elastic within the range of action with a single constant value of Youngs modulus and poissons ratio. Secondly, that the thickness of the plate is constant and thirdly that the reaction at the base of the plate due to the elastic foundation is a vertical pressure equal per unit of area to a constant  $k$  times the deflection. In support of these assumptions we can say that assuming constant thickness and constant poissons ratio is not too unrealistic. As regards Youngs modulus it is true that it will vary with temperature and position in the ice sheet. The variation with temperature we can account for by selecting a value representative of that temperature at which we are working. The variation with position in the ice sheet we cannot account for, however, since only the fourth root of Youngs modulus enters into the above expressions, it is felt that the resulting error will not be unreasonable. The assumption that the ice sheet remains elastic within the range of action could cause difficulty since it is known that ice behaves plastically. However, as we have mentioned, if the rate of loadings is rapid (above about  $7.11 \text{ lb/in}^2\text{-sec}$ ) the ice will behave elastically,



and such may realistically be assumed to be true during ramming with a modern icebreaker.

In order to better compare the previously given expressions for the force  $P$  required to rupture an ice sheet in bending, figure 33 shows a plot of the force required as a function of ice thickness for the single case of perennial sea ice at the average mean ice temperature of  $-12^{\circ}$  C. This plot shows a comparison of values obtained using each of our above expressions.

So as to evaluate the adaptability of these flat plate expressions, let us select the expression given by Timoshenko as representative of the correct solution and investigate the forces required throughout a temperature range. For this purpose, let us select the strength characteristics of perennial sea ice and using the values of Young's modulus as given in figure 3 determine the force required to overcome ice of any given thickness. These results are shown in figure 34.

Now for a conventional type icebreaker it is often quoted that the static vertical force which may be developed at the bow is approximately 10% of vessel displacement and that under dynamic conditions this value may approach 20% as a maximum. If such were the case, the conventional wind class breaker should be capable of rupturing over 18 feet of perennial sea ice. Experience, however, dictates that such a feat is quite impossible. Consequently an error exists in our reasoning.

This error was brought to light by the results of experimentation on pack ice in the field. It was observed that when the floating ice sheets were put under load the ice would crack radially from the center of the loading due to





# COMPARATIVE FORCE REQUIRED TO OVERCOME SEA ICE

FORCE REQUIRED - LBS X 10<sup>4</sup>

9.0  
8.0  
7.0  
6.0  
5.0  
4.0  
3.0  
2.0  
1.0  
0

0 20 40 60 80 100 120 140 160 180 200 220 240

ICE THICKNESS - INCHES

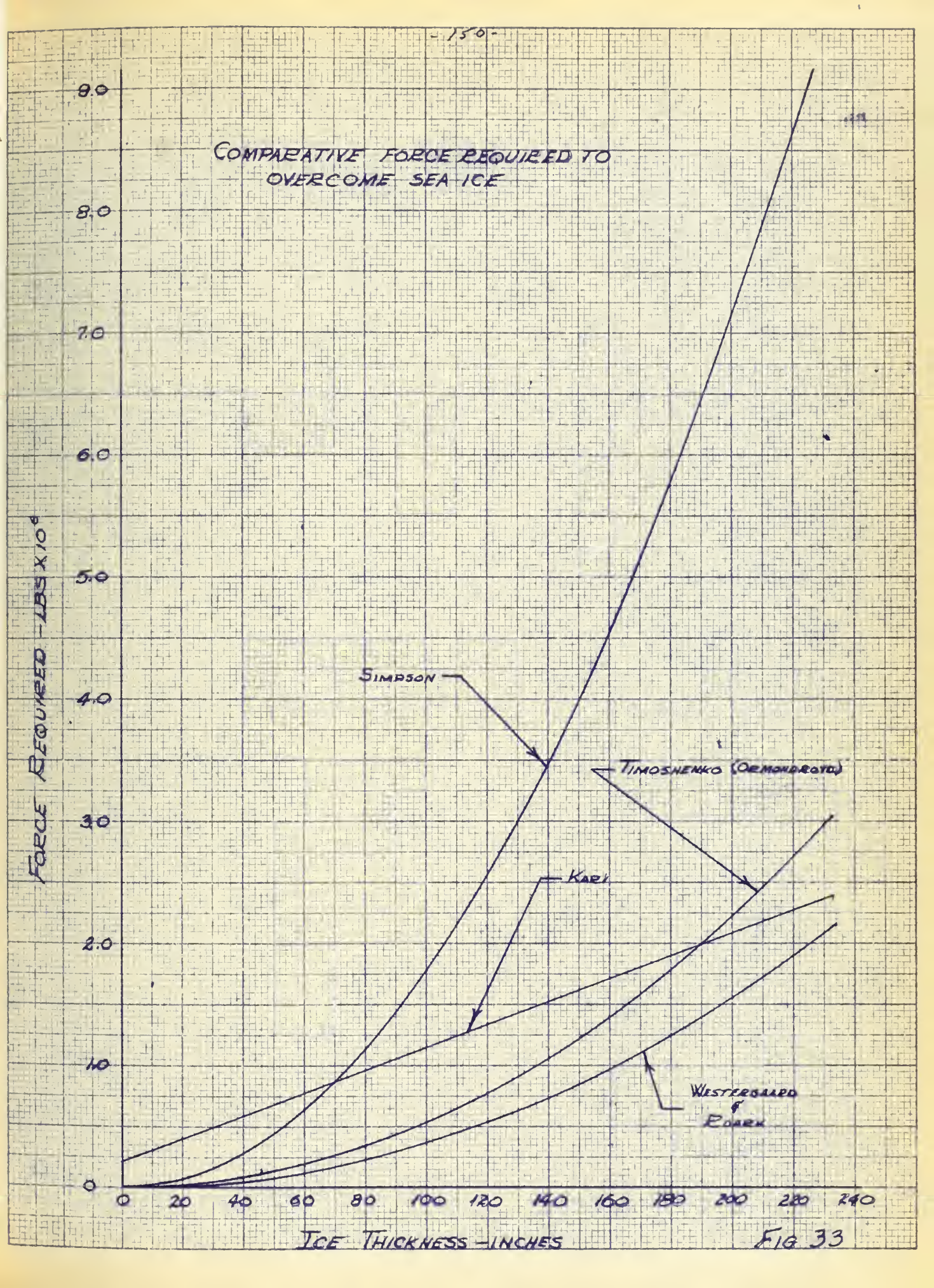
SIMPSON

TIMOSHENKO (ORMONDROYD)

KARL

WESTERGAARD  
&  
ROARK

FIG 33









# PERENNIAL SEA ICE

NOTE - PERENNIAL SEA ICE STRENGTH BEGINS  
DOWN COMPLETELY AT  $-0.8^{\circ}\text{C}$

## ICE PLATE THICKNESS VS FORCE REQUIRED TO RUPTURE

NOTE -  $^{\circ}\text{F} = 1.8(^{\circ}\text{C} + 17.78)$   
 $^{\circ}\text{C} = 0.555(^{\circ}\text{F} - 32)$

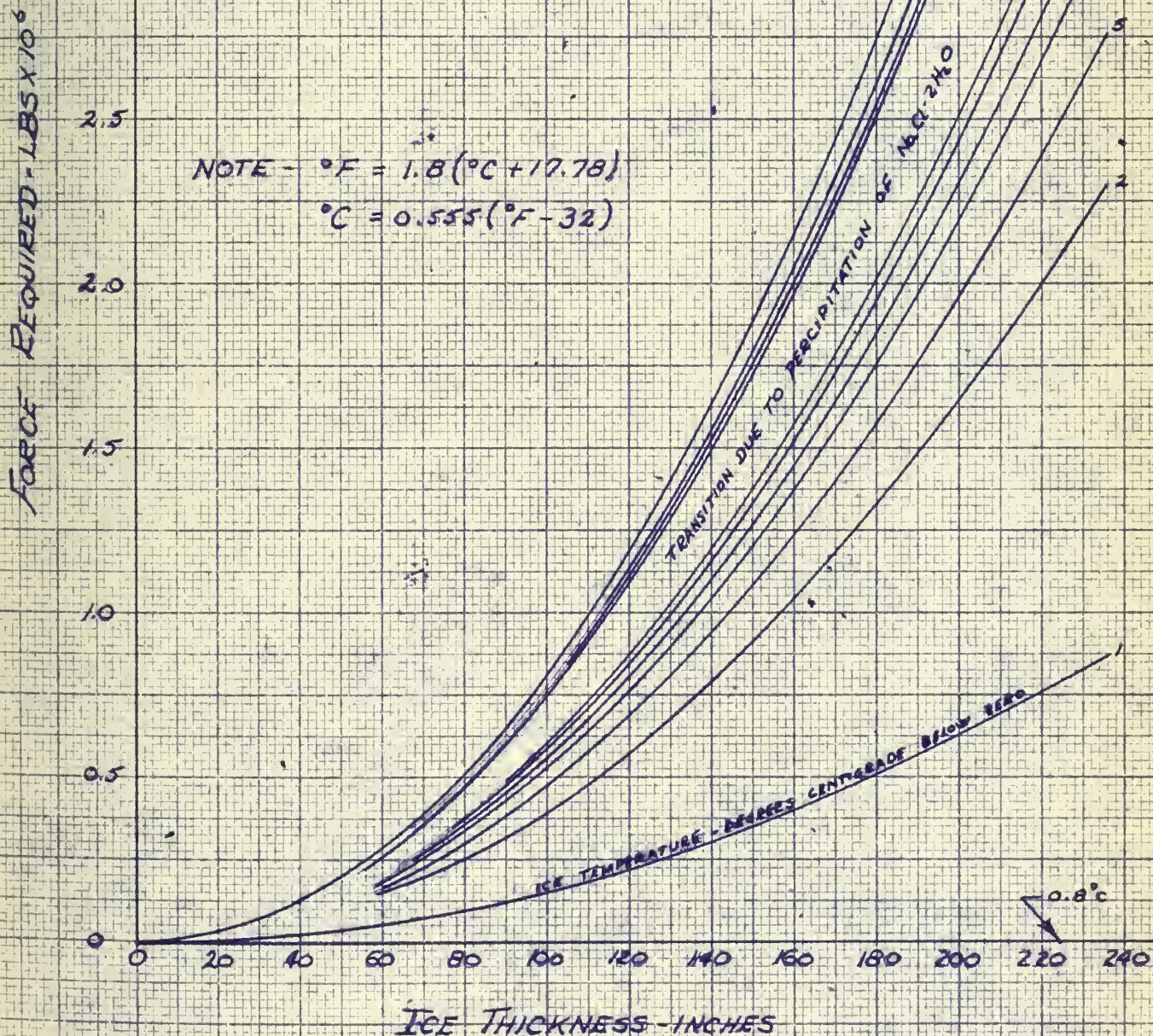


FIG. 34





tension on the bottom surface of the ice. As the loading was increased, the radial cracks lengthened and increased in number until finally a circumferential crack was formed caused by tension on the upper surface of the ice. Now the theory of the flat plate on an elastic foundation will closely predict the radial cracks. However, even after the radial cracks have formed the ice sheet still has considerable <sup>LOAD</sup> ~~local~~ carrying ability, that is, the pieces of ice shelf will not break off. Thus in our ice breaker analogy, although we have predicted the cracking of the ice we have as yet not broken it. The ice does not break until shortly after the circumferential crack has formed. Now the flat plate theory does not accurately predict the circumferential crack because the plate is already cracked. Consequently, we must consider the problem of a wedge on an elastic foundation in order to compute where and under what conditions the circumferential crack will occur. Note that although the formation of a circumferential crack does not determine the ultimate capacity of the ice, it does occur very shortly before failure. Thus it would seem that the solution to this wedge problem would more closely simulate our physical icebreaker problem and allow us to more accurately predict the vertical bow force necessary to actually break a given thickness of ice.

The only useable solution to the problem of a wedge on an elastic foundation is that developed by Mr. D. E. Nevel of the U. S. Army Snow, Ice and Permafrost Research Establishment. <sup>(115)</sup> Mr. Nevel considered the case of a narrow, free, infinite wedge composed of an elastic homogenous isotropic material and resting on an elastic foundation. The term narrow indicates that the wedge width is sufficiently small so that tangential bending may be neglected. Model studies

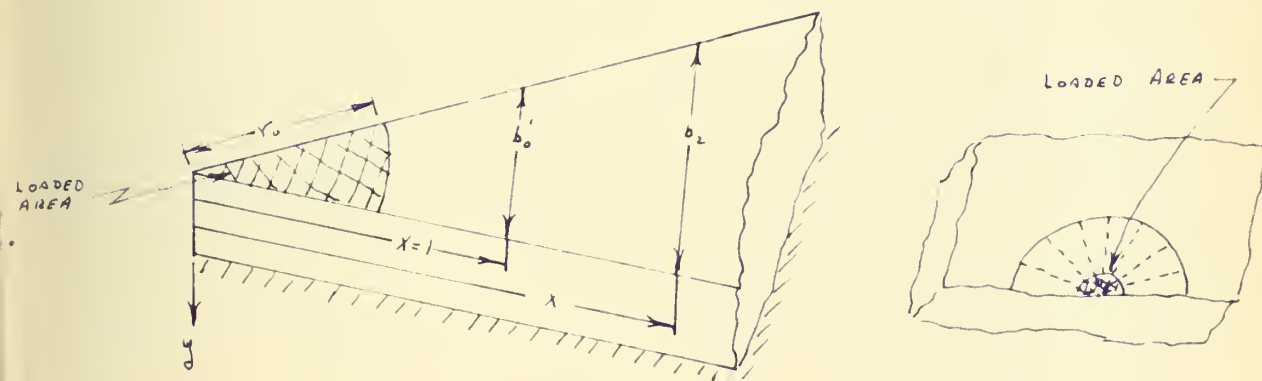




have shown that this is true if the angle of the wedge is less than 60 degrees as is normally true of sea ice under loading. The term free indicates that there are no forces exerted on the sides of the wedge by adjacent wedges and although the wedge is not infinite, this case will approach that of a finite wedge attached to a plate.

This problem involves the solution of the differential equation describing the wedge, i.e.

$$\frac{d^4 y}{dx^4} + \frac{2}{x} \frac{d^3 y}{dx^3} + y = \frac{q}{2} \quad (23)$$



The general solution of this differential equation was determined by Nevel in (115) 1958. He then considered the case of the wedge with a concentrated load applied at the apex, i.e.  $x = 0$  and expressed the deflection of the wedge as

$$y = \frac{P}{2 b_0' h'^2} \frac{\pi^{1/2}}{[\Gamma(3/4)]^4} D_{n_1}(x) \quad (24)$$

and the bending moment in these upper fibers as

$$M = Px \frac{\pi^{1/2}}{2[\Gamma(3/4)]^4} D_{n_1}''(x) \quad (25)$$

where  $D_{n_1}(x)$  describes a Forbenius power series and  $D_{n_1}''$  its second derivative. Now the bending stresses in the upper fibers of the wedge may be described as

$$\sigma_z = \frac{6 M}{b_0' x h'^2} \quad (26)$$

hence if we can determine the bending moment  $M$  we may evaluate the resulting fiber stresses. In an unpublished report, Nevel has, with the aid of electronic



(116)

computers, evaluated the series involved in the expression for  $M$ . These results he presents as a plot of  $M/PX$  versus the nondimensional distance along the wedge  $X$  for various values of the nondimensional distance of loading  $\tau$ .

In order to apply these results to the icebreaker problem we must first be able to determine the distance of loading of the wedge  $\tau = \frac{r_0}{l}$ . Now  $l = \sqrt[4]{\frac{E h^3}{12 k}}$ , hence we may evaluate it as a function of the ice thickness  $h$ , foundation modulus  $k$  and Young's modulus for the ice at the given temperature.

In determining  $r$ , however, we must make some approximation of the area of loading. The physical picture of the icebreaker climbing an ice sheet does approach that of a ~~conventional~~ <sup>CONCENTRATED</sup> loading, however, the loaded area is finite.

In order to approximate  $r_0$ , therefore, we may use the method developed by Westergaard in his treatment of the flat plate on an elastic foundation wherein he assumes a circular area of loading described by a radius factor  $b$  defined

as

$$b = \sqrt{1.6 C^2 + h^2} - 0.625 h \quad \text{for } C < 1.724 h$$

$$b = C \quad \text{for } C > 1.724 h$$

where  $h$  = thickness of the plate

$C$  = radius of circular area over which load distributed

For the icebreaker case wherein we approach a point loading we have

$$r_0 = b = 0.325 h$$

Hence we may approximate  $r_0$  solely as a function of ice thickness.

Having determined the nondimensional distance of loading  $\tau$  we may enter Nevel's curves and determine the maximum value of  $M/PX = t'$  and its location along the wedge  $X$ . From this value of  $t'$  we may determine

$$M = P X t'$$

hence

$$\delta_t = \frac{b P t'}{b_0 h^2} \quad (27)$$



(27)

The vertical force  $P$  required to break the wedge becomes

$$P = \frac{\sigma_{max} b_0' h^2}{6 t'} \quad (28)$$

where  $\sigma_{max}$  is the tensile strength of the upper fibers of the ice sheet. Now the only unknown in this expression is  $b_0'$  the width of the wedge at a distance  $X=1$ , hence the angle of the wedge. Field tests show that when the ice sheet cracks the wedges formed are less than  $60^\circ$ . Nevel, in his paper, pictures these segments as of approximately  $22.5^\circ$  each. Since the actual angle chosen has an insignificant effect upon the resultant value of  $P$  which must be developed by the icebreaker, let us assume wedges as depicted by Nevel of  $22.5^\circ$ . Hence  $b_0' = 0.398$  and

$$P = 0.0664 \frac{\sigma_{max} h^2}{t'} \quad (29)$$

Now this is the vertical force necessary to break the wedge. Since the icebreaker climbs up on to the ice and exerts a vertical force on an adjacent group of wedges (which we assume to be 8 due to the angle of  $22.5^\circ$ ) the actual vertical force which it must develop to overcome all of them and break the ice upon which it is resting becomes

$$F' = 8P$$

or

$$F' = 0.531 \frac{\sigma_{max} h^2}{t'} \quad (30)$$

In order to evaluate this expression a curve of the loci of the maximum values of  $M/P_X = t'$  for values of  $M$  in the normal icebreaker range is shown in figure 35. The expression (30) was evaluated for perennial sea ice (salinity  $\approx 2$  ppm), normal one season ice (salinity  $\approx 5$  ppm) and young sea ice (salinity  $\approx 10$  ppm) for ice thicknesses ranging from 10 inches to 225 inches as a function





LOCI OF MAXIMUM  $M/P_K = t'$  FOR VALUES  
OF  $\tau$  IN ICEBREAKER RANGE

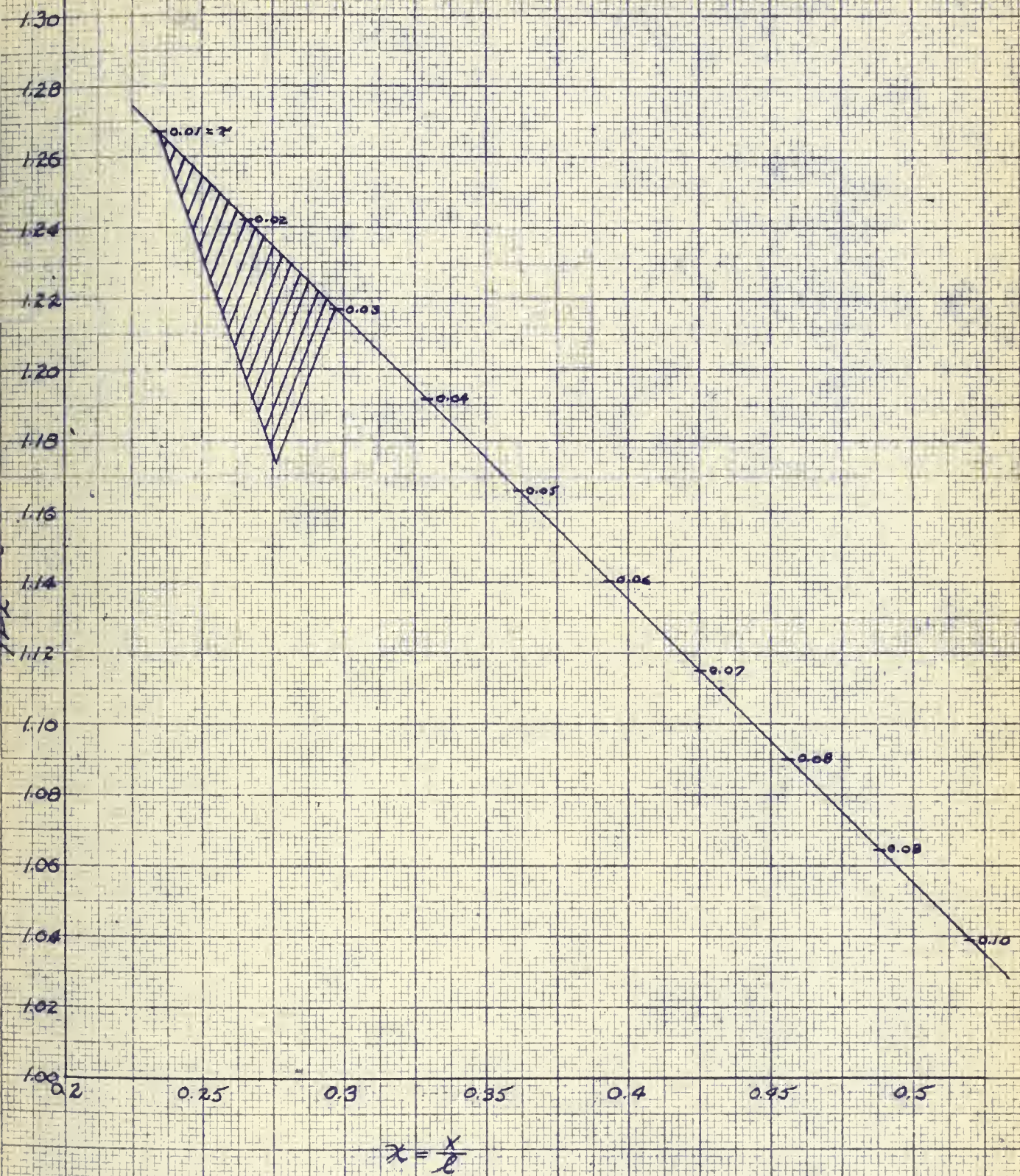


FIG 35





of ice surface temperature. These results are shown in figures 36, 37 and 38 where vertical bow reaction force  $F'$  necessary to overcome the ice sheet is plotted as a function of ice surface temperature for the above mentioned range of ice thicknesses.





VERTICAL BOW FORCE REQUIRED - LBS

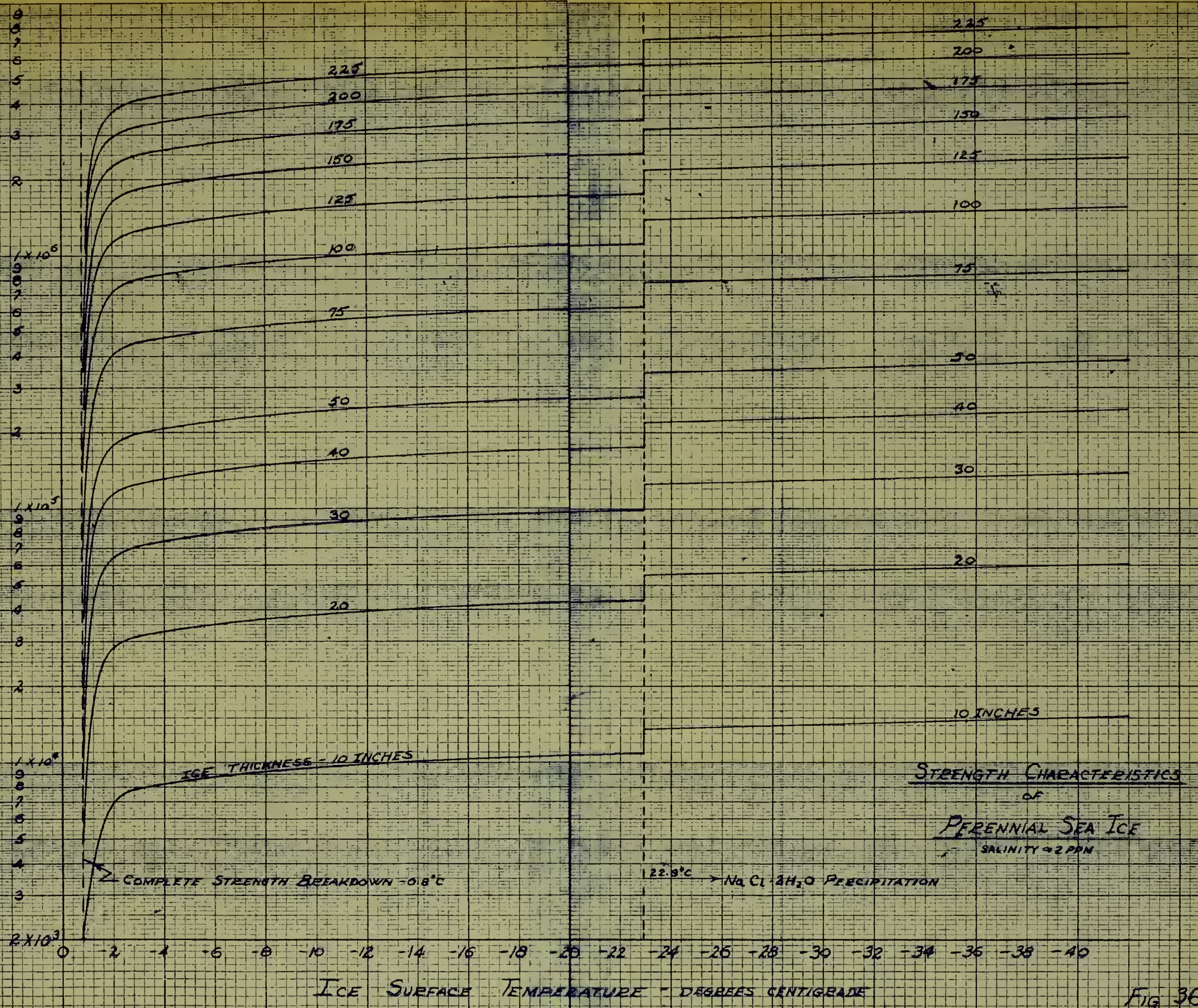


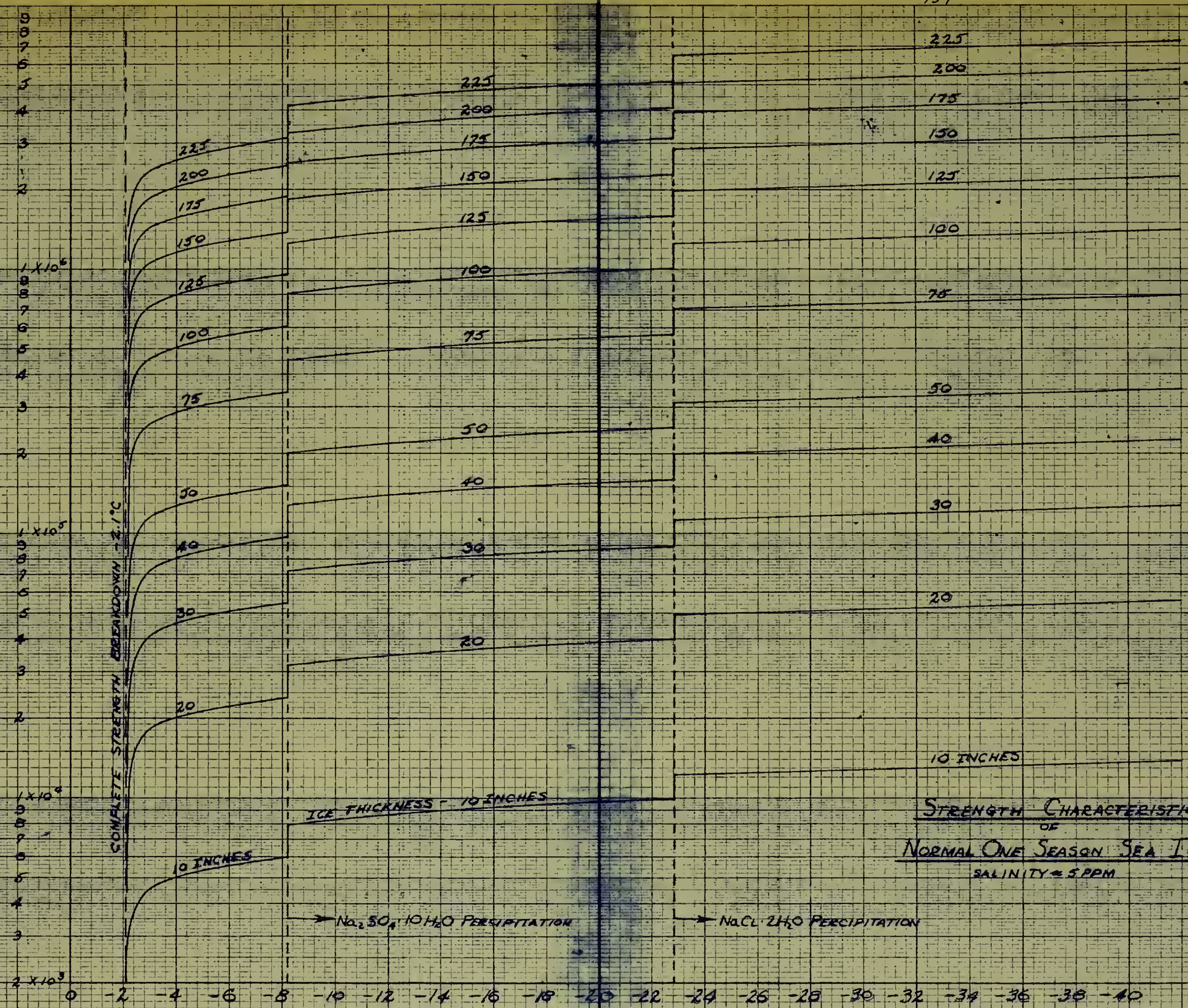
FIG 36







VERTICAL BOW FORCE REQUIRED - LBS



ICE THICKNESS - 10 INCHES

10 INCHES

→  $\text{Na}_2\text{SO}_4 \cdot 10\text{H}_2\text{O}$  PRECIPITATION

→  $\text{NaCl} \cdot 2\text{H}_2\text{O}$  PRECIPITATION

STRENGTH CHARACTERISTICS  
OF  
NORMAL ONE SEASON SEA ICE  
SALINITY ≈ 5 PPM

ICE SURFACE TEMPERATURE - DEGREES CENTIGRADE

FIG 37







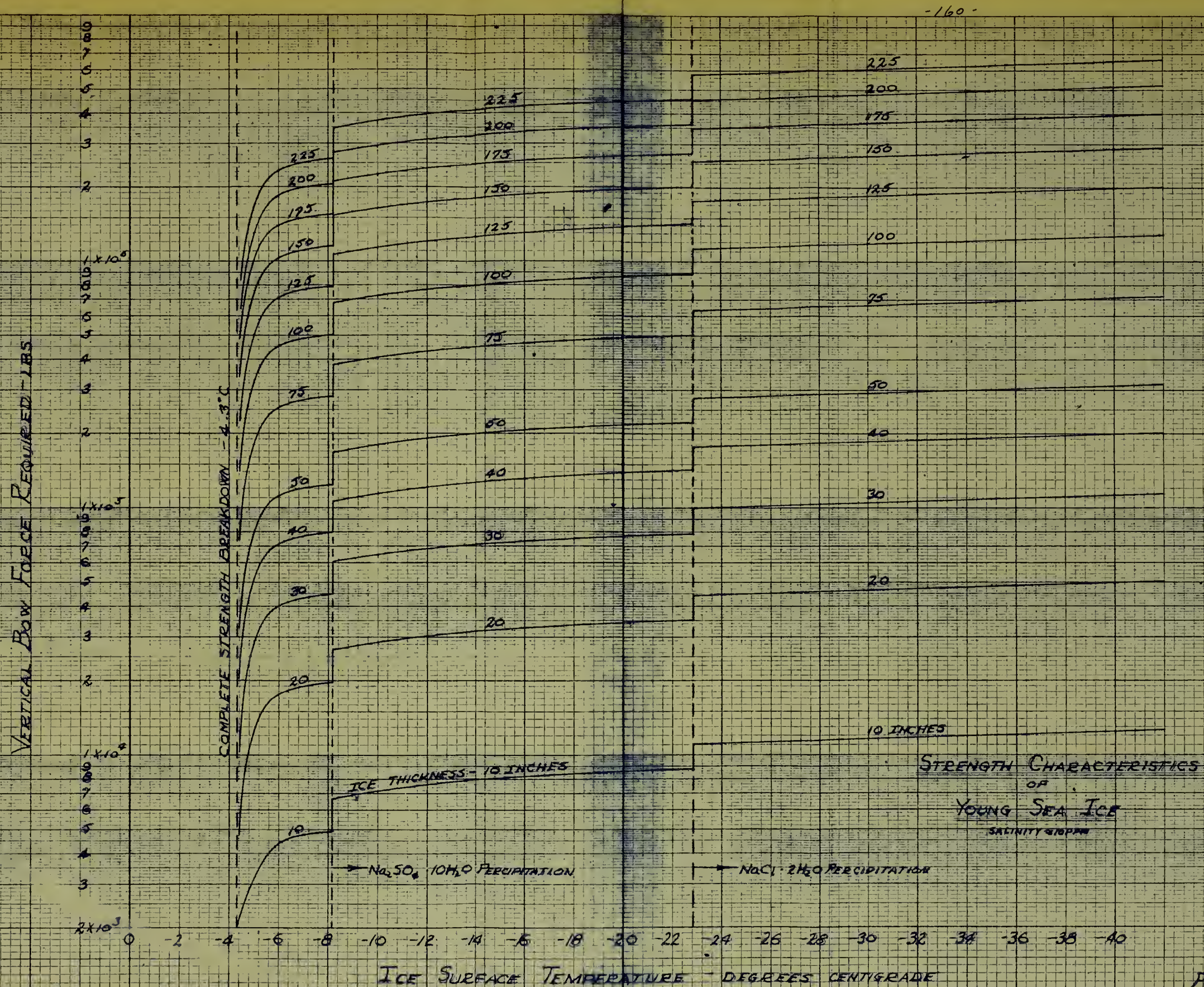


Fig 38





## Part 2

### Icebreaking Forces and Vessel Impact Velocity

Our analysis is the result of work done by I. V. Vinogradov and published in his book Vessels for Navigation in Icebound Waters, 1946. The development is based on the assumption that no vertical forefoot exists, if one does exist, that it does not strike the ice surface.

We assume an icebreaker, moving with a known velocity, to strike a uniform, continuous ice shelf such that the vessel, due to its inclined bow, rides up on to the ice until a downward pressure at the bow is developed of sufficient magnitude to rupture or overcome the ice. During the period of time that the vessel is climbing on to the ice shelf, the propellers continue to turn and exert a forward thrust which, at the *limit*, is equal to the ballard pull. In general, when the vessel is breaking ice of sufficient thickness to necessitate ramming, it may reasonably be assumed that at the instant the ice collapses the vessel's forward speed is, for all practical purposes, reduced to zero. It is true that since the ice just forward of the bow is ruptured and since practically full ballard thrust is being developed, the ship will have a tendency to continue its forward motion. However, personal experience with heavy polar ice indicates that this forward motion, if it exists, is very limited and will be reduced to zero upon contact with the still unbroken ice sheet - a distance of only several feet. In fact, icebreaker practice in heavy ice normally dictates that the engines be reversed at the instant of ice collapse so as to insure that the vessel will not become beset due to the pressure often exerted by broken slabs of ice wedged between the unbroken ice sheet and the vessel's





hull. Consequently, for the purposes of our analysis of the polar ice-breaker we may safely assume that forward motion is zero upon collapse of the ice.

The quantity which we wish to determine in this analysis is  $F$ , the maximum value of vertical bow reaction force developed at the stem of the vessel. Since this maximum value of  $F$  is a function of the distance traveled by the vessel on to the ice, it will occur at the instant the ice collapses. Therefore, only a study of the dynamic forces leading up to the collapse of the ice shelf need be made and no consideration need be given to the downward drop of the bow which occurs when the ice gives way.

The easiest approach to this problem is through a consideration of the energy forces involved and the principles of the conservation of energy. The energy expended by the vessel is its kinetic energy plus the energy of the propeller thrust acting through the distance of vessel travel. This total energy is dissipated by impact of the bow on the ice shelf, change in vessel potential energy due to its being raised and changed *IN TRIM* and by the friction loss due to rubbing of the stem against the ice shelf. In equation form this may be expressed as

$$E_1 + E_2 = E_3 + E_4 + E_5 \quad (42)$$

where

$E_1$  = kinetic energy of vessel at instant of impact

$E_2$  = energy derived from ships propeller

$E_3$  = Energy dissipated through impact

$E_4$  = change in vessel potential energy

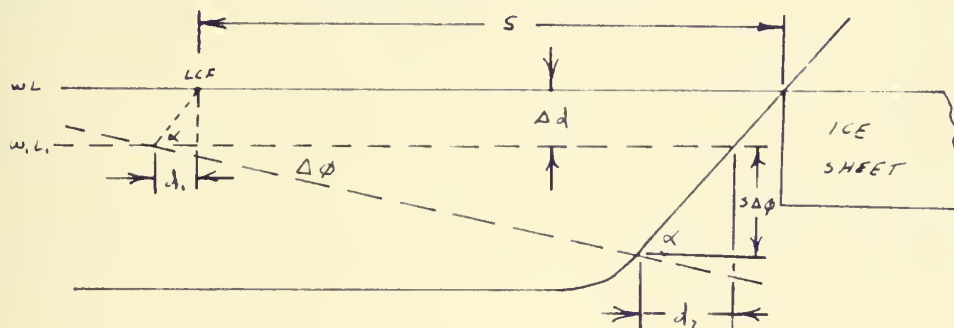
$E_5$  = energy loss due to friction



Let  $W$  represent the displacement of the vessel in tons and  $v$  its velocity in ft/sec at the instant of impact with the ice shelf, then

$$E_i = \frac{W}{2g} v^2 \quad \text{ft tons} \quad (43)$$

Next consider the energy delivered by the propellers as the vessel rides up on to the ice shelf. During this vessel motion there is a reduction in mean draft, designated  $\Delta d$ , and the ship assumes an angle of trim, designated  $\Delta\phi$ . The distance from the point of contact of the stern with the ice shelf to the longitudinal center of floatation (LCF) at the original waterline designate as  $S$ . The stern of the vessel is sloped at an angle  $\alpha$  from the horizontal. During the change in mean draft we may assume that the LCF moves in a direction parallel to the stern since the error resulting from such an assumption will be very small due to the small  $\Delta d$ .



Notice that the assumption is also made that the upper surface of the ice shelf coincides with operating waterline of the vessel. This, in reality, is not a true representation since there is a certain thickness of ice which is above the surface of the water, hence contact is first made at a point on the stern slightly above the original waterline. However, this difference is not enough to introduce any noticeable error. Consequently, from the instant of first contact with the ice until the ice collapses, the linear advance of the vessel is

$$d = d_1 + d_2$$





but

$$d_1 = \Delta d \cot \alpha$$

and since

$$\frac{\sin \alpha}{\sin \alpha} = \frac{d_1}{\sin(\gamma - \alpha)} = \frac{d_1}{\cos \alpha}$$

we have

$$d_1 = \sin \alpha \cot \alpha$$

therefore, combining we have

$$d = (\Delta d + \sin \alpha) \cot \alpha$$

If we let T represent the thrust in tons which is exerted by the propeller during this travel we have that

$$E_2 = T(\Delta d + \sin \alpha) \cot \alpha \quad (44)$$

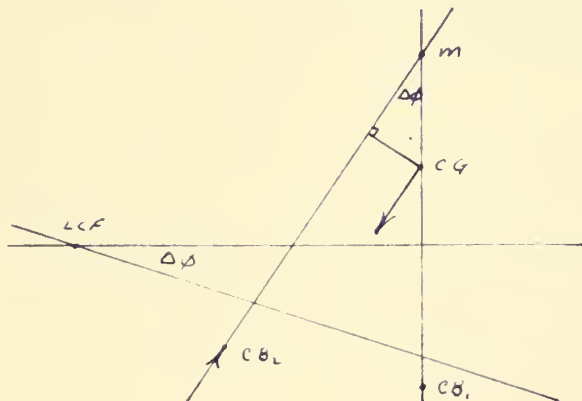
Since we are interested in the maximum vertical bow reaction force F, it would be better to express  $E_2$  as a function of F. Now if we assume that the change in draft,  $\Delta d$ , is small (seldom exceeds 10%) the properties of the waterplane will not markedly change, hence

$$F = \frac{\gamma' \Delta d A_w}{2240}$$

and

$$\Delta d = \frac{2240 F}{\gamma' A_w}$$

In addition, the change in trim resulting from impact with the ice is due to the *trimming* movement FS.



If  $\Delta \phi$  is small (normally it is less than  $5^\circ$ ) we may say that

$$FS = WGM_L \sin \Delta \phi = WGM_L \Delta \phi$$



therefore,

$$\Delta \phi = \frac{F_3}{\omega G M_L}$$

Substituting for  $\Delta d$  and  $\Delta \phi$  in (44) we have

$$E_2 = T \left[ \frac{2240 F}{\delta' A_w} + \frac{F_3^2}{\omega G M_L} \right] \cot \alpha \quad (45)$$

Now waterplane area is equal to the product of length, breadth and waterplane coefficient, i.e.

$$A_w = L B C_w$$

and vessel displacement is the product of length, breadth, draft, block coefficient and specific weight of sea water, i.e.

$$W = \frac{L B H C_B \delta'}{2240}$$

If we substitute these expressions for  $A_w$  and  $W$  in (45) and introduce the non-dimensional coefficients  $k_1$  and  $k_2$ , where

$$S = k_1 \frac{L}{2}$$

$$G M_L = \frac{k_2 C_w L^2}{H C_B}$$

we have

$$E_2 = \frac{A T F H}{W} \cot \alpha \quad \text{FT-TONS} \quad (46)$$

where

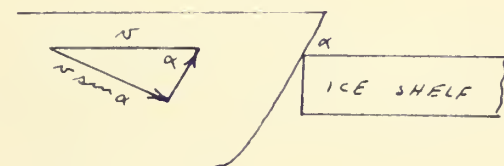
$$A = \left[ \frac{C_B}{C_w} + \frac{k_1^2 C_B}{4 k_2 C_w} \right] \quad (47)$$

Note that in establishing  $k_2$  we make the assumption that longitudinal metacentric height is essentially equal to the distance between center of buoyancy and the longitudinal metecenter.

By the theory of impact, when two bodies collide normal to each other, the loss of kinetic energy involved may be expressed in terms of their relative velocities and a constant for the materials called the coefficient of restitution. Now in the case of our vessel, the stern does not collide normal to the ice sheet since the stern is inclined at an angle  $\alpha$  with the horizontal. The



velocity component normal to the ice shelf, therefore, is  $v \sin \alpha$ . Hence if  $v$



is the vessel velocity at the instant of contact with the ice shelf, and if, as before, we assume that the vessel comes to a stop as the ice collapses, the loss of kinetic energy due to impact may be expressed as approximately

$$E_3 = \frac{W}{2g} (v \sin \alpha)^2 (1 - e^2) \quad (48)$$

where  $e$  is the coefficient of restitution between steel and ice. As far as is known, no actual data exists in the literature for the value of this coefficient of restitution. Consequently, in order to determine its approximate value simple experiments were conducted, the results of which are recorded later in this section. For the present, however, we know that it varies between values of zero for perfect inelasticity to one for perfect elasticity.

We can readily see that our elusive vertical reaction force  $F$  is a variable which increases from zero at the instant of contact to a maximum value  $F$  at the instant the ice collapses. Now if we consider the total change in vessel potential energy we have that the total rise of the point on the stern which first contacts the ice is equal to the change in vessel draft plus the rise due to the change in vessel trim. Since  $\Delta \phi$  is normally less than  $50^\circ$  we have

$$h = \Delta d + s \Delta \phi$$

The gain in vessel potential energy, therefore, is equal to the vertical bow reaction force developed moving through the vertical distance  $h$ , or

$$E_4 = \int_0^{\Delta d} F d(\Delta d) + \int_0^{\Delta \phi} F s d(\Delta \phi) \quad (49)$$





But earlier we said that

$$F = \frac{\gamma' \Delta d A_w}{2240}$$

$$F_s = W G M_L \Delta \phi$$

Therefore if we substitute and integrate we have

$$E_H = \frac{\gamma' A_w}{2240} \frac{(\Delta d)^2}{2} + W G M_L \frac{(\Delta \phi)^2}{2} \quad (50)$$

Again using the above substitutions for F and  $F_s$  plus our previously given definitions of  $k_1$ ,  $k_2$ ,  $A_w$  and  $W$  we have

$$E_H = \frac{F^2 H A}{2 W} \quad \text{ft tons} \quad (51)$$

where as before

$$A = \left[ \frac{C_B}{C_w} + \frac{k_1^2 C_B}{k_2^2 + C_w^2} \right] \quad (47)$$

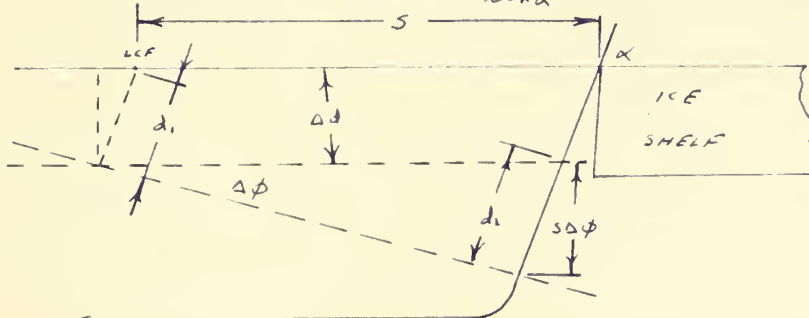
Finally we consider energy dissipated through friction of the shell plating sliding across the ice. The value of the frictional force is equal to the product of the coefficient of sliding, or dynamic, friction for steel on ice and that component of bow pressure which acts normal to the ship's hull plating. The resultant frictional force,  $F_f$ , acts in a direction parallel to the stern of the vessel and may be assumed to be evenly divided on either side of the stern.

The energy dissipated by this frictional force  $F_f$  is equal to the force moving through the distance the vessel travels in a direction parallel to the stern as a result of the change in vessel draft and *Trim*, i.e.

$$E_s = F_f h$$

where

$$h = d_1 + d_2 = \frac{\Delta d}{\sin \alpha} + \frac{S \Delta \phi}{\sin \alpha}$$

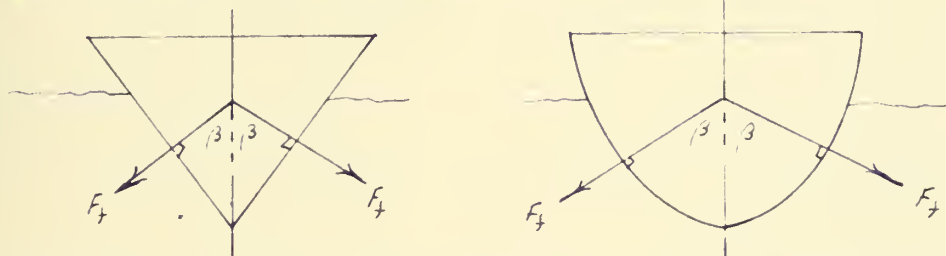




Therefore

$$F_s = \frac{1}{\sin \alpha} \int_0^{\Delta d} F_f d(\Delta d) + \frac{1}{\sin \alpha} \int_0^{\Delta \varphi} F_f d(\Delta \varphi) \quad (52)$$

Before integrating (52) we wish to know the expression for  $F_f$ . If we dissect or pass planes through the forepart of the vessel normal to the stern, the sections for the submerged portion of the vessel will be in the form of wedges with flat or slightly convex sides, i.e.



Since the vessel is being forced against the ice by its kinetic energy and propeller thrust, the ice will be deformed in the form of a wedgelike groove in which the bow slides when climbing on to the ice. Pressure is developed normal to the faces of the groove and friction forces along the faces of the groove and in the direction parallel to the stern. If we designate as  $R_t$  the resultant force acting normal to the stern then the force acting normal to the plating on each side is

$$\frac{R_t}{2 \cos \beta}$$

resulting in a friction force

$$\frac{F_f}{2} = \frac{f_0 R_t}{2 \cos \beta}$$

where  $f_0$  is the coefficient of sliding or dynamic friction of steel on ice.

The total friction force, therefore, is given as

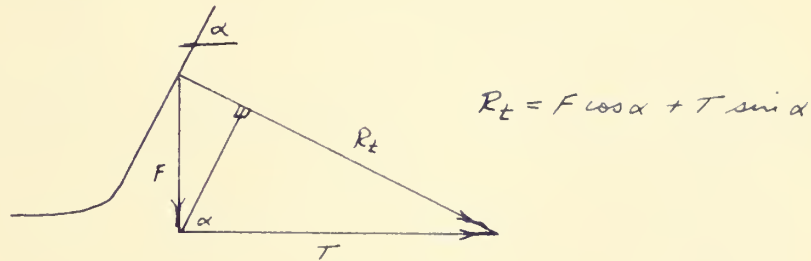
$$F_f = \frac{f_0 R_t}{\cos \beta}$$

The value of the force  $R_t$  is related to the vertical bow reaction force and the





propeller thrust such that



Therefore,

$$F_t = f_0 \left[ \frac{F \cos \alpha}{\cos \beta} + \frac{T \sin \alpha}{\cos \beta} \right]$$

substituting into (52) we have

$$\begin{aligned} E_s = & \frac{f_0}{\cos \beta} \int_0^{\Delta \phi} T d(\Delta \phi) + \frac{f_0}{\cos \beta} \int_0^{\Delta \phi} T_s d(\Delta \phi) + \frac{f_0}{\cos \beta} \int_0^{\Delta \phi} F \cot \alpha d(\Delta \phi) \\ & + \frac{f_0}{\cos \beta} \int_0^{\Delta \phi} F_s \cot \alpha d(\Delta \phi) \end{aligned} \quad (53)$$

Again using our expressions for F and F\_s, i.e.

$$F = \frac{\gamma' \Delta d A_w}{2240}$$

$$F_s = \omega G M_e \Delta \phi$$

integrating and re-substituting for  $\Delta d$  and  $\Delta \phi$  we have

$$E_s = \frac{2240 F T f_0}{\gamma' A_w \cos \beta} + \frac{F T_s^2 f_0}{\omega G M_e \cos \beta} + \frac{2240 F^2 f_0 \cot \alpha}{2 \gamma' A_w \cos \beta} + \frac{F^2 s^2 f_0 \cot \alpha}{2 \omega G M_e \cos \beta}$$

Using our previously given definitions for  $k_1$ ,  $k_2$ ,  $A_w$ ,  $A$  and  $\omega$

we have

$$E_s = \frac{A H}{\omega} \left[ \frac{F T f_0}{\cos \beta} + \frac{F^2 f_0 \cot \alpha}{2 \cos \beta} \right] \quad F T - T O N S \quad (54)$$

If we now substitute the expressions for  $E_1$  through  $E_5$  back into (42) and rearrange terms we have



$$F^2 - 2FT \left[ \frac{\cot \alpha \cos \beta - f_0}{\cos \beta + f_0 \cot \alpha} \right] + \frac{w^2 v^2}{gAH} \left[ \frac{\cos \beta}{\cos \beta + f_0 \cot \alpha} \right] \left[ \sin^2 \alpha (1 - e^2) - 1 \right] = 0$$

If we let

$$X = \frac{\cot \alpha \cos \beta - f_0}{\cos \beta + f_0 \cot \alpha} \quad (55)$$

$$Y = \frac{\cos \beta}{\cos \beta + f_0 \cot \alpha}$$

this becomes

$$F^2 - 2FTX + \frac{w^2 v^2 Y}{gAH} \left[ \sin^2 \alpha (1 - e^2) - 1 \right] = 0$$

Solving for the vertical bow reaction force F and noting that our solution must be real and that  $F > 0$  we have

$$F = XT + \sqrt{X^2 T^2 - \frac{w^2 v^2 Y}{gAH} \left[ \sin^2 \alpha (1 - e^2) - 1 \right]} \quad (56)$$

In order now to make use of expression (56) in our vessel evaluation, it is necessary to decide upon the value of propeller thrust (T) and vessel impact velocity (v) to use. T is the thrust acting during the period in which the vessel is climbing on to the ice, hence it is a function of ship speed and varies from some value T at the instant of impact to a maximum of bellard thrust T when vessel forward motion stops. The vessel impact speed v is a function of the vessel mass and the propeller thrust available to accelerate the vessel during the ramming period. Let us first investigate the expression for ship impact speed v.

When a vessel accelerates through the water, there is a certain amount of water which accompanies the vessel and which must also be accelerated. This apparent increase in vessel mass - or added mass - was first investigated by Froude who first realized the concept and attempted to estimate its effect on ship motions. Attwood and Pengally, in their book, Theoretical Naval Architecture,<sup>(97)</sup> assume a value of added mass equal to 20% of the vessel displacement. Since such an assumption does not consider the effect of vessel fineness or form in terms of its length, breadth and draft - which effects may be pro-



nounced - the results are not entirely reliable. Consequently, to more closely approach a realistic value for this added mass we must consider the hydrodynamic problem of the motion of a solid through a fluid.

When a vessel moves in calm water, the inertia forces experienced in accelerated motion are

$$F = \rho V \frac{d^2 s}{dt^2} + m_s \frac{d^2 s}{dt^2}$$

where the first term is the inertia force due to the ship itself and the second term summarizes the influence of the surrounding water. The assumption here is that the fluid is perfect, which is reasonable since as far as is known, viscosity has only a slight effect on the values obtained.

The theoretical solution of the problem of computing added mass was first presented by Lamb in his Hydrodynamics. The application of this concept to Naval Architecture did not occur until relatively recently. For ships, exact mathematical solutions are not available, however, approximate solutions, sufficiently accurate for practical purposes, can be carried out.

A comprehensive treatment of this subject is given by Weinblum and St. Denis in their paper On the Motions of Ships at Sea.<sup>(114)</sup> In this paper, the authors present the virtual mass of a vessel in terms of ~~ten~~<sup>non</sup>-dimensional inertia coefficients wherein for linear motions the additional mass is referred to the mass of water displaced by a circumscribing ellipsoid. For linear motions along the longitudinal axis of the vessel, the inertia coefficient  $k'$  may be expressed as

$$k' = \frac{m'}{\frac{4}{3} \pi \rho a b c}$$

where

$m'$  = added vessel mass - lb - sec<sup>2</sup>/ft

$a$  = one half ships length at LWL =  $L/2$  - ft.





$b$  = one half ships beam at LWL =  $B/2$  - ft.

$c$  = vessel draft =  $H$  - ft.

Therefore the added vessel mass may be expressed as

$$m' = \frac{1}{3} b' \pi \rho L B H$$

Values of the inertia coefficient  $b'$  may be obtained from figure <sup>39</sup>~~36~~ which shows the variation of  $b'$  as a function of the ratios  $B/2H$  and  $L/B$ . Based on the above expression, therefore, the total vessel mass which must be accelerated may be given as

$$m'' = \frac{2240 W}{g} + \frac{1}{3} b' \pi \rho L B H \quad \text{LB-SEC}^2/\text{ft}$$

Also, since block coefficient is defined as

$$C_B = \frac{V}{L B H} = \frac{35 W}{L B H}$$

our expression for vessel mass may be written as

$$m'' = W \left[ \frac{2240}{g} + \frac{30.7 b'/C_B}{C_B} \right]$$

For extremely long fine vessels, the  $L/B$  ratio becomes large and, consequently,  $b'$  approaches zero. In this instance the second term above approaches zero and vessel mass is given solely by

$$m'' = \frac{2240 W}{g}$$

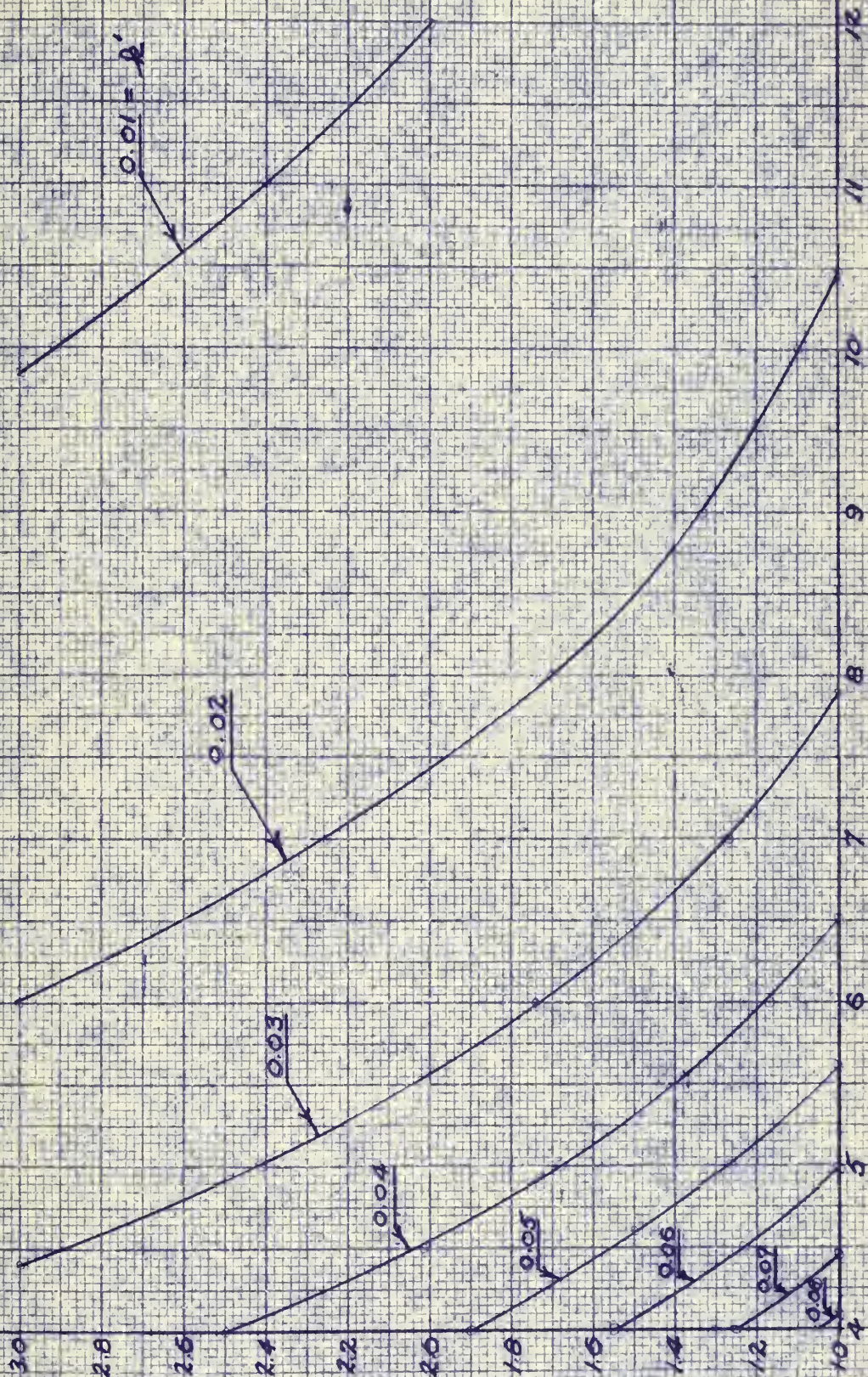
For the icebreaker type vessel, however, which is quite short and fat, we must investigate the value of  $b'$  more closely. If we consider data from approximately forty past and present icebreaker type vessels designed for ocean service we find that the value of the ratio  $b'/C_B$  varies from about 0.091 to about 0.153. Based on this range of values we may select a value of

$$b'/C_B = 0.122$$





# LINEAR INERTIA COEFFICIENT OF AN ELLIPSOID ALONG LONGITUDINAL AXIS



LENGTH TO BEAM RATIO -  $l/b$

LIMITING CASE  
 $h_1 = 0.15 \cdot l/b$

HALF BEAM TO DEPTH RATIO -  $b/h_1$

FIG 39







as typical of the polar icebreaker type vessel and representative of present practice. Using this representative value of  $\frac{4}{c_g}$  and assuming a density of sea water at 29° F. of 1.995 lb sec<sup>2</sup>/ft<sup>4</sup> we have for total vessel mass which must be accelerated

$$m'' = 78.54 W \quad \frac{46 \cdot 36 \cdot 4}{H} \quad (57)$$

It is interesting to note that the assumption given by Attwood and Pengally, is.

$$m'' = \frac{6}{5} \left[ \frac{W}{g} \times 2200 \right] = 83.5 W \quad \frac{46 \cdot 36 \cdot 4}{H}$$

is not too bad an elementary assumption for the icebreaker type vessel.

Knowing the vessel mass which must be accelerated, we may now proceed to determine vessel impact speed  $v$ . Let propeller thrust acting be given by  $T'$  and ship resistance at ~~some~~ speed which is below design maximum speed be given by  $r$ . Then the force which is acting to accelerate the vessel in open water is

$$F = T' - r$$

But

$$F = m A$$

therefore

$$T' - r = 78.54 W A$$

Acceleration is defined as

$$A = \frac{dv}{dt} = \frac{dv}{ds'} \cdot \frac{ds'}{dt} = v \frac{dv}{ds'}$$

hence

$$ds' = 78.54 W \frac{v dv}{T' - r}$$

and

$$s' = 78.54 W \int_0^v \frac{v}{T' - r} dv$$

where  $s'$  is the distance in feet over which the vessel accelerates.

The total resistance of a vessel is a function of ship speed and the common assumption is that resistance varies as the speed squared. This



assumption, however, does not hold too well for the icebreaker type vessel. In order to approximate this relationship more closely we investigate the variation of total vessel resistance plus appendages for the Glacier and wind class vessels for which some data is available. This variation is shown in figure 40 up to a ship speed of 12 knots. We are not too interested, at present, in the variation beyond this limit since we are considering only the velocity to which the vessel will accelerate during a ramming charge, and this velocity will seldom, if ever, exceed about 8 knots in open water. Also shown on figure 40 is an empirical relationship between total ship resistance and ship speed which approximates the typical icebreaker variation pretty closely. We shall assume this empirical relationship in our development rather than the more common  $r = k v^n$ . Therefore

$$r = 330 v^{1.61}$$

and

$$v' = 78.54 W \int_0^v \frac{v dv}{T' - 330 v^{1.61}} \quad (58)$$

The propeller thrust which may be developed by a given propeller with a given shaft horsepower is a function of vessel speed. This variation for the Troost series B3-50 and B4-55 propellers was developed in section E-2 and was given as approximately

$$T'_{B3.50} = 156 P^{1/3} D^{1/3} \left[ 0.489 - 0.0233 \frac{v D^{1/3}}{P^{1/3}} \right] \quad (40)$$

$$T'_{B4.55} = 156 P^{1/3} D^{1/3} \left[ 0.481 - 0.0221 \frac{v D^{1/3}}{P^{1/3}} \right] \quad (41)$$

If these expressions for  $T'$  are substituted into our expression (58) we may integrate and solve for vessel impact speed  $v$ . The result, however, is so unwieldy and difficult to apply as to make it useless in preliminary design. Consequently, in order to circumvent this difficulty, an assumption is in order.





# HULL RESISTANCE VS SHIP SPEED

TOTAL HULL RESISTANCE - WITH APPENDAGES - LBS X 10<sup>3</sup>

40  
35  
30  
25  
20  
15  
10  
5  
0

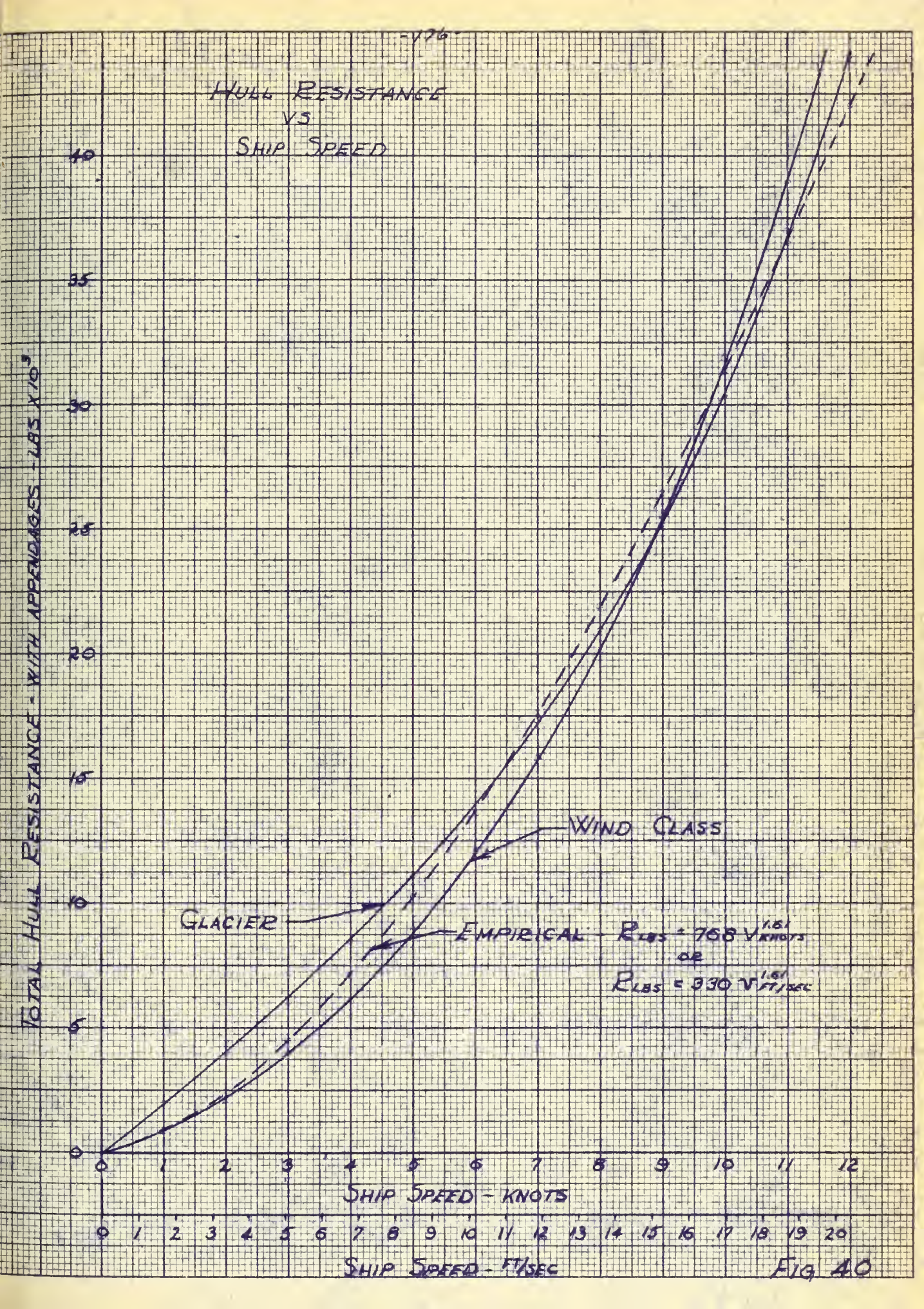
SHIP SPEED - KNOTS

0 1 2 3 4 5 6 7 8 9 10 11 12 13 14 15 16 17 18 19 20

SHIP SPEED - FT/SEC

WIND CLASS  
GLACIER  
EMPIRICAL  $R_{LBS} = 768 V^{1.61}_{KNOTS}$   
OR  
 $R_{LBS} = 330 V^{1.61}_{FT/SEC}$

FIG 40







If we visualize an icebreaker which is backing down in order to commence another charge at the ice sheet, we find that after having backed down about a ship length to a ship length and a half the engines are reversed full power ahead so as to accelerate for the charge. The actual time required for the shafts to reverse direction of motion is really unimportant to us here except that by the time astern ship motion is stopped and forward motion begins, the propellers are turning over at full power and we may, with reasonable accuracy, assume that the thrust being developed at the commencement of this forward motion is equal to the ballard pull. Once forward motion begins, it is true that the propeller thrust developed will decrease as a function of vessel speed. Consequently, the thrust <sup>ACTING</sup> ~~action~~ during the period of acceleration may be visualized as a constant and equal to the arithmetic average of ballard pull and thrust at impact velocity. When breaking ice by ramming, however, personal experience dictates that the impact velocity will seldom exceed 8 knots, and in most instances will be much less. Therefore, the actual thrust decrease over this speed range as seen from data in section E-2 is relatively small. For the present, therefore, let us assume that the thrust acting during acceleration is constant and equal to the ballard pull  $T_0'$ . If we do this rather than use the average thrust acting, the percentage error in thrust acting becomes

$$\% \text{ ERROR} = \frac{T_0' - \frac{T_0' + T_L}{2}}{\frac{T_0' + T_L}{2}} = \frac{T_0' - T_L}{T_0' + T_L}$$

In section E-2 we developed the relationships for  $T_0'$  and  $T'$  for both



the series B3-50 and B4-55 propellers, i.e.

$$T'_{B3.50} = 74.2 \rho^{2/3} D^{4/3} \quad (33A)$$

$$T'_{B3.50} = 156 \rho^{2/3} D^{2/3} \left[ 0.484 - 0.0233 \frac{v D^{2/3}}{\rho^{1/3}} \right] \quad (40)$$

$$T'_{B4.55} = 72.2 \rho^{2/3} D^{4/3} \quad (33B)$$

$$T'_{B4.55} = 156 \rho^{2/3} D^{2/3} \left[ 0.487 - 0.0277 \frac{v D^{2/3}}{\rho^{1/3}} \right] \quad (41)$$

Therefore for the B3-50 propeller by substitution

$$\% \text{ ERROR} = \frac{3.64 v - 2 \frac{\rho^{1/3}}{D^{2/3}}}{150.4 \frac{\rho^{1/3}}{D^{2/3}} - 3.64 v}$$

and in like manner for the B4-55 propeller

$$\% \text{ ERROR} = \frac{4.32 v - 3.7 \frac{\rho^{1/3}}{D^{2/3}}}{148.1 \frac{\rho^{1/3}}{D^{2/3}} - 4.32 v}$$

In order to evaluate our percentage error we could investigate the range of variation of the ratio  $\rho^{1/3}/D^{2/3}$  for past and present icebreakers. This ratio, however, has little physical meaning and its trend would be hard to predict. Consequently, let us introduce the ratio  $T'/D^2$  which is a propeller loading factor in psi and has physical significance. Since we wish to determine the expression for  $\rho^{1/3}/D^{2/3}$  in terms of our propeller loading factor we return to our expressions for propeller thrust from section E-2. For any given shaft horsepower, the ratio  $\rho^{1/3}/D^{2/3}$  must be constant with ship speed, hence for convenience let us evaluate it at the bollard condition. From section E-2 we have,

$$T'_{B3.50} = 74.2 \rho^{2/3} D^{4/3} \quad (33A)$$

$$T'_{B4.55} = 72.2 \rho^{2/3} D^{4/3} \quad (33B)$$

therefore

$$\rho^{1/3}/D^{2/3} = \sqrt{0.0135 T'_0/D^2} \quad \text{FOR B3.50}$$

$$\rho^{1/3}/D^{2/3} = \sqrt{0.0137 T'_0/D^2} \quad \text{FOR B4.55}$$





Since the difference between the three and four bladed propeller is so small (about 1.5%) we can use an average value expression to represent them both,

i.e. 
$$\frac{P^{1/3}}{D^{2/3}} = \sqrt{0.0137 \frac{T_0'}{D^2}}$$

Therefore, percentage error in  $T'$  becomes

$$\% \text{ error B3-50} = \frac{3.64 \sqrt{T_0'/D^2} - 0.234 \sqrt{T_0'/D^2}}{17.6 \sqrt{T_0'/D^2} - 3.64 \sqrt{T_0'/D^2}}$$

$$\% \text{ error B4-55} = \frac{4.32 \sqrt{T_0'/D^2} - 0.434 \sqrt{T_0'/D^2}}{17.3 \sqrt{T_0'/D^2} - 4.32 \sqrt{T_0'/D^2}}$$

Since the maximum error will occur at the impact velocity, and since this velocity will seldom exceed 8 knots (13.5 ft/sec), the maximum percentage error will be approximately

$$\% \text{ error B3-50} = \frac{49.2 - 0.234 \sqrt{T_0'/D^2}}{17.6 \sqrt{T_0'/D^2} - 49.2}$$

$$\% \text{ error B4-55} = \frac{58.3 - 0.434 \sqrt{T_0'/D^2}}{17.3 \sqrt{T_0'/D^2} - 58.3}$$

From an investigation of past and present icebreaking vessels we find that the ratio of  $T_0'/D^2$  per shaft varies from about 490 to 765. This is a considerable variation, however, we may evaluate present and possible future trends in powering so as to arrive at a reasonable value of  $T_0'/D^2$  which will be representative of future designs. The value of 490 is characteristic of river icebreakers and the smaller, lower powered arctic icebreakers up to and including the Mackinaw and wind class vessels. These breakers, as regards polar service, are somewhat outdated and underpowered. The higher value of 765 is representative of the Glacier and several of the more recent large, foreign built, polar icebreakers and typifies a trend through the <sup>y</sup>ears toward



higher shaft horsepowers per given diameter propeller.

Now as regards the so called first line polar icebreakers, it may be inferred that future designs will go to even higher shaft horsepower so as to increase developed thrust and icebreaking capability. Such an inference, however, does not seem to be really justified if we review the problem a little more closely. In any icebreaker it is desirable to have as large a propeller diameter as is possible so as to obtain maximum thrust. Due to limitations in water depths in the areas of operation in polar regions plus the desire to provide maximum propeller tip immersion so as to minimize propeller damage by contact with floating ice, there is a practical limit for the draft of a polar icebreaker. This necessarily limits the maximum useable propeller diameter. This limit becomes somewhat evident if we examine present trends. The Glacier, a twin screw vessel with 21000 installed shaft horsepower has a full load draft of about 28' 7" and a 17' 6" propeller while in contrast, the wind class vessels, all twin screw (modified) vessels with 10000 installed shaft horsepower and built about eleven years before the Glacier have a full load draft of about 28' 0" and a 17' 0" propeller. Further, the atomic powered Lenin, a triple screw vessel with 39200 installed shaft horsepower has a full load draft of 30' 3" and a design study by O. Oakley of BuShips and S. W. Lank of the U.S. Coast Guard, presented in a paper Application of Nuclear Power to Icebreakers,<sup>(21)</sup> propose a twin screw vessel of 30000 installed shaft horsepower with a 29' 0" full load draft and an 18' 0" propeller. Of course, installed shaft horsepower may still be continuously increased in future designs despite restrictions and propeller



protection considerations. If this is done, developed propeller thrust will increase, however, such increases in shaft horsepower would be extremely inefficient since the gain in thrust with increased power is severely limited by the maximum propeller disc area which can be provided. This inefficiency would be magnified by the desire to provide as much propeller tip immersion as possible so as to protect the propellers from damage from floating ice.

From the above discussion, therefore, it would seem that a value of  $\tau_o'/D^2 = 765$  per shaft is more representative of present day practice with a possible increase to a somewhat maximum efficient limit of about 1000 for future large designs. If we select a value of

$$\tau_o'/D^2 = 850 \quad \text{per shaft}$$

as representative of present and possible future trends in icebreaker powering, we find that about the highest percentage error introduced in  $\tau'$  due to the use of  $\tau_o'$  rather than average thrust over the accelerating distance becomes

$$\begin{array}{ll} \% \text{ error} & = + 9.12\% \\ & \text{B3-50} \end{array}$$

$$\begin{array}{ll} \% \text{ error} & = + 10.2\% \\ & \text{B4-55} \end{array}$$

Consequently, for our development of icebreaker impact speed, if we consider the thrust acting during the period of acceleration as constant and equal to

$$\tau' = 0.91 \tau_o' \quad (59)$$

we shall have simplified our problem with a maximum introduced error of about 0.5%. It is interesting to note that if powering trends do continue as discussed and the ratio of  $\tau_o'/D^2$  do increase to as high as 1000, the error introduced will still be less than 1.5%.

Based on our above development, therefore, expression (58) becomes





$$S' = 78.54 W \int_0^{x'} \frac{v dv}{0.91 T_0' - 330 v^{1.61}} \quad (60)$$

if we let

$$v = \left( \frac{0.91 T_0'}{330} \right)^{\frac{1}{1.61}} x'$$

$$dv = \left( \frac{0.91 T_0'}{330} \right)^{\frac{1}{1.61}} dx'$$

then we have

$$S' = 0.9577 W T_0'^{0.24} F(x') \quad (61)$$

where

$$F(x') = \int_0^{x'} \frac{x' dx'}{1 - x'^{1.61}}$$

The expression for  $F(X^1)$  cannot be integrated by elementary methods but may be reasonably approximated by a method of numerical integration such as Simpsons rule. This has been done for values in the ship range and the results presented as figure 4/. Based on the values in this figure we may determine our vessel impact speed for acceleration over a given distance in open water.

The value of  $F(X^1)$  may be determined from (61) as

$$F(X^1) = 17.35 \frac{S'}{W T_0'^{0.24}}$$

or if ballard pull is expressed in tons, as

$$F(X^1) = 2.73 \frac{S'}{W T_0'^{0.24}} \quad (62)$$

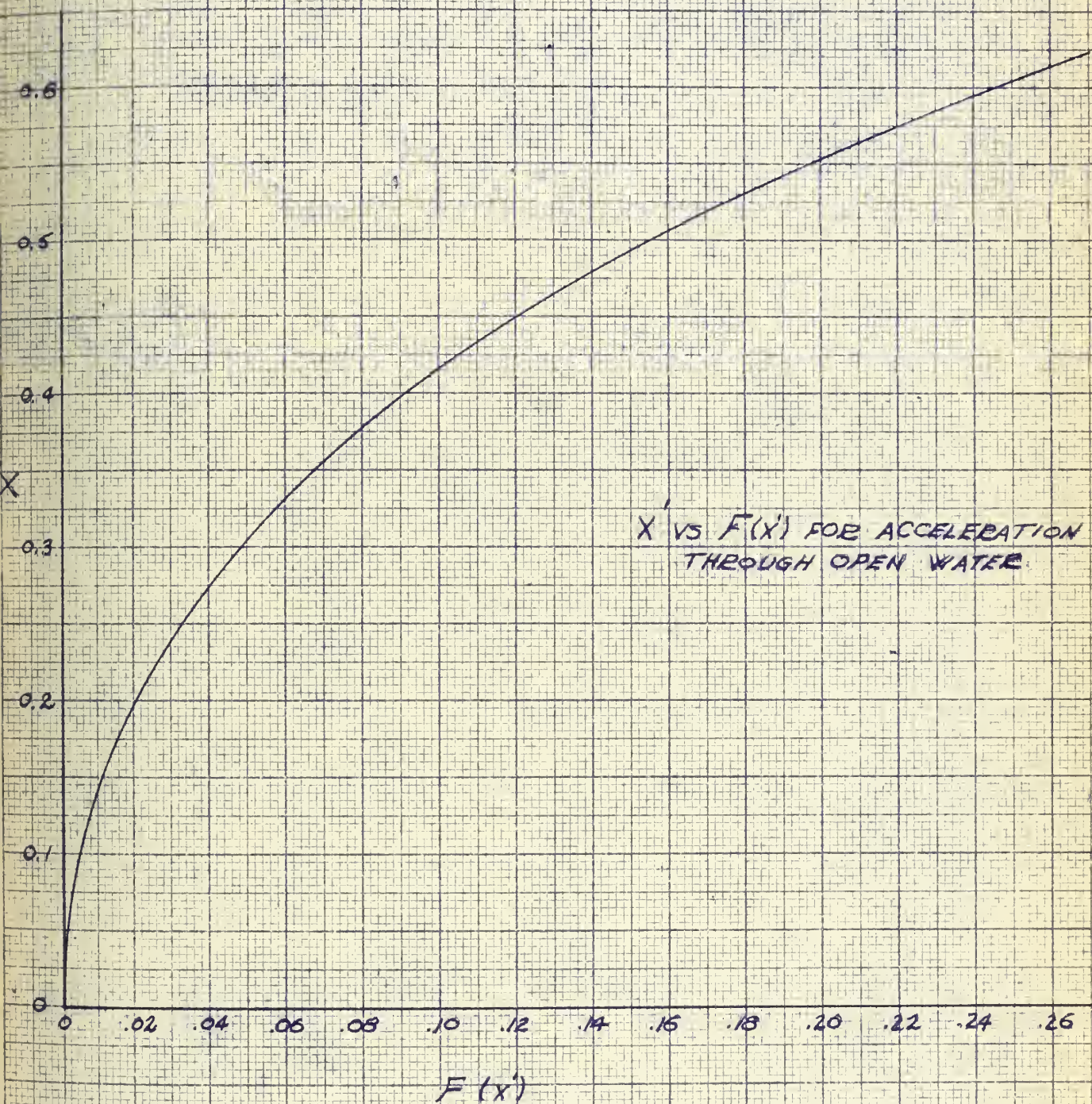
Knowing  $F(X^1)$  we can determine  $X^1$  from figure 4/ and the vessel impact speed as

$$V = 1.835 X' T_0'^{0.621} \quad \text{knots}$$

$$v = 3.1 X' T_0'^{0.621} \quad \text{ft/sec} \quad (63)$$







$$\int_0^{x'} \frac{x' dx'}{1 - x'^{1.61}}$$

FIG 41





The vessel seldom, however, operates in clear open water when engaged in breaking ice. The water soon becomes filled with pieces of ice varying in size and thickness which are the remains of previous ramming attempts. This ice filled channel which the vessel generates as it progresses, offers considerably more resistance to the passage of the vessel than that resulting in open water.

Consequently, when we consider the vessel accelerating in an ice filled channel we must, in addition to normal water resistance, include a consideration of the added resistance offered by the pieces of ice in the water. This ice resistance is the result of several forces acting against the hull as it accelerates. The largest of these forces is the inertia force which occurs when the pieces of ice are accelerated from zero to the speed of the vessel. This force can be expressed in the form

$$R_{ice} = K \frac{\rho' v^2}{2g} \delta h$$

where  $h$  is the thickness of the ice pieces and  $K$  a constant dependent upon hull form. In addition to this inertia force there also exists a displacement force of the ice pieces and a friction force of the ice pieces as they pass against the steel hull. Thus the total ice force is a combination of forces partly dependent upon the thickness of the ice and partly upon the speed of the vessel.

Since it appears from experimentation that the resistance of ice has a positive value even as zero speed is approached, the total ice resistance may theoretically be expressed as

$$R_{ice} = (C_1 + C_2 v^2) \delta h$$



The value of  $C_1$  will, in most instances be very small due to the ability of the ice pieces to move as vessel motion begins. Its value will increase as the ice pieces become larger or as the channel becomes clogged with a heavier concentration of ice pieces. In either case, however, unless we approach the ultimate wherein the ice is solid and not broken into pieces, the value of  $C_1$  will be small enough so that we can neglect it. In this case we may express total ice resistance as

$$R_{ice} = C_2 v^2 B h$$

If we generalize this expression for the normal icebreaker hull form, we have as an approximation

$$R_{ice} = 142.3 v^2 h \quad \text{Lbs/INCH}$$

which experience and experiments indicate is a fairly reasonable approximation.

The thickness of the pieces of ice in the broken channel vary in thickness from very small to quite large. We must, in order to be able to make reasonable preliminary predictions, assume some sort of statistical average thickness. Since we are considering the case of the sea going polar icebreaker, we may assume an ice thickness of 24 inches as a reasonable average for the thickness of the pieces resulting from our ramming operation. If we do this, we obtain

$$R_{ice} = 3420 v^2 \quad \text{Lbs} \quad (64)$$

Since the resistance is in addition to the total water resistance of the hull, we must add it to the values of figure 40 in order to obtain a new representative curve of total resistance versus ship speed. This is shown in figure 42. In order to more easily handle our ship acceleration problem,





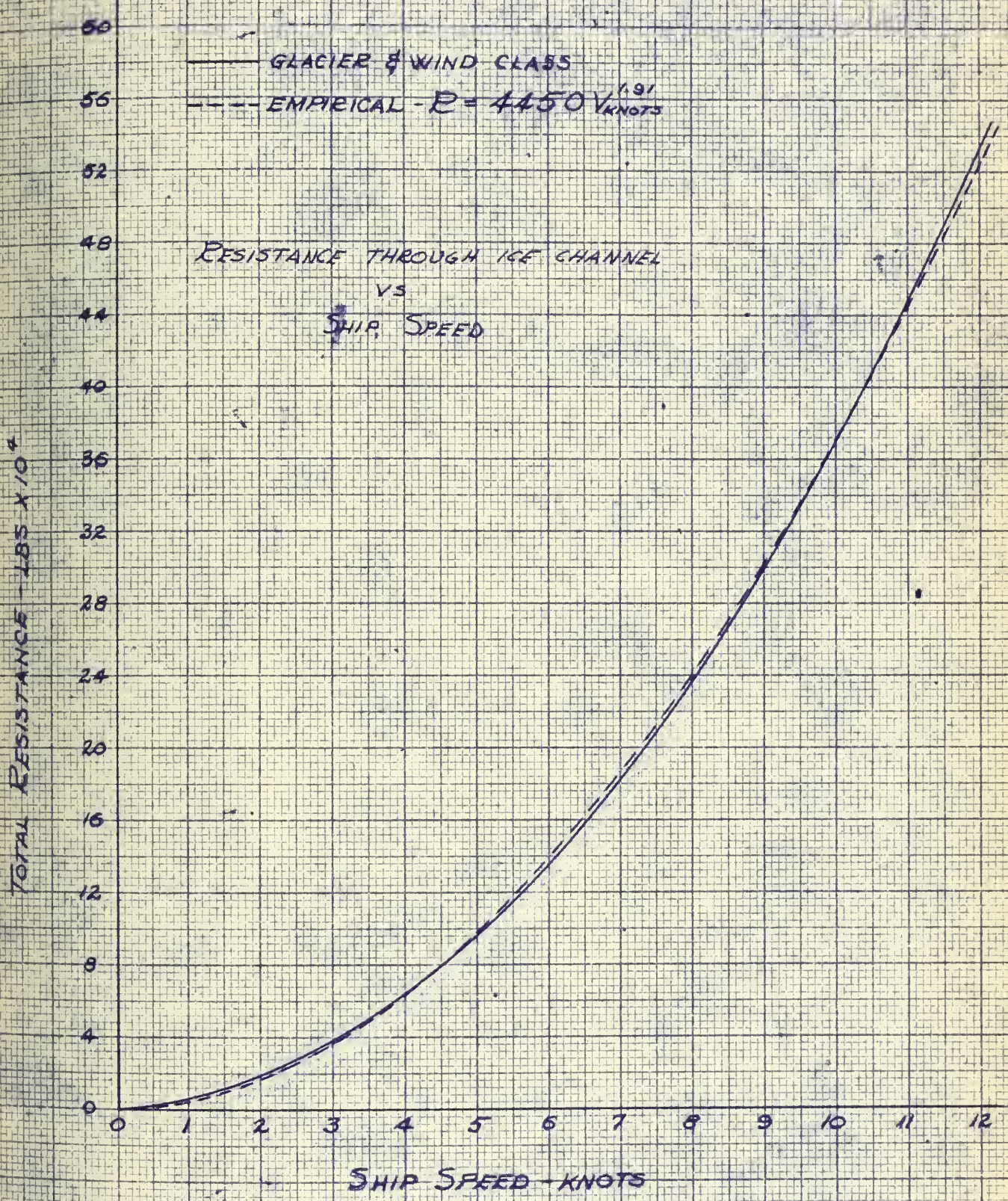


FIG 42





an empirical curve of total ship resistance versus ship speed is also given.

This empirical relationship may be expressed as

$$R_{TOTAL} = 4450 V^{1.91} \quad \text{lbs}$$

or if ship speed is expressed in ft/sec

$$R_{TOTAL} = 1640 V^{1.91} \quad \text{lbs} \quad (65)$$

If we now return to our expression for vessel acceleration (58) and substitute (65) for vessel resistance, we have

$$S' = 78.54 W \int_0^V \frac{V dV}{0.91 T_0' - 1640 V^{1.91}}$$

If we let

$$V = \left( \frac{0.91 T_0'}{1640} \right)^{\frac{1}{1.91}} X'$$

$$dV = \left( \frac{0.91 T_0'}{1640} \right)^{\frac{1}{1.91}} dX'$$

we have

$$S' = 0.0343 W T_0'^{0.047} F(X') \quad (66)$$

where

$$F(X') = \int_0^{X'} \frac{X' dX'}{1 - X'^{1.91}}$$

We again evaluate the expression for  $F(X^1)$  by means of numerical integration so as to obtain the variation of  $F(X^1)$  as a function of  $X^1$  in the ship range.

The results are shown in figure <sup>43</sup>~~40~~. As in the case of acceleration in open water we may determine  $F(X^1)$  by

$$F(X^1) = 29.2 \frac{S'}{W T_0'^{0.047}}$$

or if bollard pull is expressed in tons

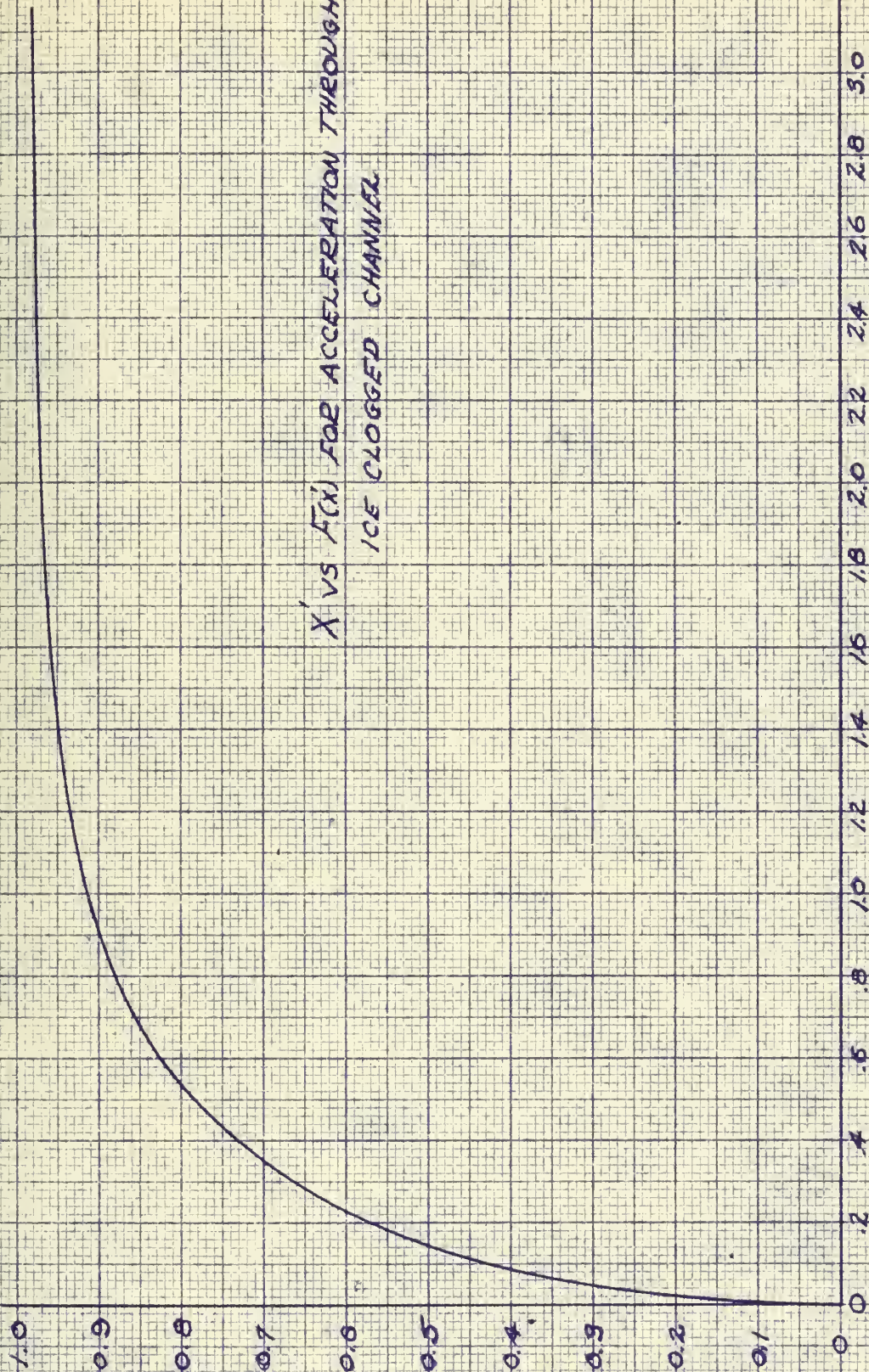
$$F(X^1) = 20.35 \frac{S'}{W T_0'^{0.047}} \quad (67)$$

Knowing  $F(X^1)$  we may determine  $X^1$  from figure <sup>43</sup>~~40~~ and vessel impact speed as





$X'$  VS  $F(X')$  FOR ACCELERATION THROUGH  
ICE CLOGGED CHANNEL



$$F(X') = \int_0^{X'} \frac{X' dx'}{1 - X'^2}$$

FIG 43





$$V = 0.665 \times T_o^{0.524} \quad \text{KNOTS}$$

(68)

$$W = 1.12 \times T_o^{0.524} \quad \text{ft/SEC}$$

It should be noted here that the values of ballard pull  $T_o$  as obtained from figure 9 and 12 are open water values, i.e. free of vessel influence. Consequently, the values should be modified by a factor which represents the influence of the hull so as to obtain the thrust actually developed by the propeller when in the "behind the ship" position. The factor we speak of here is that commonly referred to as the relative rotative efficiency.

The relative rotative efficiency which reflects the dissimilitude of flow conditions to the propeller when behind the hull as compared to when in open water, is a difficult item to determine for the icebreaker type vessel. Doctor Schoenben, in a paper on propulsion and propellers lists a value of 0.985 for twin screw vessels. <sup>(108)</sup> This, however, is for merchant ship forms and may not be too reliable for the case of the icebreaker. If we consider several icebreakers for which test tank data is available, we may obtain representative values for this quantity.

By definition

$$SHP = \frac{EHP}{\eta_r \eta_p \eta_n \eta_m}$$

The mechanical efficiency,  $\eta_m$ , which considers the losses occurring in the shaft bearings and stern tube stuffing boxes is normally about ninety eight per cent. Therefore

$$\eta_m = 0.98$$

The hull efficiency,  $\eta_n$ , is defined as

$$\eta_n = \frac{1-t}{1-w}$$

Therefore

$$\eta_r = \frac{EHP(1-w)}{0.98 SHP(1-t) \eta_p}$$

For the Glacier, at design speed this becomes

$$\eta_r = 1.077$$



For the Wind class vessels, at design speed it becomes

$$\eta_r = 0.982$$

If we try to generalize more completely we find that the ratio of effective horsepower to shaft horsepower, or propulsive efficiency, remains relatively constant throughout the vessels speed range and for the icebreaker type vessel averages about 0.58. Therefore

$$\eta_r = \frac{0.58 (1-w)}{0.58 \eta_p (1-z)}$$

Propeller open water efficiency ranges between about 0.50 to 0.65 at design speed, hence we may assume a value of  $\eta_p = 0.60$  as representative for our purposes. In section E-2 we discussed wake fraction for this type vessel and determined that a value of  $W = 0.18$  was realistic and reasonable for the twin stern screw icebreaker with no bow propeller. As regards the thrust deduction coefficient,  $t$ , we must again examine past and present vessels for which data is available so as to determine a reasonable value to use. Dr. Jansson, in his paper on icebreaker design lists a value of 0.27 as characteristic of a twin screw vessel with no bow propeller. In a paper by Nordstrom, Edstrand and Lindgren, reporting work done at the Swedish State Tank, values of 0.218 to 0.245 over a speed range of 9-14 knots are given for models which were designed with bow propellers but which had the bow propeller removed and a dummy boss and cone substituted. Model tests at the David Taylor Model basin with several classes of Coast Guard and Navy icebreakers resulted in values of 0.27 for the wind class, 0.27 for Mackinaw, 0.24 for Cactus and 0.27 for Glacier. In the case of Mackinaw and the Wind class vessels, each was built with a bow propeller, although in the wind class vessel this propeller was



later removed and replaced with a covering blank. Values listed for these vessels, therefore, are not too reliable since the data did not indicate the status of the bow propeller which could materially effect the resulting value of  $t$ . For our purposes, however, we may select a representative value of

$$t = 0.25$$

Substituting our values of  $t$ ,  $\omega$  and  $\gamma_p$  we have for representative relative rotative efficiency

$$\gamma_r = 1.077$$

Since this is only a representative value and determined from so few data it would seem advisable to ignore the possible effects of relative rotative efficiency and assume

$$\gamma_r = 1.0$$

Hence, for all practical purposes, the thrust developed by the propellers when installed behind the ship is essentially equal to open water values. In our expression for vessel impact speed, as well as all others wherein propeller thrust is a factor, we may use the open water values as tabulated in Section E-2.

Returning now to our expression (56) for the vertical bow reaction force

$$F = XT + \sqrt{X^2 T^2 - \frac{\omega^2 v^2 Y}{gAH} [\sin^2 \alpha (1 - e^2) - 1]}$$

we see that the thrust referred to is that which acts after vessel impact with the ice. This thrust increases from that which acts at the moment of impact to a maximum of bellard pull at the instant of ice collapse when vessel speed becomes zero. This, in essence, is the same condition as existed during the period of vessel acceleration, only reversed. Consequently, the reasoning used to determine the average thrust acting during the period of acceleration





applies here also and we may re write (56) as

$$F = 0.91 XT_0 + \sqrt{0.828 X^2 T_0^2 - \frac{W^2 v^2 \gamma}{g A H_L} [\sin^2 \alpha (1-e^2) - 1]} \quad (69)$$

where  $v$  as used here applies to the impact velocity as determined by (63) or (68).

Previously we alluded to the term  $(1-e^2)$  in the above expression where  $e$  is the coefficient of restitution between ice and steel. It was mentioned that a value for  $e$  could not be found in a search of existing literature. Mr. F. L. Ferris, of BuShips, in a paper on icebreaker design uses a value <sup>(10)</sup> of  $e = 0.95$ . This value, however, seems excessively high, so <sup>THE AUTHOR</sup> ~~it was~~ decided to perform a simple experiment so as to determine a little more accurately the range of values for this coefficient.

Consider two bodies, one with mass  $m_1$  and velocity  $u_1$  and the other with mass  $m_2$  and velocity  $u_2$  which collide so as to produce direct central contact. Let  $v_1$  be the velocity of  $m_1$  and  $v_2$  the velocity of  $m_2$  after the impact. It may be shown that

$$v_1 - v_2 = e (u_2 - u_1)$$

where  $e$  is the coefficient of restitution between the materials involved.

Rearranging

$$e = \frac{v_1 - v_2}{u_2 - u_1}$$

If a body be allowed to fall vertically upon the horizontal surface of a large mass, we have a special case of direct central impact. If the mass upon which the body drops is rigidly supported, its velocity at all times may be assumed equal to zero. Therefore

$$e = - \frac{v}{u}$$

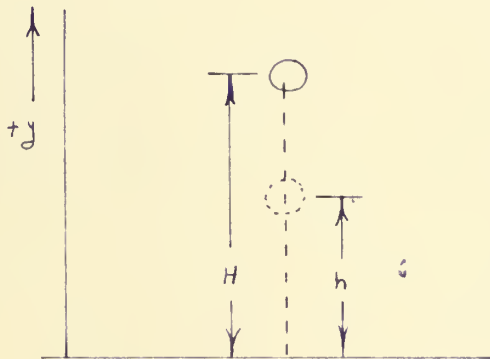


where  $u$  and  $v$  are of opposite sign to signify opposite direction. If the body be allowed to fall through a distance  $H$ , then its impact velocity is

$$u = -\sqrt{2gH}$$

and if it rebounds a distance  $h$ , its rebound velocity is

$$v = \sqrt{2gh}$$



Consequently,

$$e = \sqrt{\frac{h}{H}}$$

For this experiment, therefore, large pans of fresh and salt water were frozen. A steel ball weighing 5.44 grams was dropped from a known height through a guiding glass tube sufficiently large in diameter to pass the ball with little possibility of friction loss and the height of rebound was measured. In all instances the temperature of the ice ranged from  $-3^{\circ}\text{C}$ . to  $-10^{\circ}\text{C}$ . Due to the fact that a controlled freezing atmosphere could not be maintained during actual testing, it was necessary to perform a test immediately upon removal of the ice sample from the freezer so as to insure that subsequent <sup>MELTING</sup> ~~wetting~~ of the ice at its surface would not result in erroneous readings. This process was repeated a considerable number of times so as to insure consistent readings. The result of these tests may be





summarized as follows

$$e = 0.189 \quad \text{for fresh water ice}$$

$$e = 0.120 \quad \text{for salt water ice}$$

In the case of salt water ice it is known that the results will be effected slightly by the salinity of the water and for both fresh and salt water  $e$  will no doubt vary slightly with ice temperature. However, it is doubtful whether these variations would be of such magnitude as to materially effect the above results. Assuming the above stated values of  $e$ , therefore, as representative for the impact of steel on ice, we have that

$$e^v = 0.0359 \quad \text{for fresh water ice}$$

$$e^v = 0.0143 \quad \text{for salt water ice}$$

Since the values of  $e^v$  in both instances are very small, we may for all practical purposes assume

$$e^v = 0$$

Therefore, expression (69) becomes

$$\bar{F} = 0.91 X T_0 + \sqrt{0.828 X^v T_0^v + \frac{W^v v^v Z}{g A H}} \quad \text{TONS} \quad (70)$$

where

$$X = \frac{\cot \alpha \cos \beta - f_0}{\cos \beta + f_0 \cot \alpha} \quad (55)$$

$$Z = Y \cos^2 \alpha = \frac{\cos \beta \cos^2 \alpha}{\cos \beta + f_0 \cot \alpha}$$

$$A = \left[ \frac{C_B}{C_S} + \left( \frac{h_1}{h_2} \right)^2 \frac{C_B}{4 C_w} \right] \quad (47)$$



### Part 3

#### Vessel Advance due to Impact

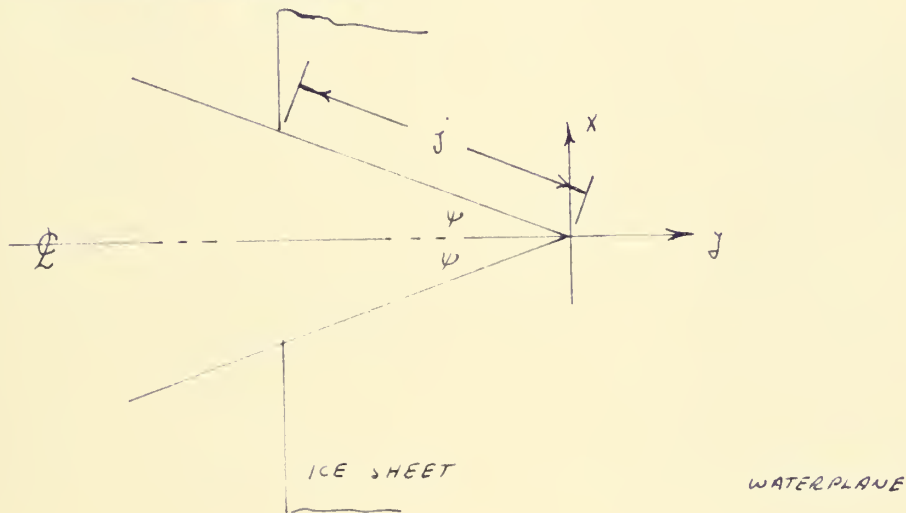
When an icebreaking vessel strikes an ice field it can overcome the ice by means of a bending stress generated when the vessel climbs up on to the ice or it may do so by means of compressive stresses as a result of impact forces and propeller thrust acting in the plane of the ice sheet. The forces <sup>IN THE</sup> ~~with~~ plane of the ice sheet cause a state of plane stress to be established in the ice which ultimately produces failure in the form of long radial cracks emanating from the bow of the ship. The bending forces, normal to the ice sheet, produce stresses in the ice which ultimately cause failure along lines roughly at right angles to the radial cracks. The details of the ice breaking process, naturally, depend upon which type of failure occur first. For relatively thin ice there is considerable photographic evidence to indicate that the radial cracks precede those due to bending. In the case of thick ice, with which we are concerned here, there is considerable reason to believe that the compressive stresses in the plane of the ice sheet are insignificant and that the ice is broken solely by means of stresses in the plate due to bending.

In order to investigate the effect of these compressive forces in the plane of the ice sheet let us consider, in an elementary manner, how they develop.

Let us again consider the bow section of the vessel to have the shape of a wedge and that the various waterplanes and bow sections are formed by straight lines inclined toward the centerline plane. As we have already mentioned, such a simplifying assumption will not lead to appreciable error



since most sea going breakers do have waterplanes and sections of small <sup>A</sup> CURVATURE at their forward end



Since the vessels waterlines are symmetrical about the centerline or  $y$  axis we need consider only one half of the vessel. If we take the  $x$  and  $y$  axis as shown we may express the load waterline in the form

$$x = a y$$

where  $a$  may be determined by an investigation of existing vessels. The length  $j$  of waterplane which has penetrated the ice sheet may be expressed as

$$j = \int_{j_1}^{j_2} \left[ \left( \frac{dx}{dy} \right)^2 + 1 \right]^{1/2} dy$$

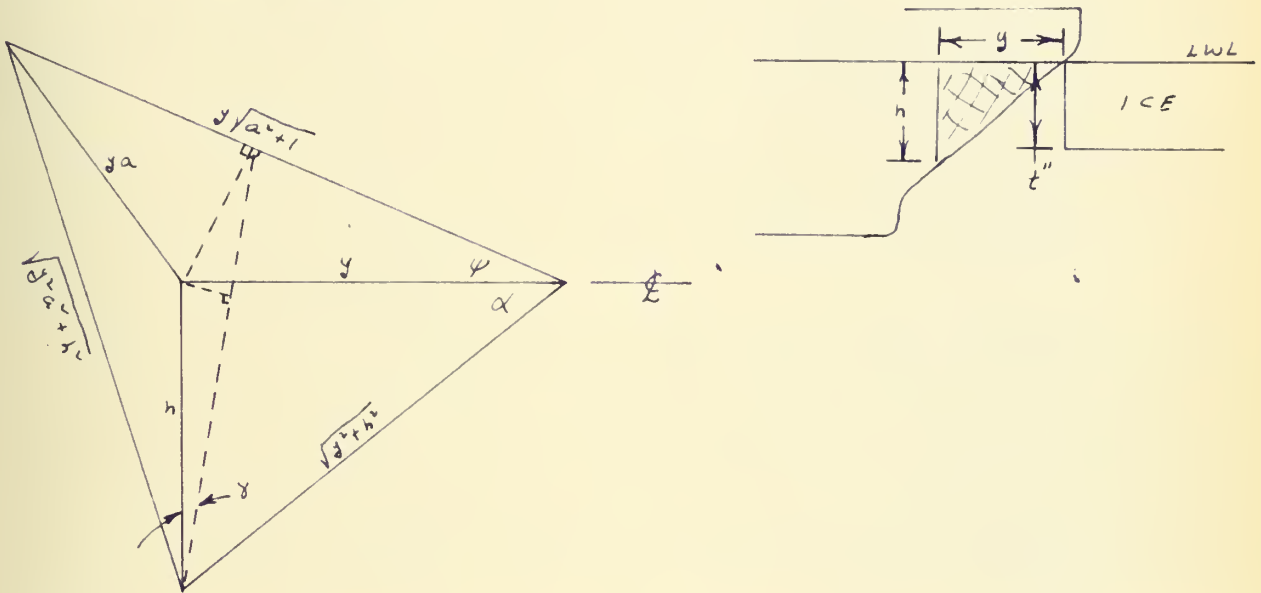
which, for our case gives

$$j = j \sqrt{a^2 + 1}$$





Therefore if we consider the bow section which has penetrated the ice in three dimension, we have



where  $h = y \tan \alpha$ . This restriction is necessary to account for the condition when forward motion due to compressive forces is such that  $h > t$ . In this instance, the above pictorial representation does not hold since  $h$  becomes a constant and equal to  $t$  the ice thickness. For the present, however, we shall consider only the case where  $h < t$  since it is the more severe condition and typical of polar conditions.

Now it is also true that the relationship

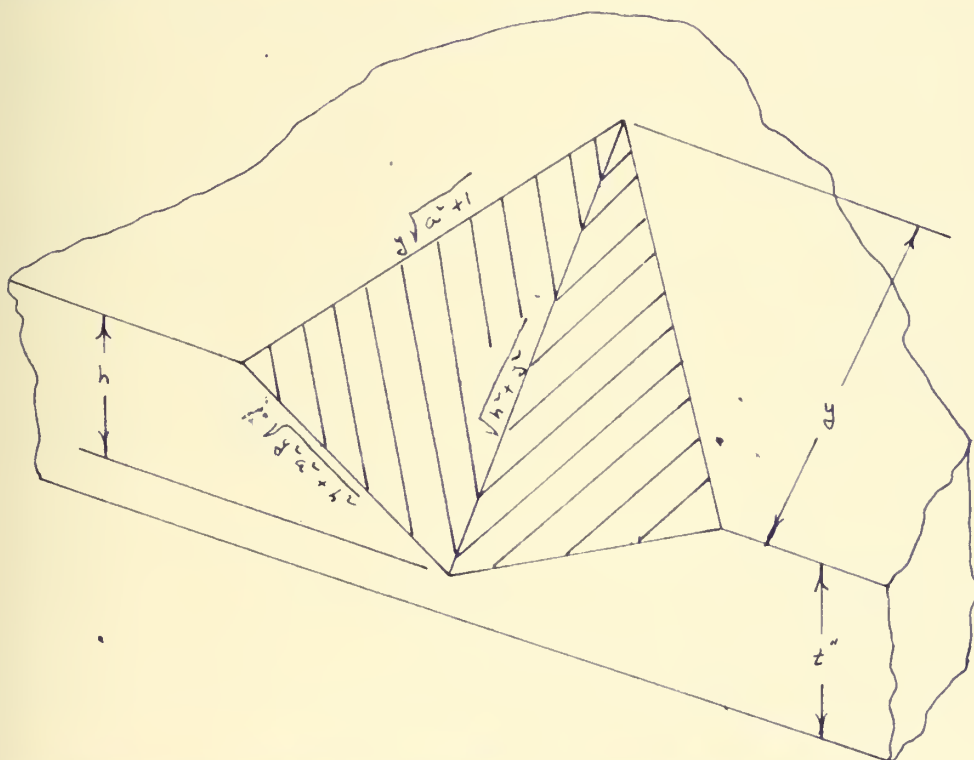
$$h = y \tan \alpha$$

does not hold if forward motion due to compressive forces is such as to cause the vertical portion of the forefoot to strike and penetrate the ice. In this instance  $h$  will again be constant and equal to vessel draft. We need not concern ourselves with this restriction, however, since in normal icebreaking by ramming the vessel will never penetrate the ice so deeply due to compression in the plane of the ice. If such penetration is accomplished, the ice is thin



enough not to require ramming since continuous forward motion can be maintained. For thick ice, where continuous forward motion cannot be maintained and ramming is necessary, the energy available to compress the ice will soon dissipate itself in crushing the ice locally and forming a wedge-like groove in which the vessel will climb on to the ice. However, we shall not belabor this point now, but rather, accept it and in a later section its truth will be substantiated.

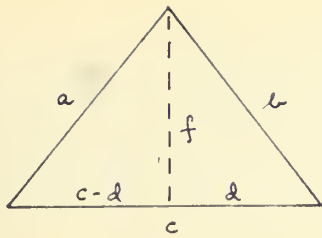
Now when the vessel strikes the ice the forces acting cause the ice to fail by compression in the immediate vicinity of the stern so as to form a wedge-like groove. If we consider that portion of the vessel's side which is actually in contact with the ice in this groove we have a triangular section such that



Now for any triangle with sides  $a$ ,  $b$  and  $c$  we have







$$\text{where } d = \frac{b^2 + c^2 - a^2}{2c}$$

$$f = \frac{\sqrt{2a^2b^2 + 2a^2c^2 + 2b^2c^2 - a^4 - b^4 - c^4}}{2c}$$

Therefore the area of the triangle becomes

$$\text{Area} = \frac{fc}{2} = \frac{1}{4} \sqrt{2a^2b^2 + 2a^2c^2 + 2b^2c^2 - a^4 - b^4 - c^4}$$

For our case above, however,

$$a = y \sqrt{a^2 + 1}$$

$$b = \sqrt{h^2 + y^2}$$

$$c = \sqrt{y^2 a^2 + h^2}$$

Therefore for one side of the groove

$$\text{Area} = \frac{y}{2} \sqrt{a^2 h^2 + h^2 + y^2 a^2}$$

but

$$h = y \tan \alpha$$

Therefore

$$\text{Area per side} = \frac{y^2}{2} \sqrt{a^2 \sec^2 \alpha + \tan^2 \alpha} = \frac{A_t}{2}$$

Now if we consider the energy available for compressing this ice as well as its dissipation, we have

$$E_1 + E_2 = E_3$$

where

$E_1$  = Component of kinetic energy acting normal to the stern and lost in impact with the ice

$E_2$  = Energy due to the propeller thrust acting through the distance of compression



$E_3$  = Energy dissipated in crushing the ice

In section F-2 we stated that the energy lost due to impact with the ice could be stated as

$$E_1 = \frac{1}{2} m v^2 \sin^2 \alpha \quad \text{ft-lb} \quad (48)$$

where

$$m = \text{vessel mass} = \frac{2240 W}{g} \quad \text{lb sec}^2/\text{ft}$$

In addition we showed that

$$v = 3.1 \times 10^{-6} T_o^{0.621} \quad \text{ft/sec} \quad (63)$$

in open water, and approximately

$$v = 1.12 \times 10^{-6} T_o^{0.524} \quad \text{ft/sec} \quad (68)$$

ice filled water. Therefore

$$E_1 = 334 \times 10^{-6} T_o^{1.242} W \sin^2 \alpha \quad \text{ft-lb} \quad (71)$$

in open water and

$$E_1 = 43.6 \times 10^{-6} T_o^{1.048} W \sin^2 \alpha \quad \text{ft-lb} \quad (72)$$

in an ice filled channel.

The energy due to propeller thrust acting may be stated as

$$E_2 = T' y$$

where

$y$  = total horizontal distance vessel advances during ice compression - ft.

Now we know that  $T'$  is a variable since, as the ice compresses, vessel speed will decrease, and hence, propeller thrust increase. In section F-2 we demonstrated how this variable thrust could be replaced by a constant average value of  $0.91 T_o$ , where  $T_o$  is the ballard pull in tons, with little introduced error. Hence

$$E_2 = 2040 T_o y \quad \text{ft lb} \quad (73)$$

The energy dissipated in crushing the ice may be deduced from the physical problem. As the vessel strikes the ice the forces normal to the shell act on



a very small area of ice, hence the compressive stress is very large and the ice will fail and deform in compression. At no time, however, does this stress exceed  $\sigma_c$ , the compressive strength of ice since as this stress is reached the ice will fail and relieve itself by continuously deforming and enlarging the area of contact with the hull. This will continue until such time as the forces acting normal to the hull act over an area of contact large enough to reduce the applied compressive stress below  $\sigma_c$ . At this instant the ice will resist further deformation and the remaining vessel energy will dissipate itself in climbing up on to the ice. Therefore, we may say that

$$\begin{aligned} E_3 &= \text{Force} \times \text{distance} \\ &= \int \sigma_c A_t d(d) \end{aligned} \quad (74)$$

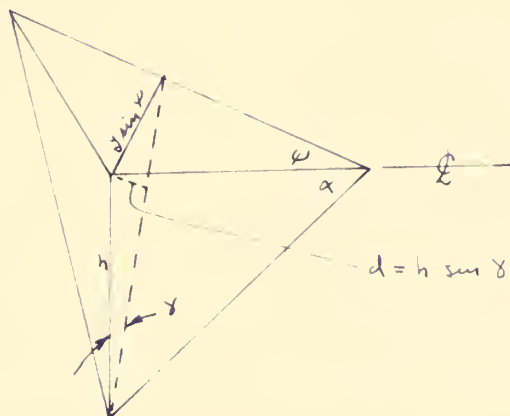
where  $\sigma_c$  = compressive strength of ice - lb/ft<sup>2</sup>  
 $A_t$  = area of contact between hull and ice - ft<sup>2</sup>  
 $d$  = distance normal to shell through which force moves - ft

Now previously we showed that

$$A_t = \int \sqrt{a^2 \sec^2 \alpha + \tan^2 \alpha}$$

In addition, we can determine that

$$d = h \sin \gamma$$







but  $h = y \tan \alpha$  therefore

$$d = y \sin \gamma \tan \alpha$$

$$d(l) = \sin \gamma \tan \alpha dy$$

hence

$$E_3 = \int_0^y \int_0^y \sin \gamma \tan \alpha \sqrt{a^2 \sec^2 \alpha + \tan^2 \alpha} dy$$

or

$$E_3 = \frac{\int_0^y y^3}{3} \sin \gamma \tan \alpha \sqrt{a^2 \sec^2 \alpha + \tan^2 \alpha}$$

In section F-6 we show that

$$\tan \gamma = \frac{\sin \varphi}{\tan \alpha}$$

therefore

$$\sin \gamma = \frac{\sin \varphi}{\sqrt{\sin^2 \varphi + \tan^2 \alpha}}$$

and

$$E_3 = \frac{\int_0^y y^3}{3} \frac{\sin \varphi \tan \alpha}{\sqrt{\sin^2 \varphi + \tan^2 \alpha}} \sqrt{a^2 \sec^2 \alpha + \tan^2 \alpha}$$

Now we said previously that  $x = ay$  defines the waterline, therefore

$$\tan \varphi = \frac{x}{y} = a$$

hence

$$\sin \varphi = \frac{a}{\sqrt{a^2 + 1}}$$

Substituting we have

$$E_3 = \frac{\int_0^y y^3 a}{3} \tan \alpha \quad ft-Lb \quad (75)$$

Considering <sup>FIRST</sup> just the case of the vessel accelerating in open water and equating (48), (73) and (75) we have

$$334 \lambda^{1/2} T_0^{1.242} \omega \sin^2 \alpha + 2040 T_0 y = \frac{\int_0^y y^3 a}{3} \tan \alpha$$

or

$$y^3 - 6120 P y - 1002 W \lambda^{1/2} P T_0^{0.242} \sin^2 \alpha = 0 \quad (76)$$

where

$$P = \frac{T_0}{\int_0^y a \tan \alpha}$$

Let

$$y = u + v \quad (77)$$

where  $u$  and  $v$  are unknowns whose sum equals a root of the cubic, then



$$u^3 + v^3 + (34v - 6120P)(u + v) - 1002Wx'vT_0^{0.242} \sin^2 \alpha = 0 \quad (78)$$

Since the two unknowns  $u$  and  $v$  have imposed on them only the condition (77), they are not determined uniquely. Hence we may impose a second condition, which, in order to simplify take as

$$34v - 6120P = 0 \quad (79)$$

We, therefore, have the simultaneous equations

$$\left. \begin{aligned} 34v - 6120P &= 0 \\ u^3 + v^3 - 1002Wx'vT_0^{0.242} \sin^2 \alpha &= 0 \end{aligned} \right\}$$

Eliminating  $v$  we have

$$u^3 - 1002Wx'u^3T_0^{0.242}P \sin^2 \alpha + 8.5 \times 10^4 P^3 = 0 \quad (80)$$

Solving as a quadratic

$$u^3 = 501Wx'u^3T_0^{0.242}P \sin^2 \alpha \pm \sqrt{(501Wx'u^3T_0^{0.242}P \sin^2 \alpha)^2 - 8.5 \times 10^4 P^3}$$

If we let

$$u^3 = 501Wx'u^3T_0^{0.242}P \sin^2 \alpha + \sqrt{(501Wx'u^3T_0^{0.242}P \sin^2 \alpha)^2 - 8.5 \times 10^4 P^3} = A'$$

$$v^3 = 501Wx'v^3T_0^{0.242}P \sin^2 \alpha - \sqrt{(501Wx'v^3T_0^{0.242}P \sin^2 \alpha)^2 - 8.5 \times 10^4 P^3} = B'$$

we can show that the roots are

$$u = \sqrt[3]{A'}, \quad \omega \sqrt[3]{A'}, \quad \omega^2 \sqrt[3]{A'}$$

$$v = \sqrt[3]{B'}, \quad \omega \sqrt[3]{B'}, \quad \omega^2 \sqrt[3]{B'}$$

where

$$\omega = -\frac{1}{2} + \frac{i}{2}\sqrt{3} \quad \omega^2 = -\frac{1}{2} - \frac{i}{2}\sqrt{3}$$

Now if we impose condition (79), then the only combinations which will satisfy it are

$$\sqrt[3]{A'} \sqrt[3]{B'}, \quad \omega \sqrt[3]{A'} \omega^2 \sqrt[3]{B'}, \quad \omega^2 \sqrt[3]{A'} \omega \sqrt[3]{B'}$$

Substituting these pairs of values in (77) we have as roots of (76)





$$y_1 = \sqrt[3]{A'} + \sqrt[3]{B'}$$

$$y_2 = \omega \sqrt[3]{A'} + \omega^2 \sqrt[3]{B'}$$

$$y_3 = \omega^2 \sqrt[3]{A'} + \omega \sqrt[3]{B'}$$

however, since ours must be a real root, we may take as the solution of (76)

$$y = \sqrt[3]{501 \omega x' T_0^{1.242} P \sin^2 \alpha} + \sqrt[3]{(501 \omega x' T_0^{1.242} P \sin^2 \alpha)^2 - 8.5 \times 10^8 P^3}^{1/2}$$

$$+ \sqrt[3]{501 \omega x' T_0^{1.242} P \sin^2 \alpha} - \sqrt[3]{(501 \omega x' T_0^{1.242} P \sin^2 \alpha)^2 - 8.5 \times 10^8 P^3}^{1/2}$$

Substituting the value of  $P$  we have

$$y = \sqrt[3]{\frac{501 \omega x' T_0^{1.242} \sin^2 \alpha}{d_c a \tan \alpha}} + \sqrt[3]{\left( \frac{501 \omega x' T_0^{1.242} \sin^2 \alpha}{d_c a \tan \alpha} \right)^2 - \frac{2040 T_0^3}{d_c a \tan \alpha}}^{1/2}$$

$$+ \sqrt[3]{\frac{501 \omega x' T_0^{1.242} \sin^2 \alpha}{d_c a \tan \alpha}} - \sqrt[3]{\left( \frac{501 \omega x' T_0^{1.242} \sin^2 \alpha}{d_c a \tan \alpha} \right)^2 - \frac{2040 T_0^3}{d_c a \tan \alpha}}^{1/2}$$

Now for the value of  $d_c$  we find that little reliable and consistent data exists. Dependent upon the investigator, values have ranged from as low as about 250 psi to as high as about 1700 psi. For the purpose of this paper, however, we shall use values which are the result of work by T. R. Butkovich of the U.S. Army Snow, Ice and Permafrost Research Establishment as reported in his paper Strength Studies of Sea Ice. The values given are the result of sixty unconfined compression tests including older near shore ice as well as younger ice. From the results of this work we may assume that

$$d_c = 1400 \text{ psi} = 202000 \text{ psf}$$



Now it is frequently claimed that the ultimate <sup>compressive</sup> strength of sea ice increases as the temperature decreases, although many workers in the field were unable to detect any temperature dependence. Butkovich does indicate a slight temperature dependence. However, reliable and consistent data as to this dependence is non existent and what variation is indicated by existing test results is very small and we can, for the purposes of this paper, consider  $\sigma_c$  constant.

As regards the value of  $a$ , if we accept the load waterplanes of the Glacier, Mackinaw and wind class icebreakers as typical of modern polar vessels, then from figure 47 we see that the slope of the waterline at the forward end may be taken as 1.835, hence

$$a \approx 0.545$$

and

$$\sigma_c a \approx 110000$$

Therefore,

$$y = \sqrt[3]{0.00228 \omega x' T_0^{1.242} \sin 2\alpha + \left[ (0.00228 \omega x' T_0^{1.242} \sin 2\alpha)^2 - (0.01855 T_0 \cot \alpha)^3 \right]^{1/2}} \\ + \sqrt[3]{0.00228 \omega x' T_0^{1.242} \sin 2\alpha - \left[ (0.00228 \omega x' T_0^{1.242} \sin 2\alpha)^2 - (0.01855 T_0 \cot \alpha)^3 \right]^{1/2}}$$

For the polar icebreaker the term

$$(0.01855 T_0 \cot \alpha)^3$$

is very small when compared to the term

$$(0.00228 \omega x' T_0^{1.242} \sin 2\alpha)^2$$

normally over 1000 to 1, therefore, we may reasonably assume that

$$(0.01855 T_0 \cot \alpha)^3 \approx 0$$





# LOAD WATERPLANE CURVES

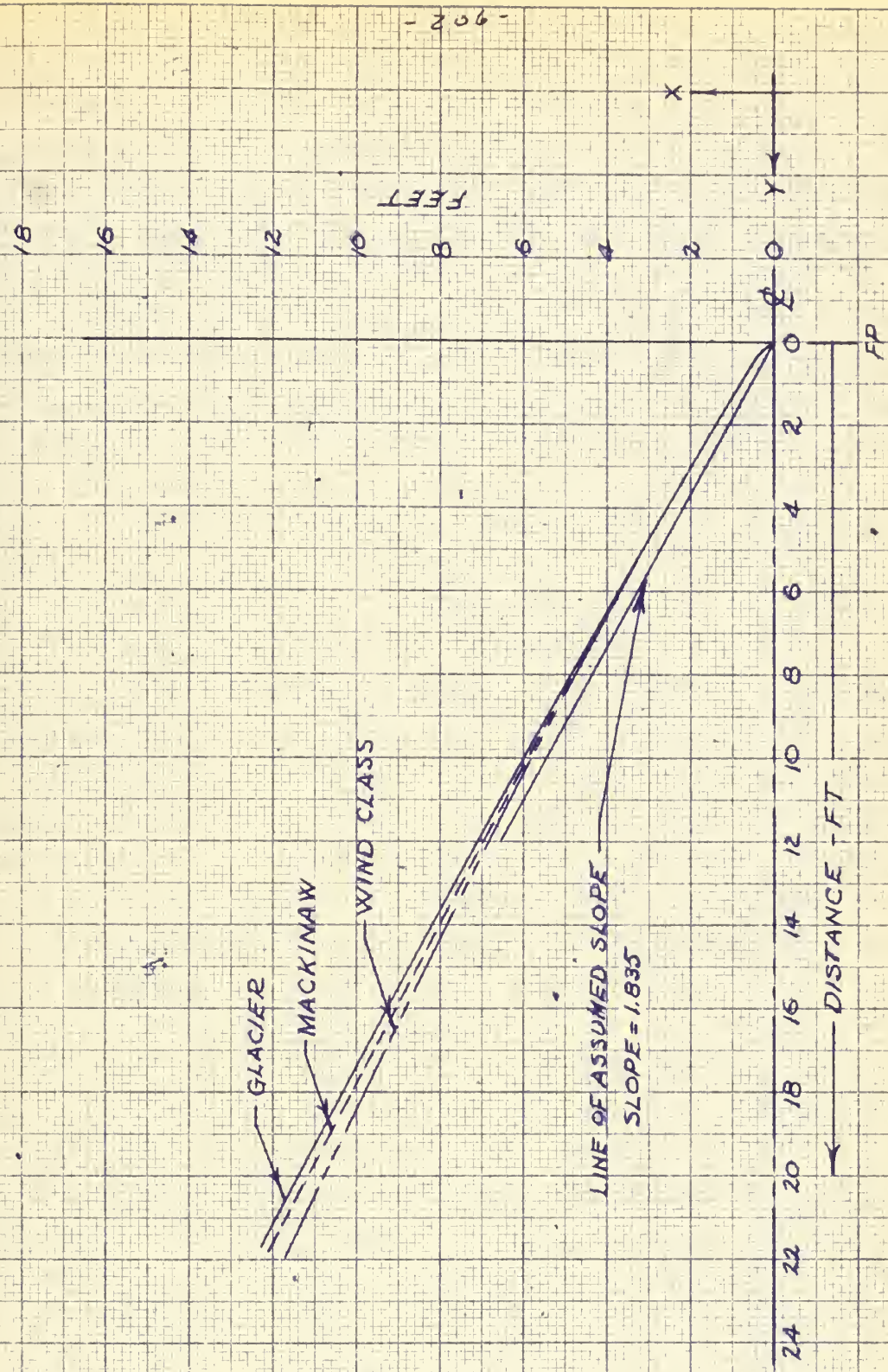


FIG 44

- 206 -





without sacrificing our accuracy. Hence

$$y = \sqrt{0.00456 \omega x^2 T_0^{1.246} \sin 2\alpha} \quad (81)$$

when acceleration was in open water.

If we now consider the case where the vessel accelerates through a channel whose water is relatively clogged with pieces of ice and whose impact velocity is given by

$$v = 1.12 x T_0^{0.524} \text{ ft/sec} \quad (68)$$

we have upon equating  $E_1$ ,  $E_2$  and  $E_3$

$$43.6 x T_0^{1.048} \omega \sin^2 \alpha + 2040 T_0 y = \frac{J_c J^3}{3} a \tan \alpha$$

or

$$J^3 - 6120 P y - 130.8 x T_0^{0.048} \omega P \sin^2 \alpha = 0 \quad (82)$$

where

$$P = \frac{T_0}{J_c a \tan \alpha}$$

Solving for  $J$  as before we get

$$y = \sqrt[3]{0.000297 \omega x^2 T_0^{1.048} \sin^2 \alpha + \left[ (0.000297 \omega x^2 T_0^{1.048} \sin^2 \alpha)^2 - (0.01855 T_0 \omega \tan \alpha)^3 \right]^{1/2}} \\ + \sqrt[3]{0.000297 \omega x^2 T_0^{1.048} \sin^2 \alpha - \left[ (0.000297 \omega x^2 T_0^{1.048} \sin^2 \alpha)^2 - (0.01855 T_0 \omega \tan \alpha)^3 \right]^{1/2}}$$

Again for the polar icebreaker, the second term above is very small as compared to the first term, about 500 to 1, hence we may assume that

$$(0.01855 T_0 \omega \tan \alpha)^3 \approx 0$$

and

$$y = \sqrt[3]{0.000594 \omega x^2 T_0^{1.048} \sin 2\alpha} \quad (83)$$

for acceleration in an ice filled channel.



In order to observe the order of magnitude of the horizontal advance due to compression, let us evaluate the expression (83) as the most typical case in polar operations for both the Glacier and wind class vessels. For the purposes of discussion we shall assume that the vessel accelerates through a distance of one ship length which is typical icebreaker practice, therefore

$$s' = LBP$$

and we find that

$$y = 8.06 \text{ ft. Glacier}$$

$$y = 6.92 \text{ ft. Wind}$$

Now it will be recalled that our development was based on the assumption that

$$h < z'', \text{ i.e.}$$

$$z'' \geq h = y \tan \alpha$$

Therefore

$$h = 4.65 \text{ ft. Glacier}$$

$$h = 3.99 \text{ ft. Wind}$$

Now practical experience dictates that an ice thickness of 4.65 ft for the Glacier and 3.99 ft for the Wind class is hardly such as to require breaking by heavy ramming except perhaps in those cases where the ice field is under considerable pressure. In the majority of instances, therefore, this is relatively light ice. Consequently, for all practical purposes we can say that

$$z'' \geq h$$

and horizontal advance due to compression in the plane of the ice sheet is





relatively insignificant.

Now the question arises as to whether or not these compressive forces should contribute to the icebreaking force development of section F-2. To an extent they do. The component of the vessel kinetic energy which acts normal to the stern is completely expended in impact due to the extremely low coefficient of restitution of steel on ice. This energy acts to deform the ice in compression and its complete loss is accounted for in the development above. In addition, the thrust developed by the propeller during the initial impact stage also acts to deform the ice in compression. This force acting through the distance  $y$  constitutes an energy expenditure which is not considered in the development of section F-2. However, this is proper since its action also is limited to compressive deformation only.

To reiterate, ice may be broken by compressive forces, i.e. cracking radially from the point of impact of the bow, or by bending due to the development of a vertical bow force when the vessel climbs on to the ice. Dependent upon the thickness of the ice, one of these methods will become dominant.

In relatively thin ice where vessel forward motion is continuous, rupture of the ice is primarily by compressive loading in the plane of the ice sheet (radial cracking). In this instance the vessel does not climb up on to the ice. As the thickness of ice increases the vessel may begin to encounter difficulty in breaking by compression loading alone in which case the vessel will climb up on to the ice sheet until the combined compressive loading and bending due to developed vertical bow force overcomes the ice sheet. Here, the vessel forward motion may still be continuous, i.e. the vessel is not



stopped, however, forward speed is not constant since the bow of the vessel describes a motion which is similar in character to a saw tooth wave.

The problem we are considering, however, is the case of very thick ice, where vessel forward motion cannot be maintained continuous, but rather, is periodic wherein the vessel advances a certain distance with each charge. Hence the process of backing and ramming. In this instance the compressive forces discussed above do act, but only during the very beginning of the ramming process. These forces compress the ice locally into the form of a wedge due to the shape of the vessels stern. During this period some radial cracks may develop, due to impact, which act to weaken the ice. However, since the rate of loading is normally not too high, large cracks seldom occur in thick ice. The local compressive deformation will produce very small radial cracks which, though they weaken the extreme edge of the ice sheet somewhat, do not materially effect the strength of the ice sheet for any distance from the immediate point of contact. Consequently, if the ice is to be overcome, it must be done by the development of a vertical bending force which ruptures the ice sheet due to large developed tensile stresses in the top fibers of the ice sheet. Now, as long as the vessel can develop forces in the plane of the ice sufficient to overcome the ice in compression no climbing on to the ice will occur. However, once the distance  $y$  (developed above) is reached, sufficiently large compressive forces can no longer be developed and the ice will resist further deformation in the plane of the ice sheet. Consequently, the forces which are still acting at this time (propeller thrust and unexpended vessel kinetic energy) will expend themselves in forcing the vessel on to the ice



and developing a vertical bow force to put the ice sheet in bending. Hence, for very thick ice the actions of compressive deformation and vertical bow force development may be considered two separate and distinct phenomenon. First, a partial local deformation due to compressive loading, then the development of vertical bending forces which cause ice to break in large slabs. Now there is no doubt that the forces in the plane of the ice sheet will tend to act in conjunction with the vertical bending force so as to increase the stress in the ice due to bending. However, due to the thickness of our ice sheet the effects of the compressive loading, once compressive ice failure has ceased, are small and our problem is basically one of pure bending. Therefore, we are justified in our development of section F-2 in considering bending only. In that development, the energy available is the vessel kinetic energy plus the propeller thrust acting through the horizontal distance moved during the process of climbing on to the ice. The energy due to propeller thrust acting through the distance  $y$  is not considered there since this energy is completely dissipated in causing local compressive failure. As for the energy expended, however, we must consider the kinetic energy lost in impact since it too is completely expended in local compressive deformation and does not contribute to the vessels climbing motion.

Hence we may conclude that although forces do act in the plane of the ice sheet and do cause local deformation, the effect is small and the energy developed is soon dissipated leaving the remainder of the energy to force the vessel on to the ice to cause failure, if possible, by bending. The energy balance as shown in section F-2, therefore, is proper as shown.





Part 4

Vessel Advance and Evaluation of the Vertical Forefoot

Let us consider the horizontal distance traveled by the vessel from the moment of first impact with the ice until vessel forward motion is stopped. This horizontal distance  $r'$  may be given by

$$r' = d + y$$

where

$d$  = horizontal movement of vessel while climbing on to the ice

$y$  = horizontal movement of vessel due to ice compression after impact

Now in section F-2 we showed that the distance  $d$  could be expressed as

$$d = \Delta d \cot \alpha + s \Delta \phi \cot \alpha \quad \text{ft}$$

where

$\Delta d$  = change in vessel draft due to climbing on to ice - ft.

$\Delta \phi$  = change in vessel ~~trim~~ <sup>rise</sup> due to climbing on to ice - radians

$s$  = distance from point of impact on stem to horizontal center of floatation - ft

$\alpha$  = angular ~~rise~~ <sup>rise</sup> of forefoot

In addition we showed that

$$\Delta d = \frac{2240 F}{\delta' A_w} \quad \text{ft}$$

$$\Delta \phi = \frac{F s}{w G M_L} \quad \text{radians}$$

Therefore

$$d = \left[ \frac{2240 F}{\delta' A_w} + \frac{F s^2}{w G M_L} \right] \cot \alpha \quad \text{ft.}$$



since by definition

$$A_w = L B C_w$$

$$w = \frac{L B H C_B \gamma'}{2240}$$

and if we again introduce the non dimensional quantities  $k_1$  and  $k_2$  where

$$s = k_1 L/2$$

$$G M_1 = \frac{k_2 C_w L^2}{H C_B}$$

we have

$$d = \frac{F H A}{w} \cot \alpha \quad (91)$$

where  $A$  is the dimensionless coefficient

$$A = \left[ \frac{C_B}{C_w} + \frac{k_1^2}{4 k_2} \frac{C_B}{C_w^2} \right]$$

In section ~~F-1~~<sup>G</sup> we show that the vertical bow reaction force  $F$  can be expressed as

$$F = 0.91 \times T_0 + \sqrt{0.828 \times T_0^2 + \frac{w^2 v^2}{A g H}} \quad \text{tons}$$

In addition if we consider the normal icebreaking condition where the vessel accelerates through an ice clogged channel then we showed ~~we showed~~ in section F-2 that impact velocity could be expressed as

$$v = 1.12 \times T_0^{0.524} \quad \text{ft/sec} \quad (68)$$

Therefore

$$F = 0.91 \times T_0 + \sqrt{0.828 \times T_0^2 + \frac{1.25 w^2 \times T_0^{1.048}}{A g H}}$$

and

$$d = \frac{0.91 \times T_0 H A}{w} \cot \alpha + \frac{H A}{w} \cot \alpha \sqrt{0.828 \times T_0^2 + \frac{1.25 w^2 \times T_0^{1.048}}{A g H}} \quad (92)$$

In section F-3 we showed that the distance the vessel would advance due to ice compression  $J$  could be given as

$$J = \sqrt[3]{0.000594 \times w T_0^{1.048} \sin 2\alpha} \quad (83)$$





Therefore, the total horizontal distance travelled is

$$r' = \frac{0.91 \times T_0 \cdot HA}{w} \cot \alpha + \frac{HA}{w} \cot \alpha \sqrt{0.828 \times \frac{H^2 T_0^2}{w^2} + \frac{1.25 w^2 \times \frac{H^2 T_0^2}{w^2}}{A_2 H}} + \sqrt[3]{0.000594 \times \frac{H^2 T_0^2}{w^2} \sin 2\alpha} \quad (93)$$

In section G-1 we show that the values of  $\alpha$  and  $\beta$  for optimum ice breaker effectiveness are

$$\alpha = 26^\circ$$

$$\beta = 45^\circ$$

hence

$$\chi = 1.26$$

$$z = 0.557$$

we also show that for the conventional polar icebreaking vessel

$$A \approx 4$$

Substituting into (93) above we have

$$r' = \frac{9.4 T_0 H}{w} + \sqrt{88.3 \frac{H^2 T_0^2}{w^2} + 0.362 \times \frac{H^2 T_0^2}{w^2}} + \sqrt[3]{0.000468 \times \frac{H^2 T_0^2}{w^2}} \quad (94)$$

Now let us investigate the forward ship advance so as to determine the probability of the vertical forefoot, if one exists, striking the ice sheet. If no vertical forefoot is designed into the stern of the vessel, as is true in many modern icebreakers, (especially foreign built) our problem here of horizontal advance is somewhat academic with the exception of its effect on vessel stability when sitting with the bow up on the ice. This is a problem we shall consider at a later point in the paper.

Assuming, therefore, that a vertical forefoot does exist, then our vessel advance consideration becomes of practical significance since from an ice breaking viewpoint it is probably desirable that the vertical forefoot not strike the ice sheet. Some authorities hold that such a striking blow against



the ice sheet by the vertical forefoot is good and desirous since it tends to crack the ice and aid the icebreaking process. This is, in a sense, true for light ice or free floating floes of thick ice but for solid continuous ice this opinion is not subscribed to by this author since such a conclusion does not seem reasonable nor does practical icebreaking experience substantiate the claimed advantage. The bow of the conventional arctic icebreaker is rather blunt and spoon shaped. In addition, by the time the vessel has run up on to the ice sufficiently to cause the vertical forefoot to hit the major portion of the original vessel energy has been expended. Consequently, it is doubtful if the remaining energy acting through the vertical forefoot portion is sufficient to cause any appreciable radial cracks or even be of much assistance in breaking ice which has resisted failure due to bending stresses in the outer fibers. But even supposing that the ice did crack radially as a result of the impact - the icebreakers job has not been done since the ice has not broken off. We know from experimentation and the theory of ice mechanics that it does not take much force in bending to cause this ice sheet to crack, but it takes a considerably greater force to actually break the ice off. This theory we reviewed in section F-1 when we considered the force required to break a wedge on an elastic foundation. Consequently, our cracking the ice does not materially aid the icebreaking process. Either the ice has already been cracked into wedges by the vertical bow reaction force  $F$ , but this force has not been sufficient to break the wedges, or else the vertical bow reaction force has not been large enough to crack the ice in which case it is entirely insufficient to ever break it. In either



case, additional cracking of the ice due to the impact of the vertical forefoot will be totally ineffective. If, sufficient power is available in the vessel to propell it far enough on to the ice so that the vertical forefoot strikes, it would seem desirable to move this vertical portion further aft or remove it completely so as to allow generation of a larger vertical bow reaction force  $F$  which is effective in actually breaking the ice. It would therefore seem that the most desirable arrangement would be either the complete absence of a vertical forefoot or its location far enough aft to permit the vessel to develop the largest bow reaction force  $F$  possible with the power installed.

There are two limiting considerations to the above discussion. One is that the vessel should be able to extract itself if she becomes beset. Consequently, the powering of the vessel should be such as to satisfy the conditions outlined in section F-5 where this problem of vessel retraction is considered. Secondly, the vessel must not be so overpowered as to climb up on to the ice to such an extent that vessel stability is jeopardized. Admittedly the intact stability of this type vessel is inherently very large. However, when sitting in the inclined position with the bow on the ice this stability can be markedly reduced and care must be taken that the vessel not be able to propell itself so far as to become unstable. This problem is considered in a later section.

In regard to these limiting considerations, it might be proposed that a vertical forefoot be used to prevent the vessel from advancing too far on to the ice thus limiting the vertical bow reaction force which may be developed in accordance with the above considerations of vessel stability and retraction



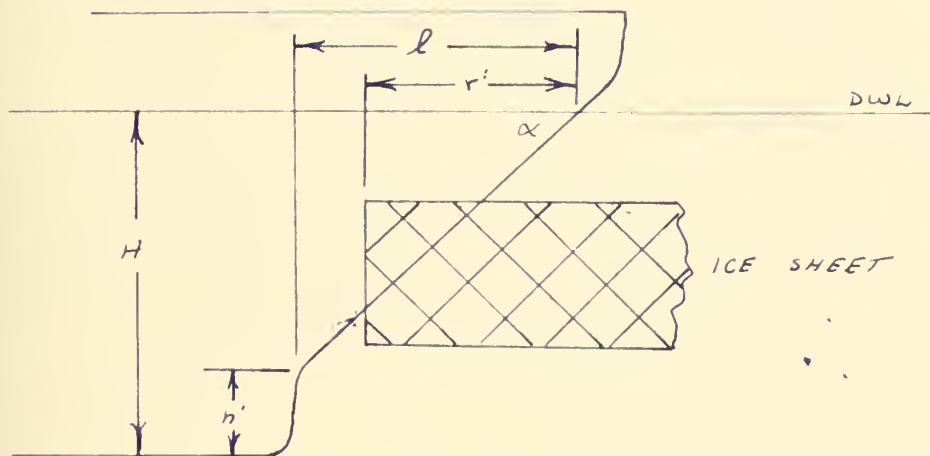


ability. Such a proposal is justifiable in that the vessel impact energy is a direct function of the impact velocity, and though the powering of the vessel may be such as to keep the vessel from climbing too far out of the water when accelerated through a reasonable distance (say two ship lengths), it is possible that increasing the accelerating distance or accelerating in open water could cause the vessel to climb so far as to be unable to retract or impair vessel stability. In such instances the vertical forefoot would act as a preventer. In addition, it might be desired to considerably overpower the vessel so that it could more effectively force leads, tow in ice or have a higher design speed. In this instance, even if a reasonable accelerating distance is used, the vessel could again climb so far as to be unable to retract or impair vessel stability. Here again the vertical forefoot could act as a preventer. In both these instances the use of a vertical forefoot would be desirable. Its location, however, must not be so far forward as to materially reduce the vertical bow force which may be developed. Consequently, if the vertical forefoot is used, it must be located far enough aft as to allow the vessel to develop the maximum vertical bow force possible with the power installed yet be able to retract in accordance with section F-5 and not have its stability endangered in accordance with section G-2. It must be reiterated, however, that vessel energy remaining at the instant of vertical forefoot contact is completely lost and useless to the icebreaking process.

Let us now consider the present day conventional arctic icebreaker so as to determine the probability of the vertical forefoot striking the ice



sheet



Now let

$$h' = k H$$

where  $k$  is some constant. Therefore

$$l = H(1 - k) \cot \alpha$$

Now if  $r' > l$  the vertical forefoot will strike the ice sheet with subsequent loss of remaining ship inertia energy. If we consider our selected value of

$\alpha = 26^\circ$  we may state that the vertical forefoot will strike if

$$2.05 H (1 - k) \leq r' \quad (95)$$

Substituting (94) for  $r'$  we have

$$2.05(1 - k) H \leq 9.4 \frac{T_0 H}{W} + \sqrt{38.3 \frac{H^2 T_0^2}{W^2} + 0.362 \frac{H^2 T_0^{1.048}}{W}} + \sqrt[3]{0.000468 \frac{H^2 T_0^{1.048}}{W}} \quad (96)$$

or if we rearrange terms we have that the vertical forefoot will strike if

$$k \geq C$$

where

$$C = 1 - \left[ 4.58 \frac{T_0}{W} + \sqrt{21 \frac{T_0^2}{W^2} + 0.0862 \frac{H^2 T_0^{1.048}}{W}} + \sqrt[3]{0.000544 \frac{H^2 T_0^{1.048}}{W^3}} \right]$$





In order to examine these relationships for present and past icebreaker designs let us assume that the vessel is twin screw and accelerates through a distance of either one or one and one half ship lengths, i.e.

$$S' = L \quad \text{or} \quad 1.5L$$

From an analysis of existing and past vessels we can determine representative variations of draft,  $T_0 / \text{Dia}^2$  and  $T_0 / W$  as a function of ship length and also a representative variation of propeller diameter as a function of vessel draft. These are shown in figures 45, 47, 50 and 51. Based on these characteristic values we may evaluate the above expression for C. The results are shown as figure 52.

An investigation of past and present vessels which have a vertical forefoot installed reveals that for the conventional arctic icebreaker with a bow propeller

$$k \approx 0.60$$

and for those without bow propellers

$$k \approx 0.46$$

Based on these values of  $k$  we see from figure 52 that for the conventional arctic icebreaker using full installed power

$$k > C$$

therefore when breaking ice by ramming the vertical forefoot will always strike the ice sheet. This fact can also be seen from figure 53 wherein are plotted  $r'$  (vessel horizontal advance) and  $l$  (advance possible before vertical forefoot strikes) as a function of ships length for the representative present day icebreaker. Here again we see that  $k$  must be almost zero in order for the





PROPELLER DIAMETER  
VS  
VESSEL DRAFT

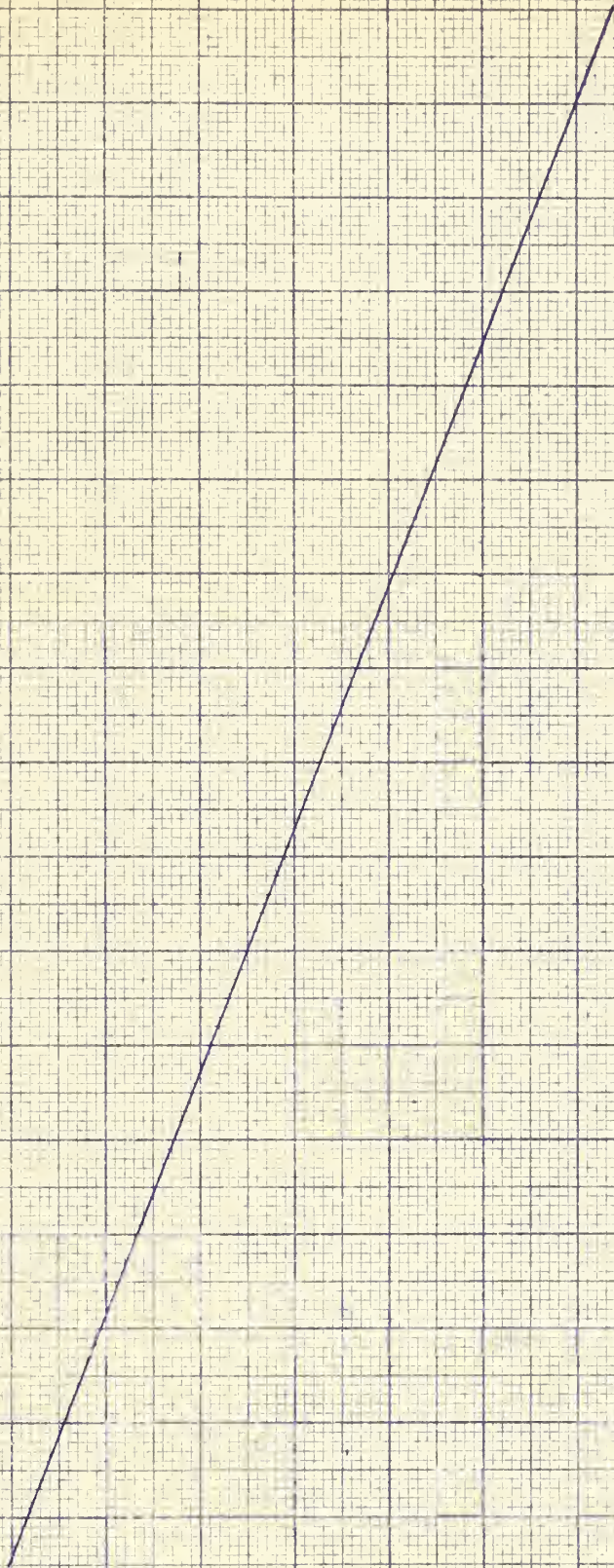
RATIO - PROPELLER DIA  
DRAFT

54-914

- 220 -

0.55 13 14 15 16 17 18 19 20 21 22 23 24 25 26 27 28 29 30

FULL LOAD DRAFT







PROPELLER DIAMETER  
VS  
VESSEL BEAM

RATIO - PROPELLER DIA  
BEAM

BEAM - FT

20 2 4 6 8 30 2 4 6 8 40 2 4 6 8 50 2 4 6 8 60 2 4 6 8 70 2 4 6 8 80

0.40  
0.38  
0.36  
0.34  
0.32  
0.30  
0.28  
0.26  
0.24  
0.22

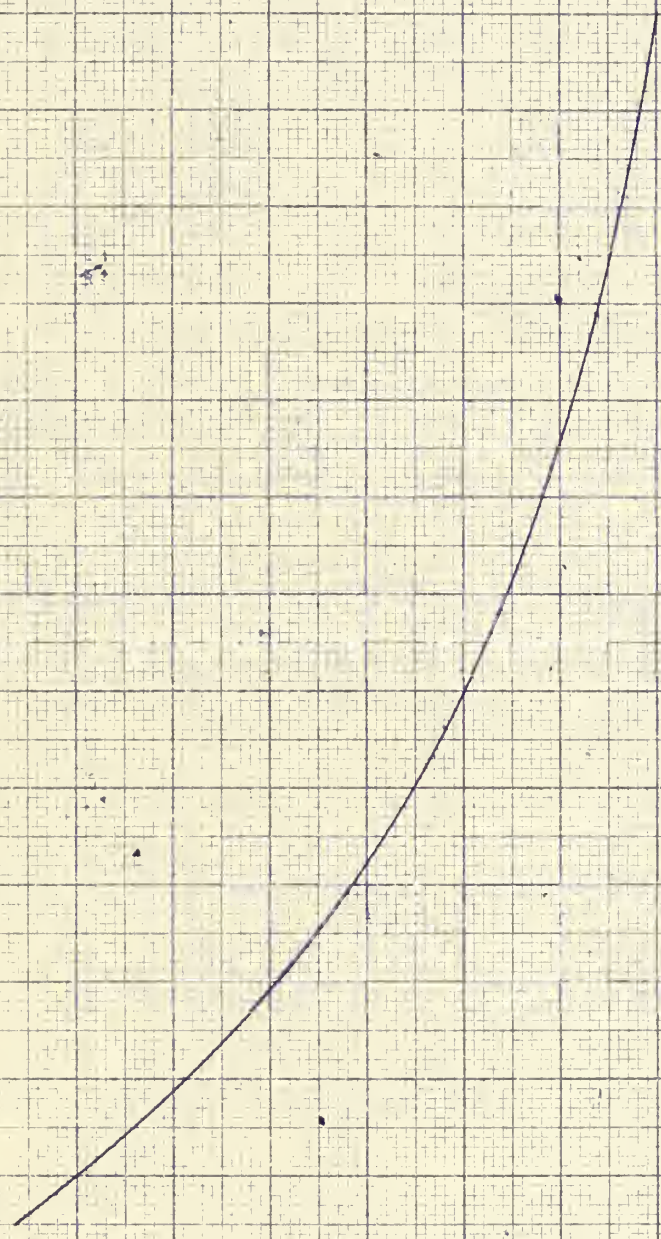


FIG 46





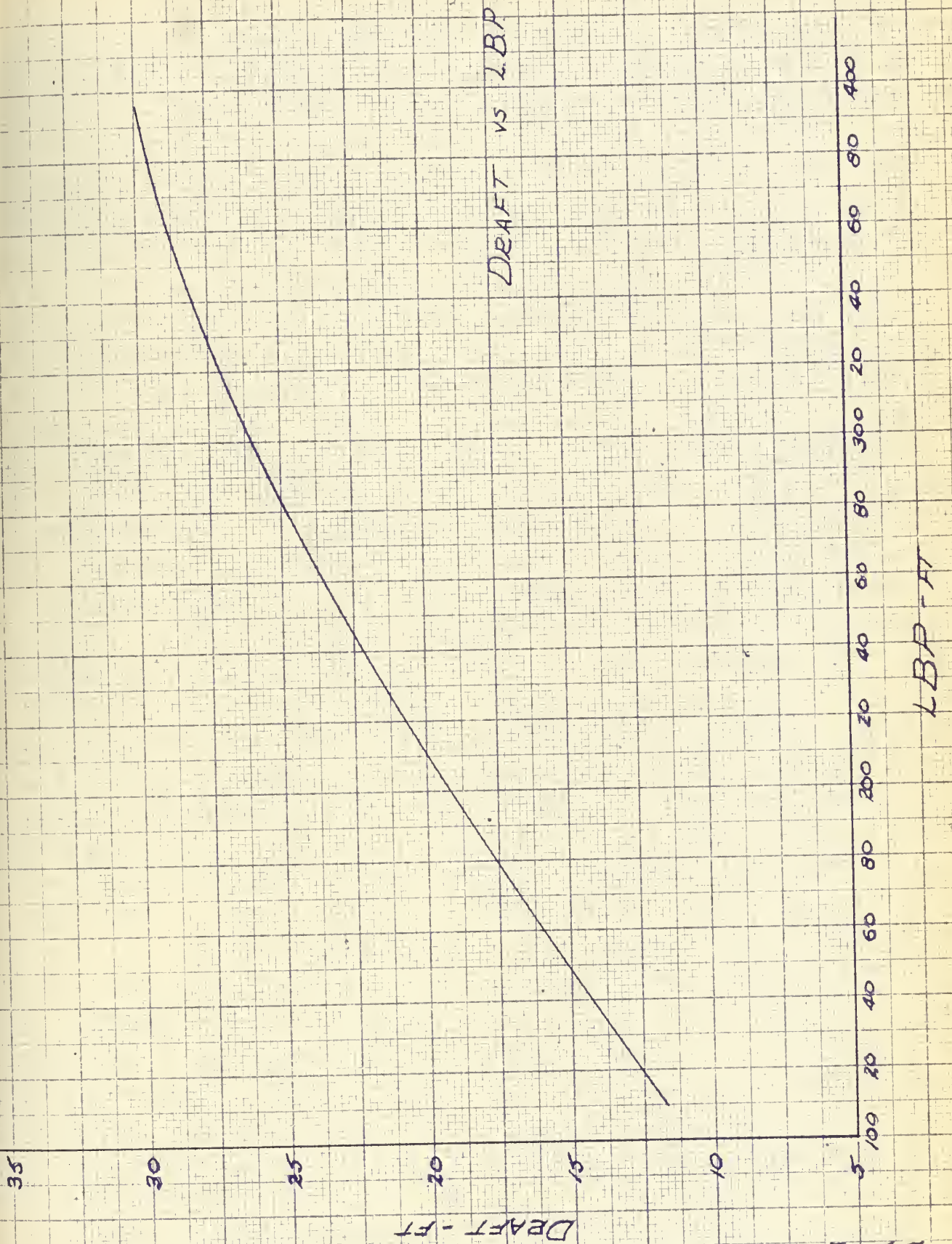


FIG 47



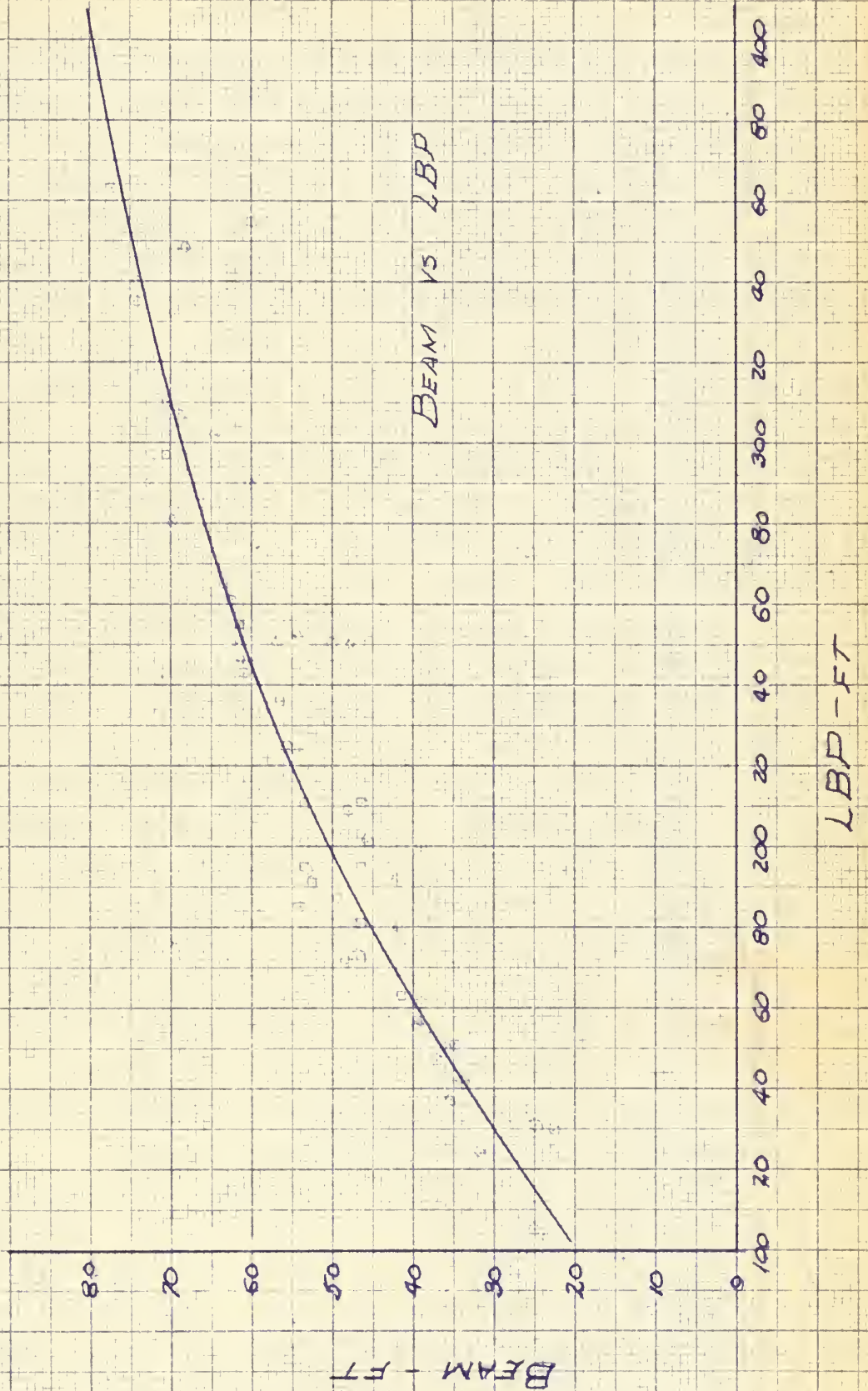


Fig 48







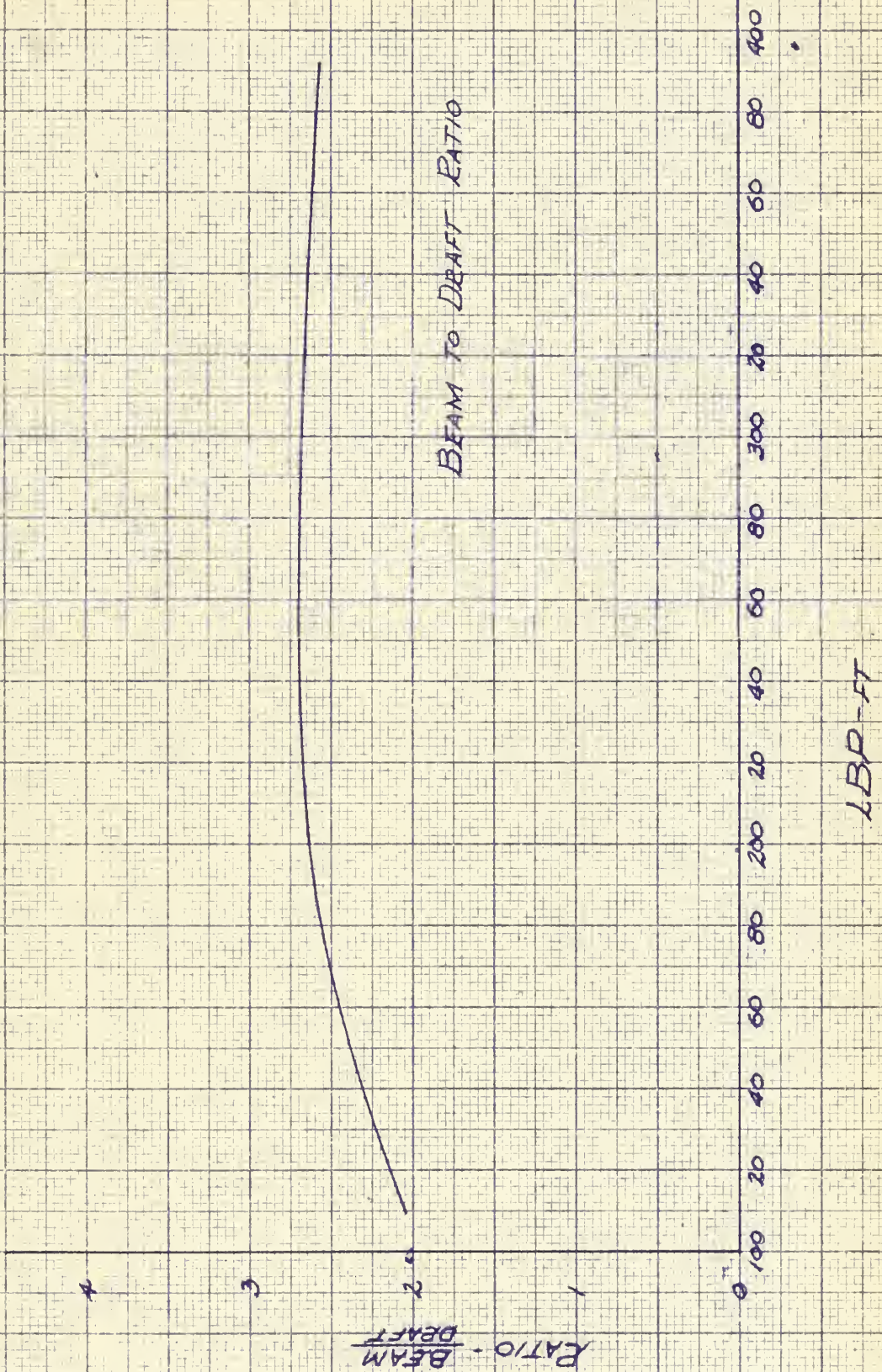


FIG 49





TREND IN PROPELLER LOADING FACTOR

0.40

0.35

0.30

0.25

0.20

0.15  
100

$\frac{10}{\text{DIA}^2}$  PER SHAFT - TONS/FT<sup>2</sup>

-850

-800

-750

-700

-650

-600

-550

-500

-450

-400

$\frac{10}{\text{DIA}^2}$  PER SHAFT - LBS/FT<sup>2</sup>

300

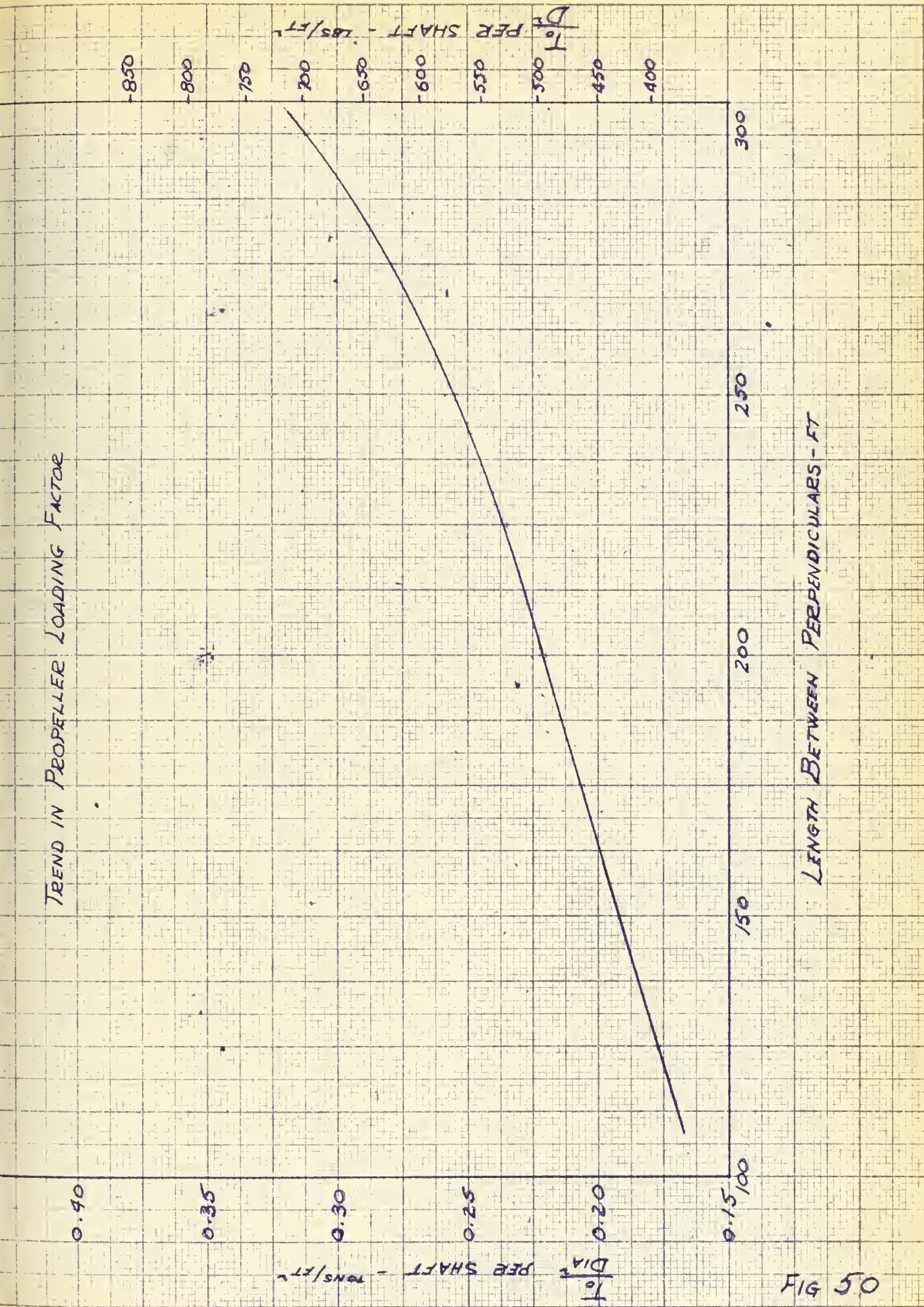
250

200

150

LENGTH BETWEEN PERPENDICULARS - FT

Fig 50







THRUST TO DISPLACEMENT RATIO

0.030

0.025

0.020

0.015

0.010

100

150

200

250

300

LENGTH BETWEEN PERPENDICULARS - FT

DIMENSIONLESS

$\frac{F}{10 - \text{total}}$

FIG 5.1



922 -





TENDENCY OF VERTICAL FOREFOOT  
TO STRIKE ICE SHEET

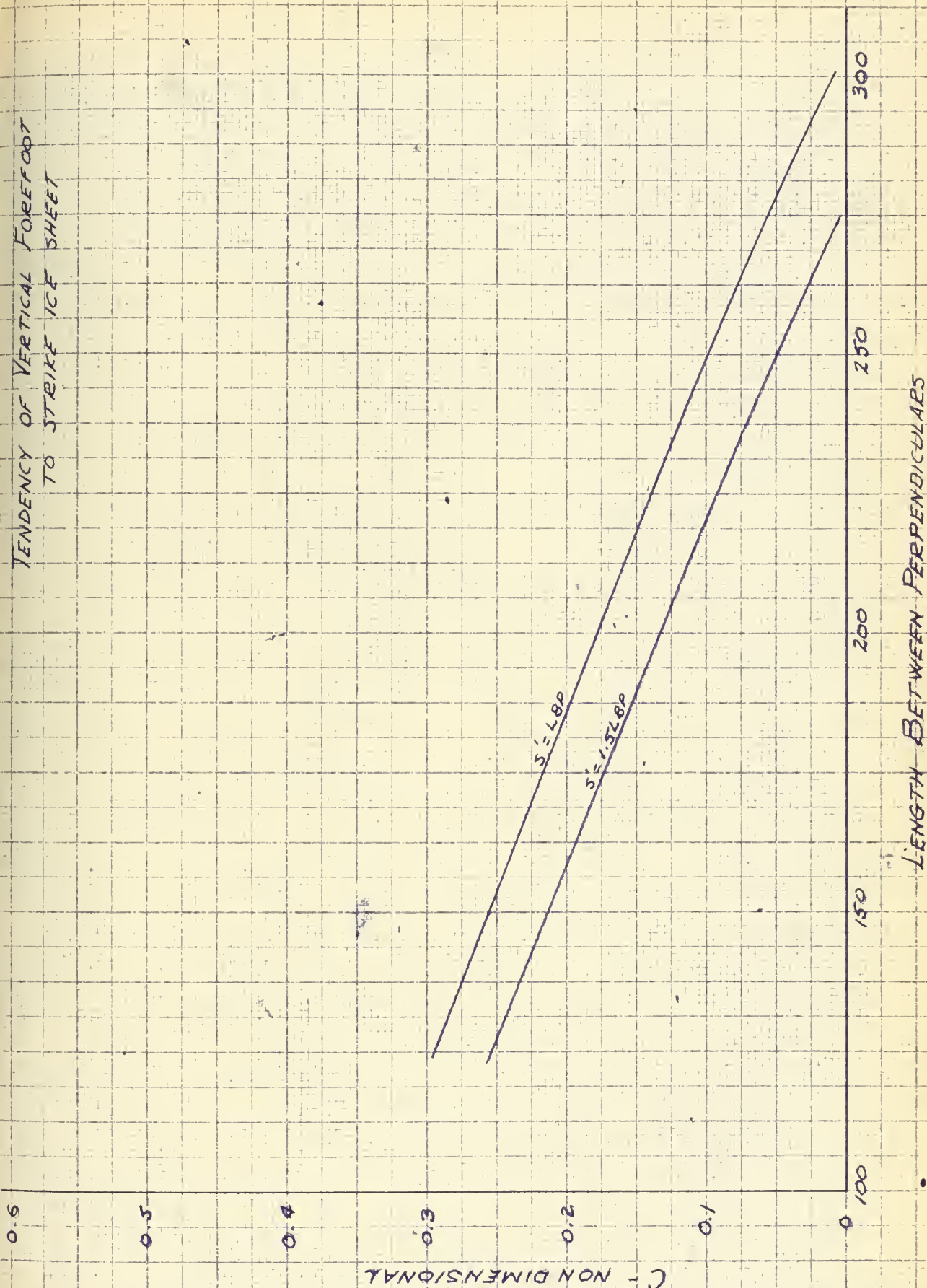
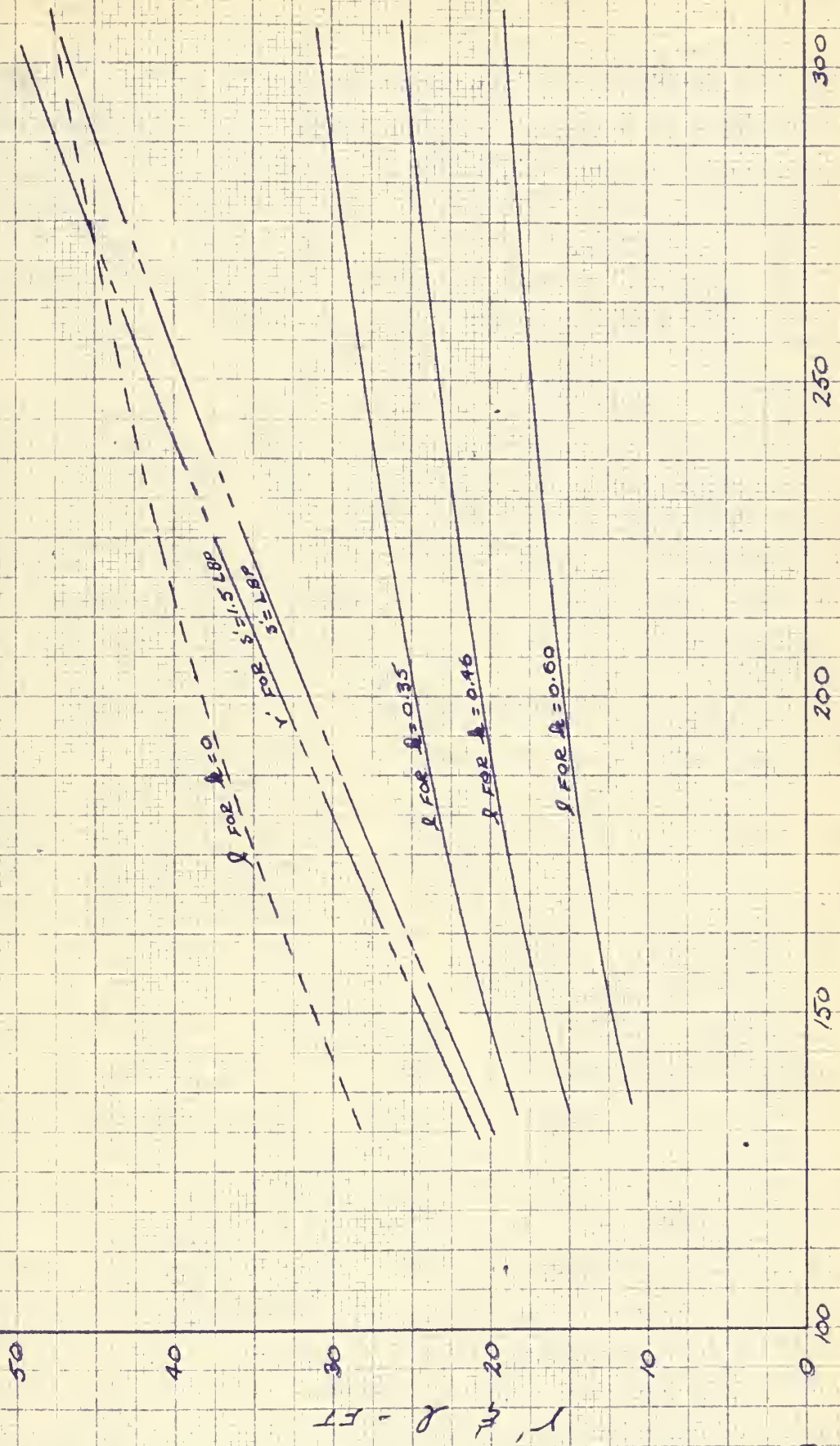


FIG 5.2



VESSEL FORWARD ADVANCE FOR VARYING  
VERTICAL FOREFOOT TO DRAFT  
RATIOS



- 228 -

FIG 53

LENGTH BETWEEN PERPENDICULARS - FT





vertical forefoot not to strike. There is really no sound reason for  $h$  ranging so high as from 0.46 to 0.60, and proposed future designs do indicate a trend towards reducing this ratio to about  $h = 0.35$ . However, figure 53 indicates that even this value is too high and with present powering trends will cause loss of inertia energy by striking of the vertical forefoot. It would therefore seem that the complete elimination of the vertical forefoot (i.e.  $h=0$ ) or the installation of a very small one would be advantageous. Reiterating that the only restriction to such a move is the vessels ability to retract and the retention of adequate stability when sitting up on the ice.

Now let us consider the condition where the vertical forefoot does strike and calculate the percentage of energy lost and the maximum vertical bow reaction force which may be developed. If the vertical forefoot strikes the ice sheet then ship horizontal motion due to climbing on to the ice ( $d$ ) is limited to  $(l-y)$  where  $y$  taken for most common condition of acceleration in ice channel.

We have shown that  $d$  could be expressed as

$$d = \frac{FHA}{\omega} \cot \alpha \quad (91)$$

therefore

$$\frac{FHA}{\omega} \cot \alpha = l - y$$

$$\frac{FHA}{\omega} \cot \alpha = H(1-h) \cot \alpha - \sqrt{0.000574 \omega x' T_0^{1.048} \sin 2\alpha}$$

and the maximum bow reaction force which we may develop becomes

$$F = \frac{\omega}{A} (1-h) - \frac{\omega}{HA} \tan \alpha \sqrt{0.000574 \omega x' T_0^{1.048} \sin 2\alpha} \quad (97)$$

Again we may consider  $A = 4$  as characteristic of conventional polar ice-breakers. Substituting this and our selected value of  $\alpha$  we have



$$F_1 = \frac{\omega}{4} (1-k) - 0.0095 \frac{\omega}{H} \sqrt[3]{\omega x'^2 T_0^{1.018}} \quad (98)$$

This represents the maximum bow reaction force which may be developed if the vertical forefoot strikes. This must be compared to that which could be developed as expressed by

$$F_2 = 0.91 x T_0 + \sqrt{0.828 x^2 T_0^2 + \frac{\omega^2 v^2}{49 H}}$$

where

$$v = 1.12 x' T_0^{0.524} \quad (68)$$

for the ship accelerating in ice filled water. If we substitute the value of  $v$  into  $F_2$  and using our value of  $\alpha = 26^\circ$  and  $\beta = 45^\circ$  we have

$$F_2 = 1.14 T_0 + \sqrt{1.315 T_0^2 + 0.00543 \frac{\omega^2 x'^2 T_0^{1.018}}{H}} \quad (99)$$

If, for the purposes of comparison we again make use of the representative polar icebreaker size and powering characteristics previously depicted in figures 45, 47, 50 and 51 we may evaluate expression (98) and (99) for a percentage comparison. The results of this comparison are shown in figure 54. Here we can see the amount of vertical bow reaction force which we may develop when a vertical forefoot of a given  $k$  value is installed ( $F_1$ ) as compared to that which could possibly be developed without the vertical forefoot ( $F_2$ ) for a vessel accelerating in our ice filled channel for a distance of one ship length. It can be seen that for a vessel comparable to the <sup>GLACIER</sup> ~~wind~~ class where  $k = 0.46$  about <sup>50%</sup> ~~45%~~ of the vessels potential icebreaking force (vertical reaction  $F$ ) is completely lost when the vertical forefoot strikes the ice.

In order to better visualize the percentage of vertical bow reaction





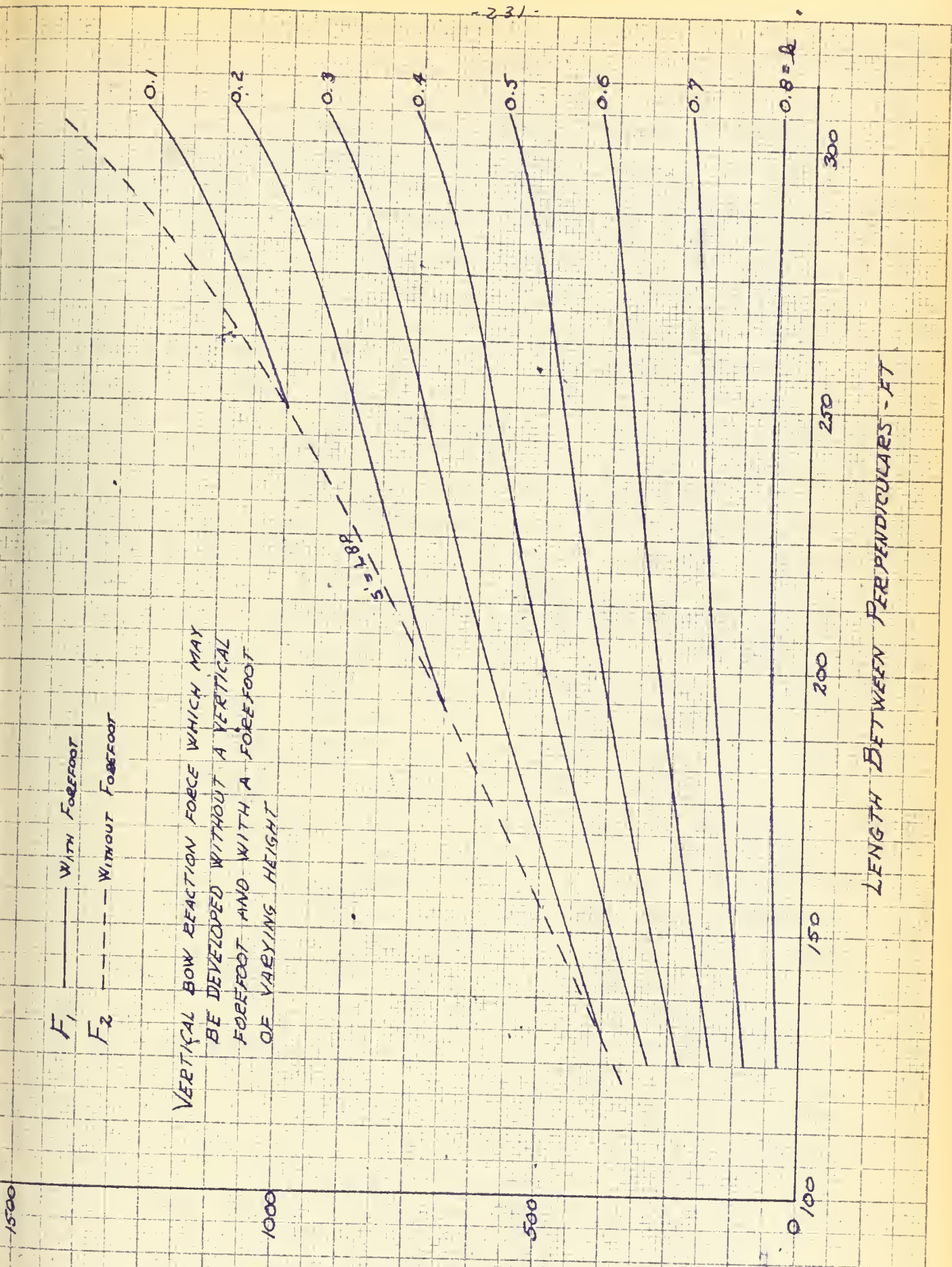
VERTICAL BOW REACTION FORCE - TONS

$F_1$  ——— WITH FOREFOOT  
 $F_2$  - - - WITHOUT FOREFOOT

VERTICAL BOW REACTION FORCE WHICH MAY  
 BE DEVELOPED WITHOUT A VERTICAL  
 FOREFOOT AND WITH A FOREFOOT  
 OF VARYING HEIGHT

$$\frac{1}{5} = 1.88$$

LENGTH BETWEEN PERPENDICULARS - FT







force which is unattainable due to the vertical forefoot striking the ice sheet, let us consider the ratio of  $F_v/F_L$ , where again

$F_v$  = Vertical bow reaction force which may be developed  
if a vertical forefoot exists and strikes the  
ice sheet (98)

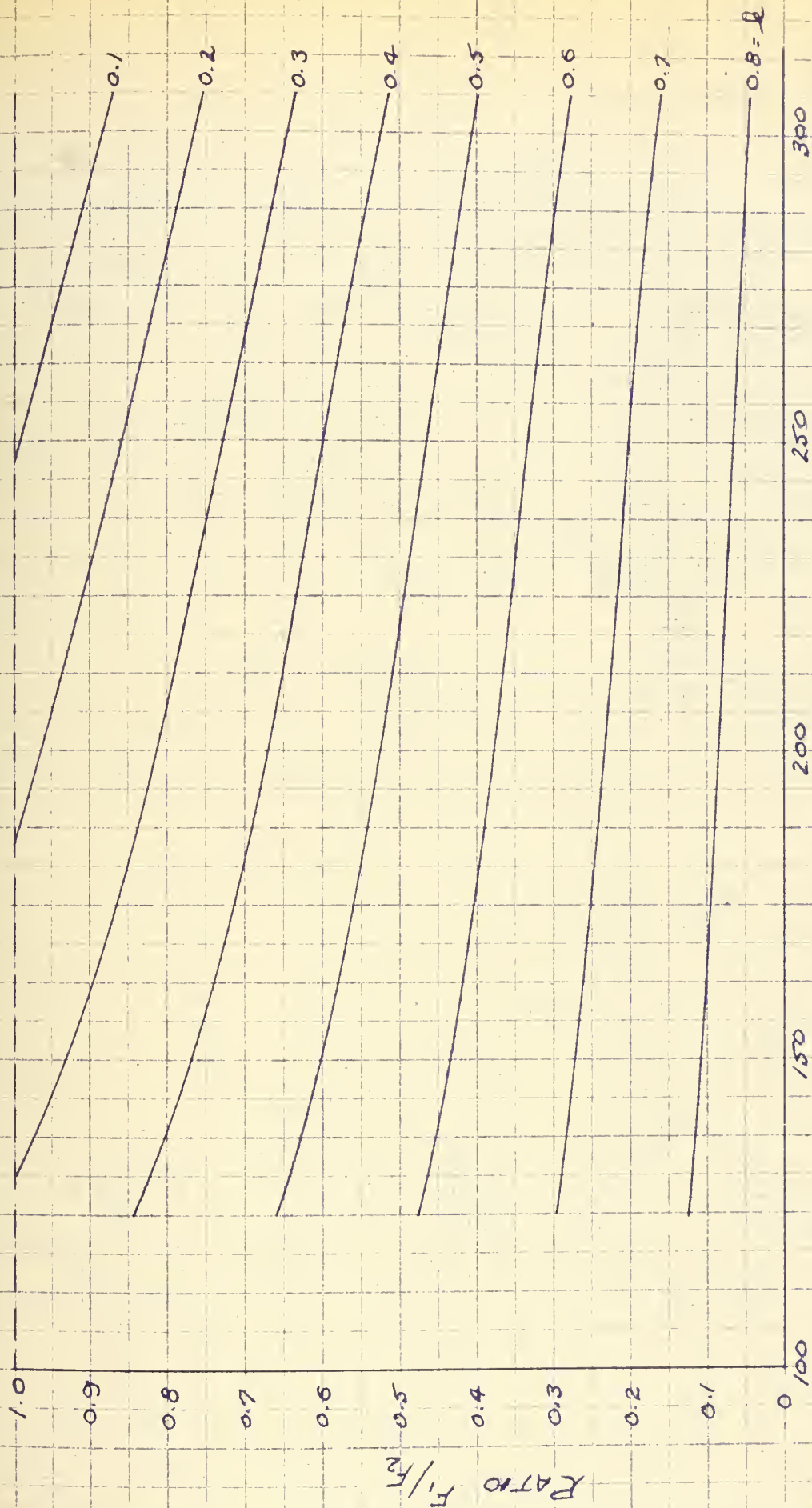
$F_L$  = Vertical bow reaction force which can be developed  
if no vertical forefoot is installed (99)

The results are shown in figure 55 where  $F_v/F_L$  <sup>ACE</sup> is based on the vessel accelerating for one ships length in an ice clogged channel. Again it is seen that for a vessel comparable to the <sup>GLACIER</sup> ~~wind-class~~, only about <sup>48%</sup> ~~54%~~ of its potential ice breaking force is realized before the vertical forefoot strikes the ice sheet.

From our past discussion it can be seen that the use of a large vertical forefoot is expensive in terms of lost potential icebreaking force. Two alternatives exist. Reduce vessel powering to a point where full vessel ice breaking potential may be realized despite the forefoot. This is not too desirable an alternative since it seriously limits the vessels' ability to force a lead thereby hampering her successful operation in field ice. The other alternative is to reduce the size of the vertical forefoot or remove it completely. In this instance the vessel may climb out on to the ice so as to realize her full icebreaking potential commensurate with her powering. This seems the better of the two alternatives with the reduction in vertical forefoot size preferred over its complete removal. It must be reiterated, however, that care must be taken to insure that the vessel does not climb up so far as to endanger transverse stability or that once on the ice she will be unable to retract. See Sections F-5 and G-2.



PERCENTAGE OF VERTICAL BOW REACTION FORCE  
LOST DUE TO PRESENCE OF VERTICAL  
FOREFOOT OF VARYING SIZE



LENGTH BETWEEN PERPENDICULARS - FT

RATIO  $F_1/F_2$

FIG 55



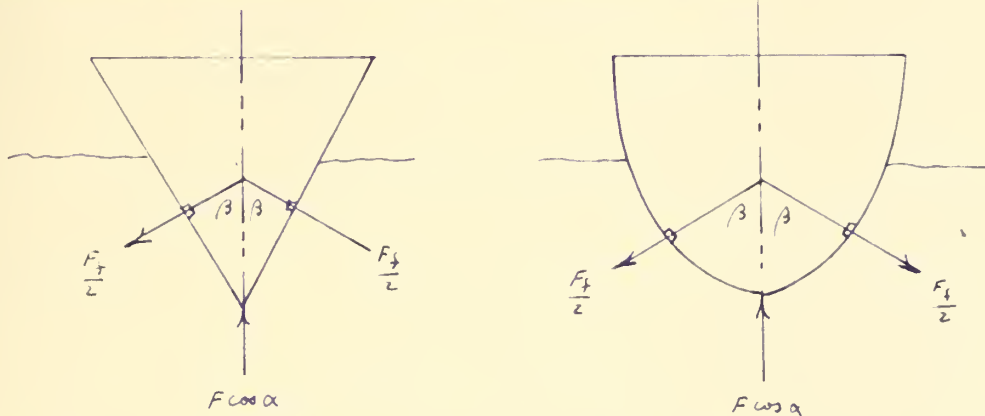


## Part 5

### Ability to Retract once Beset

Suppose the vessel has climbed up on to the ice sheet but the ice fails to break and the vessel becomes beset. According to the theory of mechanical friction, the force which is acting to impede the retraction of the vessel is the static frictional force which is equal to the product of the coefficient of static friction for steel on ice and the component of the bow force which acts normal to the ships hull plating. The resultant mechanical friction force  $F_f$  acts parallel to the stern and may be assumed evenly divided either side of the stern.

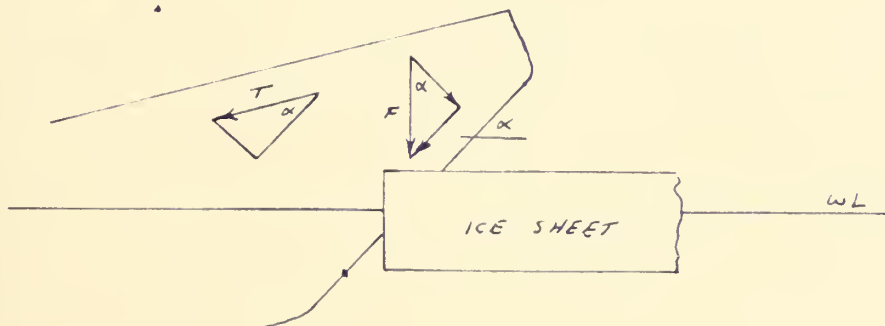
If, for the present, we assume no stepped forefoot, and if we pass planes through the bow of the vessel normal to the stern, the sections will be in the form of wedges with flat or slightly convex sides.



Since the ice has been deformed in the form of a groove in which the bow slides when climbing, pressure is developed normal to the faces of the groove causing friction forces along the faces of the groove and in a direction parallel to the stern.



As the ship sits in this beset condition there is a vertical bow reaction force  $F$  acting.



The component  $F \cos \alpha$  acts normal to the stern, hence the force which acts normal to the shell plating on each side is

$$\frac{F \cos \alpha}{2 \cos \beta}$$

resulting in a friction force of

$$\frac{F_f}{2} = \frac{f_s F \cos \alpha}{2 \cos \beta}$$

Therefore, the total friction force becomes

$$F_f = \frac{f_s F \cos \alpha}{\cos \beta}$$

where  $f_s$  = coefficient of static friction

The force  $F \sin \alpha$  also acts, but parallel to the stern and tends to overcome the friction force holding the vessel. In addition, if the vessel is beset, the propeller will be put full power astern in order to aid retract. For lack of better data on astern propeller operation we may assume that full ballard pull is being developed.



Now the component of propeller thrust  $T_0 \cos \alpha$  acts to aid the vessel extract itself since it acts parallel to the stern. In addition, the component  $T_0 \sin \alpha$  tends to reduce the normal force hence reducing the force of friction which must be overcome. If we consider the propellers acting then the total normal force becomes

$$F \cos \alpha - T_0 \sin \alpha$$

resulting in a total friction force of

$$F_f = f_s \left( \frac{F \cos \alpha - T_0 \sin \alpha}{\cos \beta} \right)$$

and the force tending to overcome this friction force becomes

$$F \sin \alpha + T_0 \cos \alpha$$

consequently if

$$F \sin \alpha + T_0 \cos \alpha \geq f_s \left( \frac{F \cos \alpha - T_0 \sin \alpha}{\cos \beta} \right) \quad (100)$$

the vessel will be able to extract itself once beset. We may re write this as

$$T_0 \geq F \left[ \frac{f_s - \tan \alpha \cos \beta}{f_s \tan \alpha + \cos \beta} \right] \quad (101)$$

If we let

$$U = \frac{f_s - \tan \alpha \cos \beta}{f_s \tan \alpha + \cos \beta}$$

we have

$$T_0 \geq F U \quad (102)$$

Now  $U$  can be either positive or negative dependent upon whether  $\tan \alpha \cos \beta$  is greater or less than  $f_s$ . If  $U$  is negative, then

$$\tan \alpha \cos \beta > f_s$$

If we consider the vessel in the static condition at the end of a charge without the propellers acting the forces acting are the friction force

$$F_f = \frac{f_s F \cos \alpha}{\cos \beta}$$





tending to prevent retraction and the force

$$F \sin \alpha$$

acting parallel to the stern tending to cause the vessel to retract. Now if

$$F \sin \alpha \geq \frac{f_s F \cos \alpha}{\cos \beta}$$

the vessel will not become beset since the friction force will not be great enough to hold the vessel. We may reduce this expression to

$$\tan \alpha \cos \beta \geq f_s$$

But this is exactly the condition that exists if  $U$  is negative. Consequently, if we can, in the design of our vessel, assure that

$$\tan \alpha \cos \beta > f_s$$

we need not worry about the vessel becoming beset at the end of a charge.

This, however, is not always possible or feasible since the value of  $f_s$  is an elusive thing and difficult to predict since it is so dependent upon existing atmospheric and ice conditions.

In section G-1 we show that the values of  $\alpha$  and  $\beta$  most conducive to maximum icebreaking effectiveness are

$$\alpha = 26^\circ$$

$$\beta = 45^\circ$$

Consequently, so long as  $f_s \leq 0.345$  we can design for maximum icebreaking effectiveness and still satisfy the condition

$$\tan \alpha \cos \beta \geq f_s$$

However, in section D-3 we showed that  $f_s$  could vary up to approximately 0.5 and perhaps greater if temperatures are low, the ice very dry and the vessel sitting in the beset condition for a period of time so as to allow adhesion between the hull and ice surface. In such a condition  $U$  is positive, i.e.

$$\tan \alpha \cos \beta < f_s$$



Hence, let us reconsider our expression for the vessels ability to retract,  
ie.

$$T_0 \geq FV$$

Now in section F-2 we showed that the bow reaction force  $F$  could be expressed as

$$F = 0.91 \times T_0 + \sqrt{0.828 \times T_0^2 + \frac{W^2 V^2 L}{4gH}} \quad \text{tons}$$

where  $\lambda$  and  $z$  are the dimensionless quantities

$$\lambda = \frac{\cot \alpha \cos \beta - f_0}{\cos \beta + f_0 \cot \alpha}$$

$$z = \frac{\cos \beta \cot^2 \alpha}{\cos \beta + f_0 \cot \alpha}$$

$f_0$  = dynamic coefficient of friction

In addition we gave expressions for  $V$  dependent upon whether the vessel accelerated through open water or an ice clogged channel prior to impact with the ice. Since the severity of this retraction problem increases directly with an increase in bow reaction force  $F$  and since  $F$  increases as impact speed  $V$  increases let us consider the more severe case where the vessel has accelerated through open water. Therefore

$$V = 3.1 \times T_0^{0.621} \quad \text{ft/sec} \quad (63)$$

Hence, when  $V$  is positive, i.e.

$$f_0 \geq \tan \alpha \cos \beta$$

the condition we must satisfy in order for the vessel to be able to free itself becomes

$$T_0^{0.758} \geq \frac{0.0245 W^2 V^2 \lambda^2}{H(1 - 0.828 \lambda V)} \quad (103)$$





As previously mentioned, in section G-1 we establish values of  $\alpha$  and  $\beta$  based on an  $\alpha$  and  $\beta$  which would produce the greatest ice breaking effectiveness, i.e. greatest vertical bow reaction force  $F$ , and still be consistent with accepted icebreaker design practice. It does not seem logical at this point to alter these values of  $\alpha$  and  $\beta$  so as to minimize  $U$  since the vessels primary task is to break ice and this can only be accomplished by the greatest bow force  $F$  we can develop. Our only concern here is that the vessel will be able to extract itself after ramming under the normally encountered ice conditions. Consequently, we shall continue to accept our values of

$$\alpha = 26^\circ$$

$$\beta = 45^\circ$$

unless we can subsequently show that such values of  $\alpha$  and  $\beta$  will prevent the vessel from extracting itself. If such is the case, then we will modify  $\alpha$  and  $\beta$  and accept a reduced bow reaction force  $F$  so as to increase the vessels probable ability to retract. Consequently, accepting the above values of  $\alpha$  and  $\beta$  we have

$$\alpha = 1.26$$

$$\beta = 0.557$$

and our desired condition becomes

$$\frac{0.758}{f_s} \geq \frac{0.0415 W^{0.5} X^{0.5}}{H(1 - 2.27U)} \quad (104)$$

Now as we've seen, the value of  $U$  is a direct function of the coefficient of static friction  $f_s$ . In section D-3 we stated that the value of  $f_s$  could, for steel on salt water ice, vary from about 0.3 to as high as 0.5. Existing experimental data indicates that the value of 0.5 is quite severe and would



probably be indicative of a condition where the vessel remains in the beset condition for a considerable length of time so as to allow the steel hull to completely freeze to or adhere to the contacting ice surface. In normal ice breaking this is not the case since the vessel attempts to retract shortly after the completion of the ram. Hence the length of time that she actually sits in the beset condition, assuming ice conditions are such as to cause her to become beset, is relatively short and probably only equal to the time it takes to reverse her engines to full power astern. Therefore, to evaluate our ship characteristics on the basis of a value of  $f_s = 0.5$  would be overly severe and not at all realistic or consistent with icebreaker operating practice. To be more realistic and rational in our evaluation it would probably be best if we accepted an average value of

$$f_s = 0.4$$

and reserve consideration of the condition where  $f_s = 0.5$  for those instances when the vessel moors itself to the ice by ramming it and remaining beset for a considerable period of time.

From figure 56 we see that based on our previously selected values of  $\alpha$  and  $\beta$  and  $f_s = 0.4$  we have

$$U = 0.061$$

Therefore, a reasonable condition which we must satisfy so as to ensure that the vessel will be able to extract itself once beset is

$$T_0^{0.758} \geq 0.0001195 \frac{\omega^2 x^2}{H} \quad (105)$$

For the very extreme condition where the vessel has remained beset for a considerable length of time and the temperature is very low, i.e.  $f_s = 0.5$



$$U = \frac{f_s - \tan \alpha \cot \beta}{f_s \tan \alpha + \cot \beta}$$

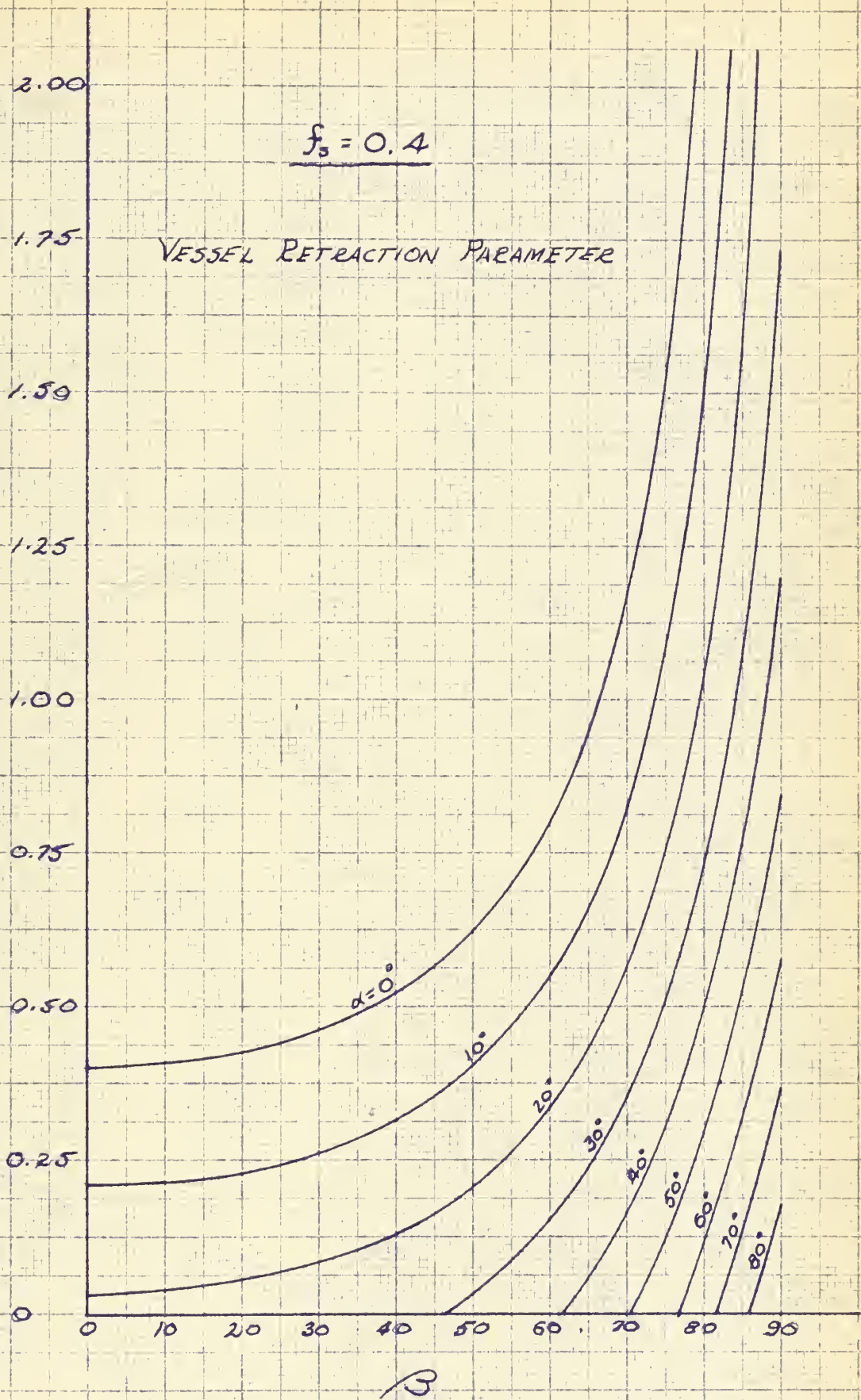


FIG 56





$$U = \frac{f_s - \tan \alpha \cos \beta}{f_s \tan \alpha + \cos \beta}$$

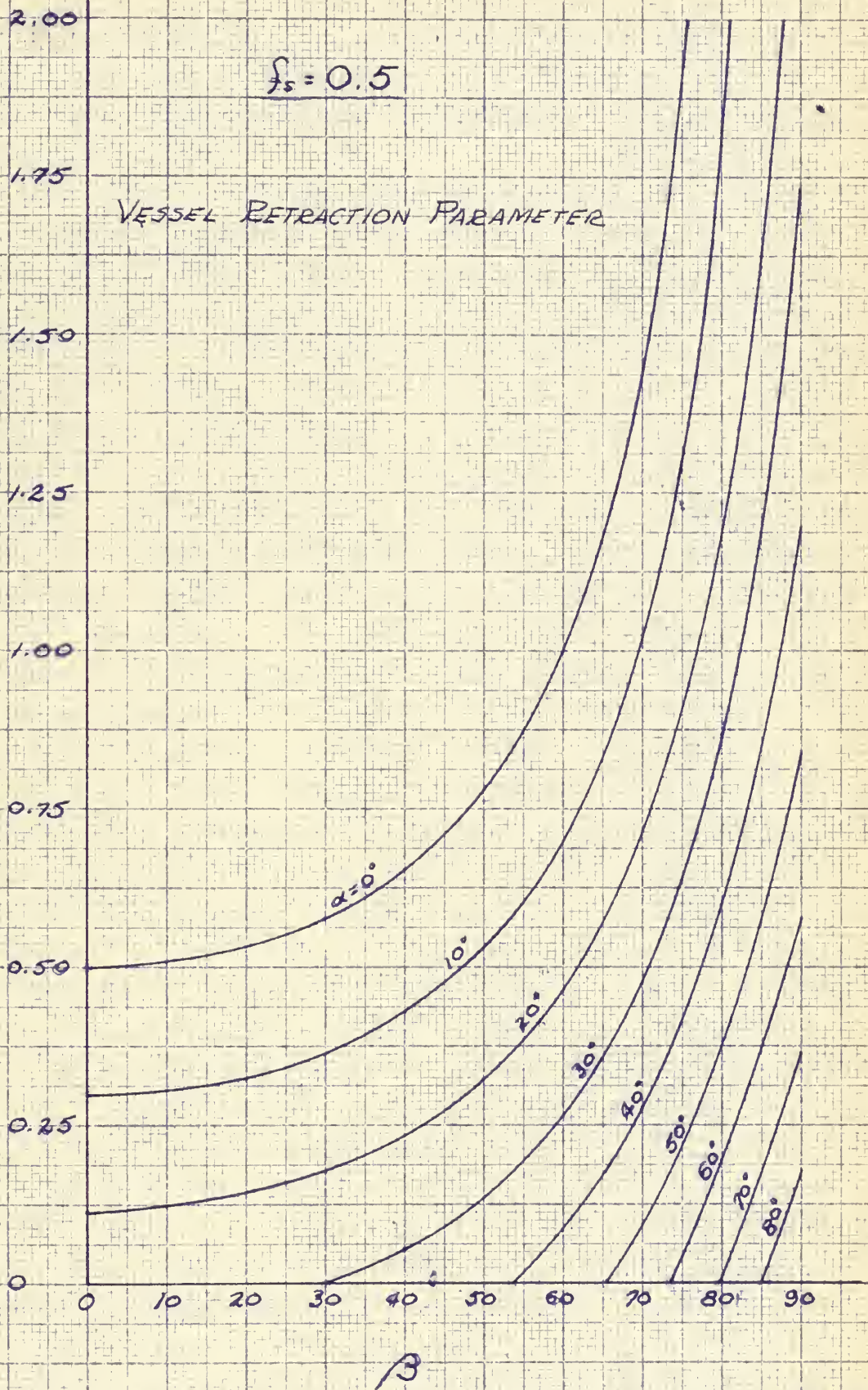


Fig 57



we have from figure 5?

$$U = 0.163$$

and the more severe condition to MEET that

$$T_0^{0.258} \geq 0.001765 \frac{\omega^2 x^2}{H} \quad (106)$$

Now, admittedly, these two conditions above are rather severe since they assume that the vessel has rammed the ice after accelerating in open water.

This is seldom the case in heavy icebreaking for a channel is soon found, and when the vessel accelerates, it does so through this ice clogged channel.

In this instance the impact velocity  $v$  is given by

$$v = 1.12 x T_0^{0.524} \quad \text{ft/sec} \quad (68)$$

hence the condition we must meet so that the vessel will be able to extract is

$$T_0^{0.952} \geq \frac{0.00972 \omega^2 20^2 x^2}{H(1-1.82 x U)} \quad (107)$$

Applying the same reasoning as before as regards  $x$  and  $\beta$  and based on

$f_s = 0.4$  we have

$$x = 1.26$$

$$\beta = 0.557$$

$$U = 0.061$$

Hence the condition we must satisfy is

$$T_0^{0.952} \geq 0.0000634 \frac{\omega^2 x^2}{H} \quad (108)$$

or the more severe condition when  $f_s = 0.5$  that

$$U = 0.163$$

hence

$$T_0^{0.952} \geq 0.000227 \frac{\omega^2 x^2}{H} \quad (109)$$





Now previously we mentioned the probable feasibility of modifying  $\alpha$  and  $\beta$  so as to make  $U = 0$ , i.e.

$$f_s = \tan \alpha \cos \beta$$

and therefore ensure that the vessel would be able to retract solely by virtue of the component of the vertical bow reaction  $F$  which acts parallel to the stern. We could do this based on a static coefficient of friction of 0.4 which would then leave that component of propeller ballard pull acting parallel to the stern as reserve power to account for the possibility of the static coefficient of friction rising above 0.4.

If such a modification as described above is made, it might be best to vary  $\alpha$  while keeping  $\beta$  constant since any variation in  $\beta$  would have to act to increase  $\beta$  and cause the vessels forepart to become excessively spoon shaped which is undesirable. Consequently, for our case where we have selected a value of  $\beta = 45^\circ$  we see from figure 66 that we need increase  $\alpha$  to approximately  $29.5^\circ$  to meet the condition.

$$f_s = 0.4 = \tan \alpha \cos \beta$$

and make  $U = 0$ . Now this is not too rash a modification and would only reduce the vertical bow reaction  $F$  by about 2-3% which in reality is insignificant. Therefore, it seems that a modification <sup>COULD</sup> ~~should~~ be made and <sup>MIGHT</sup> ~~would~~, in the end, be beneficial. Hence it seems the best selection <sup>MIGHT</sup> ~~would~~ be

$$\beta = 45^\circ$$

$$\alpha = 29.5^\circ \text{ say } 30^\circ$$



## Part 6

### Evaluation of Optimum Flare at Side

Vessels of the icebreaking type are usually provided with a generous flare aft of the stern which is carried back to amidships and normally varies from about 10 to 20 degrees from the vertical. There are several reasons for this practice. The one most often quoted results from the epic experiences of the "Fram" wherein the flare will cause the vessel to lift up rather than be crushed when subjected to the extreme pressures due to the compressive forces of drifting floes. In addition, the flare and the waterline can be laid out so that extensive portions of the buttock lines in the forebody will be parallel to the sloping portion of the stern. This is felt to be advantageous since it causes the entire periphery of the forward end of the vessel to bear down uniformly on the ice so as to make the entire forebody, from bow to maximum beam, act effectively to break ice.

The exact angle of flare which is used, or should be used, is subject to controversy. It is agreed, however, that some flare should be used since a normal ship with vertical sides amidships, fitted with a cut away bow gives comparatively poor ice breaking performance. Such a flat sided vessel will break ice continuously until the vertical sides are reached, where all breakage will stop and forward progress halt due to the friction between the ice and vertical sides.

In many instances, angles less than the 10° - 20° quoted above have been used. As early as 1898, Admiral Makarev of the Russian Navy, expressed his



feeling that such a reduced angle produced a more effective vessel. To this end he wrote "..... I find that sharpness of the bow outlines plays a large part in icebreaking and that excessively sloping frames, although useful in the initial breaking of ice, cause difficulties. It seems to me that with sloping frames ice does not get into the vertical position at which it can slide along the side. It only inclines somewhat and its whole snow covered surface tightly adheres to the vessel. This produces enormous friction which stops advance. Steamships with more vertical sides, to my observation, can cope more easily with ice." And he continued, "The more sloping is the outline of the frames the more the forepart of the ship approaches a spoonlike shape which, in my opinion, is worthless in breaking ice." These observations were fully confirmed by the improved breaking ability of the Russian breaker "Ernak" after her forepart was altered so as to give more near vertical side frames. This same view concerning the slope of an icebreakers frames in the forebody has also been expressed by many others since Makarev. In the present larger icebreaking vessels the flare angle is often small since a large flare angle amidships will result in a certain degree of flatness of the sides which causes some shouldering of the buttocks where they turn into the bow. The smaller flare angle results in an easier buttock curvature and the generally rounder lines so produced seem to result in better ice breaking performance with less tendency for the vessel to stick. In addition, the form which results due to high angles of flare amidships makes it necessary to harden up the bilges so as to provide adequate deck area in the engine rooms. This form will prevent the early rise of ice driven under



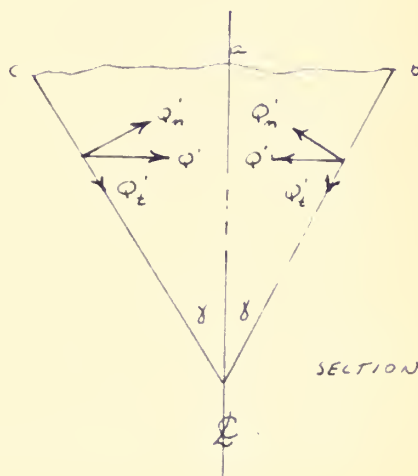
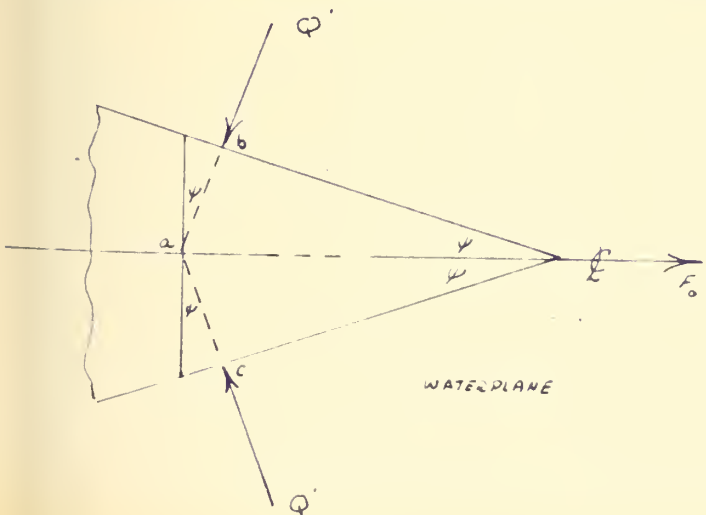


the vessel, causing more of it to come up into the propeller.

In making the choice of flare to use on a new design, therefore, we must consider the effect of this flare on the ability of the vessel to withstand crushing as well as its effect on the icebreaking effectiveness of the vessel. As regards crushing, it is felt that with the modern all welded, heavily constructed icebreaker hull there is little if any possibility of the vessel actually being crushed by an ice field. Consequently, the practical choice of flare normally will evolve about its effect on the vessels ice breaking effectiveness.

In order to more properly evaluate this point let us evaluate the influence of the separate elements of the vessels forepart on its mobility in ice. To do this we shall consider movement in broken ice since this is where the effect of the shape of the frames is most critical.

For simplicity, assume that the bow of the vessel has the shape of a wedge and that the load waterplane and bow sections are formed by straight lines inclined toward the centerline plane. Such a simplifying assumption will greatly facilitate the solution of our problem yet will not lead to appreciable error since most sea going ice breakers have waterplanes and sections of small curvature at their forward end.





When a vessel of such configuration moves under the action of a force  $F$  through ice, it is opposed by forces representing the pressure of the ice which acts normal to the sides of the vessel. The value of this normal force is

$$Q' = \frac{F'}{2 \sin \psi}$$

where  $\psi$  = angle between center line plane and load waterplane

The frictional forces caused by the pressure  $Q'$  will be

$$F_f = f_0 Q' = \frac{f_0 F'}{2 \sin \psi}$$

where  $f_0$  = coefficient of dynamic friction between the ice and steel

Let us dissect the bow of the vessel with vertical planes coinciding with the direction of force  $Q'$  as shown in <sup>THE</sup> figure (planes ab and ac). Force  $Q'$  may be broken into component forces  $Q'_t$  and  $Q'_n$  tangent and normal to the sides. We may now say that once the ice is broken, the force tending to push the ice cakes down under the water so as to give way to the vessel is  $Q'_t$  and the force opposing this motion of the ice is  $f_0 Q'_n$ . Therefore, when

$$f_0 Q'_n < Q'_t \quad (110)$$

the ice cakes pressing on the hull plating will slide down along the plating under water and give way to the vessel. This may also be expressed as

$$f_0 < \tan \delta \quad (111)$$

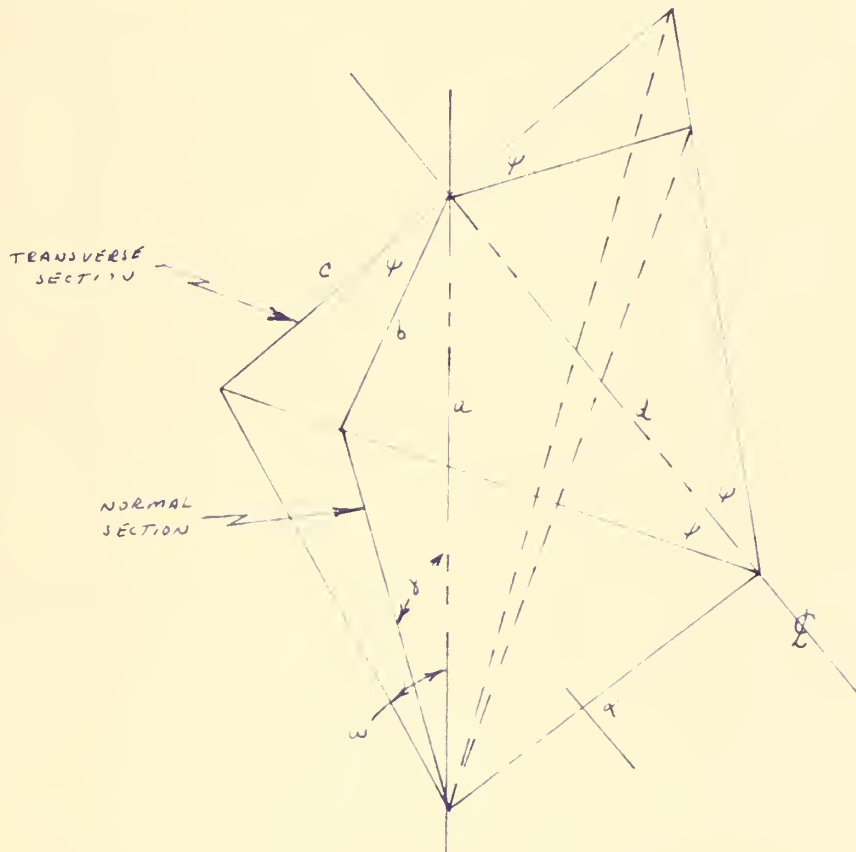
When the angle  $\delta$  is large, ice cakes may easily go down under the stern and bottom and, as experience shows may even, due to the resulting spoon shaped bow, adhere to the sides. If this occurs, successive cakes of ice will adhere





to the first so that the vessels motion is soon impeded. On the other hand, if the angle  $\gamma$  is small and the tangent  $\gamma$  only slightly larger than the coefficient of dynamic friction, then the ice will be forced down, turn on its side and give way.

Now we have been considering the section normal to the ships side. If we consider the transverse section at this point



where  $\omega$  = angle between the centerline plane and the ships side at the transverse section

$\alpha$  = angular rise of forefoot

In order to develop a relationship between the angle  $\gamma$  and  $\omega$  we may note that

$$b = a \tan \gamma$$



also

$$b = c \cos \phi$$

$$c = a \tan w$$

Therefore

$$a \tan \delta = a \tan w \cos \phi$$

hence

$$\tan \delta = \tan w \cos \phi \quad (112)$$

In like manner

$$a = d \tan \alpha$$

also since

$$c = a \tan w$$

$$c = d \tan \phi$$

Therefore

$$a \tan w = \frac{a \tan \phi}{\tan \alpha}$$

hence

$$\tan w = \frac{\tan \phi}{\tan \alpha} \quad (113)$$

If we combine the expressions for  $\tan \delta$  and  $\tan w$  we have

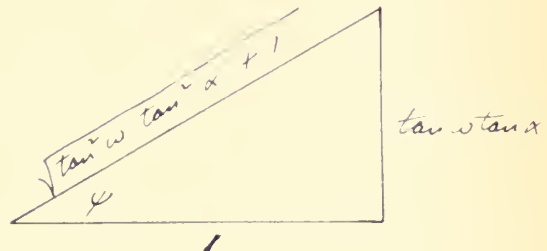
$$\tan \delta = \frac{\sin \phi}{\tan \alpha} \quad (114)$$

hence our expression (111) becomes

$$f_D < \frac{\sin \phi}{\tan \alpha} \quad (115)$$

but

$$\tan \phi = \tan w \tan \alpha$$



therefore

$$f_D < \frac{\tan w \tan \alpha}{\tan \alpha \sqrt{\tan^2 w \tan^2 \alpha + 1}}$$

$$f_D < \frac{\tan w}{\sqrt{\tan^2 w \tan^2 \alpha + 1}} \quad (116)$$



From figure 64 we see that for maximum  $z$  which is beneficial to icebreaking force

$$22^\circ < \alpha < 31.5^\circ$$

Therefore, if we assume our value of coefficient of dynamic friction of

$$f_D = 0.15$$

The condition we wish to achieve is

$$\frac{\tan w}{\sqrt{\tan^2 w \tan^2 \alpha + 1}} \stackrel{\text{SLIGHTLY}}{>} 0.15 \quad (117)$$

hence as a minimum condition

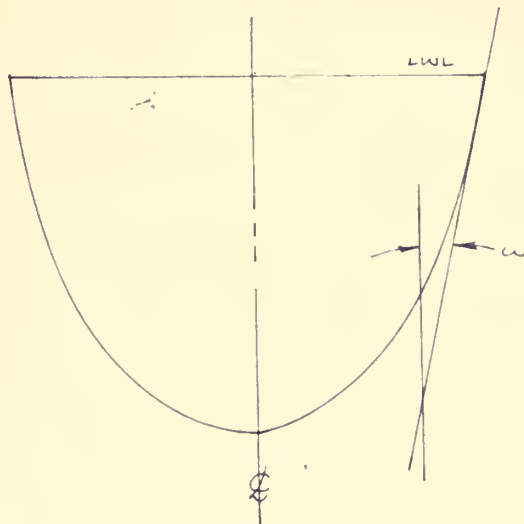
$$\tan w = \frac{0.15}{\sqrt{1 - 0.0225 \tan^2 \alpha}} \quad (118)$$

but  $0.0225 \tan^2 \alpha$  is extremely small compared to 1 when we consider the range of  $22^\circ < \alpha < 31.5^\circ$  hence the minimum condition becomes

$$\begin{aligned} \tan w &= 0.15 \\ w &= 8.5^\circ \end{aligned} \quad (119)$$

We may therefore say that the ideal condition would be when  $w$  is slightly greater than  $8.5^\circ$  say about  $10^\circ$ .

Now in an actual design the sides of the transverse section are not straight as assumed above, but rather, slightly curved. Our results







above, therefore, must be interpreted to mean that the angle between the tangent to the side at the load waterline and the vertical should be  $W = 10^{\circ}$ . We may therefore conclude that the flare of side which is most conducive to effective icebreaking effectiveness is about  $10^{\circ}$ .



## Part 7

### Ability to Break Ice without Ramming

Consider an icebreaker which is attempting to proceed through a continuous field of sea ice. Assume that the vessel approaches the ice from open water and has considerable momentum at the instant it just strikes the ice shelf. This kinetic energy in conjunction with propeller thrust acts to force the vessel on to the ice breaking it by bending. Soon, however, the vessel's kinetic energy is completely expended and the vessel's propeller thrust must act alone to continue forcing the vessel up on to the ice so as to develop sufficient vertical bow reaction to overcome the ice. If the thrust available is such that it cannot force the vessel up on to the ice sufficiently to develop a vertical bow reaction force large enough to overcome the encountered thickness of ice, then vessel forward motion will cease and the vessel must back down so as to accelerate and again ram the ice.

It seems logical, therefore, that when undergoing a design study of a proposed icebreaker it would be desirable to insure that sufficient propeller thrust will be available so as to allow the vessel to proceed continuously through a reasonable thickness of ice without the necessity for having continuously to back down and ram.

Let us imagine, therefore, that the vessel has just completed a charge and has broken sufficient ice as a result of that charge so as to reduce its forward speed to zero. As the propellers continue to turn at full power the stern touches the unbroken ice shelf and the vessel attempts to continue its forward motion through the ice. The ensuing events may be described in equation





form as

$$E_1 = E_2 + E_3 \quad (120)$$

where

$E_1$  = Energy derived from the ships propeller

$E_2$  = Change in potential energy of the vessel

$E_3$  = Energy loss due to friction

In section F-2 we showed that the energy derived from the propeller could be expressed as

$$E_1 = T(\Delta\theta + s\Delta\phi) \cot \alpha \quad \text{ft tons} \quad (44) \quad (45)$$

If we put this in terms of the vertical bow reaction force (F) this became

$$E_1 = \frac{ATFH}{W} \cot \alpha \quad \text{ft tons} \quad (46)$$

where

$$H = \left( \frac{C_B}{C_W} + \frac{2_i C_B}{4k_i C_W} \right) \quad (47)$$

In like manner we showed that the change in vessel potential energy could be expressed as

$$E_2 = \frac{F^2 HA}{2W} \quad \text{ft tons} \quad (51)$$

and the energy loss due to friction as

$$E_3 = \frac{AH}{W} \left[ \frac{FTf_0}{\cos \beta} + \frac{F^2 t_0 \cot \alpha}{2 \cos \beta} \right] \quad \text{ft tons} \quad (54)$$

If we substitute the value of  $E_1$ ,  $E_2$ , and  $E_3$  back into (120) we have

$$\frac{ATFH}{W} \cot \alpha = \frac{AH}{W} \left[ \frac{FTf_0}{\cos \beta} + \frac{F^2 t_0 \cot \alpha}{2 \cos \beta} \right] + \frac{F^2 HA}{2W} \quad (121)$$

If we rearrange this expression and solve for the vertical bow reaction force F we have

$$F = 2T \left( \frac{\cot \alpha \cos \beta - t_0}{t_0 \cot \alpha + \cos \beta} \right) \quad (122)$$



but we have already defined the non dimensional quantity X as

$$X = \frac{\cot \alpha \cos \beta - f_0}{f_0 \cot \alpha + \cos \beta}$$

Therefore

$$F = 2T\lambda \quad (123)$$

Since the series of events which we are here describing take place after the complete loss of kinetic energy, that is at ship speed zero, the thrust developed by the propellers in causing the above described motion is practically equal to bellard thrust and we may, since the vessels forward velocity is practically nil as it climbs on to the ice, assume that in our expression

(123)

$$T = T_0$$

Therefore

$$F = 2T_0\lambda \quad \text{tons} \quad (124)$$

Since the larger we can make F the greater the thickness of ice we can overcome, it behooves us in our preliminary design to make  $T_0$  and  $\lambda$  as large as possible.  $T_0$  is a direct function of propeller diameter and installed horsepower hence there is not too much we can do other than insure that we use the largest diameter propeller allowed by the vessels draft or beam limitations and attempt to have as high an installed horsepower as can effectively and efficiently be absorbed by the selected propeller. We discussed this problem of power limitation in section F-2 wherein we described a propeller loading factor  $T_0/D^2$  and discussed how from an economic point of view the highest we could reasonably expect this factor to go in the foreseeable future was about

$$\frac{T_0}{D^2} = 850 \text{ per shaft}$$



Hence, in tons, a reasonable limiting approximation could be given as

$$T_0 = 0.379 D^2 \text{ per shaft}$$

As regards  $X$  we do have some latitude of variation in that it is solely a function of geometry, i.e. angular rise of forefoot  $\alpha$  and angle between the centerline plane and the normal to the vessels side at the bow  $\beta$ .

From figure <sup>65</sup> we see that for any given value of  $\beta$  the value of  $X$  increases with decreasing  $\alpha$ . It would seem, therefore, desirable to decrease  $\alpha$ . Unfortunately, however, we see from figure <sup>64</sup> ~~44~~ that a decrease in  $\alpha$  beyond the value of  $\alpha = 26^\circ$  we have already chosen will materially reduce  $Z$ . We show in section G-1 that the effect of the value of  $Z$  upon the vessels' capability of breaking ice by ramming is greatly in excess of the effect caused by varying  $X$  and we stated that if any choice were made it would be best to make  $Z$  as large as possible even if at the expense of a reduced value of  $X$ . It was at that time that we selected  $\alpha = 26^\circ$  and  $\beta = 45^\circ$  as our optimum values. Consequently, if we were now to dictate a decreased value of  $\alpha$  so as to increase our vessels' ability to break ice in continuous motion we would seriously effect its capability for breaking by ramming. Since the ramming consideration will dictate the thickest ice that the vessel will be able to penetrate it is felt that it should have overriding consideration and our values of  $\alpha$  and  $\beta$  remain at  $26^\circ$  and  $45^\circ$  respectively.

In like manner, when we discussed the vessels ability to retract from the ice once it was beset we stated that from the point of view of retraction it might be desirable to increase the value of  $\alpha$  to about  $30^\circ$ . If this is done however, our value of  $X$  decreases from 1.26 to 1.09 or a 13.5% decrease.





This in turn would mean a 13.5% decrease in the vertical bow reaction force developed in (124) above - a considerable decrease. Since vessels of the icebreaker type are normally equipped with heeling and *Trim* tanks to aid in breaking the adhesion bond between the ice and the vessels hull if the vessel becomes beset and since these tanks are so very effective in breaking the bond allowing the reverse propeller thrust to retract the vessel, it is felt that our present consideration of the vessels continuous icebreaking ability should take precedence and that  $\alpha$  should not be increased.

Consequently, it would seem that our previous choice of  $\alpha = 26^\circ$  and  $\beta = 45^\circ$  is still the most desirable as regards the ships general operational ability in the ice. Based on these values we have

$$\lambda = 1.26$$

and our expression (124) becomes

$$F = 2.52 T_0 \quad (125)$$

If we make use of our approximation of propeller loading ratio we may express this as

$$F = 0.955 D^2 \quad \text{tons} \quad (126)$$

Figures 58 to 60 show <sup>plots</sup> ~~plates~~ of the approximate number of inches of ice through which a vessel may proceed continuously based on expression (125) above and as a function of ice salinity and surface temperature.

There is one other item which we should consider here. That is, when selecting the actual value of  $\alpha$  and  $\beta$  to use in a proposed design we must in all instances insure that  $\lambda > 0$ . To do otherwise would make the ship incapable of breaking ice except by ramming wherein it made use of its kinetic





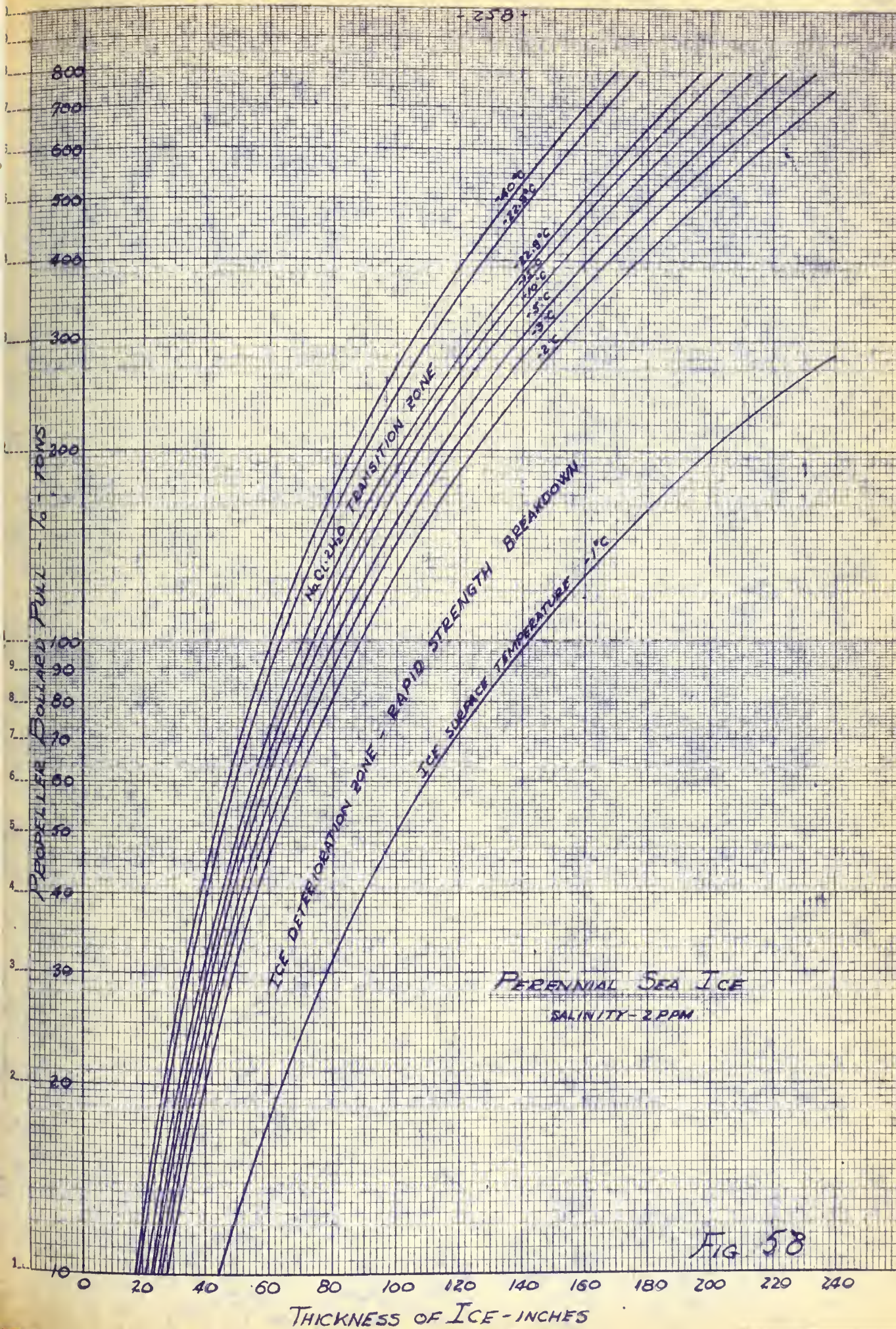
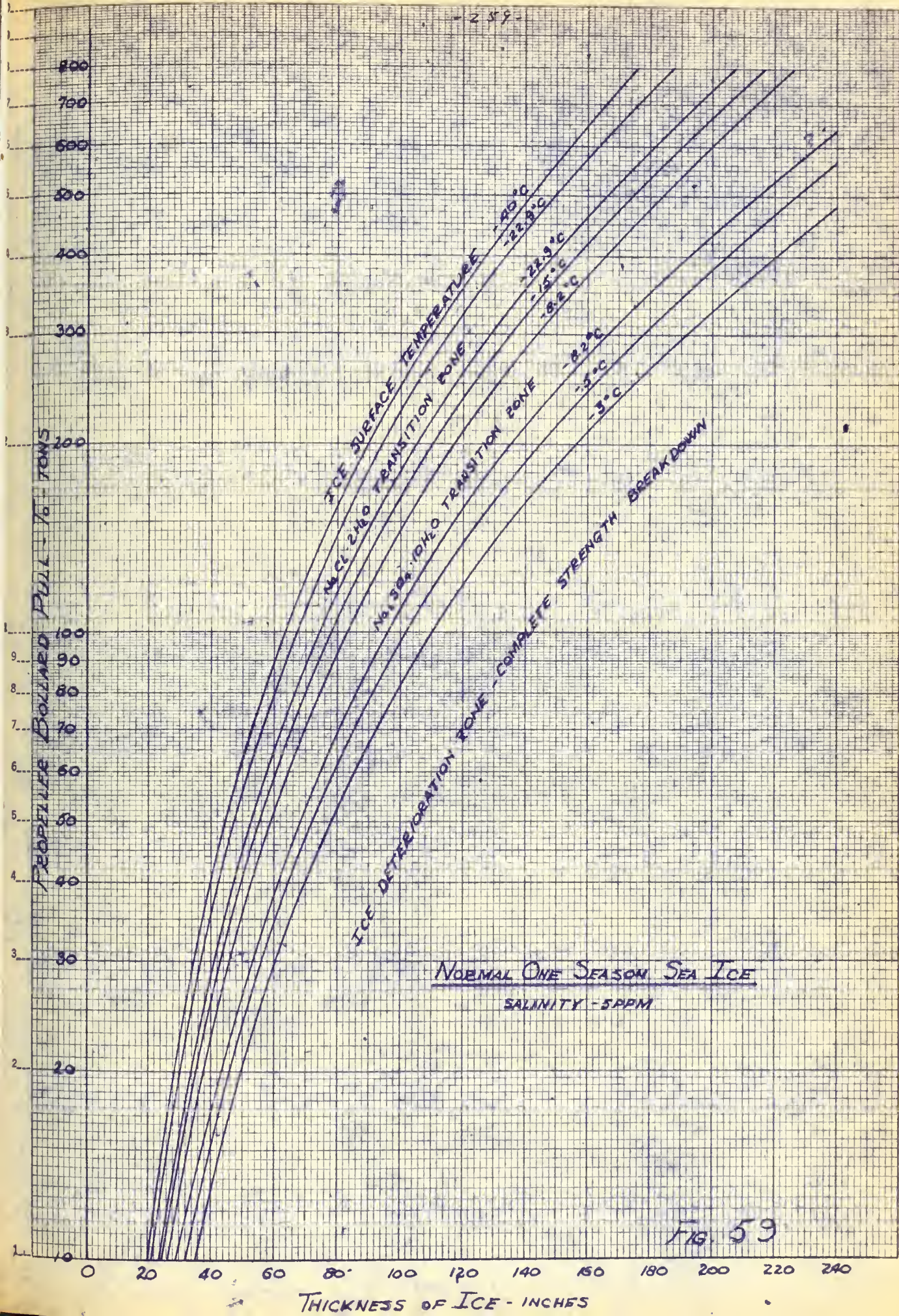


Fig 58

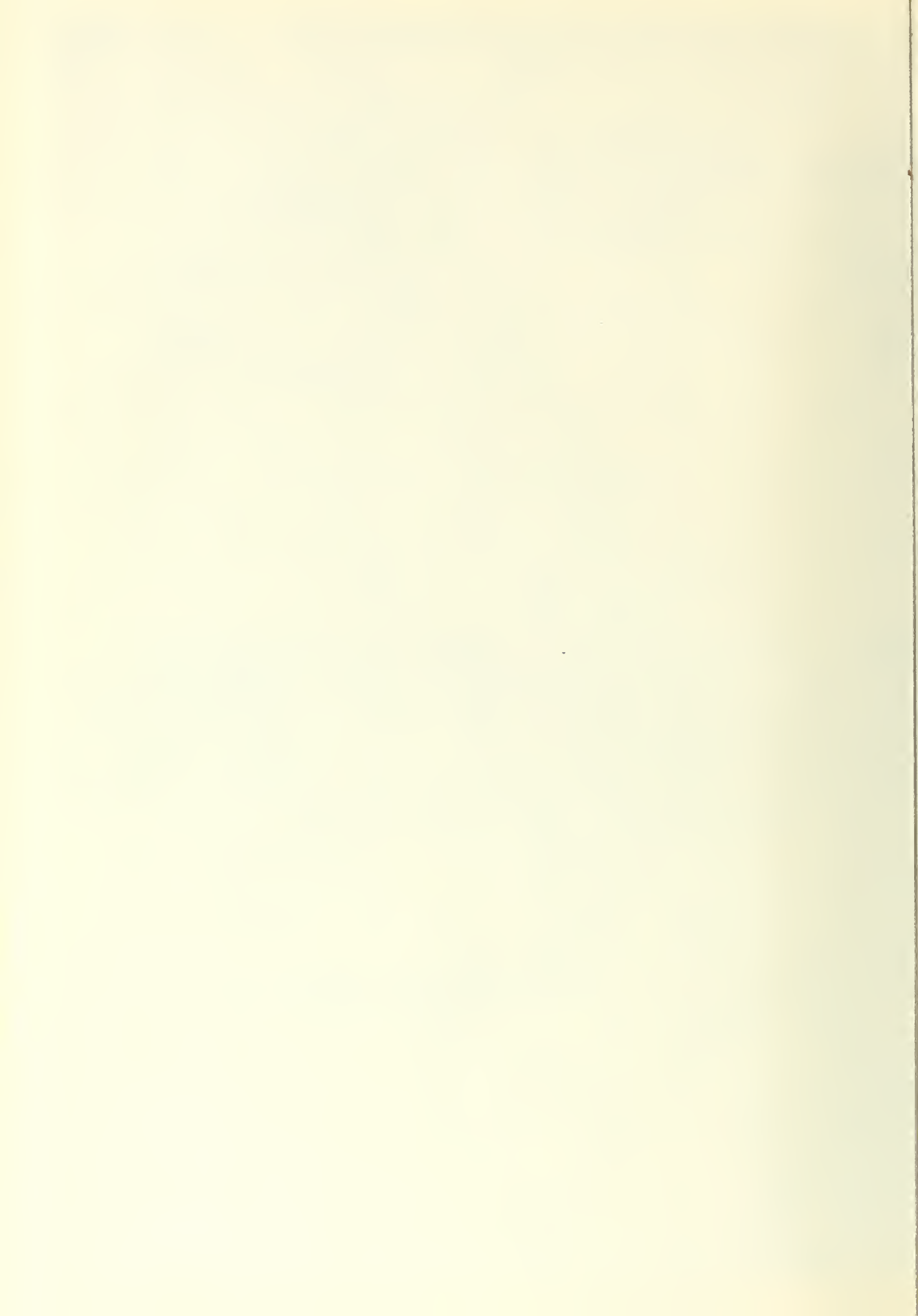


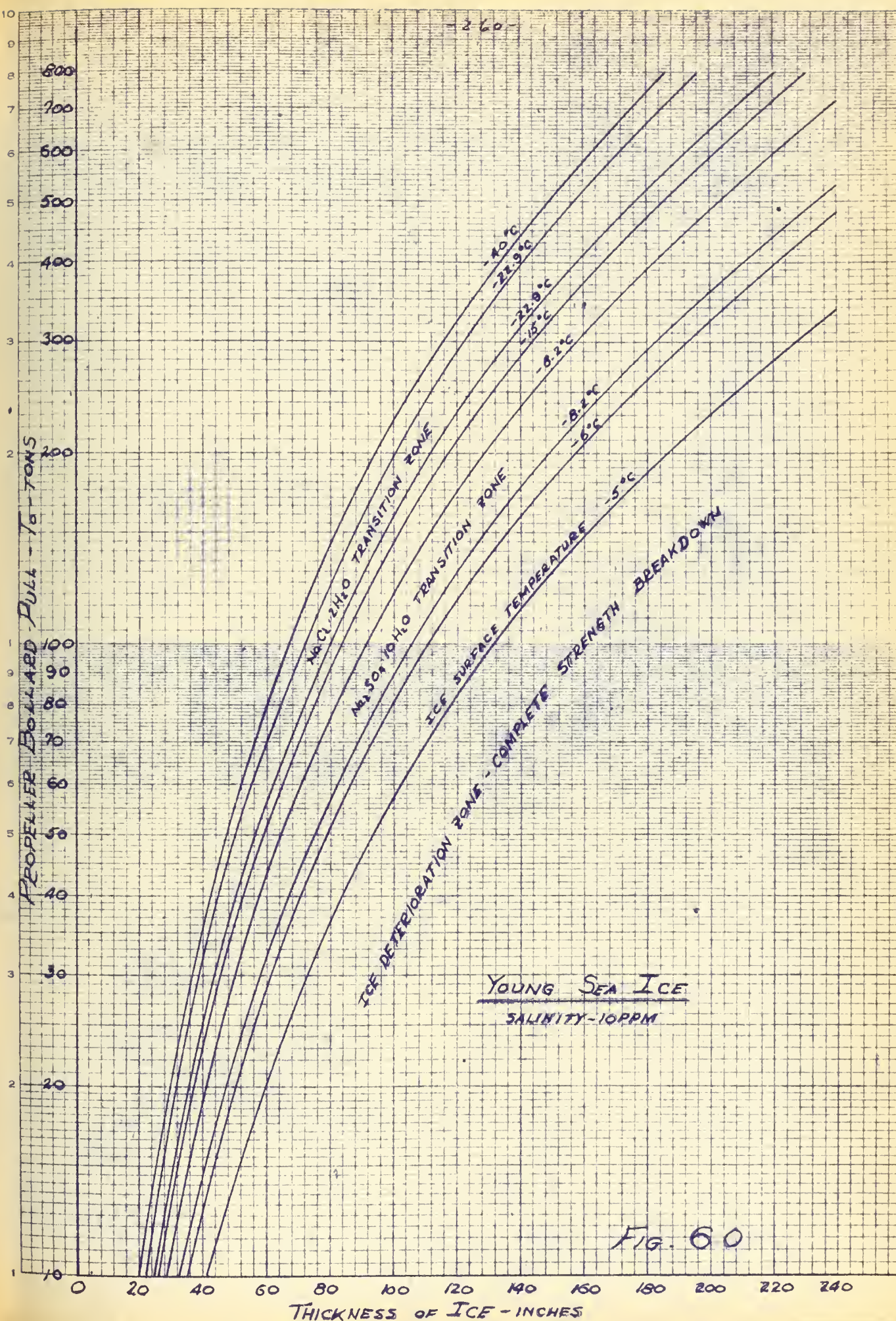
















energy. Consequently, not only do we desire  $\lambda$  as large as possible, but as an actual limit we must insure that

$$\lambda = \frac{\cot \alpha \cos \beta - f_0}{f_0 \cot \alpha + \cos \beta} > 0$$

or that

$$\cot \alpha \cos \beta > f_0 \quad (127)$$

In section D-3 we discussed friction and stated that the values of the dynamic coefficient of friction for sea ice on steel plate normally ranged from about 0.1 to 0.2. These values are rather low and for most <sup>DESIGNS</sup> designers past and present, we can show that

$$\cot \alpha \cos \beta > 0.1 \text{ to } 0.2$$

However, this is a consideration and the designer of any proposed vessel should insure that his selection of  $\alpha$  and  $\beta$  are not so radical as not to satisfy (127). Figure 61 shows a plot of  $\cot \alpha \cos \beta$  with the dotted lines indicating the probable upper limits of the dynamic and static coefficient of friction. As long as the selected values of  $\alpha$  and  $\beta$  fall above these two dotted lines our above condition is satisfied.





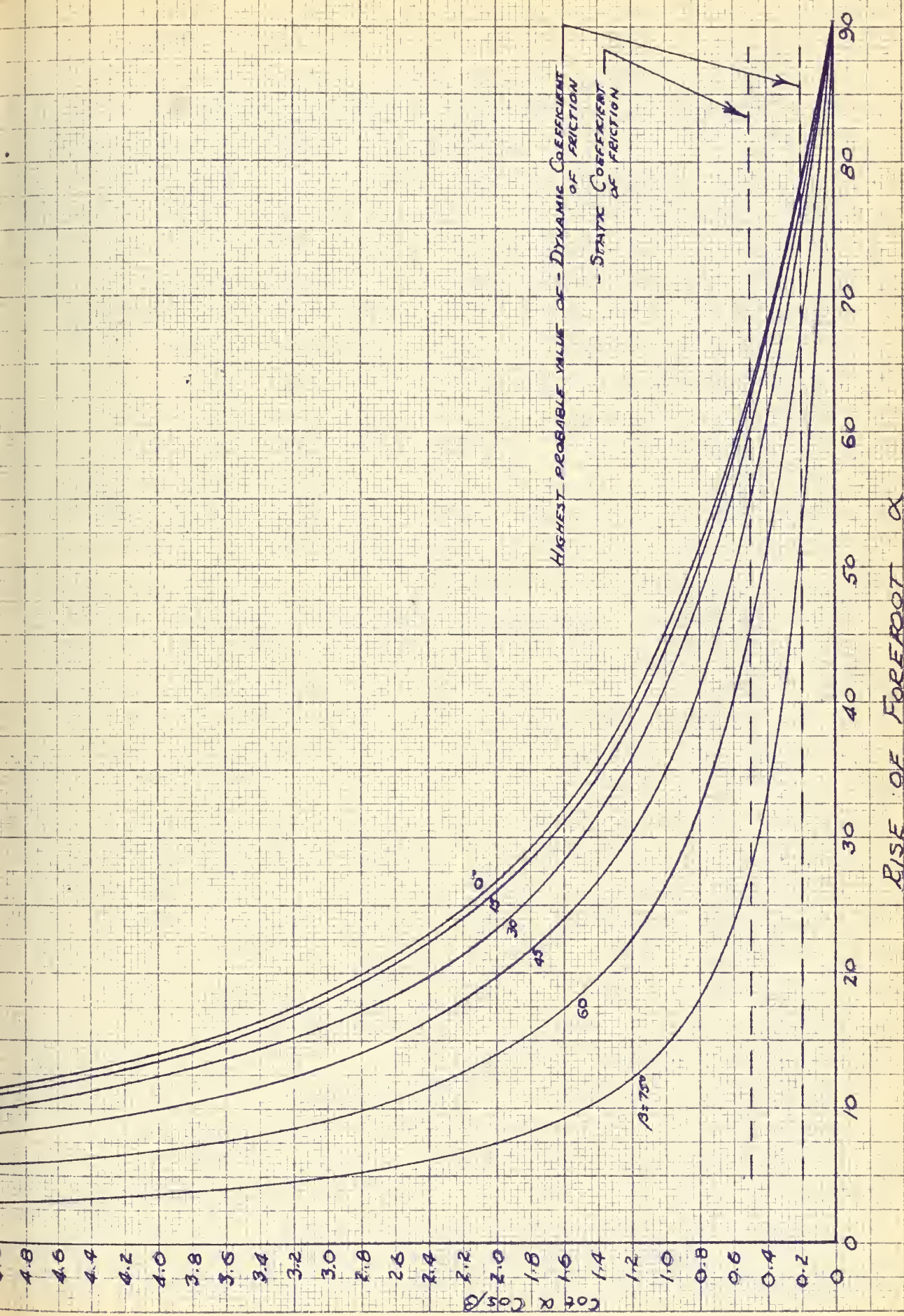


Fig 01



Section G

Preliminary Design Considerations





## Part 1

### Preliminary Estimate of Vessel Proportions

Let us consider our expression for the vertical force developed by the bow of our vessel, i.e.

$$F = 0.71 X T_0 + \sqrt{0.828 X T_0^2} + \frac{\omega^2 v^2 z}{g A H} \quad (70)$$

where

$$X = \frac{\cot \alpha \cos \beta - f_0}{\cos \beta + f_0 \cot \alpha}$$

$$z = \frac{\cos \beta \cos^2 \alpha}{\cos \beta + f_0 \cot \alpha} = Y \cos^2 \alpha$$

$$A = \left[ \frac{C_0}{C_w} + \left( \frac{b_1}{b_2} \right)^2 \frac{C_0}{4 C_w} \right]$$

$$S = b_2 \cdot L/2$$

$$GM_2 = \frac{b_2^2 C_w L^2}{H C_0}$$

If we solve this expression for vessel development, we have

$$\omega^2 = \frac{g A H}{2 v^2} \left[ F^2 - 1.82 X T_0 F \right] \quad (84)$$

Now when we investigate the non dimensional quantity A we find that it may be considerably simplified for the purposes of a preliminary displacement estimate. If we examine past American built icebreaker type vessels we find



that the value of  $k_1$ , is relatively constant, varying from about 1.01 to 1.034. In like manner the value of  $k_2$  for these vessels is also relatively constant, varying from about 0.266 to 0.272. We may, therefore, select representative values of  $k_1$  and  $k_2$ , tending in our selection to favor the more recent icebreaker types. Doing this, we may say

$$k_1 = 1.031$$

$$k_2 = 0.267$$

Therefore, the ratio

$$\frac{k_1}{k_2} = 3.83$$

which value varies by only about 0.5% from the average value for the vessels considered. Based on this ratio, our expression for A becomes

$$A = \frac{c_b}{c_w} \left[ 1 + \frac{3.67}{c_w} \right] \quad (85)$$

Due to the peculiar requirements for the underwater hull shape of icebreaker type vessels, it would seem that the non dimensional ratio  $c_b/c_w$  would remain relatively constant with vessel size. This ratio was investigated for seventeen past and present icebreaker vessels of the polar type of all sizes and it was found to vary from about 0.625 to 0.73. We may select a mean value of

$$c_b/c_w = 0.6735$$

as representative of modern icebreaker practice. Therefore, expression (85) becomes

$$A = 0.6735 \left[ 1 + \frac{3.67}{c_w} \right] \quad (86)$$

This selected value of  $c_b/c_w$  is further justified if we examine the five most recent American built icebreakers. In this instance we have a variation



of from 0.626 to 0.683 where the higher value is more representative of the larger types such as Glacier and Mackinaw.

In order to arrive at a value of  $C_w$  for use in our first estimate of vessel displacement we investigate icebreaking vessels built since 1940 and determine a trend in  $C_w$  as a function of speed length ratio. The results of this investigation are shown as figure 02 . The mean value, if used for our preliminary estimate, will only involve a maximum percentage difference of 4% from extreme values. This percentage difference is felt to be within acceptable limits for our purposes.

A further investigation was made of over thirty five past and present icebreakers so as to determine the variation of design speed length ratio. The values varied from about 0.849 to 1.20. This seems a wide variation, however, closer inspection reveals that for these thirty five vessels, depending upon the year in which they were built, the following variations exist:

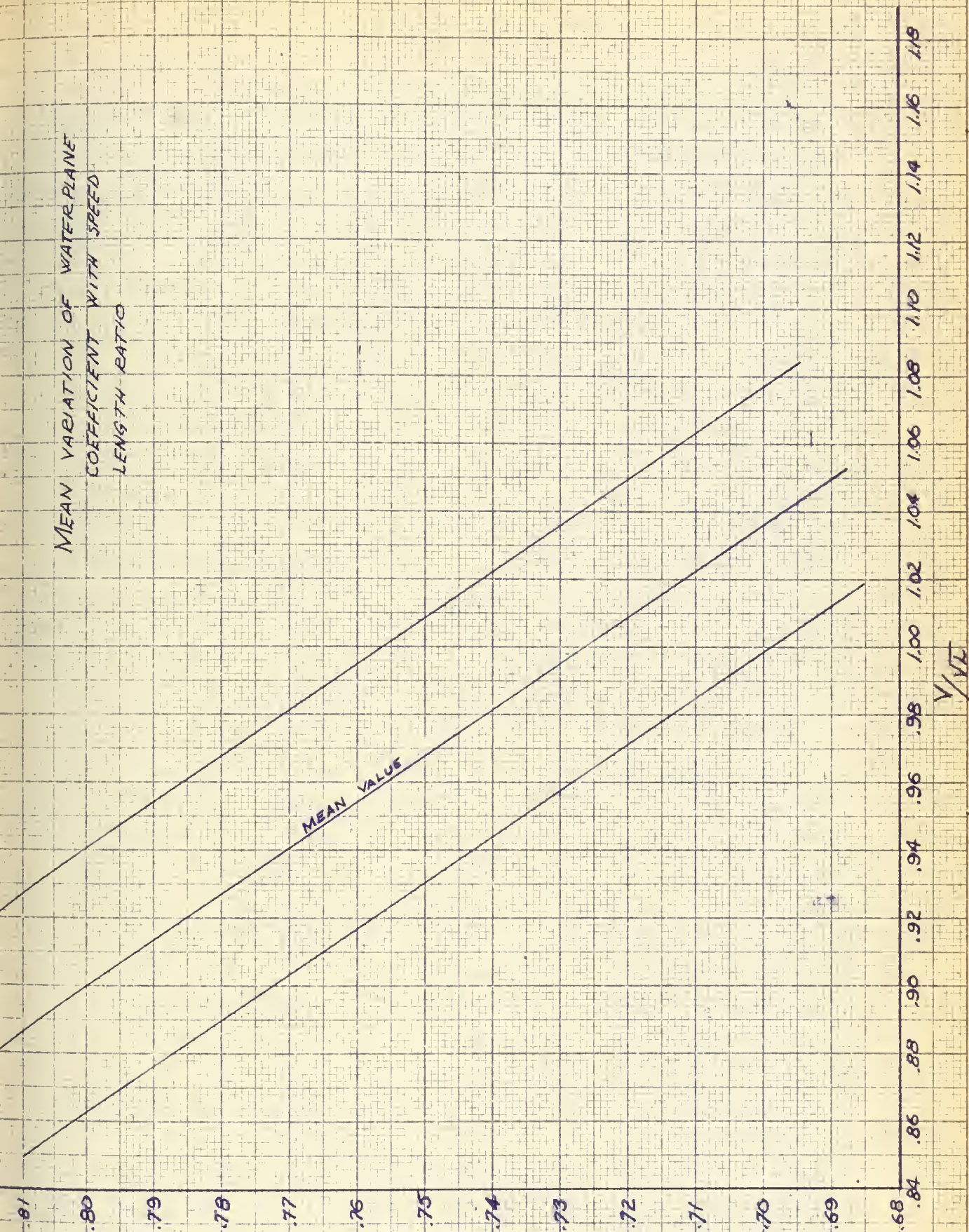
<u>Year Built</u>	<u>Range of Design <math>\sqrt{V/L}</math></u>
1920-1929	0.829 - 1.12
1930-1939	0.849 - 1.22
1940-1949	0.946 - 1.044
1950-1959	0.865 - 1.052

The trend is towards a higher average vessel design speed. Now it may be inferred that future designs will go to even higher design speeds due to increased powering and hence higher speed length ratios. This is somewhat doubtful, however, as explained in section F-2 since vessel draft limitations will severely restrict the maximum size of propeller which may be used





MEAN VARIATION OF WATERPLANE  
COEFFICIENT WITH SPEED  
LENGTH RATIO



C

FIG 62



to absorb these increased powers. This in essence becomes an economic problem of how much power can a given propeller absorb efficiently. This coupled with the fact that a definite limitation as to vessel length does exist so as to insure adequate maneuverability in the ice field, it seems hardly reasonable that the values of design speed length ratio of future vessels will ever go materially above *unity*. It is true that in earlier vessels values up to 1.22 were used, but these vessels were extremely short and light and were able to use much larger propeller diameters per given shaft horsepower than is true today, as will be true in the future. Consequently, it would seem that the values listed for the 1950-1959 period are the most realistic and representative of possible future trends. Hence for our preliminary purposes let us assume a representative value of

$$V/L = 0.978$$

which represents an average of the ten most recent icebreaker designs for which data was available, i.e.

<u>Name</u>	<u>V/L</u>	<u>Year built</u>
Kapitan Class	0.986	1954
Labrador	1.013	1954
General San Martin	1.030	1954
Glacier	0.941	1955
Montcalm	0.899	1957
ODEN	1.052	1957
Moscow	0.956	Building





<u>Name</u>	<u><math>V/\sqrt{L}</math></u>	<u>Year built</u>
Canadian hull 620	0.928	Building
Finnish design	0.998	Proposed
American design	0.978	Design Study

If we assume this representative average value of speed length ratio at design speed, we have from figure 62

$$C_w = 0.7425$$

Therefore, our expression (86) becomes

$$A \approx \text{CONSTANT} = 4.0 \quad (87)$$

and expression (84) becomes

$$\omega^2 = \frac{128.84}{2 V^2} \left[ F^2 - 1.92 \times T_0 F \right] \quad (88)$$

Let us now investigate the expression  $\chi$  and  $z$  which appear in (88) above and which are given as

$$\chi = \frac{\cot \alpha \cos \beta - f_0}{\cos \beta + f_0 \cot \alpha}$$

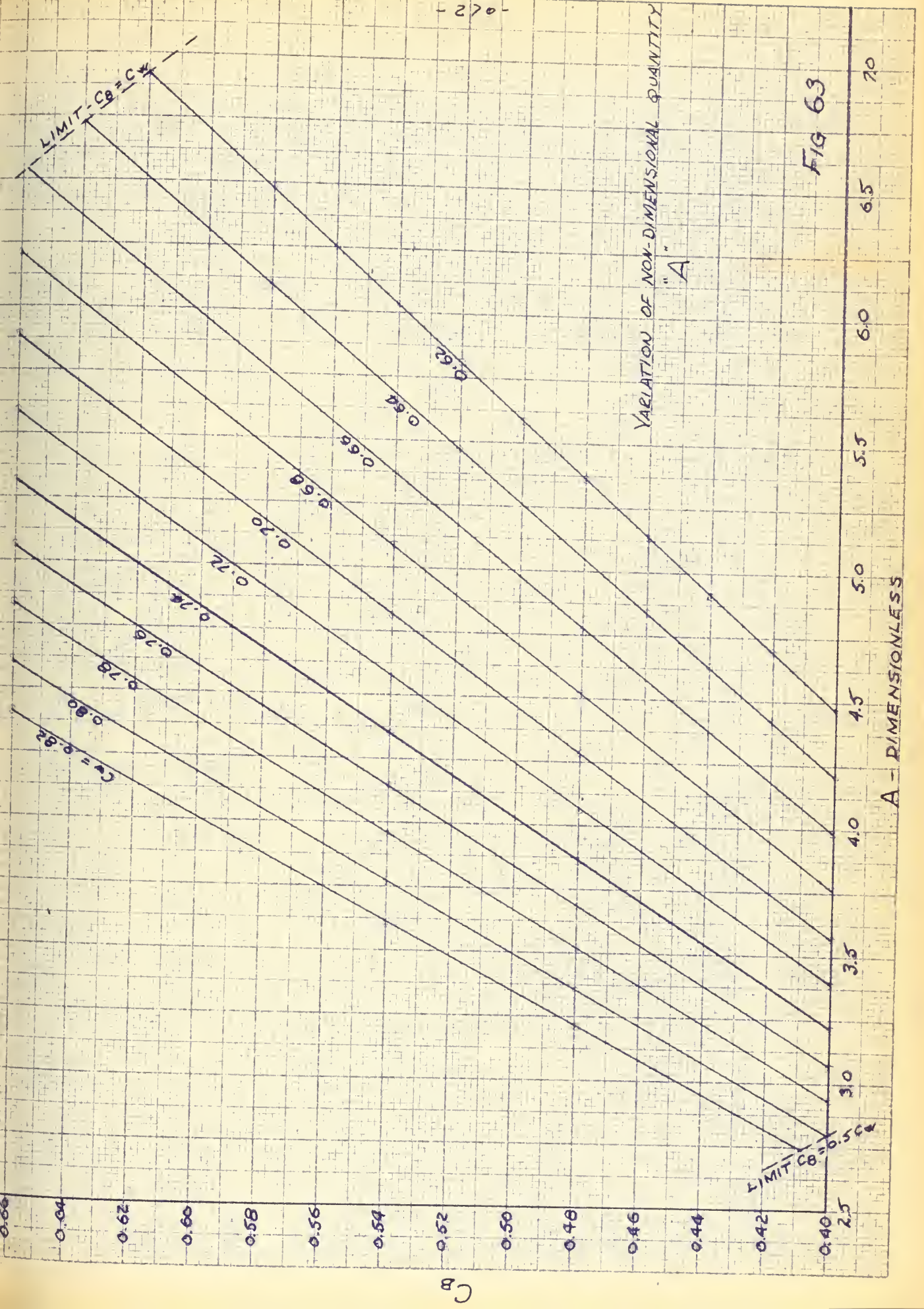
$$z = \frac{\cos \beta \cos^2 \alpha}{\cos \beta + f_0 \cot \alpha}$$

Each expression is a function of the dynamic coefficient of friction between steel and ice,  $f_0$ , the angular rise of the forefoot,  $\alpha$ , and the angle between the centerline plane and the normal to the shell at the bow  $\beta$ .

Let us consider the coefficient of friction first.

As outlined in section D-3, little reliable information exists concerning an absolute value of the dynamic coefficient of friction. It is known that it varies with ice temperature and salinity, however, due to insufficient









data, accurate predictions of this variation is impossible. We can, however, use what data is available in order to arrive at a realistic representative value which we shall consider constant with temperature and salinity. This, of course, admits to some inherent error, however, such error is small enough not to materially effect our results. Section D-3 describes the reasoning involved in the selection of this representative value of  $f_D$  which was given for salt water ice as

$$f_D = 0.15$$

It must be recalled that the above assumption is based on dry salt water ice. If the ice is wet this coefficient of dynamic friction approaches zero as a limit and there is a marked increase in the value of  $\chi$  and  $z$  as shown by the dotted lines in figures 64 and 65. This fact is one of the principal arguments given by the proponents of the bow propeller who maintain that such a propeller can be used to keep the ice directly forward of the ship wet, hence increase the vessels breaking ability. For polar operation, however, the thickness of ice encountered and its hardness are such as to cause propeller damage which far outweighs the icebreaking advantage. Besides, when the normal polar breaker with no bow propeller rams the ice and then backs off at full power, sufficient backwash is generated so as to cause that ice surrounding the bow to become awash, hence partially achieving results similar to the bow propeller. Despite the benefit accruing from a reduced coefficient of friction, we shall consider only dry ice as the most severe condition and that which should be considered in the preliminary design.



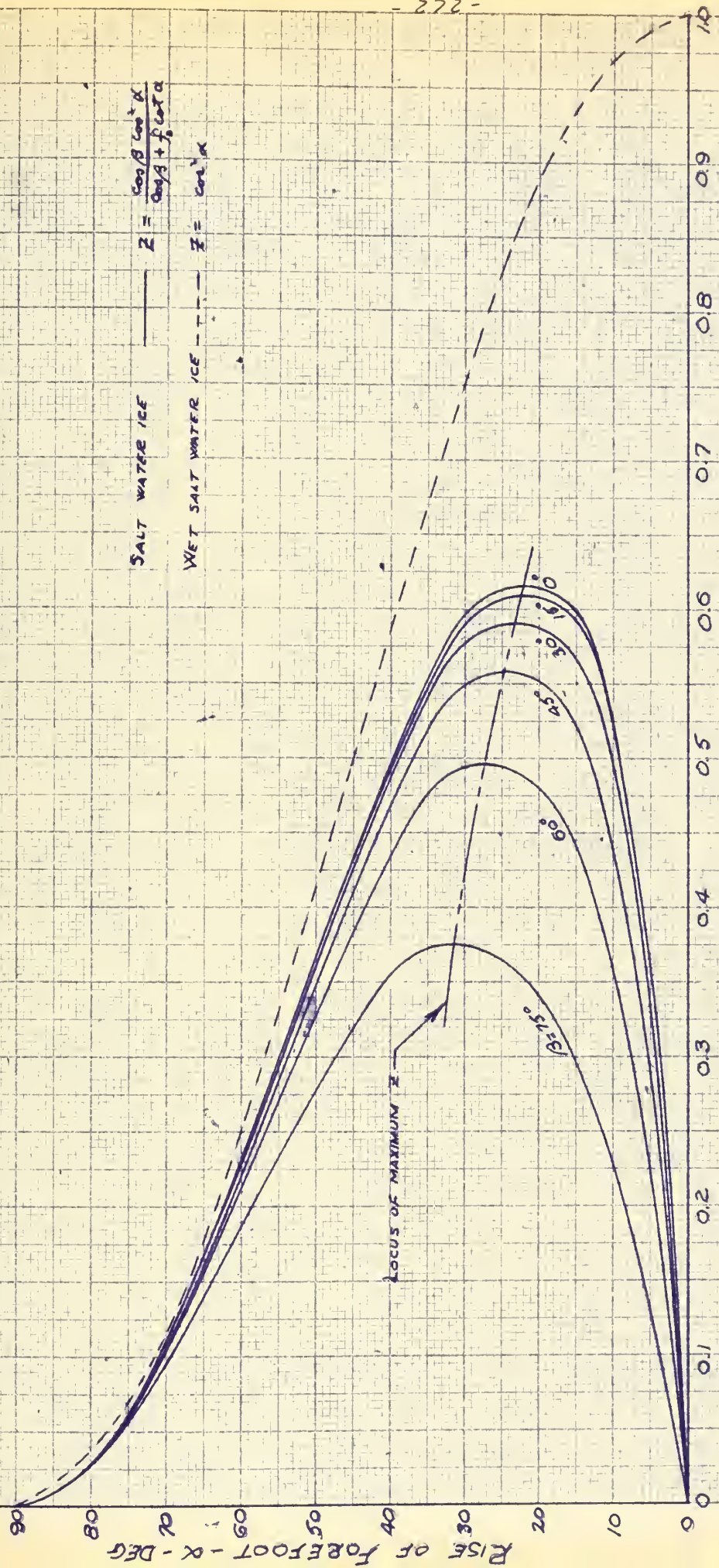


VARIATION OF  $Z$  AS A FUNCTION OF  $\alpha$

17

SALT WATER ICE  $Z = \frac{\cos \beta \cos^2 \alpha}{\cos \beta + f \cos \alpha}$

WET SALT WATER ICE  $Z = \cos^2 \alpha$



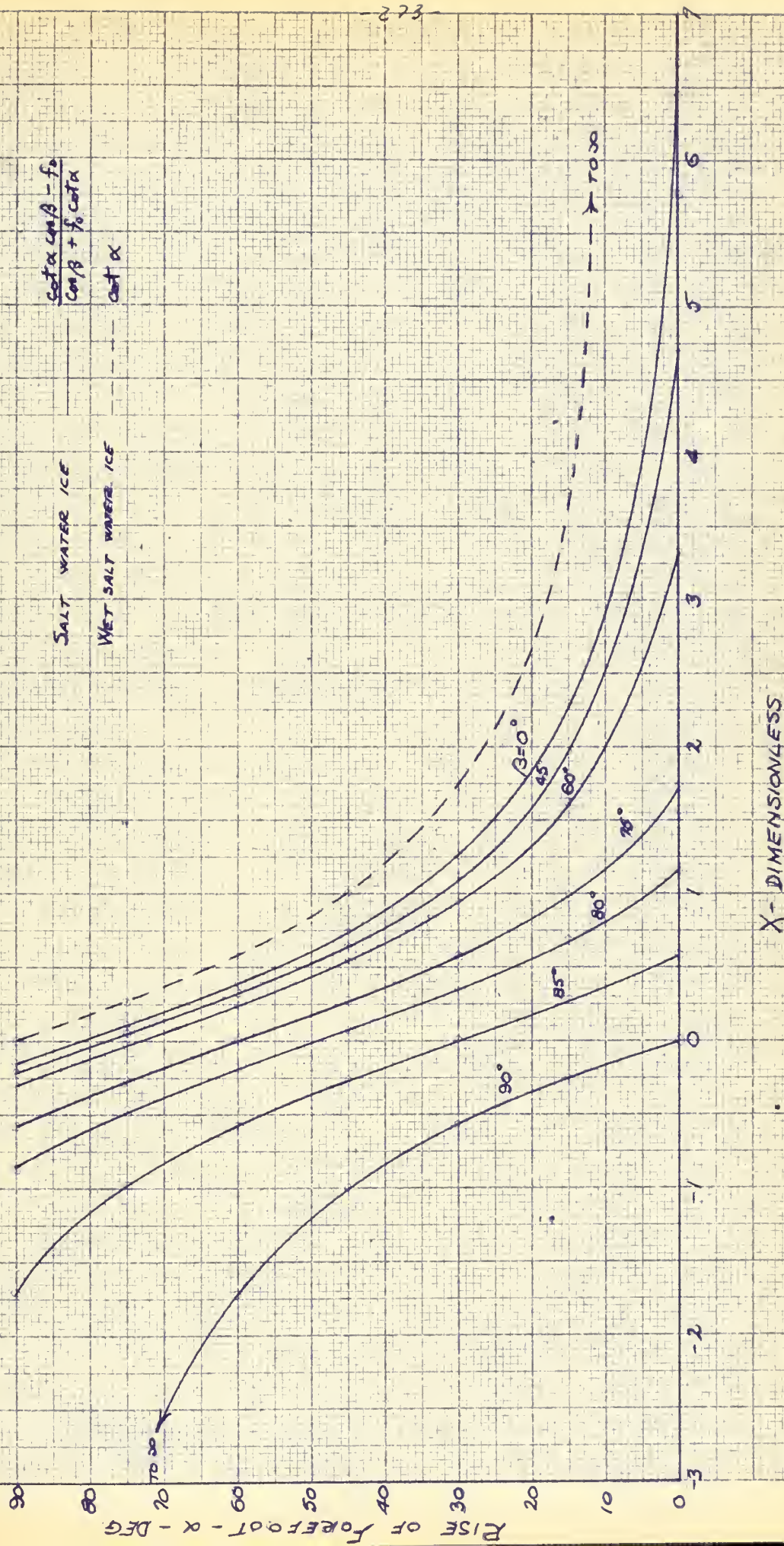
$Z$  - DIMENSIONLESS

FIG 64





- 223 -







DIMENSIONLESS QUANTITIES  $Z$  &  $X$  AS A  
FUNCTION OF RISE OF FOREFOOT -  $\alpha$   
AND BOW NORMAL ANGLE  $\beta$

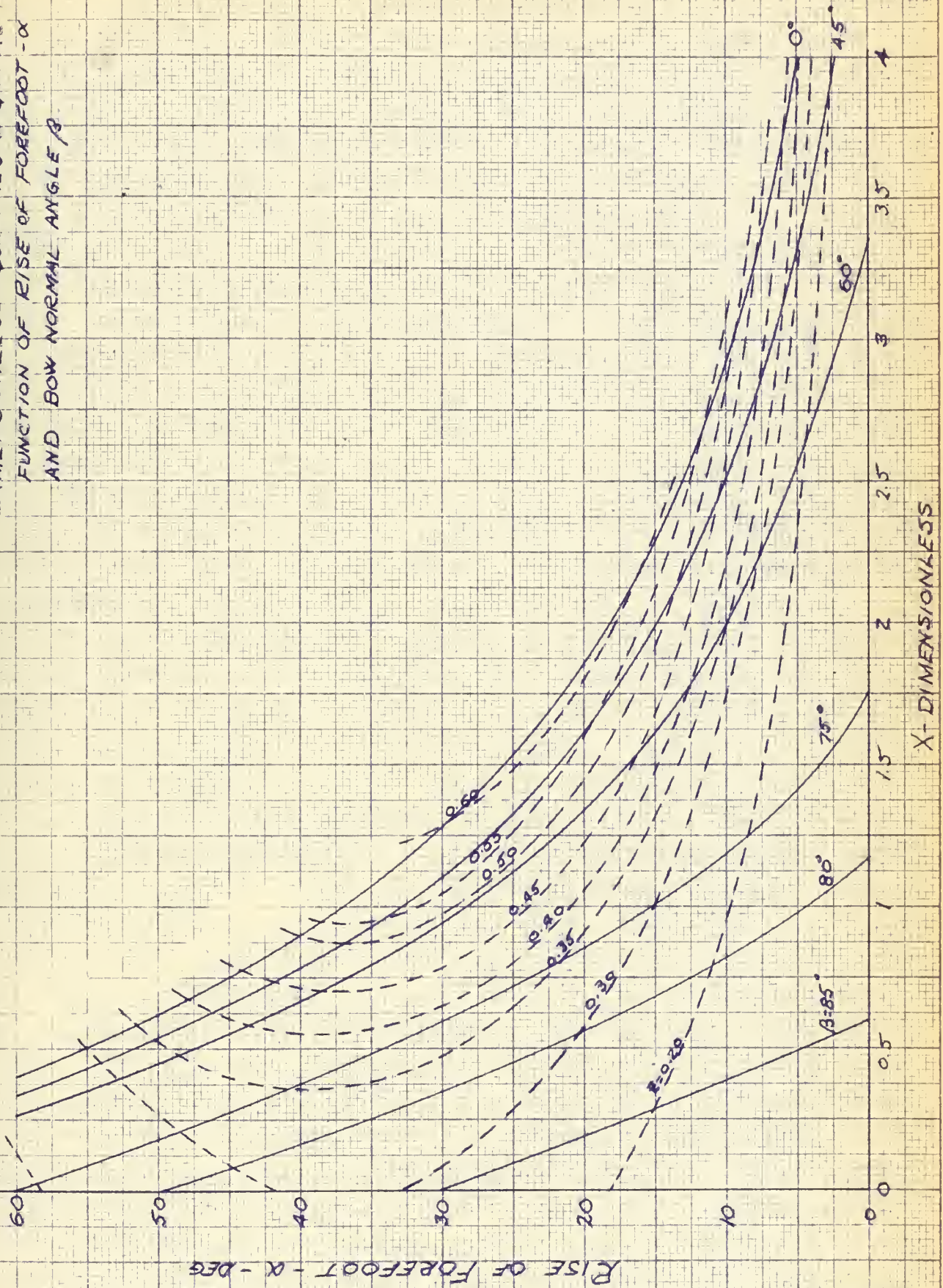


Fig 66



The angle  $\beta$  is a difficult one to consider in that it may have a wide range of values and still produce a reasonable and effective design. Since the value of  $\beta$  <sup>A</sup>ffects solely the friction force developed and since for minimum friction force  $\beta$  should be small, it would be advantageous to use as small a  $\beta$  in our design as possible. From an investigation of twenty five previous icebreakers we see that  $\beta$  has varied from  $39^\circ$  to about  $68^\circ$  over the years. Now the smaller the angle  $\beta$ , the more spoon shaped is the bow section and the greater the area over which the developed bow reaction force  $F$  must be distributed. In addition, experience shows that an excessive spoon shaped bow causes a rapid reduction of vessel forward energy when breaking ice due to the tendency of ice slabs to adhere to the bow and be pushed forward with the vessel. Hence a smaller flare angle at the bow or sharper stern would be desirable. This in essence means a larger value of  $\beta$ . This, however, is in conflict with the requirements of icebreaking force in that for maximum icebreaker effectiveness it would be desirable to have  $\chi$  and  $z$  as large as possible and from figures 64 and 65 we see that both  $\chi$  and  $z$  increase with decreasing  $\beta$ . Consequently, our selected value of  $\beta$  must be a compromise, and based on past operational experience of American breakers it would seem that a value of

$$\beta = 45^\circ$$

is an acceptable choice.

Based on our above value of  $\beta$ , we can proceed to select a value for the <sup>RISE</sup> use of forefoot  $\chi$  so as to give as large a value of  $\chi$  and  $z$  as possible so as to optimize icebreaker effectiveness. A review of figures 64 and 65 shows that these quantities are in opposition, i.e. as  $\chi$  increases  $z$  increases





to a maximum then begins to decrease while  $\lambda$  decreases continuously. As regards  $\lambda$ , therefore, the smaller the value of  $\lambda$  the better for our ice-breaking problem. However, there is a practical limit as to the minimum acceptable value of  $\lambda$ . If  $\lambda$  is very small and the vessel climbs up on to the ice but the ice does not break, the component of bow reaction force  $F$  acting normal to the ice surface will be a major portion of  $F$  hence causing a large friction force and an increased possibility of the vessel becoming beset. If  $\lambda$  is larger, the component of the vertical bow <sup>REACTION</sup> ~~reaction~~ force  $F$  normal to the ice surface is smaller giving a smaller friction force, and the component parallel to the stern is larger increasing the tendency of the vessel to retract. Hence, as regards  $\lambda$  our selection of  $\lambda$  must be a compromise. However, if we consider our expression for vertical bow reaction force  $F$ , i.e.

$$F = 0.91 \lambda T_0 + \sqrt{0.828 \lambda^2 T_0^2 + \frac{\omega^2 v^2 z}{AgH}}$$

we note that the expression  $\omega^2 v^2 z / AgH$  is very large as compared to either  $0.91 \lambda T_0$  or  $0.828 \lambda^2 T_0^2$ , therefore, in order to insure maximum  $F$  it would seem logical to select  $\lambda$  so as to make  $z$  a maximum even if such  $\lambda$  is not ideal as regards  $\lambda$ . From figure 64 we see that for  $\beta = 45^\circ$ , the  $\lambda$  for maximum  $z$  is

$$\lambda = 25^\circ$$

From figure 65 we see that for  $\beta = 45^\circ$  and for maximum  $z$  and the highest possible  $\lambda$  we should use an  $\lambda$  which is a little bit greater, say

$$\lambda = 26^\circ$$

Based on our selected values of  $\lambda$  and  $\beta$  we have





$$z = 0.557$$

$$x = 1.26$$

Hence our expression (88) becomes

$$w^2 = \frac{231H}{v^2} \left[ F^2 - 2.24 T_o F \right] \quad (89)$$

or

$$w = \frac{15.2}{v} \sqrt{F^2 H - 2.24 T_o F H} \quad (90)$$

If we use this expression in conjunction with those for vessel impact speed, i.e.

$$v = 3.1 \times T_o^{0.62} \quad \text{acceleration in open} \quad (63)$$

water

$$v = 1.12 \times T_o^{0.524} \quad \text{acceleration in ice} \quad (68)$$

clogged channel

we have two expressions which we may use for the determination of a preliminary estimate of vessel displacement.

Previously we stated that in order to commence a design study there were certain items of information which should be known. Among these are limiting draft or minimum vessel beam, thickness of ice desired to be capable of overcoming, mean air temperature for the proposed area of operation during the earliest month of planned ice penetration and possibly the desired design free route speed. Based on these known or estimated conditions we may proceed in our preliminary ship estimates.

Investigation of past and present icebreaker type vessels with twin stern



screws indicate that the maximum useable propeller diameter may be represented as a function of vessel draft or load waterline extreme beam. Figures 45 and 46 show a plot of these variations. Hence based on either known limiting draft or minimum desired load waterline beam we may select a reasonable value of propeller diameter. In addition, based on this known limiting draft or minimum load water line beam, we can, by means of figures 45 through 48 determine a first rough approximation of vessel length between perpendiculars and either vessel draft or extreme beam whichever was unknown above. It must be reiterated that these estimates of vessel length and beam are only rough approximations since with limiting draft fixed, the length and beam must reflect desired displacement so as to result in a reasonable block coefficient.

In section F-2 we discussed a propeller loading factor  $T_0/D^2$  which we said could be used to estimate the powering of a vessel. If we investigate past and present icebreakers we can determine a characteristic variation of  $T_0'/D^2/\text{SHAFT}$  as a function of vessel length. A plot of the variation <sup>was</sup> is shown as figure 50.

Based on our estimated vessel length we may select a reasonable propeller loading ratio and hence, estimate the ballard pull which we can reasonably expect under present and foreseeable future standards of icebreaker powering. Knowing the expected ballard pull per shaft and the approximate propeller diameter, we may, from figure 9 or 12 determine the shaft horsepower per shaft necessary to produce this propeller thrust and from figure 10 or 13 the shaft RPM necessary for its attainment. If on the other hand, the proposed installed shaft horsepower is known in the preliminary design stage, the above approach





may be reversed so as to employ figures 9 and 12 to more accurately determine the ballard pull which will be available. Note, however, that in either case, the estimated value of ballard pull will represent that obtainable from a Troost series propeller and must be modified as shown in section E-2 to account for the larger hub diameters and thicker blade sections normally used on icebreakers, i.e.

$$T_{ACTUAL} = K_1 K_2 T_{TROOST}$$

where

$K_1 = 0.97$	solid propeller
$= 0.86$	built up propeller
$K_2 = 0.885$	3 bladed propeller
$= 0.980$	4 bladed propeller

In order to determine the vertical bow reaction force which we must be capable of developing, we make use of the estimated mean air temperature in the probable area of vessel operation during the earliest month of expected penetration (table 1 and 2) and the desired thickness of ice which must be overcome. Based on this mean air temperature and assuming ice with no snow cover we may estimate the ice surface temperature with our expression (12). Knowing the ice surface temperature and ice thickness we can, from figures 36, 37, or 38, dependent upon type of ice involved, determine an estimate of the vertical bow reaction force F which we must develop.

If we assume that the vessel will accelerate through one ship length in ramming the ice, which is reasonable from practical experience, we can say that

$$S' = LBP$$



In addition, based on our representative design speed length ratio estimate for polar icebreakers we can estimate our vessel design free route speed as

$$V = 0.978 \sqrt{L} \text{ knots}$$

We now have reasonable estimates of our expected ballard pull ( $T_0$ ), vessel length (L), design draft (H), maximum DWL beam (B), design free route speed (V), vertical bow reaction (F) and vessel accelerating distance. Consequently, the only unknowns in expressions (90) and (63) or (68) are vessel displacement (W) and vessel impact speed ( $V$ ). If we first evaluate expression (90) for various assumed values of vessel impact speed, we can obtain a plot of displacement versus impact speed. If we then evaluate expression (68), as the most severe case, for the same assumed values of vessel impact speed we can determine a variation of  $X'$  with impact speed. Knowing the variation of  $X'$  we can determine the variation of vessel displacement with impact speed from our expression (67), i.e.

$$W = \frac{21.25 V^3}{F(X') T_0^{0.547}}$$

where  $F(X')$  is determined from figure 43 for our values of  $X'$ . The resulting variation of vessel displacement as a function of impact speed can also be plotted as before and where the two plots intersect we have a simultaneous solution for vessel displacement. This shall be our preliminary displacement estimate.

We should now correct our vessel length and beam approximations so as to reflect a reasonable block coefficient. Figure 67 presents a plot of prismatic coefficients as a function of speed length ratio and displacement length ratio. Based upon our first estimate of vessel length and displacement and our assumed





VARIATION OF  $C_p$  AS A FUNCTION OF  $V/\sqrt{L}$

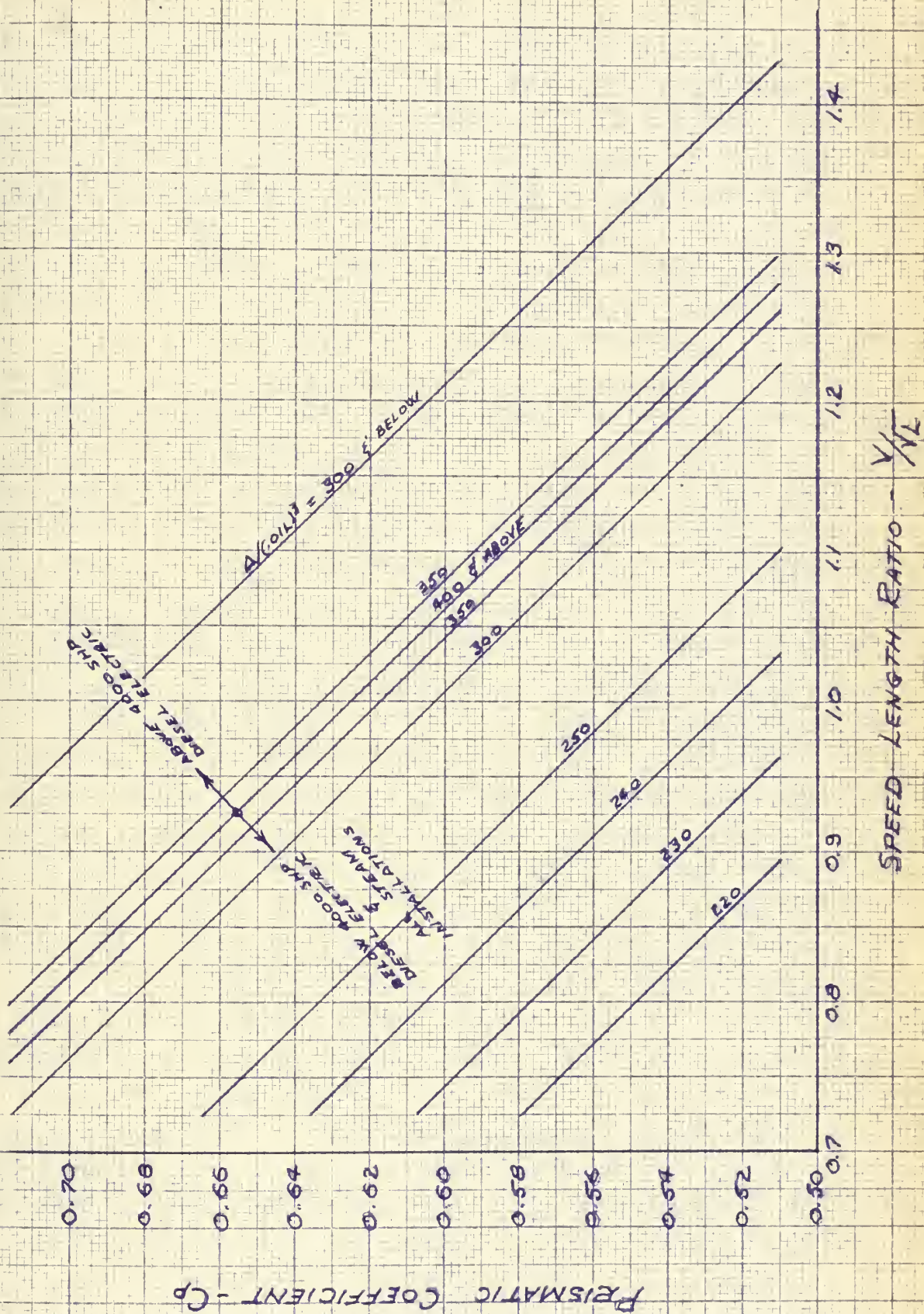


FIG. 67





average value of speed length ratio we may determine a reasonable  $C_p$  for our vessel. Figure 68 presents a plot of block coefficient as a function of speed length ratio and prismatic coefficient. Both figure 67 and 68 are representative of current icebreaker practice and suitable as a guide in the selection of a representative block coefficient. Since block coefficient

$$C_B = \frac{35 W}{L B H}$$

and since our vessel draft is fixed, we have

$$L/B = \frac{35 W}{C_B H}$$

But for the large polar icebreaker it is desirable that

$$L/B \approx 4.5$$

hence

$$L = 12.57 \sqrt{W/C_B H}$$

and

$$B = 0.2225 L$$

We now have corrected estimates of vessel length and maximum load waterline beam compatible with a reasonable block coefficient. Based on these second estimates of vessel length and beam we can re-evaluate our estimates of vessel powering and displacement, which in turn will allow a second estimate of prismatic and block coefficient. Convergence toward reasonable and compatible values of length, beam, powering, displacement, prismatic and block coefficient will be rapid and require only about two trial calculations as described above. The resulting values shall form our final preliminary estimates. In addition, since midship section coefficient

$$C_x = \frac{C_B}{C_p}$$

we can also, at this time, select a reasonable value of midship section coefficient either by direct application of our selected values of  $C_p$  and  $C_B$



VARIAION OF BLOCK COEFFICIENT

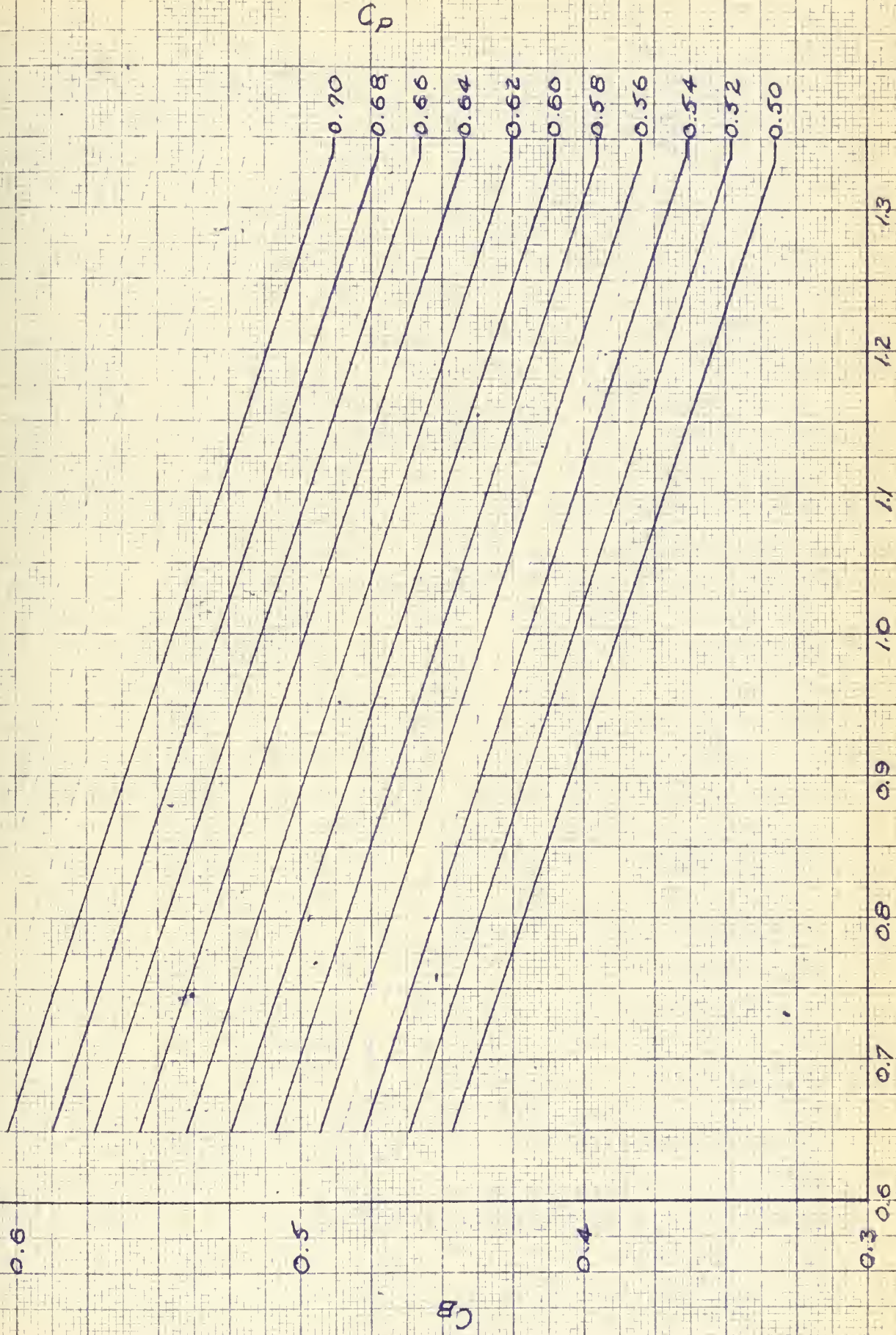
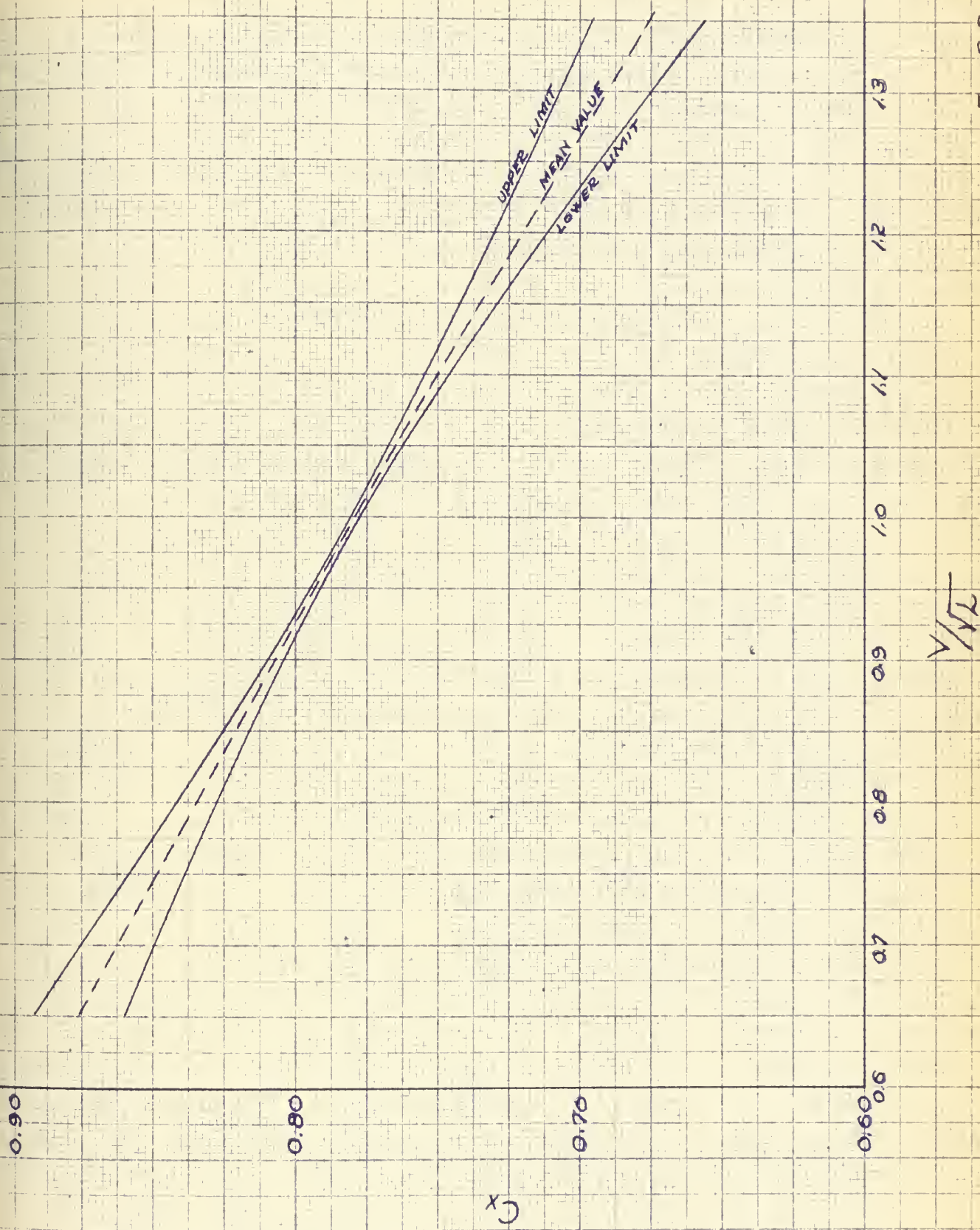


Fig 68





RANGE OF MIDSHIP SECTION COEFFICIENT



- 284 -



or by use of figure 69 which shows a variation of midship section coefficient as a function of speed length ratio.



## Part 2

### Transverse and Longitudinal Stability Evaluation

Icebreakers are normally vessels with extremely large beams. Consequently, they normally have large met<sup>A</sup>centric heights and resulting high intact stability. Because of this fact it is normal for the designer not to be too concerned with the problem of stability early in the design stages. Unfortunately, however, adequate stability may not be assumed solely by virtue of a high initial met<sup>A</sup>centric height.

Icebreaking operations are such as to make a large initial met<sup>A</sup>centric height desirable so as to insure adequate stability under all operating conditions. Probably the most serious instance in which transverse stability may be jeopardized is when the vessel has completed a charge at the ice resulting in her bow being raised a considerable distance out of the <sup>WATER</sup>crater on to the ice. Such a situation is made even more serious if there is considerable iced top *hAMPER*.

Consequently, it would seem desirable to be able to investigate this problem of stability early in the design stages while vessel characteristics and parameters are still in a state of flux. Let us, therefore, <sup>first</sup> ~~just~~ consider the initial transverse and longitudinal stability of the vessel after which we can investigate the effect upon this stability of the icebreaking process.

The height of the center of buoyancy above the baseline can be easily, and quite accurately, estimated for the icebreaking type vessel by the well known expression

$$KB = \frac{c_w}{c_B + c_w} (H) \quad (128)$$





where all coefficients are, as throughout the paper, based on length between perpendiculars. Earlier in the paper we presented methods and graphical aids for the determination of first approximations of vessel displacement, length, maximum load waterline beam, draft, prismatic coefficient and block coefficient. In order to determine a reasonable value of waterplane coefficient to use in our above expression we make use of figure 70 which shows a variation of waterplane coefficient as a function of prismatic coefficient. Again, the values plotted are very typical of current and past icebreaker design practice.

The transverse metacentric radius or height of met<sup>A</sup>center above center of buoyancy may be given as

$$BM_t = \frac{I}{V} = \frac{C_{it} LB^3}{C_B LBH} = \frac{C_{it} B}{C_B H} \quad (129)$$

where  $C_{it}$  is the transverse inertia coefficient. An investigation of icebreaker type vessels indicate that the transverse inertia coefficient can be expressed as a function of load waterplane coefficient. The results are shown in figure 71 .

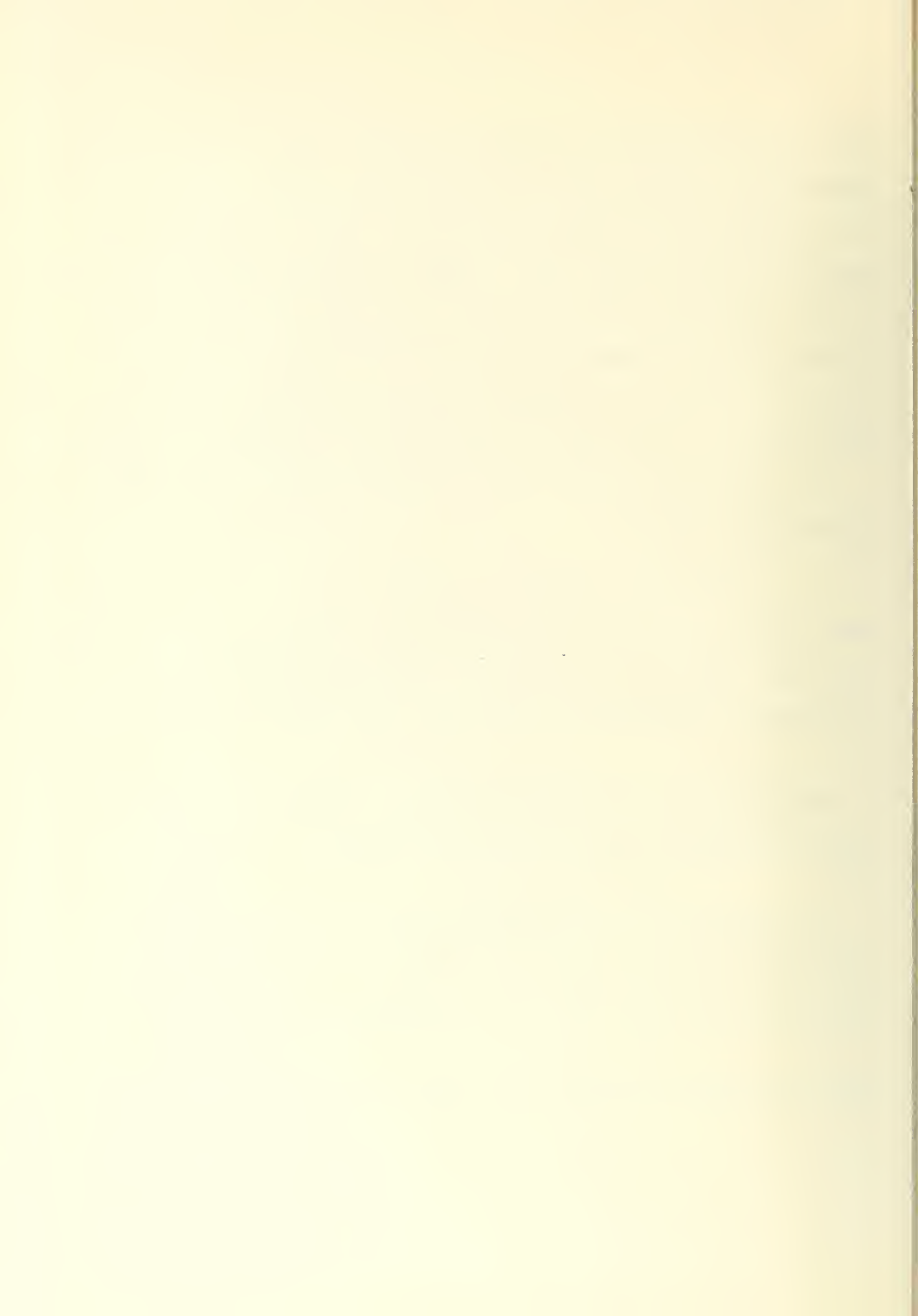
We now have all the information necessary to estimate the location of transverse met<sup>A</sup>center from (128) and (129). Therefore

$$KM_t = KB + BM_t$$

In a similar manner we can examine longitudinal stability. Since the vertical distance from the baseline to the center of buoyancy in the longitudinal direction is equal to that in the transverse direction we have

$$KM_L = KB + BM_L$$

where  $KB$  is given by expression (128). The longitudinal met<sup>A</sup>centric radius



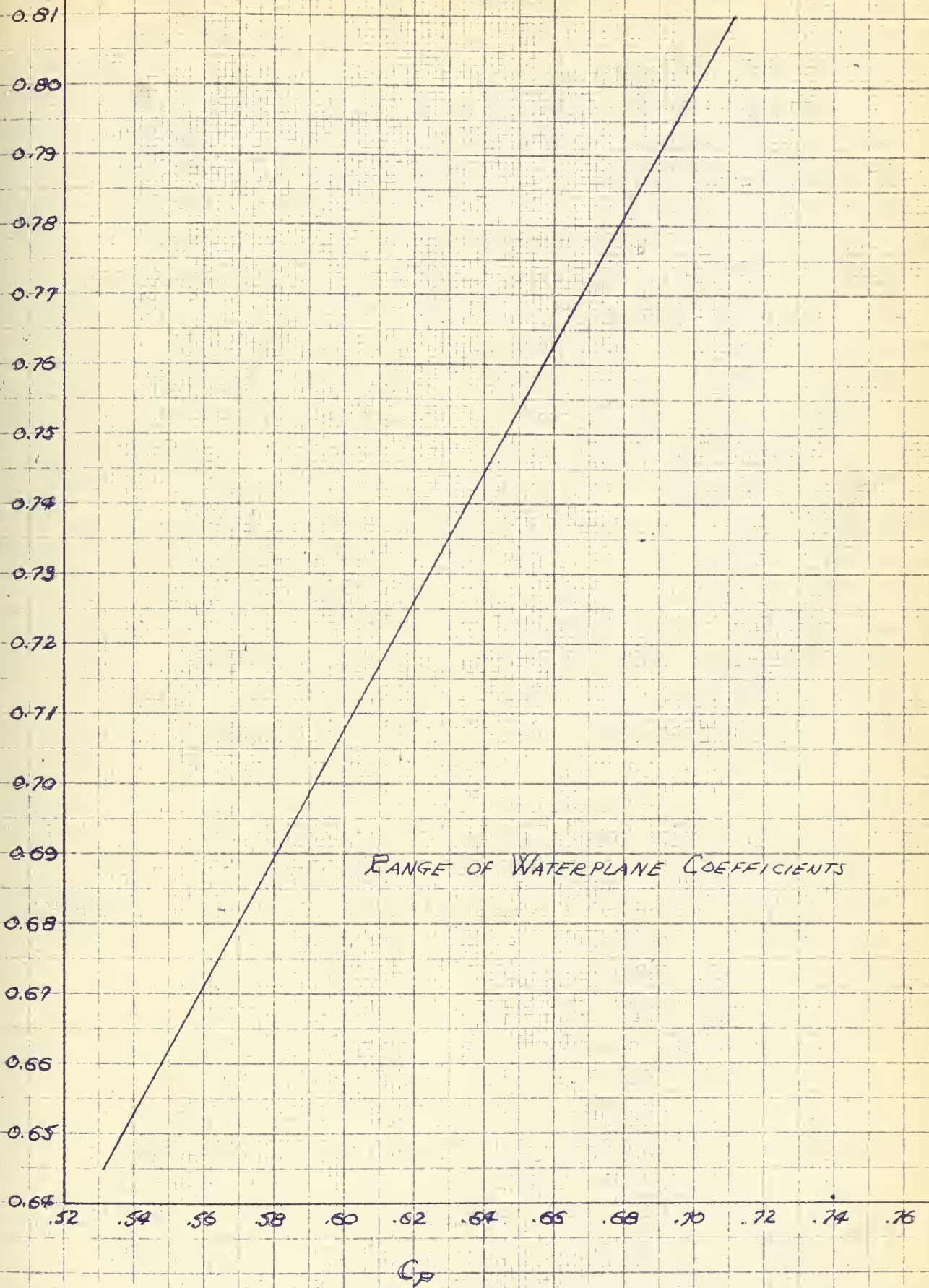


FIG 70





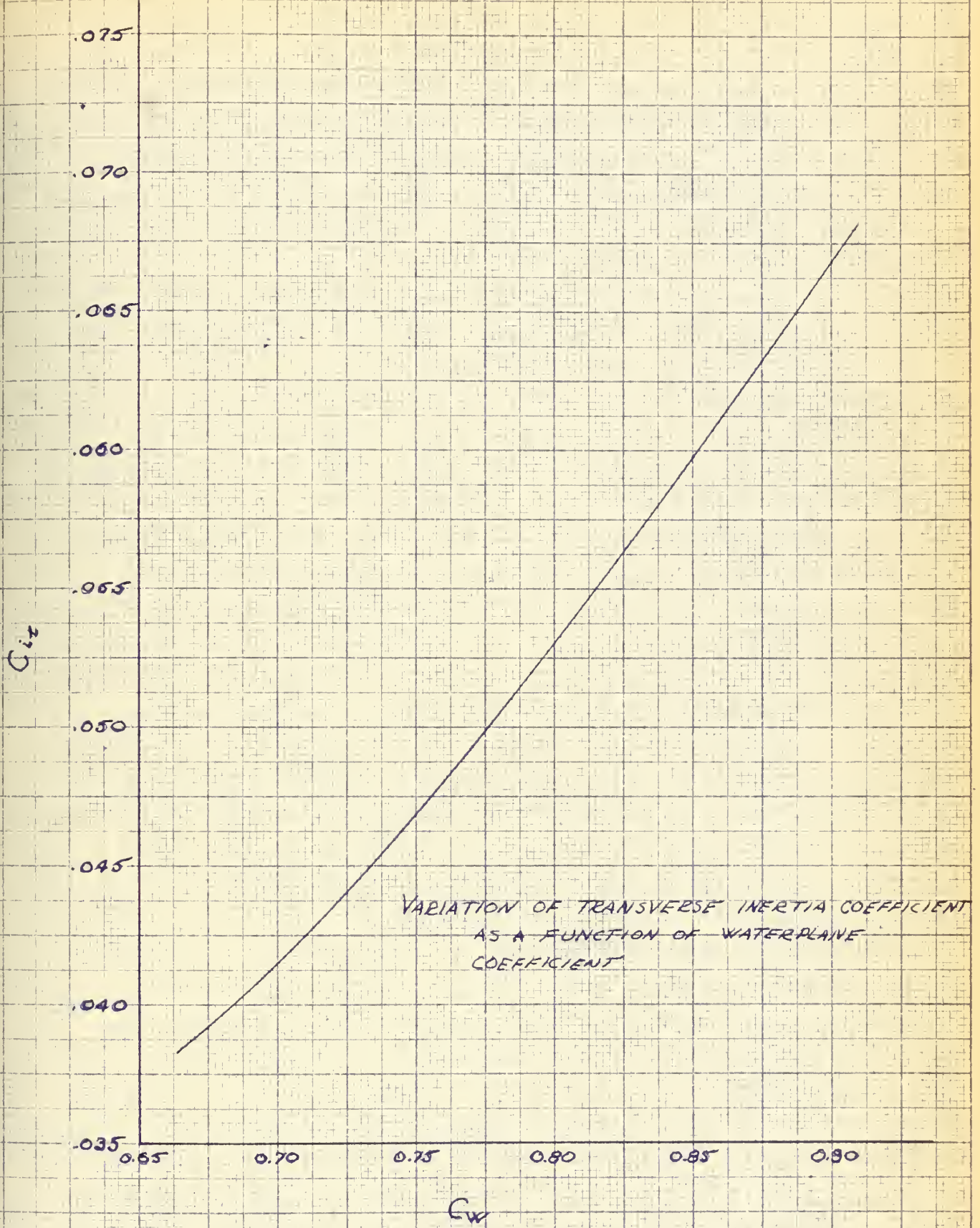


FIG 71



or height of met<sup>A</sup>center above center of buoyancy is given as

$$Bm_L = \frac{I_L}{V} = \frac{C_{iL} \delta L^3}{C_{\delta} L B H} = \frac{C_{iL} L^2}{C_{\delta} H} \quad (130)$$

where  $C_{iL}$  is the longitudinal inertia coefficient. An investigation similar to that conducted for the transverse condition reveals that the longitudinal inertia coefficient may also be expressed as a function of load water-plane coefficient. The results for the icebreaking type vessel are shown in figure 72. Hence in a manner similar to that used in the case of transverse stability we may with reasonable accuracy determine the location of longitudinal met<sup>A</sup>center. For this longitudinal case there is one qualification we can make. In icebreaker type vessels the vertical height of center of gravity varies from about 0.95 to 1.2 times the full load draft, therefore, we may assume that the center of gravity is at the load waterline and say that

$$Gm_L = LB + Bm_L - H$$

Having estimated the position of longitudinal and transverse met<sup>A</sup>center from the principal dimension and form characteristics of the vessel in the full load or design draft condition, it would be desirable now to be able to predict the effect on stability of typical operating conditions. When operating in an icefield the ice conditions are often such as to require the vessel to overcome the ice by ramming. When an icebreaking vessel rams solid ice of considerable thickness the kinetic energy of the vessel in conjunction with the developed propeller thrust act to force the vessel up on to the ice due to the inclined stern. This act of climbing on to the ice results in a reduction of vessel draft and a change in vessel ~~turn~~.

trim





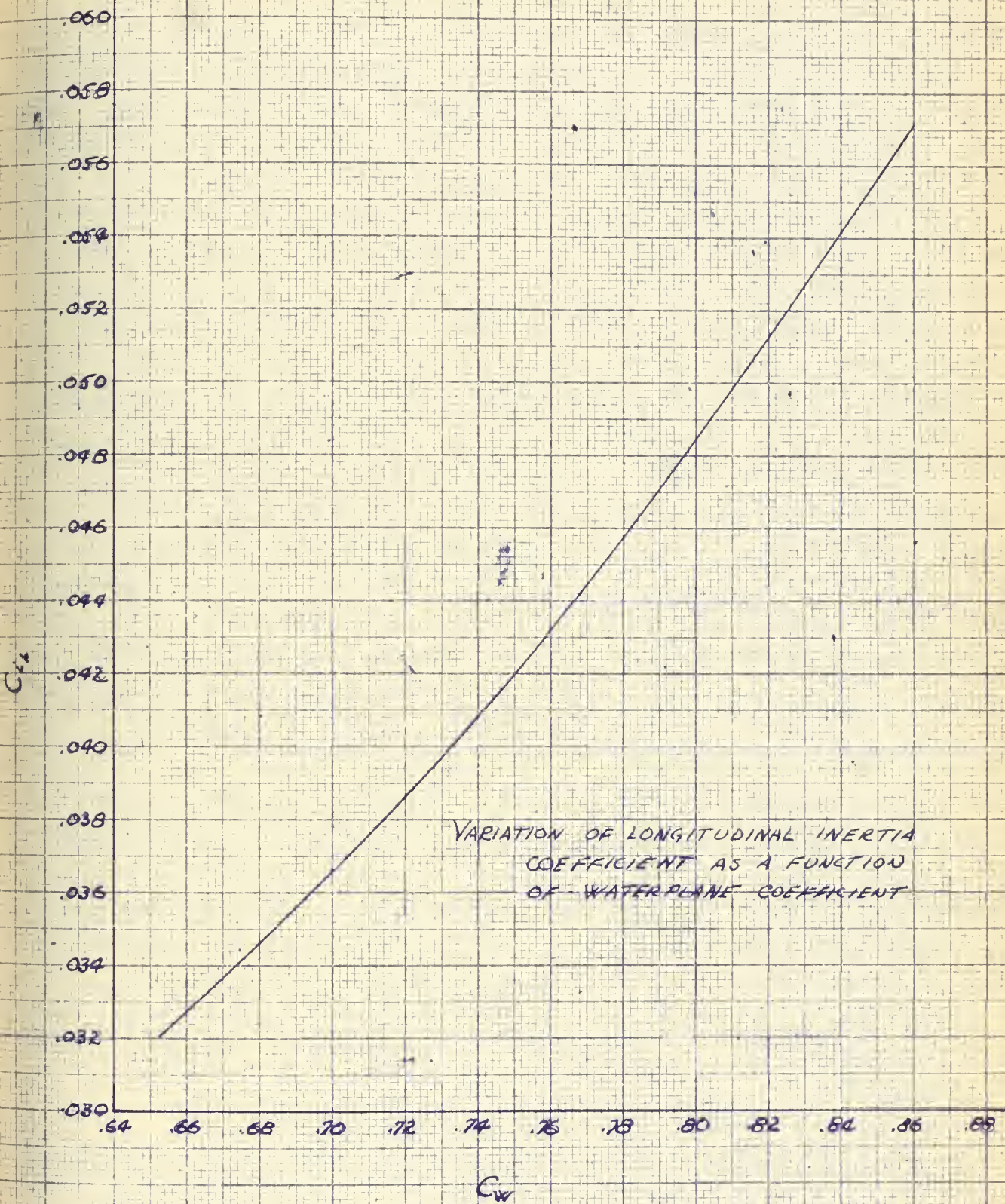


FIG 72





If we consider the transverse stability first we can see that this change of draft may materially reduce the vessels stability due to a reduction in height of met<sup>c</sup>center. In addition, since the vessels stem is sitting on the ice shelf exerting a vertical force  $F$ , stability is still further reduced due to the virtual rise in  $KG$  caused by the partial vessel support by the ice sheet. This later consideration is similar to that encountered in drydocking a vessel with trim. The effect of change in vessel trim can normally be neglected if the trim is not excessive (more than about 1% of the length). However, even in those instances where the trim does exceed the above limits due to the vessel riding up onto the ice, the vessel will be trimmed by the stern and due to vessel shape the effect will be to increase  $KM$ . Consequently, we can normally ignore the effect of trim and consider as the more severe case only the effect of change in vessel draft and grounding of the stem. As regards the effect of this vessel motion on longitudinal stability we may state that the distance from the keel or baseline to the longitudinal met<sup>c</sup>center is normally so large that any effect due to a change in vessel draft or vessel trim will be quite small and insignificant. Hence, we can safely ignore the longitudinal consideration so long as we have insured that the intact longitudinal met<sup>c</sup>centric radius is adequate.

In considering the effect of change in vessel draft on the transverse stability it is useful to consider the concept of vertical prismatic coefficient for the representation of vertical distribution of displacement. This is given

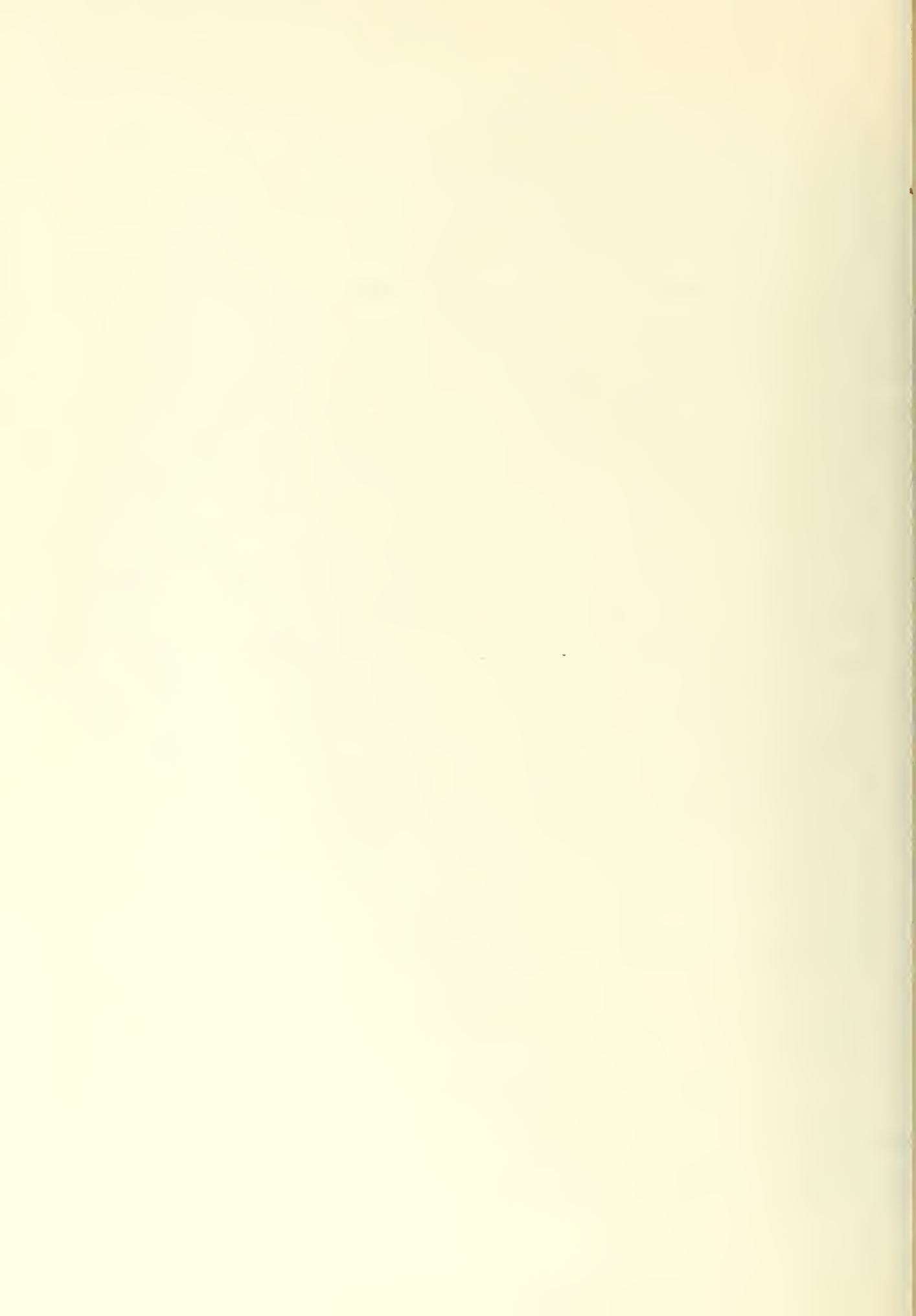
as

$$C_v = C_b / C_w$$

and has been indirectly employed in our expression

$$KB = \frac{C_w}{C_b + C_w} (H) = \frac{1}{C_v + 1} (H) \quad (128)$$

Since both block coefficient and waterplane coefficient vary by the same factor with changing drafts for the normal type vessel, we may justifiably assume that



vertical prismatic coefficient remains constant with draft. In order to determine the ordinary range of values of vertical prismatic coefficient for ice-breaker type vessels an investigation was made of past and present vessels. The results of this investigation are shown in figure 73 wherein vertical prismatic coefficients are plotted as a function of full load prismatic coefficients and vessel length between perpendiculars. Consequently, we see that by using expression (128) and the vertical prismatic concept which is constant with draft we may determine the vertical center of buoyancy at any draft.

In section F-2 we showed that the change in vessel draft due to riding up on to the ice could be approximated as

$$\Delta d = \frac{35F}{A_w} \quad f \quad (131)$$

where  $A_w$  is the waterplane area at full load condition. Here the assumption was made that change in vessel draft would be small (less than 10%) hence the waterplane properties would not be materially effected. This is not really true since waterplane area will vary. The use of (131), however, will not lead to too serious an error in  $\Delta d$  but if greater accuracy is required we can improve our approximation.

There have been a considerable number of attempts to investigate the variation of form characteristics with varying draft but the most consistent and simple to apply seem to be those published by Dyer in his The Draft-Displacement Curves and their Derivitives wherein he formulates

$$\frac{w}{w_i} = \left( \frac{H}{H_i} \right)^{\frac{1}{C_v}} \quad (132)$$

and

$$\frac{C_B}{C_{B_i}} = \frac{C_w}{C_{w_i}} = \frac{A_w}{A_{w_i}} = \left( \frac{H}{H_i} \right)^{\frac{1-C_v}{C_v}} \quad (133)$$





VERTICAL PRISMATIC COEFFICIENT -  $C_v$

RANGE OF VERTICAL PRISMATIC COEFFICIENT

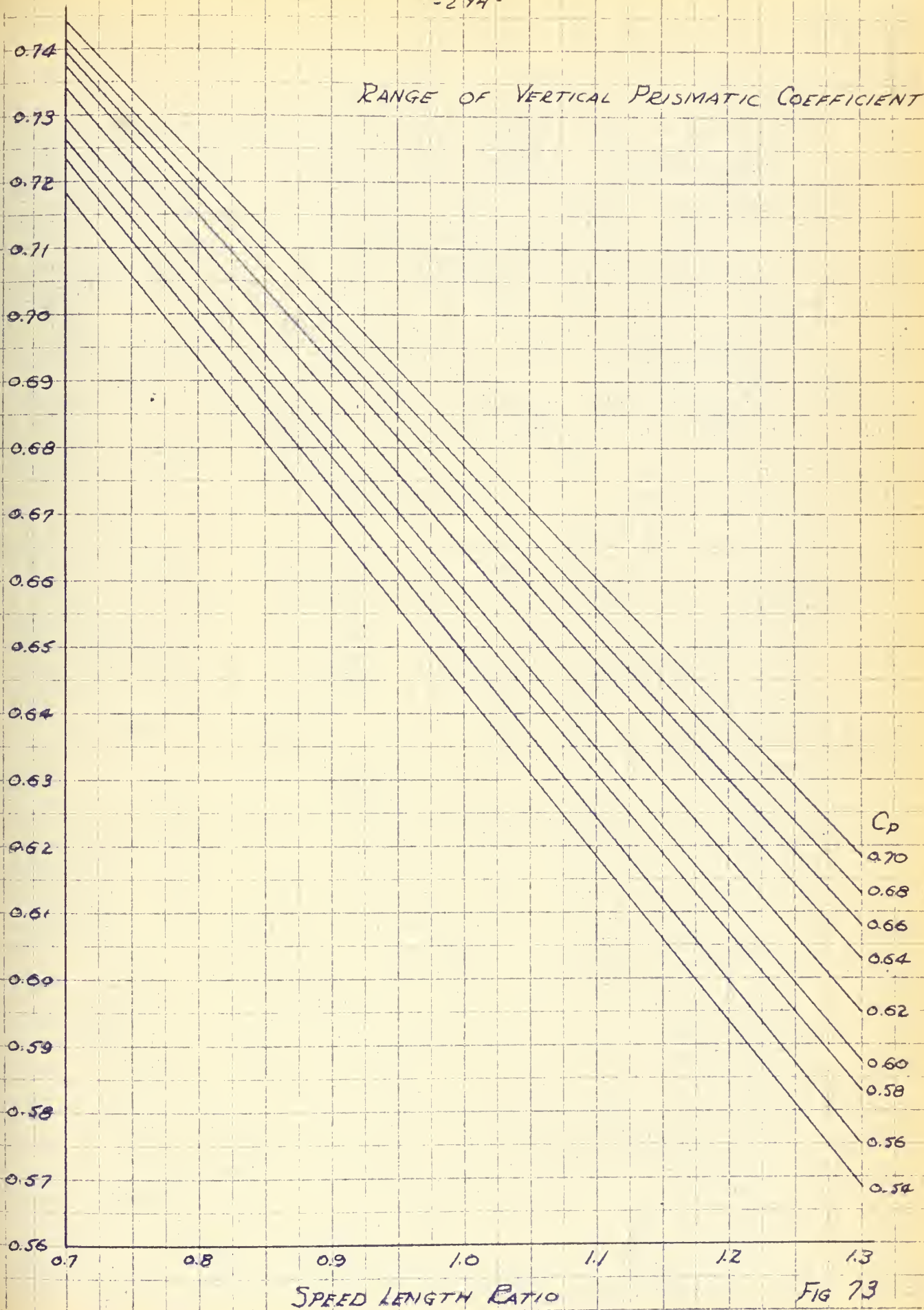


FIG 73



where the subscript one refers to any intermediate draft as distinguished from the full load or design draft. Consequently, in order to improve our estimate of  $\Delta d$  we can use the expression as given in (131) as our first estimate to determine

$$H_1 = H - \Delta d \quad (134)$$

Based on this first estimate draft  $H_1$ , we can determine the final water-plane area,  $A_{w_1}$ , for this draft by use of (133). Then we can correct (131) to get a more accurate estimate of change in draft as

$$\Delta d_1 = \frac{70F}{A_w + A_{w_1}}$$

$$H_2 = H - \Delta d_1 \quad (135)$$

This process can be repeated until the desired accuracy is achieved, however, for most instances in the preliminary design study it is sufficient to use either (131) or (135) to estimate the change in vessel draft.

We must next consider the effect of this change in vessel draft upon

$$B M_t = \frac{C_{L_t} B^3}{C_B H} \quad (129)$$

This is not as easily done since we cannot predict the variation in vessel beam with draft. We can, however, circumvent this difficulty. Let us consider the expression for  $K M_t$ , i.e.

$$K M_t = K B + B M_t$$

$$= \frac{1}{C_V + 1} (H) + \frac{C_{L_t} B^3}{C_B H}$$

If we divide through by vessel draft this becomes

$$\frac{K M_t}{H} = \frac{1}{C_V + 1} + \frac{C_{L_t}}{C_B} \left( \frac{B}{H} \right)^3 \quad (136)$$



Since the flare at side for a normal icebreaker type vessel is carried well above the normal full load or design draft, vessel beam will decrease with decreased draft. Consequently, the beam to draft ratio will remain approximately constant. We may, therefore, justifiably assume that the beam to draft ratio is constant with draft for the range of drafts in which we are interested. Hence in (136) above, since  $C_v$  is also constant with draft, transverse inertia coefficient and block coefficient are the only variables we must consider as functions of changing draft. From expression (133) we may determine  $C_w$  for our new draft and from figure 71 the transverse inertia coefficient  $C_{1t}$  corresponding to this new waterplane coefficient. Expression (133) will also allow us to estimate the block coefficient at our new draft. Consequently, we have

$$\frac{km_{t_2}}{H_2} = \frac{1}{C_v + 1} + \frac{C_{1t_2}}{C_{B_2}} \left( \frac{B}{H} \right)^2 \quad (137)$$

where  $B/H$  and  $C_v$  are constant and evaluated at the full load draft and items with the subscript two refer to evaluation at the new draft  $H_2 = H - \Delta d$ . Hence, we can estimate the height of transverse met<sup>A</sup>center at our new draft,  $km_{t_2}$ , and reasonably predict the effect of draft reduction upon met<sup>A</sup>centric radius.

When the vessel sits with its bow on the ice shelf, part of the vessel weight is borne by the ice sheet and part of it is water borne.





That portion of vessel weight (equal to the vertical bow reaction force  $F$ ) supported by the ice sheet effects stability in a manner similar to the removal of a weight of magnitude  $F$  from the point of contact between the vessel and the ice sheet. Because of this, there will be a rise in the vertical center of gravity. This virtual height of center of gravity may be expressed as

$$K G_{T_v} = \frac{W \cdot K G - F H_2}{W - F}$$

where it is assumed that the average height of the point of contact of the stem and ice sheet is  $H_2$  and  $K G$  refers to the intact height of center of gravity at full load of design draft. Therefore, the virtual metac<sup>A</sup>centric height of the vessel as it sits on the ice sheet is

$$G M_v = K M_{t_2} - K G_{T_v}$$

By the above described methods we have been able to predict the effect of the icebreaker ramming process upon stability during the early stages of design. We have considered this ramming and climbing up onto the ice as the most serious operational evolution which could materially effect vessel intact stability. However, we must realize that our approach was idealized, ~~in that it~~



~~considered the vessel center of gravity fixed.~~ In actual vessel operation in arctic or antarctic waters there will often be the perplexing and serious problem of topside iceing. The presence of such ice on the upper reaches of the ship can be extremely serious and especially when breaking ice by ramming. The possible reduction in transverse metac<sup>A</sup>entric radius when the vessel rides up on to the ice in conjunction with the often serious rise in vessel center of gravity due to top side ice can act to produce a dangerous reduction in vessel transverse stability. It is impossible to predict the actual quantitative effect of this topside ice upon stability since the amount formed and its location above the main deck is so definitely a function of unpredictable weather and sea conditions as well as the amount of spray which is being taken by the vessel. Since this iced top <sup>hampers</sup> can have such serious effect upon vessel intact stability it must be considered by the designer of an ice-breaking type vessel, and he must insure that his vessel has sufficient intact stability so as to be able to withstand the substantial <sup>rise</sup> ~~use~~ in vessel center of gravity caused by topside ice. Invariably, the prudent ship operator will attempt to keep this ice formation to a minimum, however, it may not be assumed since weather and sea conditions may often make this topside ice removal too hazardous or impossible to accomplish. Consequently, it behooves the ship designer to assume the probable presence of this topside ice and provide adequate intact stability to withstand it.

One other item which will effect ship stability and which should be considered early in the design stage is the question of vessel depth or freeboard. The selection of a proper freeboard for the vessel will greatly contribute to





its performance both in an ice field and in the open sea.

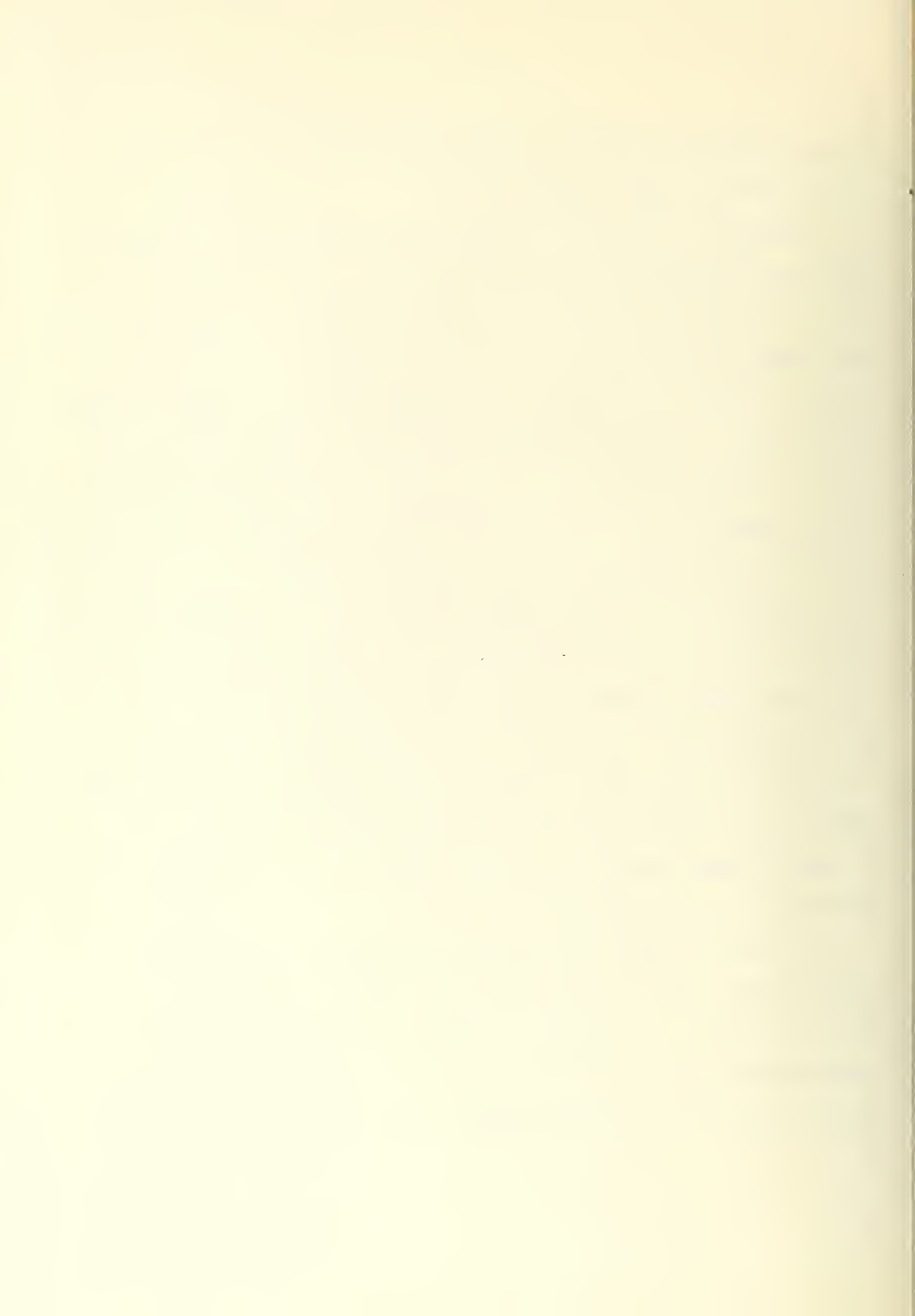
Since icebreakers are normally such short fat ships with near round bottoms, they are invariably bad performers in a heavy sea. Their reputation for heavy rolling is well known and in any type of a head sea they pitch quite violently. Many types of ships which pitch badly are provided with a high freeboard at the bow plus a steeply rising sheer and strongly flared sections so as to help keep solid green water off the deck in heavy weather. Icebreakers could well use such a configuration of bow, especially so when in the higher or polar latitudes where air temperatures are low and spray coming over the bow causes serious ice formation on the topside structure. Several disadvantages to such a bow configuration have, however, been raised in the past. The steeply rising sheer makes it difficult for men to keep their footing when the main deck forward is iced over and, consequently, makes ice removal or handling of ground tackle difficult and dangerous in polar regions. It is possible, by use of a raised forecastle deck to provide necessary freeboard forward and yet eliminates all, or about all, sheer. The use of this large freeboard forward, whether in the form of a raised forecastle deck or steep deck sheer, will, to some extent, hamper the conning officers view of the ice just forward of the bow. Some designers raise serious objection to such a restriction of vision, however, it is felt that any such restriction of vision will not be severe and that the bridge deck is normally high enough above the water to provide the conning officer with as much freedom of forward vision as he need have or even desires to have. The very slight reduction in visible area forward caused by a raised forecastle deck



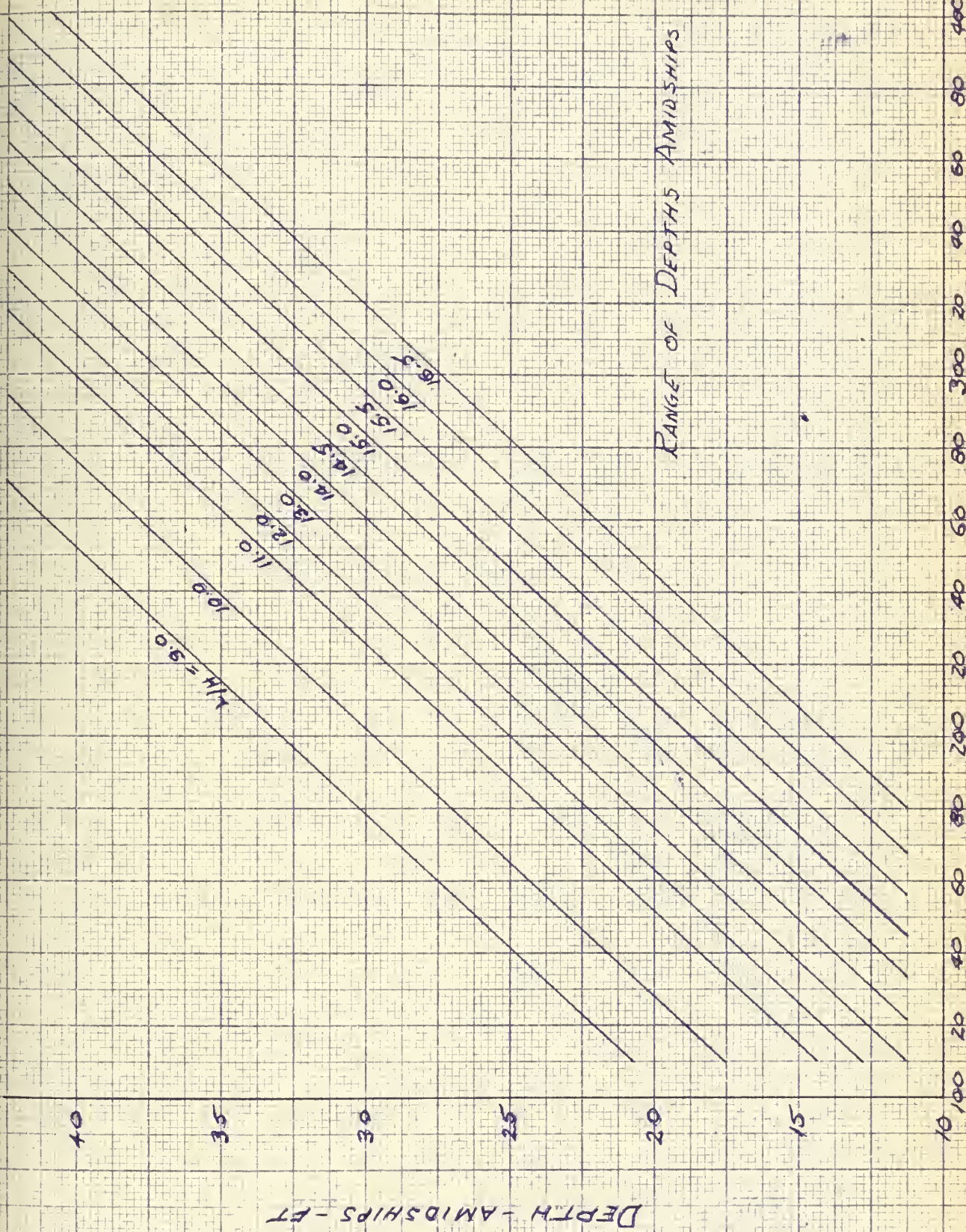
or high freeboard is certainly negligible when compared to the seriousness of heavy topside iceing forward.

As mentioned previously, icebreakers roll fantastically. In heavy seas a  $30^{\circ}$  roll is commonplace, a  $40^{\circ}$  roll not unusual and  $50^{\circ}$  or more not unheard of. In such situations, the danger to intact transverse stability due to deck edge immersion must be realized. It would be beneficial, therefore, if as generous a freeboard as is possible be provided over the midships half length. In this regard it might be beneficial or desirable to combine the need for generous freeboard forward as well as amidships and provide for a completely enclosed damage control or main deck to extend aft to about the after quarter point. This would provide adequately generous freeboard and, in addition, since the covered main or damage control deck is that for which floodable length is computed, it would be feasible to provide for continuous fore and aft inside passage ways so that personnel need not traverse weather decks during heavy weather. In the selection of vessel depth amidships, figure 24 can serve as a useful guide. It shows the representative variation of depth amidships as a function of length between perpendiculars for varying ratios of length between perpendiculars to draft. The variation shown is typical of present day icebreaker practice.

The choice of freeboard at the stern is again influenced by stability considerations. When a vessel breaks ice by ramming and her bow climbs up on to the ice there is a tendency for the stern to depress. If the deck becomes awash due to this change in vessel trim then the transverse metacentric height will be materially reduced. This will aggravate the loss of







RANGE OF DEPTHS AMIDSHIPS

FIG 74





metac<sup>A</sup>centric height already incurred due to change in vessel draft when riding up on to the ice and intact transverse stability could be endangered. It is desirable, therefore, to provide sufficient freeboard aft to keep the deck from becoming awash when the vessel experiences a change in *TRIM* defined by the angular change of Section F-2, i.e.

$$\Delta \phi = \frac{FS}{\omega GM_2}$$

In order to estimate the value of  $\mathcal{S}$ , the distance from the intersection of stern and load waterline and the longitudinal center of flotation, we can say that

$$\mathcal{S} = \frac{LBP}{2} + M$$

where  $M$  = distance from amidships to longitudinal center of flotation with aft positive and forward negative. Figure 75 shows the variation of  $M$  for icebreaking type vessels as a function of waterplane coefficient. For values of  $C_w < 0.715$  we may assume that  $M = 0$  with negligible introduced error.

In summation, therefore, the effects of freeboard are increased vessel weight, rise in vessel center of gravity and increased lateral plane area. Weight is no problem in an icebreaker, in fact, it is in a way desirable so as to increase ice breaking effectiveness. As regards vertical center of gravity, it is true it will rise but the transverse metac<sup>A</sup>centric height of an icebreaker is normally very large and some slight reduction due to an increased  $KG$  can be tolerated and probably absorbed without noticeable ill effect. Since winds in the polar regions are very strong, the increased lateral plane area will cause increased wind resistance to motion. How serious an increase



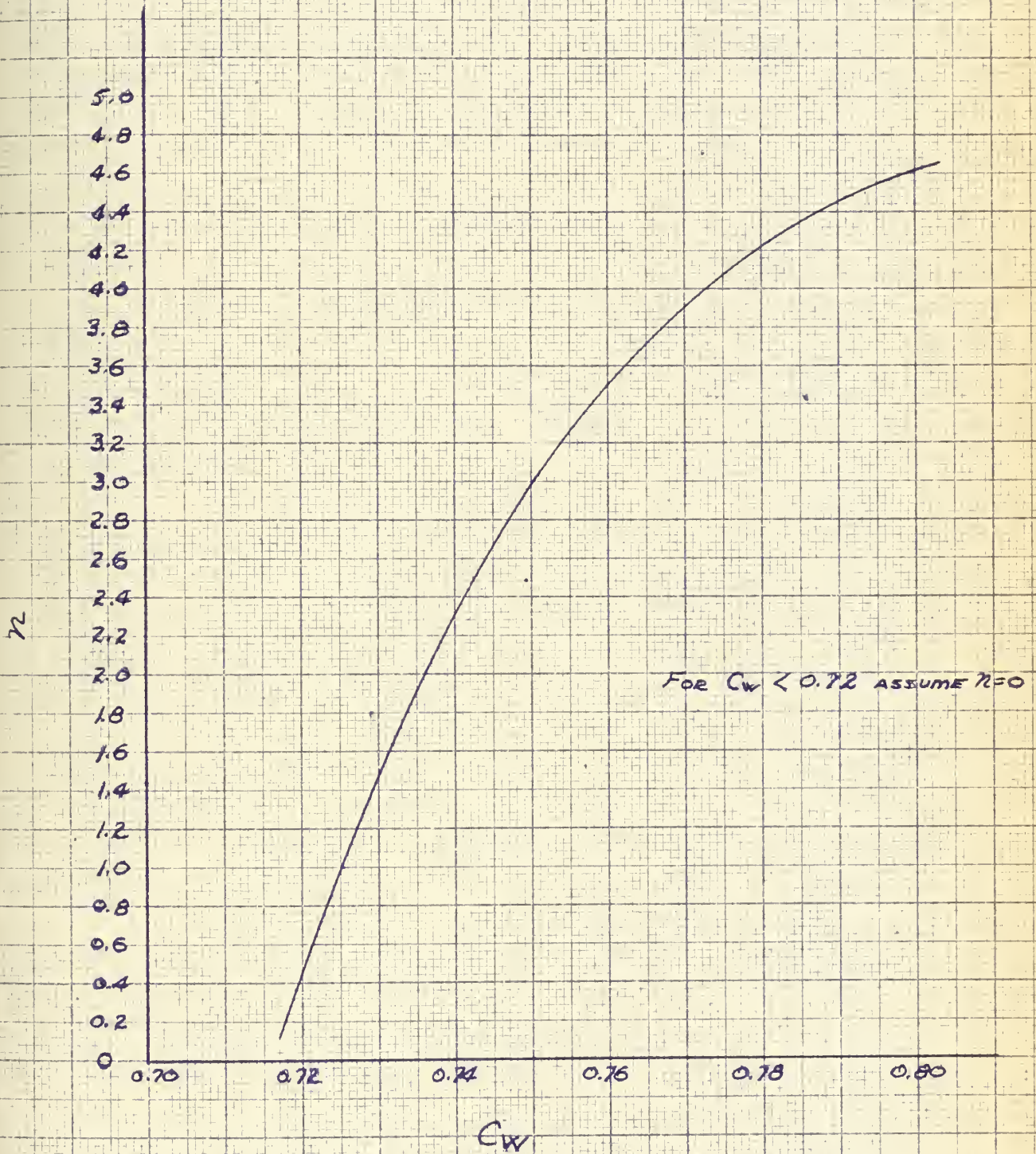


FIG 75





is difficult to predict but it is doubtful if the magnitude will be such as to cause serious effects upon vessel acceleration ability. This increased lateral plane area could also cause a slight effect upon vessel directional stability or course keeping ability due to wind action. However, since ice-breakers are usually such deep drafted vessels, the noticeable effects should be negligible.



### Part 3

#### Illustrative Example of Methods

##### A. Preliminary Design Estimates

Consider an icebreaking vessel to be built for polar service whose primary area of operation is to be the Antarctic with possible alternate summer deployment in the Arctic. The vessel is to be a first line breaker capable of early independent penetration of the pack ice under normal ice conditions during the month of October in the Kanian Bay, Little America area.

Based on a study of the probable areas of vessel operation in the Antarctic, let us assume that it is necessary to restrict vessel design full load draft to 30'-0". In addition, let us assume that this area study has revealed that the probable maximum ice thickness to be encountered during late winter or early spring is 15'-0" of one season ice with some possibility of older ice.

The items known at the beginning of our study are,

Maximum draft	= 30'-0"
Maximum ice thickness	= 15'-0"
Month of First Penetration	= October

From table 1 we see that the mean air temperature for the Kanian Bay, Little America area for October is

$$\Theta_a = -38^{\circ} \text{ F.} = -38.9^{\circ} \text{ C.}$$



The ice surface temperature, assuming no snow cover may be approximated as

$$\begin{aligned}\theta_o &= 0.86 (\theta_a + 0.17) - 0.4 \text{ } ^\circ\text{C.} & (12) \\ &= -33.7^\circ \text{ C say } - 34^\circ \text{ C.}\end{aligned}$$

Since there is a possibility of old ice as well as younger one season ice in the area we shall consider perennial sea ice as the most severe case.

Based on our limiting draft of 30'-0" we have from figure 45

$$\frac{\text{propeller diameter}}{\text{Draft}} = 0.615$$

Therefore

$$\text{Propeller Diameter } D = 18'-5"$$

In addition, from figure 47

$$\text{LBP} = L = 398' - 0" \text{ (First Estimate)}$$

Based on this estimate of vessel length, the extreme beam at the design water line is from figure 48

$$B' = 79' - 3" \text{ (First Estimate)}$$

From figure 50 we note that characteristic propeller loading factors  $\tau_o' / D^2$  are not given for vessel lengths in excess of 300' - 0". In order to determine a value for use with our problem we must try to interpret the indicated trends. As can be seen, the ratio  $\tau_o' / D^2$  tends to rise rapidly for vessels beyond 275' - 0" in length. In section F-2, however, we indicated that from an economic viewpoint the value of this ratio approaches a limit of about 850. In our problem, therefore, we may assume the limiting value, hence

$$\tau_o' / D^2 = 850 \text{ lb/ft}^2 \text{ per shaft}$$

$$\tau_o' \text{ per shaft} = 289000 \text{ lbs.}$$

$$\tau_o' \text{ TOTAL TROOST} = 578000 \text{ lbs.} = 258 \text{ tons}$$





Assuming the conventional practice of a built up three bladed propeller with thick strength sections, we have

$$T_{ACTUAL} = K_1 K_2 T_{TROOST} \\ = 196 \text{ tons}$$

Knowing the ideal propeller thrust (Troost) per blade and propeller diameter, we can, from figure 9 determine an approximation of shaft horsepower required as

$$SHP/Shaft = 13800$$

$$SHP \text{ Total} = 27600$$

and from figure 10 the propeller RPM as

$$RPM = 150$$

If the thickness of ice we wish to overcome is 180" and surface temperature is  $-34^{\circ}$  C. we can estimate from figure 36 for perennial sea ice that vertical bow reaction force F required as

$$F = 4900000 \text{ lbs.} = 2185 \text{ tons}$$

Let us assume that in normal breaking by ramming the accelerating distance is equal to one ships length, therefore

$$S' = L = 398' - 0"$$

In addition, based on our vessel length, a first approximation of vessel free route speed is

$$V = 0.978 \sqrt{398} = 19.5 \text{ knots}$$

We can now apply the expression for icebreaking force and vessel impact speed so as to obtain a reasonable first estimate of vessel displacement. Dealing first with icebreaker force we have the modified expression (90), i.e.

$$W = \frac{15.2}{V} \sqrt{F^2 H - 2.29 T F H}$$



Substituting our known values this can be simplified to

$$W = \frac{200000}{v}$$

Assuming various values of  $v$  we can obtain a plot of vessel displacement versus vessel impact speed as shown in figure 76 . Now consider vessel impact speed due to acceleration both in open water and in an ice clogged channel. Considering first acceleration in open water we have

$$v = 3.1 x' T_o^{0.621}$$

therefore, substituting known values

$$x' = 0.0121 v$$

Assuming various values of vessel impact speed  $v$  we can obtain a variation of  $x'$  as a function of  $v$  . From figure 4' we obtain values of  $F(x')$  corresponding to each value of  $x'^1$  . These values of  $F(x'^1)$  used in our expression for open water

$$W = \frac{2.86 v^2}{F(x'^1) T_o^{0.24}} = \frac{307}{F(x'^1)}$$

will give a variation of vessel displacement as a function of impact speed as shown on figure 76 . Since this curve and the one above give a simultaneous solution to our problem, we have from the intersection of the two curves a first estimate of displacement of

$$W = 10200 \text{ tons}$$

This, however, is an optimistic estimate since the vessel will seldom accelerate in open water. Instead, the working channel will soon become full of ice pieces and the vessel will, under normal circumstances be accelerating in an ice filled channel. For acceleration in an ice channel,





# EXAMPLE PROBLEM SOLUTION FOR VESSEL DISPLACEMENT

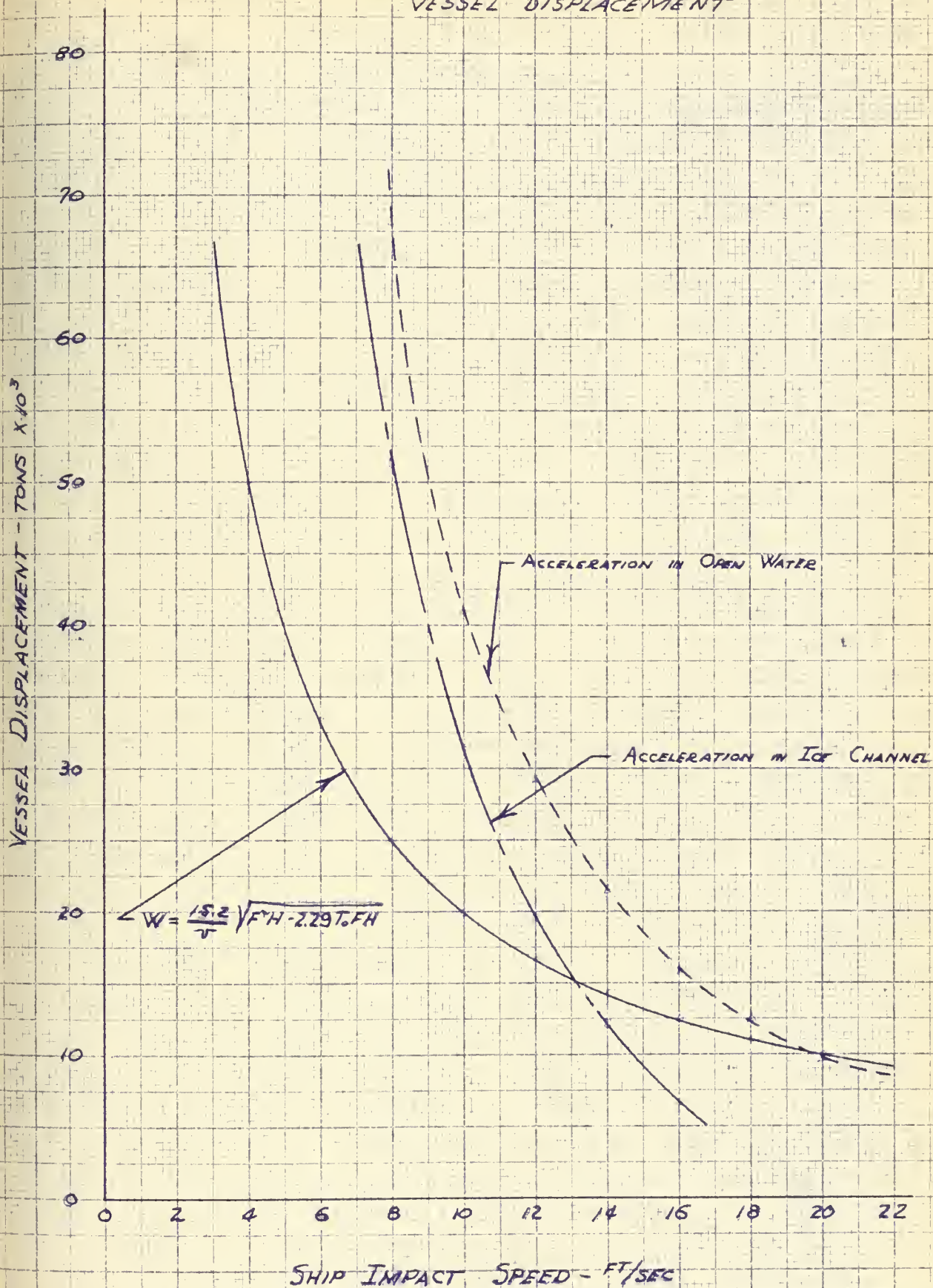


FIG 76



Sample Calculation

$$W = \frac{15.2}{V} \sqrt{F^2 H - 2.24 T_o F H}$$

$$= \frac{15.2}{V} \sqrt{(2185)^2 (30) - (2.24)(196)(2185)(30)}$$

$$W = \frac{200000}{V}$$

open water

$$V = 3.1 X' T_o^{0.621}$$

$$X' = \frac{V}{(3.1)(196)^{0.621}}$$

$$X' = 0.0121 V$$

$$W = \frac{2.86 V^2}{F(X') T_o^{0.24}}$$

$$= \frac{(2.86)(19.5)^2}{F(X')(196)^{0.24}}$$

$$W = \frac{307}{F(X')}$$

ice channel

$$V = 1.12 X' T_o^{0.524}$$

$$X' = \frac{V}{(1.12)(196)^{0.524}}$$

$$X' = 0.0566 V$$

$$W = \frac{21.25 V^2}{F(X') T_o^{0.047}}$$

$$= \frac{(21.25)(19.5)^2}{F(X')(196)^{0.047}}$$

$$W = \frac{6300}{F(X')}$$

2	100000	0.0242	0.0003	1024000	0.113	0.004	1573000
4	50000	0.0484	0.0013	236500	0.226	0.025	252000
6	33350	0.0726	0.0025	123000	0.339	0.06	105000
8	25000	0.0969	0.0045	68300	0.452	0.12	52500
10	20000	0.121	0.0075	41000	0.566	0.20	31500
12	16700	0.145	0.0105	29300	0.679	0.32	19700
14	14300	0.1693	0.0142	21600	0.792	0.515	12230
16	12500	0.1936	0.0193	15900	0.906	0.95	6630
18	11100	0.218	0.0245	12530			
20	10000	0.242	0.0310	9930			
$V$	$W$	$X'$	$F(X')$	$W$	$X'$	$F(X')$	$W$



therefore,

$$v = 1.12 x' T_o^{0.524}$$

and

$$\omega = \frac{21.25 v^2}{F(x') T_o^{0.047}}$$

Substituting our known values these expressions become

$$x' = 0.0566 v$$

$$\omega = \frac{6300}{F(x')}$$

By a method identical to that used for acceleration in open water and with figure 73, we can obtain a new curve of vessel displacement versus impact speed as shown in figure 76. Again, the intersection of this curve and our first curve gives a simultaneous solution to our problem. Hence a more reasonable displacement estimate is

$$W = 15200 \text{ tons}$$

In order to now consider the compatibility of our estimated dimensions with a reasonable block coefficient, we proceed next to an estimate of vessel form parameters. Figure 67 shows a plot of prismatic coefficient as a function of speed length ratio and displacement length ratio. For our case

$$v/\sqrt{L} = 0.978$$

$$\omega/(0.01L)^3 = 241$$

Since ours will be a diesel electric vessel, we see that figure 67 does not extend to as low a displacement length ratio as ours. We can, however, use the curve for the lowest value listed, i.e.  $\omega/(0.01L)^3 = 300$ . Thus

$$C_p = 0.696$$

Based on this value of  $C_p$  and our speed length ratio we can determine a





representative value of block coefficient from figure 68, i.e.

$$C_B = 0.545$$

and

$$C_x = \frac{C_B}{C_P} = \frac{0.545}{0.696} = 0.784$$

Now

$$C_B = \frac{35W}{LBH}$$

Assuming that for our vessel we desire

$$L/B = 4.5$$

which is reasonable for a large polar icebreaker, we have

$$L = 12.57 \sqrt{\frac{35W}{C_B H}} = 384 \text{ ft}$$

hence our first estimate of length was a bit high and for our second estimate we shall assume

$$LBP = 384 \text{ ft}$$

Therefore our second estimate of vessel maximum beam becomes

$$B = 0.2225 L = 85.4 \text{ ft}$$

Now we shall investigate the effect of these modifications in vessel length and beam on our other selected vessel characteristics.

Since our vessel draft is still fixed at 30' - 0" our propeller diameter cannot be modified. Our altered vessel length would normally modify the ratio  $T_0'/D^3$ , however, since our vessel is still considerably in excess of 300' - 0" we are justified in continuing to assume that powering will be at or near our discussed economic maximum

$$T_0'/D^3 = 850$$



Therefore, our previously determined values of actual propeller thrust, shaft horsepower and shaft RPM remain unchanged. Vessel vertical bow reaction force,  $F$ , necessary to overcome ice 15' - 0" thick is not a function of vessel length or beam, hence it too remains unchanged.

Again we assume

$$S' = L = 384 \text{ ft}$$

Therefore our estimated vessel free route speed becomes

$$V = 0.978 \sqrt{384} = 19.2 \text{ knots}$$

If we now reapply our expression for vessel displacement

$$W = \frac{15.2}{0.0001} \sqrt{F^2 H - 2.24 T_0 F H}$$

and that for vessel impact speed in an ice channel

$$V = 1.12 \times T_0^{0.544}$$

$$W = \frac{21.25 V^2}{F(x) T_0^{0.544}}$$

we obtain a new graphical solution for vessel displacement. Doing this, however, we note only a minor increase in our displacement estimate due solely to the modification of vessel free route speed with length since all other items remain constant, i.e.

$$W = 15300 \text{ tons}$$

Since the effect of this minor change in displacement will produce a negligible effect upon our estimated prismatic and block coefficients we now have a reasonable and compatible preliminary estimate of vessel proportions.

To further determine the adequacy of these proportions, we should now investigate vessel stability. Based on our value of  $C_p$  we can from figure 70 determine a reasonable value of load waterplane coefficient, i.e.





$$C_w = 0.7955$$

From expression (128) we can determine height of center of buoyancy as

$$KB = \frac{C_w}{C_b + C_w} (H) = 17.8 \text{ ft}$$

The height of transverse metacenter above center of buoyancy is given as  
(129)

$$Bm_t = \frac{C_{it} B^2}{C_b H}$$

where transverse inertia coefficient  $C_{it}$  determined from figure 71 as

$$C_{it} = 0.0525$$

therefore

$$Bm_t = 23.4 \text{ ft}$$

and

$$KM_t = KB + Bm_t = 41.2 \text{ ft}$$

Since we have shown that for icebreakers the vertical height of center of gravity may be taken at the design water line, we have

$$KG = 30'-0"$$

Therefore metacentric height for our vessel is

$$GM_t = KM_t - KG = 11.2 \text{ ft}$$

Considering now the longitudinal condition

$$Bm_L = \frac{C_{il} L^2}{C_b H} \quad (130)$$

where  $C_{il}$  is obtained from figure 72 as

$$C_{il} = 0.0478$$

therefore

$$Bm_L = 431 \text{ ft}$$



Let us now consider the effects of one of the most severe operating conditions on this stability, i.e. the vessel sitting with its bow up on the ice shelf. Since resulting vessel trim is small we can neglect its effect and consider only change in vessel draft. A first approximation of this change in draft was given as (131)

$$\Delta d = \frac{35 F}{A_w}$$

where

$$A_w = 413 C_w = 26050 \text{ ft}^2$$

hence

$$\Delta d = 2.94 \text{ ft}$$

This, however, assumed constant waterplane area, hence as a closer approximation

$$\Delta d_1 = \frac{35 F}{A_w + A_{w_1}}$$

where

$$\frac{A_{w_1}}{A_w} = \left( \frac{H}{H_1} \right)^2 \frac{1 - C_v}{C_v} \quad (133)$$

$$H_1 = H - \Delta d = 27.06 \text{ ft}$$

Now

$$C_v = \frac{C_B}{C_D} = 0.685$$

hence

$$A_{w_1} = 24900 \text{ ft}^2$$

and

$$\Delta d_1 = 3.01 \text{ ft}$$

Therefore

$$H_2 = H - \Delta d_1 = 26.99 \text{ ft}$$



Since vertical prismatic coefficient,  $C_v$ , is constant with draft, the new height of center of buoyancy is

$$KB_1 = \frac{1}{C_v + 1} (H_2) = 16.0 \text{ ft}$$

we have shown that

$$\frac{KM_{t_2}}{H_2} = \frac{1}{C_v + 1} + \frac{C_{L_{t_1}}}{C_{B_1}} \left( \frac{B_1}{H} \right)^2 \quad (132)$$

where  $C_v$  and  $B/H$  are constant with draft and

$$\frac{C_{B_1}}{C_{B_2}} = \frac{C_w}{C_{w_1}} = \left( \frac{H_1}{H_2} \right)^{\frac{1-C_v}{C_v}} \quad (133)$$

therefore

$$C_{B_1} = 0.520$$

$$C_{w_1} = 0.260$$

and from figure 71

$$C_{L_{t_1}} = 0.0481$$

Hence

$$\frac{KM_{t_2}}{H_2} = 1.345$$

$$KM_{t_2} = 36.2 \text{ ft}$$

and

$$BM_{t_2} = 20.2 \text{ ft}$$

The vertical location of virtual center of gravity is given as

$$KG_v = \frac{W \cdot KG + F H_2}{W - F} = 30.45 \text{ ft}$$

hence

$$GM_{t_2} = KM_{t_2} - KG_v = 5.75 \text{ ft}$$

This certainly is an adequate  $GM_t$  for the inclined condition and seems sufficient to care for any rise in center of gravity due to possible topside ice. Our preliminary vessel proportions, therefore, seem adequate and reasonable.





At this point there are several other items we can investigate based on our preliminary proportions. These are: size of vertical forefoot and location, vessel retraction ability and vessel icebreaking potential without ramming.

Considering first the forefoot we have that the vertical forefoot will not strike the ice sheet if

$$b \leq C$$

where  $C$  is given as

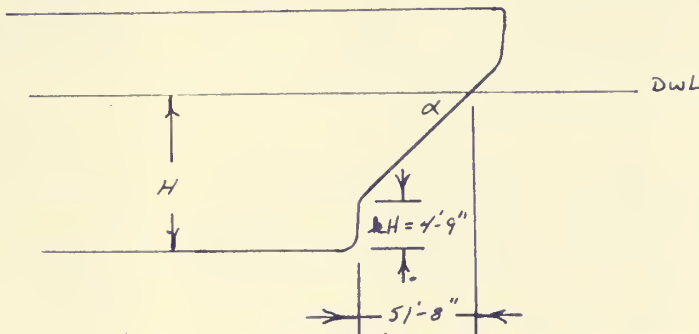
$$C = 1 - \left[ \frac{4.58 T_0}{w} + \sqrt{\frac{21 T_0^2}{w^2} + 0.0862 \frac{x'^2 T_0^{1.048}}{H}} + \sqrt[3]{0.0000544 \frac{x'^2 w T_0^{1.048}}{H^3}} \right]$$

Substituting we have

$$C = 0.1583$$

Hence, in order for the vertical forefoot not to strike

$$b \leq 0.1583$$



or since vessel draft is 30'-0", the height of vertical forefoot

$$bH \leq 4.75 \text{ ft}$$



Based on our value of  $\alpha = 26^\circ$ , therefore, the vertical forefoot should be 4'-9" high and located about 51'-8" aft of the forward perpendicular.

Considering now the ability of the vessel to retract if once beset we have for acceleration in an ice channel

$$T_o^{0.952} \geq 0.0000234 \frac{\omega^2 X'^2}{H}$$

in order that the vessel be able to retract under normal conditions. For our vessel

$$T_o^{0.952} = (196)^{0.952} = 153 \text{ tons}$$

$$0.0000234 \frac{\omega^2 X'^2}{H} = (0.0000234) \frac{(15300)^2 (0.65)^2}{30} = 77.3 \text{ tons}$$

hence since

$$T_o^{0.952} > 0.0000234 \frac{\omega^2 X'^2}{H}$$

our vessel should be capable of extracting itself under normal breaking conditions. For the more severe case where the vessel has been moored into the ice for a period of time and the stem has adhered to the ice we must satisfy the condition

$$T_o^{0.952} \geq 0.000229 \frac{\omega^2 X'^2}{H}$$

$$153 \text{ tons} < 756 \text{ tons}$$

In this instance, therefore, the vessel will not be able to extract itself and heeling tanks or some other auxiliary method must be used to free the vessel.

Turning now to the vessels icebreaking ability without ramming, i.e. continuous breaking, we see from section F-7 that the forces involved may be expressed as

$$F = 2.52 T_o$$





Based on our value of ballard pull, the vertical bow reaction force continuously available without ramming is

$$F = 2.52 \times 196 = 494 \text{ tons}$$

$$= 1107000 \text{ lbs}$$

If we assume ice conditions as in the statement of our original problem we find from figure 58 that the maximum thickness of ice which our vessel can break continuously is

$$t'' \approx 86'' = 7.17 \text{ ft}$$

At this point we have arrived at pretty reasonable estimates of vessel proportions and parameters. We may now proceed to a determination of vessel lines. Reiterating those items which we have thus far determined we have

LBP =	384'-0"	W =	15300 tons
H =	30'-0"	$C_p$ =	0.696
B =	85'-5"	$C_B$ =	0.545
D =	18'-5"	$C_A$ =	0.784
V =	19.2 knots	$C_w$ =	0.7955
SHP =	27600	$\alpha$ =	30°
RPM =	150	$\beta$ =	45°
Blades =	3	$e$ =	0.1583



## B. Evaluation of an Existing Vessel

The method outlined in this paper may be used to evaluate the effectiveness of an existing vessel as well as provide a basis for preliminary design estimates. In this regard it gives the designer a means whereby he can compare several existing vessels to determine their relative icebreaking effectiveness.

Contrasted to the preliminary design consideration where only relatively few items concerning the proposed vessel are known, we now have the condition where we know all vessel dimensions and parameters. As an example of our approach in this instance let us consider the potential icebreaking abilities of the Glacier as representative of a typical present day polar icebreaker.

The characteristics of the vessel are as follows:

LBP = 290'-0"	$C_B = 0.537$
B = 74'-0"	$C_W = 0.800$
H = 25'-9"	$C_D = 0.698$
V = 16 knots	$S = 149.6'$
SHP = 21000	$GM_t = 9.95'$
D = 17'-6"	$RM_t = 35.6'$
W = 7750 tons	$KB = 15.4'$
KG = 25.65'	$\chi = 30^\circ$
$BM_t = 20.2'$	$\beta = 46^\circ$
$LM_L = 283$	$\bar{z} = 0.466$

Since this is a twin screw vessel, the shaft horsepower per shaft is



one half the total given above. The vessel was designed for three bladed propellers, hence from figure 9 based on SHP/shaft and propeller diameter

$$\text{SHP/shaft} = 10500$$

$$D = 17'-6"$$

$$\therefore T_{\text{TROOST}} = 235000 \text{ lbs/shaft}$$

$$T_{\text{TROOST}} = 470000 \text{ lbs total}$$

$$= 210 \text{ tons}$$

Correcting for blade thickness and increased hub diameter due to use of built up propellers

$$T_{\text{ACTUAL}} = K_1 K_2 T_{\text{TROOST}}$$

$$= (0.86)(0.885)(210) = \underline{160 \text{ tons}}$$

$$k_1 = \frac{2.5}{1} = \frac{(2.5)(17.6)}{270} = 1.031$$

$$k_2 = \frac{H - 0.75}{C_w L} = \frac{(2.5)(17.6) - 0.75}{(0.8)(270)} = 0.257$$

$$H = \left[ \frac{C_0}{C_w} + \frac{k_1^2}{k_2} \frac{C_0}{4 C_w} \right] = \left[ \frac{.53}{.8} + \frac{(1.031)^2}{(.25)(.64)} \frac{.53}{4} \right] = 4.051$$

For acceleration in open water, based on an accelerating distance of one ship length





$$A =$$

$$=$$

$$= 4.051$$

For acceleration in open water, based on an accelerating distance of one ship length

$$W = \frac{2.86 V^2}{F(X^1) \tau_o^{0.24}}$$

$$\therefore F(X^1) = \frac{(2.86)(16)^2}{(7750)(160)^{0.24}} = 0.028$$

$$\therefore X^1 = 0.229$$

$$\begin{aligned} v &= 3.1 \times \tau_o^{0.621} \\ &= (3.1)(0.229)(160)^{0.621} \\ &= 16.6 \text{ ft/sec} \end{aligned}$$

If acceleration is in an ice channel

$$W = \frac{21.25 V^2}{F(X^1) \tau_o^{0.047}}$$

$$\therefore F(X^1) = \frac{(21.25)(16)^2}{(7750)(160)^{0.047}} = 0.552$$

$$\therefore X^1 = 0.806$$

$$\begin{aligned} v &= 1.12 \times \tau_o^{0.524} \\ v &= (1.12)(0.806)(160)^{0.524} \\ &= 12.9 \text{ ft/sec} \end{aligned}$$

$$\alpha = 30^\circ, \beta = 46^\circ$$

$$\therefore \lambda = 1.09$$

$$\epsilon = 0.548$$



Assuming for the moment that the vertical forefoot does not strike the ice shelf, the vertical bow reaction, F, which may be developed is

Open water acceleration:

$$\begin{aligned}
 F &= 0.91 \times T_0 + \sqrt{0.828 \times T_0^2 + \frac{W^2 \times 2}{g \Delta H}} \\
 &= 0.91 \times (1.08 \times 100) + \sqrt{(0.828 \times (1.08 \times 100)^2 + \frac{(2750)^2 \times (10.0) \times (0.548)}{(32.2) \times (4.05) \times (25.25)}} \\
 &= 1808.5 \text{ tons} \\
 &= 4040000 \text{ lbs}
 \end{aligned}$$

Ice channel acceleration:

$$\begin{aligned}
 F &= 1443.5 \text{ tons} \\
 &= 3230000 \text{ lbs}
 \end{aligned}$$

There is, however, a possibility that the vertical forefoot will strike the ice sheet and hence restrict the vertical bow reaction force which may be developed. In order for the vertical forefoot not to strike

$$b = 0$$

therefore assuming acceleration in an ice channel as most characteristic

$$\begin{aligned}
 C &= 1 - \left[ \frac{4.53 \times 10^{-5}}{2750} + \sqrt{\frac{21 \times 100^2}{(2750)^2} + 0.0862 \times \frac{1.08 \times 100}{25.25}} \right. \\
 &\quad \left. + \sqrt[3]{0.0000544 \times \frac{(1.806)^2 \times (2750) \times (100) \times 1.048}{(25.25)^3}} \right] \\
 &= 1 - \left[ \frac{(4.53 \times 100)}{2750} + \sqrt{\frac{(21)(100)^2}{(2750)^2} + \frac{0.0862 \times (1.08 \times 100) \times 1.048}{25.25}} \right. \\
 &\quad \left. + \sqrt[3]{0.0000544 \times \frac{(1.806)^2 \times (2750) \times (100) \times 1.048}{(25.25)^3}} \right]
 \end{aligned}$$

$$C = 0.083$$

$$b = 0.46$$

$$\therefore b > C$$





Hence the vertical forefoot will strike and the vertical bow reaction force,  $F$ , which may be developed is limited. Therefore, the vertical bow reaction force we can develop is

$$F = \frac{10}{14} (10 \cdot 2) = \frac{10}{14} \sin x \cdot 0.000574 \cdot 10 \cdot 10^6 \cdot 0.048 \sin x$$

$$= \frac{275}{4.057} (0.460) = \frac{275 \cdot 0.460 \cdot 3.5}{(4.057)(4.057) \cdot 0.000574 \cdot 10^6 \cdot (0.048)^2 \cdot (160) \sin 0}$$

$$F = 674 \text{ lbs}$$

$$F = 451 \text{ + 200 lbs}$$

This represents a considerable loss of potential icebreaking ability.

However, if we assume, as we did in Part A, that the vessel is to be used in the Antarctic, Little America area during the month of October we have

$$\theta_0 = -34^\circ \text{ C.}$$

Hence the amount of ice which can be broken by this vessel is, from figure 36

$$z'' = 101''$$

$$= 8.43 \text{ feet}$$

Of course, this assumes 10/10 coverage or a continuous unbroken icefield.

Let us now investigate the effect upon stability of the vessel sitting on the ice sheet.



As a first approximation of change in vessel draft

$$\Delta d = \frac{35F}{A_w}$$

where

$$A_w = LBC_w = 17200 \text{ ft}^2$$

$$\therefore \Delta d = 1.37 \text{ ft}$$

This assumes constant waterplane area. For a closer approximation

$$\Delta d_1 = \frac{35F}{A_w + A_{w_1}}$$

where

$$\frac{A_w}{A_{w_1}} = \left( \frac{H}{H_1} \right)^{1-C_v}$$

$$H_1 = H - \Delta d = 24.38 \text{ ft}$$

$$C_v = \frac{C_B}{C_w} = 0.621$$

hence

$$A_{w1} = 16750 \text{ ft}^2$$

and

$$\Delta d_1 = 1.39 \text{ ft}$$

Therefore

$$H_2 = H - \Delta d_1 = 24.36 \text{ ft}$$

Now

$$\frac{K_{M_{T_2}}}{H_2} = \frac{1}{C_v + 1} + \frac{C_{it}}{C_{B_1}} \left( \frac{B}{H} \right)^2$$

where  $C_v$  and  $B/H$  are constant with draft. Also

$$\frac{C_B}{C_{B_1}} = \frac{C_w}{C_{w_1}} = \left( \frac{H}{H_2} \right)^{1-C_v}$$



Therefore

$$C_{B_1} = 0.523$$

$$C_{W_1} = 0.778$$

and from figure 71

$$C_{L_t} = 0.0503$$

Hence

$$\frac{KM_{t_2}}{H_2} = 1.396$$

$$KM_{t_2} = 34.0 \text{ ft}$$

The vertical location of virtual center of gravity

$$KG_v = \frac{W \cdot AG - FH_2}{W - F} = 25.8 \text{ ft}$$

Hence

$$GM_{t_2} = KM_{t_2} - KG_v = 8.2 \text{ ft}$$

This is certainly adequate even allowing for topside icing. It is interesting to note that this negligible loss of stability is due solely to the serious restriction in bow reaction force  $F$  and vessel climbing potential due to the vertical forefoot striking the ice sheet.





Section H

Table of Characteristics of Past and Present

Icebreaking Vessels



\* Note - all values given are for the design condition as far as possible.  
Under item #27 SHP refers to diesel electric installation, IHP to steam installation

	ABEGWEIT	ALEXANDER HENRY	ALGONQUIN	ALTE	APU	CACTUS	D'IBERVILLE
1. Name							
2. Year Built	1947	1960	1934	1926	1899	1942	1953
3. Nationality	CANADA	CANADA	U.S.	SWEDEN	FINLAND	U.S.	CANADA
4. LBP	348-0		150-0	194-7	141-9	170-0	285-0
5. LOA	372-6	210-0	165-0	204-1	144-0	180-0	310-0
6. LWL	355-0						302-0
7. B (Extreme)	62-0	43-6	36-0	55-9	35-6	37-0	66-6
8. B (LWL)	60-0		36-0	53-2	34-0	35-0	64-6
9. Depth	24-9	21-0	21-0	28-9		17-5	40-0
10. Draft - H	19-0	16-0	12-0	19-8	18-0	12-0	27-6
11. Displacement - W	7600	2400	1000	2464	800	940	8700
12. Design Speed - V	16.5	13.5	12.8	15.5	12	13	15
13. Block Coeff - $C_b$	0.513	0.650	0.538	0.418		0.461	0.580
14. Prismatic Coeff - $C_p$	0.571		0.632	0.571		0.565	0.690
MIDSHIP SECTION							
15. Coeff - $C_x$	0.90		0.852	0.733		0.817	0.840
16. Waterplane Coeff - $C_w$	0.791			0.662		0.728	
17. KB						7.7	
18. KG						14.71	
19. $KM_t$						17.57	
20. $KM_L$						215	
21. $GM_t$						2.86	
22. $BM_t$						9.87	
23. LCF from $\bar{x}$						1.85 aft	





24. LCG from $\phi$						3.7 aft	
25. type propulsion	Diesel Electric	Direct Diesel	Steam	Steam	Steam	Diesel Electric	Steam
26. Number of shafts-aft	2	2	1	1	1	1	2
Fwd	2	0	0	1	0	0	0
27. SHP or IHP (total)	15400	3550	1500	4000	1350	1000/ 1200	10800
28. Wetted Surface						6583	
29. Propelled dia - D	13-0	8-6				8-6	14-0
30. Number of blades						5	4
31. Propeller pitch	13-6	6-0				7-0	13-6
32. RPM at design speed	128/ 155	300	140	100/ 125	84/ 90	208	145
33. Mean width Ratio						0.333	
34. Blade thickness fraction						0.0458	
35. Thrust deduction factor						0.240	
36. Wake fraction						0.205	
37. Propeller top clearance						0.6	2.35
38. Rise of forefoot $\alpha$	23.5°	26°	33°	24°	20°	30°	30°
39. $\beta$ (approx)							57°
40. Flare Amidships	9°	0°	4°	16°		20°	6°
41. Rudder Area	142.5						172.6
42. Lateral Plane Area	6750						8400
43. Propeller developed area ratio	0.528						0.50



[illegible]



Steam		Steam	Steam	Steam	Steam	Diesel Electric	Steam	Diesel Electric
2	1	3	2	2	1	2	1	2
0	1	1	0	0	0	0	1	0
3500	2700	9000	2000	7000	1300	6500	3800	21000
								25920
10-6			10-0					17-6
								3
11-9			10-9					12-1
130/ 140	160	105	140	125	83/ 94	135	120	175
								0.322
								0.049
								0.75
25°		25°	20°	52°	30°		23°	30°
		67.5°						46°
0		20°		4°			20°	20°
								173
								6670
			0.446					0.382





HOLGER DANSK	HUDSON	HULL 614	HULL 620	INTO	ISBJORN	ISBRYTAREN	ISBRYTAREN II	JAAKARHU
1942	1934				1923	1895	1914	1926
DENMARK	U.S.	CANADA	CANADA	FINLAND	DENMARK	SWEDEN	SWEDEN	FINLAND
210-4	104-0		280-0	254-1	156-2	134-0	190-7	246-0
226-0	110-6	223-6	315-0	273-10	170-7	139-9	200-0	263-0
			307-3					
55-6	24-0	48-0	70-0	63-6	40-2	35-6	55-10	63-1
53-5	24-0		69-0	61-2	39-4	34-0	52-6	60-2
24-6	12-7	21-0	41-0		21-0		28-8	31-10
17-10	9-6	16-0	28-0	20-4	18-6	18-10	20-9	21-10
3000	308	2700	8974	4415	1330	720	2350	4850
15	12	13.5	15.5	16.5	12.5	12	14	13.5
0.533	0.456	0.650	0.560	0.482	0.408	0.410	0.397	0.525
0.634	0.618						0.527	0.666
0.842	0.738						0.755	0.789
0.730								0.741
	7.95							
	12.40							
	14.12							
	106.95							
	1.72							
	6.17							
	2.53 aft							



	Diesel Electric	Diesel Electric	Diesel Electric	Diesel Electric		Steam	Steam	Steam	Steam
5.									
6.	2	1	2	3	2	1	1	1	2
	1	0	0	0	2	0	0	1	1
7.	6610	800	4250	15000		2500	1200	2600	7840
8.									
9.		7-6	11-6	13-6	13-10				
0.		3							
1.		6-3	12-9	13-0					
2.	123	250	145	136/ 170		90	102	130	117
3.									
4.									
5.									
6.									
7.				2.5					
8.	87°	30°	26°	30°		20°	31°	20°	26°
9.	46.5°			50°					
0.	16°	22°	0°	6°			11°	24°	20°
1.				204.1					
2.				8820					
3.			0.519						





[illegible]



Diesel Electric	Diesel Electric	Steam	Diesel Electric	Steam	Diesel Electric	Steam	Steam	Atomic Turbo-Electri
2	2	1	3	1	2	3	2	3
2	2	0	0	1	0	0	1	0
10500	7500	850	12000	5200	10000	10000	7500	39200
				16-0	15-0			
				4	3			
					12-6			
120				122	105/ 145			205
22°	25°	29°		33°	30°	25°	18°	
65°					50°			
20°		0°		17°	20°	20°	25°	
					137			
					6430			



MACKINAW	MIKULA SELIANINOV- ITCH	MONTCALM	MOSCOW	MURTAJA	NADESHNIJ	NAUGATUCK CLASS	N.B. McLEAN	NORTHLAND
1944	1916	1957	1960	1890	1897	1939	1929	1927
U.S.	RUSSIA	CANADA	RUSSIA	FINLAND	RUSSIA	U.S.	CANADA	U.S.
280-0	275-0	201-10	368-9	137-5	180-0	105-0	260-0	200-0
290-0	292-0	220-0	400-7	156-0	192-0	110-0	277-0	216-7
		209-10						
74-4	57-6	48-0	80-4	36-1	42-11	26-5	60-4	39-0
70-0		48-0		35-4	42-0	25-0	59-4	39-0
28-1	32-0	21-0		24-11	25-5	15-0	31-0	24-9
19-2	19-3	16-0	34-5	15-7	17-9	11-4	19-6	13-8
5252	4950	2756	15000	825	1710	361'	5034	1785
16	15.5	13	18.3	12.5	10/14	12.5	15	11.7
0.497	0.574	0.690		0.382	0.443	0.417	0.582	0.611
0.612						0.572		0.635
0.812						0.728		0.963
0.728						0.738		
11.13						7.13		
16.52						11.45		
34.68						13.45		
338						105		
18.16						2.0		
23.55						6.32		
1.0 aft								
1.1 aft						1.23 fwd		





Diesel Electric	Steam	Steam	Diesel Electric	Steam	Steam	Diesel Electric	Steam	Diesel Electric
2	2	2	3	1	1	1	2	1
1	0	0	0	0	0	0	0	0
10000	8000	4000	22000	1200	2475	1000	6500	1025
18975								
17-0		11-6				8-4	14-6	
3								
11-7		11-3				5-0	18-0	
136/ 170	103	145		83	95/ 106	265	105	132
0.327								
0.0559								
0.27								
0.207								
0.75		1.78						
30°	22°	26°		33°	30°	30°	22°	27°
43°		61°		63°		39°		
20°	10°	0°		10°		20°	15°	0°
		88.2						
		3360						
		0.509					0.461	



ODEN	PETRI VELIKIJ	SAMPO	SAUREL	SISU	SOYA MARU	STADT REVAL	STALIN CLASS	STEPHAN MACAROW
1957	1912	1898	1929	1938	1932	1895	1939	1917
SWEDEN	RUSSIA	FINLAND	CANADA	FINLAND	JAPAN		RUSSIA	RUSSIA
261-6	170-7	191-6	200-0	194-9	310-0	147-4	335-0	236-0
273-0	182-1	202-0	212-0	210-6	327-10	148-8	350-0	248-0
63-9	50-10	43-0	42-0	47-6	46-6	38-10	76-0	57-0
62.5	48-7	42-0		46-6		37-1	74-6	
31-3	27-5	21-9	21-0	18-6	30-0	18-8	30-0	30-4
21-11	19-1	18-3	14-0	16-1	15-2	14-0	26-3	22-0
5020	1610	1850	1860	2000	3770	865	9300	4570
16/17	14.4	10/13	15	16	17	11.5	15.5	15
0.483	0.378	0.441		0.482		0.396	0.520	
0.592	0.533						0.610	
0.817	0.708						0.850	
0.706	0.723						0.720	





	Steam	Steam	Steam	Diesel Electric	Steam	Steam	Steam	Steam
2	1	1	2	2		1	3	2
2	1	1	0	1		0	0	1
10340	3200	3000	3600	4005	5500	1600	10050	5550
			11-6		12-6			
			11-9		17-8			
	130/ 143		155	140	112		125	90/105
23°	30°	22°	23°	24°		30°	30°	18°
65°			61°				69°	20°
20°	20°		10°					
			0.408					



STORE BJORN	STORIS	SUNDEW	SUUR- TOOL	TARMO	THULE	PROPOSED	TROUVOR	VACTIONLAND
1931	1942	1944	1914	1907	1953		1896	1952
DENMARK	U.S.	U.S.		FINLAND	SWEDEN	RUSSIA		U.S.
180-5	220-0	170-0	236-4	210-5	187-0	363-5	161-5	348-0
196-10	230-0	180-0	247-4	219-6	204-0	390-0	166-0	362-0
49-2	43-0	37-0	57-1	47-0	52-9	80-5	40-3	73-6
46-11	41-0		56-1	46-5	49-11	77-1	39-0	68-0
23-11	19-3	17-3	22-10		27-0	46-0	22-3	25-4
18-2	14-0	12-8	18-8	18-2	17-6	31-2	18-9	16-6
2500	1916	1027	3562	2300	2100	12800	1450	6740
13.5	14	14.8	12/14	13		19	9.5/13	13/16
0.533	0.478		0.505	0.454	0.462	0.507	0.430	0.603
0.628	0.572				0.570	0.600		0.706
0.848	0.835				0.810	0.850		0.854
0.734	0.761					0.650		0.808
	15.64							
	20.08							
	322							
	4.44	3.16						
	3.58 aft							
	2.33 aft							



Steam	Diesel Electric	Diesel Electric	Steam	Steam	Diesel Electric	Diesel Electric	Steam	Diesel Electric
2	1	1	2	1	2	3	1	
1	0	0	1	1	1	0	0	
5400	1800	1675	4500	3500	5040	22000	2000	9440
	10-6	9-0						
	5	5						
	7-4	6-4						
125	160/ 195	205	100	89/ 102	145	330	110	162
	0.236	0.236						
		0.045						
24°	30°		18°	20°	23°	26°	25°	
					64°	66°		
11°	20°				20°	18°		20°





VOIMA	VOIMA II	WALTER FOSTER	WILLIAM PARSON	WIND CLASS	YMER	PROPOSED	PROPOSED	ALATNA
1924	1953	1954	1955	1944	1932			1957
FINLAND	FINLAND	CANADA	CANADA	U.S.	SWEDEN	U.S.	FINLAND	U.S.
200-10	254-4		325-0	250-0	246-1	340-0	224-0	290-0
210-7	274-0	229-2	351-0	269-0	257-11	361-0	243-6	302-0
46-7	63-7	42-6	68-0	63-9	63-4	75-6	57-4	60-11
45-11	61-5		67-0	62-0	61-0	74-0	54-10	60-0
18-9	31-2	19-6	34-9	37-9	33-0		28-10	26-6
16-9	21-0	16-7	18-5	25-9	21-0	29-0	19-0	19-0
2070	4415	2850	7108	5300	3465	10500	3280	5700
14		13.5	15	16.5	14/16	18	16/17	12
0.469	0.485	0.65	0.615	0.465	0.476	0.50	0.489	0.606
	0.594			0.618	0.593		0.601	0.654
	0.817			0.752	0.801		0.814	0.926
	0.701			0.724	0.725	0.80	0.725	0.775
				15.4				10.8
				22.63				16.7
				31.04				26.2
				224		360		314
				8.41				7.5
				15.64				15.4
				1.0 aft 1.22 aft		5.0 aft		4.0 aft 0.5 fwd



Steam	Diesel Electric	Steam	Diesel Electric	Diesel Electric	Diesel Electric	Nuclear Turbo-Elec	Diesel Electric	Diesel Electric
1	2	2	2	2	2	2		2
1	2	0	1	0	1	0		0
3700	10500	2500	13333	10000	9000	30000	8800	2530
				13423				
		10-0	14-0	17-0		18-0		12-0
				3		4		4
		9-7	9-11	11-10				11-2
111		145/ 156	136/ 170	105/ 145	140			145
				0.228				0.240
				0.059				0.051
				0.27				
				0.235				
				0.51				
23°	23°	18°	25°	30°	25°	30°	25°	30°
	65°			43°	59°	43°	64°	67°
15°	20°	0°	5°	20°	18°		23°	9°
								140
			0.481	0.317				





1.	TAK-270
2.	1957
3.	U.S.
4.	250.0
5.	263-0
6.	
7.	50-6
8.	50-0
9.	26-5
10.	19-0
11.	3710
12.	13
13.	0.543
14.	0.595
15.	0.911
16.	0.649
17.	10.8
18.	16.96
19.	22.45
20.	254
21.	5.49
22.	11.65
23.	3.8 aft
24.	0.1 fwd



5.	Diesel
6.	Electric
7.	2
8.	0
9.	2700
10.	11-0
11.	
12.	125
13.	
14.	
15.	
16.	
17.	
18.	30°
19.	
20.	10°
21.	120
22.	
23.	
24.	



Section I

Table of References





## Section D - References and Bibliography

### Icebreakers and Icebreaker Design

1. Alexandrov, A. P., The Atomic Icebreaker Lenin, SNAME transactions, 1959
2. Barnhart, R. E. and Browning, R. C., An Investigation into the Form, Size and Power Requirements of Icebreaking Vessels, Thesis, Webb Institute of Naval Architecture, 1941
3. Bradley, F. D., Maneuvering Tests on Model 3705 Representing Twin Screw Icebreakers (AGB-1 and 2) with Inward and Outward Turning Screws, DTMB Report 900, 1954
4. Bureau of Ships Journal, Ships Against Ice, U. S. Navy, August 1954
5. Canadian Shipping, HMCS Labrador, July 1954
6. Compass Points, Atomic Icebreaker Proposed, Vol. XVII, September 1959
7. Diesel Progress, Fern, February 1943, also Motorship, February 1943
8. Electric Boat Division, A Report on the Feasibility of a Nuclear Powered Icebreaker, General Dynamics Corporation, 1959
9. Engineer, Russian Icebreakers, London, December 1919
10. Ferris, L. W., The Proportions and Form of Icebreakers, SNAME transactions, 1959
11. Fisher, R. E. and Bradley, F. D., AGB-1 and 2, Predictions of Performances with and without Ice Guards, Part I - Propulsion, DTMB Report 734, 1950; Part II - Maneuvering, DTMB Report 745, 1951



12. Flodin, J., Icebreakers, Marine Engineering, September 1920
13. German, J. G., Design and Construction of Icebreakers, SNAME transactions, 1959
14. Gover, S. C., Rolling Characteristics of Model 3705 Representing USS Burton Island, DTMB Report 685, 1949
15. Hinterthan, W. B. and Yeh, H. Y., Prediction of Power Performances for AGB-1 Class fitted with Kort Nozzles as Ice Guards, DTMB Report 1197, 1958
16. Jansson, Jan-Erik, Icebreakers and their Design, European Shipbuilding, Vol. 5, 1956
17. Johnson, H. F., RADM, USCG (RET), Development of Icebreaking Vessels for the U. S. Coast Guard, SNAME transactions, 1946
18. Kari, A., The Design of Icebreakers, Shipbuilding and Shipping Record, Vol. 18
19. Kassell, B. M., LCDR, USN, Russia's Icebreakers, Journal, American Society of Naval Engineers, February 1951
20. Lank, R. B., Influence of Arctic Operations on Future Ship Designs, Journal, American Society of Naval Engineers, May 1947
21. Lank, R. B. and Oakley, O. H., Application of Nuclear Power to Icebreakers, SNAME transactions, 1959
22. Marine Engineering and Shipping Review, Icebreaker N. B. McLean, November 1930
23. Marine Engineering and Shipping Review, Soya Maru, May 1933





24. Marine Engineering and Shipping Review, Icebreaker Ymer, May 1933;  
also Shipbuilding and Shipping Record, August 1932;  
Motorship, January 1933; Motorship, London,  
April 1933
25. Marine Engineering and Shipping Record, Coast Guard Icebreaking  
Vessels, December, 1944; also Motorship, London,  
June 1945
26. Marine Engineering and Shipping Record, Icebreaker Design, April  
1945
27. Marine Engineer and Naval Architect, Canadian Naval Icebreaker  
Labrador, August 1954
28. Marine Engineer and Naval Architect, Elbjorn, April 1954
29. Marine Engineer and Naval Architect, General San Martin, December  
1954
30. Marine Engineer and Naval Architect, Labrador, August 1954
31. Marine Engineer and Naval Architect, Lena, Ob and Yenesei, August  
1954
32. Marine Engineering and Shipping Review, U.S.S. Glacier, Navy's  
Answer to Arctic Pack Ice, July 1955
33. Mathews, F. W., Capt. RCN, Stability and Control of HMCS Labrador,  
SNAME transactions, 1959
34. Mathews, S. T., An Investigation into Icebreaking, SNAME, Eastern  
Canadian Section
35. Mendl, W. V., Icebreakers, Shipbuilder and Marine Engineer Builder,  
Vol. 45



36. Motorship, London, The Largest Icebreaker, April 1933
37. Motorship, London, Sisu, April 1939
38. Motorship, London, Into, August 1950
39. Motorship, London, Soviet Icebreakers, February 1955
40. Motorship, London, Icebreaker, December 1956
41. Nardstrom, H. F., Edstrand, H. and Lindgren, H., Model Tests with Icebreakers, Swedish State Shipbuilding Experimental *TANK, 1952*
42. Ormondroyd, J., Investigation of Structural Stresses in Ice-Breaking Vessels, Engineering Research Institute, University of Michigan, 1950
43. Reedy, E. E., Protection of Ships Against Ice, SNAME, Hampton Roads Section, 1958
44. Rogers, G. F. and Reece, J. W., Operational Aspects of Wind Class Icebreakers, SNAME, New England Section, 1959
45. Runeberg, P., Steamers for Winter Navigation and Icebreaking, Institute of Civil Engineers, Proceedings, Vol. 98, 1889; Vol. 107, 1900
46. Russell, H. E. LT USCG, Some Operational Aspects of Icebreaker Design, SNAME Pacific Northwest Section, 1958
47. Shipbuilding and Marine Engineer Builder, Icebreakers for the Port of Stockholm, January-June 1914
48. Shipbuilding and Shipping Record, Swedish Icebreakers, March 1925
49. Shipbuilding and Shipping Record, Design of Icebreakers, February 1941, November 1941



50. Shipbuilding and Shipping Record, Kista Dan, June 1952
51. Shipbuilding and Shipping Record, Elbjorn, February 1954
52. Shipbuilder and Marine Engineer Builder, General San Martin,  
February 1955
53. Shipbuilding and Shipping Record, Kapitan Class, September 1956
54. Shipbuilding and Shipping Record, Research Ship John Busco, December  
1956, also Shipbuilder and Marine Engineer Builder,  
February 1957
55. Shipbuilding and Shipping Record, U.S.S. Glacier, World's Largest  
Icebreaker, 1956
56. Shipbuilding and Shipping Record, Canadian Government Icebreaker  
CAMSHELL, November 1959
57. Shipbuilding and Shipping Record, Canadian Government Icebreaker  
Wolfe, December 1959
58. Shipbuilder, Russian Icebreakers, July 1925; also Journal, American  
Society of Naval Engineers, August 1925; Shipbuilding  
and Shipping Record, March 1926
59. Shipbuilder and Marine Engineer Builder, Icebreaker Goleta Lejon,  
February 1933
60. Shipbuilder and Marine Engineer Builder, Icebreakers, March 1935  
and October 1938
61. Shipbuilder and Marine Engineer Builder, Ernest La Pointe, January 1942
62. Shipping World, Three Recent Icebreakers, 1954
63. Simonson, D. R., LT USN, Bow Characteristics for Icebreaking, Journal,  
American Society of Naval Engineers, 1936





64. Slifer, G. A., U.S.S. Glacier, Icebreaker, Hospital, Laboratory and Warship, Bureau of Ships Journal, U. S. Navy, December 1955
65. Smith, R. M., The Design of Icebreakers, Shipbuilding and Shipping Record, February 1941
66. Swan, H. F., Icebreakers, Institute of Naval Architects, Vol. 41, 1899
67. Tarskis, M. K., The Ice Loads acting upon a Ship, Rechner Transport #12, 1957
68. Thiele, E. H., RADM USCG, Technical Aspects of Icebreaker Operation, SNAME Transactions, 1959
69. U. S. Naval Institute Proceedings, Icebreakers, Vol. 66, 1940
70. U. S. Senate, Report No. 1931 from Committee on Interstate and Foreign Commerce, Eighty Fifth Congress on HR 9196, July 1958
71. U. S. House of Representatives, Hearings Before Committee on Merchant Marine and Fisheries, Eighty Fifth Congress, on HR 9196, HR 9978 and HR 10122, January 1959
72. Vinogradov, I. V., Vessels for Navigation in Icebound Waters, 1946
73. Wasmund, J. A., U.S.S. Glaciers Electrical Plant, Marine Engineering and Shipping Review, July 1955
74. Watson, A., Operation of Department of Transport Icebreakers in Canada, SNAME, transactions, 1959



75. Watson, A., The Design and Building of Icebreakers, London transactions, Institute of Marine Engineers, 1959
76. <sup>z</sup>Palite, J. A. and Balsys, L., Some Structural Aspects of Canadian Postwar built Icebreakers, SNAME, Montreal, 1955

#### Ice Mechanics

77. American Geophysical Union, Bending and Shear Tests on <sup>L</sup>Fake Ice, transactions, 1948
78. Anderson, D. L. and Weeks, W. F., A Theoretical Analysis of Sea Ice Strength, American Geophysical Union, transactions, 1958
79. Anderson, D. L., Preliminary Results and Review of Sea Ice Elasticity and Related Studies, Engineering Institute of Canada, transactions, 1958
80. Assur, S., Composition of Sea Ice and Its Tensile Strength, National Academy of Sciences, National Research Council Publication 598, 1958
81. Barnes, H. T., Ice Engineering, Renouf Publishing Company, Montreal, 1928
82. Boyle, R. W. and Sproule, D. O., Velocity of Longitudinal Vibration in Solid Rods with Specific Reference to the Elasticity of Ice, Canadian Journal of Research, Vol. 5, 1951
83. Brill, R., Structure of Ice, U. S. Army, Snow, Ice and Permafrost Research Establishment, Report #33, 1957





84. British Antarctic Pilot, Ice, 1948
85. Bureau of Yards and Docks, Arctic Engineering, U. S. Navy, 1955
86. Bureau of Ships, Bureau of Ships Cold Weather Handbook, U. S. Navy,  
Nav. Ships 250-533-7
87. Butkovich, T. R., Ultimate Strength of Ice, U. S. Army, Snow, Ice  
and Permafrost Research Establishment, Research Paper  
#11, 1954
88. Butkovich, T. R., Strength Studies of Sea Ice, U. S. Army Snow, Ice,  
and Permafrost Research Establishment, Research Report #20,  
1956
89. Cambridge Philosophical Society, Theoretical Determination of Elastic  
Constants of Ice, Proceedings, Vol. 44, Part 3, 1948
90. Engineering Institute of Canada, The Bearing Strength of Ice,  
Technical Memorandum No. 56, Transactions, 1958
91. Hess, H., On the Elastic Constants of Ice, Journal of Glaciology,  
Berlin, 1950, Translated by U. S. Army, Snow, Ice and  
Permafrost Research Establishment
92. Institute of Civil Engineers, Snow and Ice Mechanics, London, Vol.  
45, 1950
93. Mantis, H. T., Review of the Properties of Snow and Ice, University  
of Minnesota for U. S. Army Snow, Ice and Permafrost  
Research Establishment, Report #4, 1951



94. Northwood, T. D., Sonic Determination of Elastic Properties of Ice, Canadian Journal of Research, Vol. 25, 1947

95. U. S. Navy Hydrographic Office, Manual of Ice Seamanship, H.O. Publication #551

96. University of Minnesota, Friction on Snow and Ice, for U. S. Army Snow, Ice and Permafrost Research Establishment, 1955

Vessel Powering and Preliminary Design

97. Attwood, E. L. and Pengally, H. S., Theoretical Naval Architecture, 1931

98. Brideweser, D. W., The Estimation of Tugboat Towline Pull and Effects of Types of Propelling Systems, Thesis, Webb Institute of Naval Architecture, 1957

99. Burrill, L. C., Calculations of Marine Propeller Performance Characteristics, North East Coast Institution of Engineers and Shipbuilders, Transactions, 1943

100. Chase, H. J. and Ruiz, A. L., A Theoretical Study of the Stopping of Ships, SNAME, Transactions, 1951

101. Curran, T. M., Construction of Design Charts for Tow Boat Propellers, Thesis, College of Engineering, New York University, 1941



102. Gortler, M., The Prediction of Effective Horsepower of Ships by Methods in Use at the David Taylor Model Basin, DTMB Report 576, 1947
103. Hewins, E. F., Chase, H. J. and Ruiz, A. L., The Packing Power of Geared Turbine Driven Vessels, SNAME, transactions, 1950
104. Hewins, E. F. and Ruiz, A. L., Calculation of the Stopping Ability of Ships, SNAME, Technical and Research Bulletin No. 3-4, 1954
105. Kari, A., Design and Cost Estimating of Merchant and Passenger Ships, Technical Press, 1938
106. Ridgely-Nevitt, C., The Development of Graphical Aids to Preliminary Design, Journal, American Society of Naval Engineers, 1950
107. Roach, C. D., Tugboat Design, SNAME, Transactions, 1954
108. Russell, H. E. and Chapman, L. B., Principals of Naval Architecture, Vol. I and II, SNAME, 1942
109. Saunders, H. E., Hydrodynamics in Ship Design, SNAME, 1957
110. Shultz, J. W. CDR USN, The Ideal Efficiency of Optimum Propellers having Finite Hubs and Finite Numbers of Blades, DTMB Report 1148
111. Taylor, D. W., Speed and Power of Ships, U. S. Government Printing Office, 1943
112. Troost, L., Open Water Test Series with Modern Propeller Forms, North East Coast Institution of Engineers and Shipbuilders, London, 1951





113. Troost, L., A Simplified Method for Preliminary Powering of Single Screw Merchant Ships, SNAME, Transactions, 1957
114. Weinblum, G. and St. Denis, M., On the Motions of Ships at Sea, SNAME, Transactions, 1950

#### Stress Analysis

115. Nevel, D. E., The Narrow Infinite Wedge on an Elastic Foundation, U. S. Army Snow, Ice and Permafrost Research Establishment, Technical Report 56, 1958
116. Nevel D. E., The Narrow, Free, Infinite Wedge on an Elastic Foundation with Applications, Unpublished Manuscript, 1960
117. Roark, R. J., Formulas for Stress and Strain, McGraw Hill, 1943
118. Sturm, R. G., The Behavior of Rectangular Plates under Concentrated Loads, Journal of Applied Mechanics, 1937
119. Timoshenko, S., Vibration Problems in Engineering, Van Nostrand Co., 1928
120. Timoshenko, S., Theory of Plates and Shells, McGraw Hill, 1940
121. Westergaard, H. W., Stresses in Concrete Pavements Computed by Theoretical Analysis, Public Roads, U. S. Department of Agriculture, Bureau of Public Roads, 1926
122. Westergaard, H. W., Stress Concentrations in Plates Loaded over Small Areas, American Society of Civil Engineers, 1942
123. Westergaard, H. W., New Formulae for Stresses in Concrete Pavements of Air Fields, American Society of Civil Engineers, 1947
124. Wyman, M., Deflection of An Infinite Plate, Canadian Journal of Research, 1950









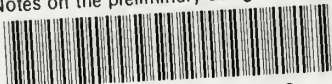






thesM582

Notes on the preliminary design of icebr



3 2768 001 88336 6  
DUDLEY KNOX LIBRARY